



HAL
open science

Initial molecular steps of bone regeneration: cellular scale modulation

Valia Khodr

► **To cite this version:**

Valia Khodr. Initial molecular steps of bone regeneration: cellular scale modulation. Biotechnology. Université Grenoble Alpes [2020-..], 2021. English. NNT: 2021GRALS031 . tel-04627615

HAL Id: tel-04627615

<https://theses.hal.science/tel-04627615>

Submitted on 27 Jun 2024

HAL is a multi-disciplinary open access archive for the deposit and dissemination of scientific research documents, whether they are published or not. The documents may come from teaching and research institutions in France or abroad, or from public or private research centers.

L'archive ouverte pluridisciplinaire **HAL**, est destinée au dépôt et à la diffusion de documents scientifiques de niveau recherche, publiés ou non, émanant des établissements d'enseignement et de recherche français ou étrangers, des laboratoires publics ou privés.



THÈSE

Pour obtenir le grade de

DOCTEUR DE L'UNIVERSITÉ GRENOBLE ALPES

Spécialité : BIS - Biotechnologie, instrumentation, signal et imagerie pour la biologie, la médecine et l'environnement

Arrêté ministériel : 25 mai 2016

Présentée par

Valia KHODR

Thèse dirigée par **Catherine PICART**, Ingénieur Chercheur,
Université Grenoble Alpes

préparée au sein du **Laboratoire CEA / Biomimetism and Regenerative Medicine**
dans l'**École Doctorale Ingénierie pour la Santé la Cognition et l'Environnement**

Premières étapes moléculaires de la régénération osseuse : modulation au niveau cellulaire

Initial molecular steps of bone regeneration: cellular scale modulation

Thèse soutenue publiquement le **6 décembre 2021**,
devant le jury composé de :

Madame CATHERINE PICART

INGENIEUR HDR, CEA CENTRE DE GRENOBLE, Directrice de thèse

Madame VERONIQUE MAGUER-SATTA

DIRECTEUR DE RECHERCHE, CNRS DELEGATION RHONE AUVERGNE, Rapporteur

Monsieur ULRICH VALCOURT

PROFESSEUR DES UNIVERSITES, UNIVERSITE LYON 1 - CLAUDE BERNARD, Rapporteur

Madame SABINE BAILLY

DIRECTEUR DE RECHERCHE, INSERM DELEGATION AUVERGNE-RHONE- ALPES, Examinatrice

Madame CORINNE ALBIGES-RIZO

DIRECTEUR DE RECHERCHE, CNRS DELEGATION ALPES, Examinatrice

Monsieur FRANK LUYTEN

PROFESSEUR EMERITE, Katholieke Universiteit Leuven, Examineur

Madame DELPHINE MEYNARD

CHARGE DE RECHERCHE HDR, INSERM DELEGATION OCCITANIE PYRENEES, Examinatrice

Monsieur FRANZ BRUCKERT

PROFESSEUR DES UNIVERSITES, GRENOBLE INP, Président

**Initial molecular steps of bone
regeneration: modulation at the cellular
scale**

Acknowledgments

First, I would like to thank Dr. Catherine Picart, my PhD advisor for the continuous support and guidance that she has provided me during this thesis. I greatly appreciated the opportunity to have done my research in her laboratory as it has provided me with a multidisciplinary training that would most definitely help me develop my career.

I would like to thank Dr. Véronique Maguer-Satta and Dr. Ulrich Valcourt for accepting to evaluate my work. In addition to Dr. Franz Bruckert, Dr. Corinne Albiges Rizo, Dr. Sabine Bailly, Dr. Frank Luyten and Dr. Delphine Meynard for accepting to participate in this thesis committee and evaluate my work.

Additional thanks for Corinne, Sabine and Dr. Marianne Weidenhaupt for being part of my supervising committee and for the scientific discussions and advices all along these past three years.

I would like to extend my gratitude for several people who played an essential role in my thesis. I first thank Dr. Elisa Migliorini for all of the scientific discussions and remarks. Furthermore, I thank both Dr. Liliane Guerente and Elisa for the role that they played in me joining the team. I thank Paul Machillot for guiding me at the beginning of my PhD and for providing training for the techniques in the team, in addition to his valuable work in the BLI experiments. Also, I thank Laura Clauzier with whom I really enjoyed working on the drugs assay project, for all of the guidance, brainstorming and scientific discussions that we had. She made the challenging phases of this work more enjoyable, and for that I am grateful.

I am thankful for all of my colleagues for creating an excellent working environment, notably Adrià for his valuable advices and discussion, as well as Julius for his support during these last months of writing the thesis, in addition to Joao, Charlotte, Jean, Lauriane, Arun and all the members of LMGP laboratory.

This work would have not been possible without the financial support for Grenoble INP that provided my thesis grant. In addition to the Agence nationale de recherche (ANR CODECIDE, ANR-17-CE13-022) and the Fondation Recherche Medicale (FRM, grant DEQ20170336746) grants for our team. Furthermore, I thank Annie Ducher, Michèle San-Martin, Josiane Viboud and Isabelle Zanotti for their administrative assistance.

Lastly, I would like to thank my parents for the continuous support and for always encouraging me to pursue my dreams, as well as my siblings Vanessa and Alaa, and my aunt Nana for always being there for me. I finally thank my partner and best friend Tamtam, for being my support system and for always motivating me, especially in this recent challenging period that the world has been through.

Abbreviations

ACTR-IIA: Activin receptor type-2A	hMSCs: human mesenchymal stem cells
ACTR-IIB: Activin receptor type-2B	hPDSCs: human periosteum-derived stem cells
ALK1: Activin receptor-like kinase 1	HUVEC: Human umbilical vein endothelial cells
ALK2 (ACVR1): Activin receptor-like kinase 2, also known as Activin receptor like 2	Juvenile polyposis syndrome (JPS)
ALK3 (BMPR-IA): BMP receptor type IA, also known as Activin receptor-like kinase 3	IC50: Half-maximal inhibitory concentration
ALK5 (TGF- β -I): TGF- β receptor type I	IF: Immunofluorescence
ALK6 (BMPR-IB): BMP receptor IB, also known as Activin receptor-like kinase 6	JNK: c-Jun N-terminal kinase
ALP: Alkaline phosphatase	JPS: Juvenile polypos syndrome
BCA: Bicinchoninic acid	LAP: Latency-associated peptides
BE: Barrett esophagus	LHLTBP: Latent TGF- β binding protein
BISC: BMP-induced signaling complex	Mad: mothers against dpp
BLI: bio-layer interferometry	MH1: Mad-homology 1
BMPs: Bone morphogenetic proteins	MH2: Mad-homology 2
BMPR: BMP receptor	MIS: Mullerian inhibiting substance
BMPR-II: BMP receptor II	MKK: Mitogen activated kinase kinase
BSA: Bovine serum Albumin	NES: Nuclear export signal
Co-Smad: Co-mediator Smads	NHS: N-hydroxysuccinimide
DMSO: Dimethyl sulfoxide	NLS: Nuclear basic localization signal
DIPG: Diffuse intrinsic pontine glioma	NPC: Nuclear pore complex
EC50: Half-maximal effective concentration	PAH : Pulmonary arterial hypertension
ECD: Extracellular domain	PEI: Poly(ethyleneimine)
ECM: Extracellular matrix	PEG: poly(ethylene glycol)
EDC: 1-ethyl-3-(3-dimethylaminopropyl) carbodiimide hydrochloride	PFA: Paraformaldehyde
EGF: Epidermal growth factor	PFC : Preformed complex
EMT: Epithelial-Mesenchymal transition	PDB : Protein data bank
FBS: Fetal bovine serum	PLL: Poly(L-lysine) hydrobromide
FDA: Food and Drug Administration (FDA)	PLGA : Poly(lactic-co-glycolic acid)
FN: Fibronectin	qPCR: Quantitative polymerase chain reaction
FOP: Fibrodysplasia ossificans progressive	RGD: Arginylglycylaspartic acid
GAGs: Glycosaminoglycans	RIfS: Reflectometry interference spectroscopy
GDF: Growth differentiation factors	R-Smad: Receptor-regulated Smads
GDNFs: Glial cell line-derived neurotrophic factors	RT: Reverse transcription
GM: Growth medium	RUNX: Runt-related transcription factor
GS: Glycine-serine	siRNA: Small interfering RNA
HA: Sodium hyaluronate	SLC: Small latent complex
hESCs: Human embryonic stem cells	SPR: Surface plasmon resonance
HHT2: Hereditary hemorrhagic telangiectasia 2	TGF- β s: Transforming growth factors
	TGF- β R: TGF- β receptor
	TGN: Trans-Golgi network
	VEGF: Vascular endothelial growth factor

Table of contents

Acknowledgments	5
Abbreviations	7
Table of contents	9
Chapter I: Introduction	13
I.A. Bone Regeneration.....	14
I.A.1. Tissue structure	14
I.A.2. Bone repair	17
I.B. Bone morphogenetic proteins (BMP), transforming growth factors (TGF- β) and their receptors	18
I.B.1. History of the discovery of BMPs and TGF- β s.....	18
I.B. 2. BMP and TGF- β	19
I.B.3. Type I and type II receptors	36
I.C. BMP and TGF- β signaling	39
I.C.1. Interactions between BMP/BMPR and TGF- β /TGF- β R	39
I.C.2. Regulation of the early steps of BMP and TGF- β signaling.....	43
I.D. BMP and TGF- β signaling pathways.....	51
I.D.1. Smad-dependent signaling pathway	51
I.D.2. Smad-independent pathways.....	57
I.D.3. BMP-responsive cells	58
I.D.4. Pharmaceutical strategies targeting BMP/TGF- β signaling	59
I.E. Biomaterials to study BMPs	62
I.E.1. Biomaterials to study BMPs	62
I.E.2. Development of BMP-containing self-assembled films by our team.....	64
Objectives of the PhD thesis	71

Chapter II: Materials and Methods	75
II.A. BMP/BMPR affinity experiments	76
II.A.1. Bio-layer interferometry (BLI) kinetic experiments	76
II.A.2. Kinetic analysis of BLI sensograms	77
II.A.3. Surface plasmon resonance (SPR) kinetic experiments	79
II.A.4. Kinetic analysis of SPR sensograms	80
II.B. Preparation of the biomimetic film	81
II.B.1. Preparation of polyelectrolyte solutions	81
II.B.2. Film buildup and crosslinking.....	81
II.B.3. Loading of BMP and TGF β in the film and UV sterilization	83
II.B.4. Quantification of bound BMP with Bicinchoninic acid (BCA) assay	83
II.C. Cell culture	85
II.C.1. Cell culture.....	85
II.C.2. Cell lysis and study of BMPR expression by quantitative polymerase chain reaction (qPCR).....	86
II.C.3. Evaluation of pSmad signaling	89
Chapter III: High throughput measurements of bone morphogenetic protein (BMP)/BMP receptors interactions using bio-layer interferometry	95
III.1. Article Summary	96
III.II. Article	98
Chapter IV: Differential bioactivity of four BMP-family members as function of biomaterial stiffness	127
IV.1. Article Summary	128
IV.2. Cellular characterization.....	130
IV.3. Role of BMPR in adhesion, spreading and signaling	135

Chapter V: Development of an automated high-content screening immunofluorescence assay of pSmad quantification: proof-of-concept with drugs inhibiting the BMP and TGFβ pathways	141
V.I. Article Summary	142
V.II. Article	143
Chapter VI: General discussion	165
I. Determining BMP/BMPR interaction using BLI	166
1. BLI as a technique	166
2. Effect on signaling.....	167
3. Crosstalk between the BMP and TGF- β pathway	170
4. BMP/BMPR interaction limitations	171
II. Drug screening on biomaterials	172
Chapter VII: Conclusions and Perspectives	175
References	181
Abstract.....	203
Résumé.....	204
Annexes	205
CV	253

Chapter I: Introduction

I.A. Bone Regeneration

I.A.1. Tissue structure

The human skeleton constitutes a large part of the organism, composed of 213 bones, apart from the sesamoid bones. It has various roles in providing structural support for the body, allowing movement, protecting internal organs, as well as containing a reservoir of growth factors and ensuring hematopoiesis within bone marrow (Clarke, 2008).

In their composition, bones are composed of two phases: >60% of mineral phase consisting mainly of hydroxyapatite (HAP) mineral crystals ($\text{Ca}_{10}(\text{PO}_4)_6(\text{OH})_2$) capable of storing the citrate, carbonate, ions such as F^- , K^+ , Zn^{2+} , Cu^{2+} and Fe^{2+} , in addition to the calcium needed for cellular function. The remaining 30% form the organic phase, which is made up of proteins such as collagen I involved in mechanical properties of the bone, in addition to non-collagenous proteins like sialoprotein, osteopontin, osteonectin, osteocalcin, Bone morphogenetic proteins (BMPs), as well as lipids, polysaccharides and primary bone cells. The remaining 10% is composed of water (Chai *et al.*, 2012).

Bones are composed of two types of osseous tissue: the cortical bone and trabecular bone (Clarke, 2008; Iaquina *et al.*, 2019). In humans, 80% of all bones are cortical bones, which are dense compact bones present in the outer layer of the bone and whose role is to carry the total load of the skeleton (Augat and Schorlemmer, 2006). While the 20% remaining are the trabecular bones composed of trabecular plates and rods containing the bone marrow (**FIG.I.1.**) (Clarke, 2008; Iaquina *et al.*, 2019). The trabecular and cortical bone are usually separated by an epiphyseal growth plate, which is the site of longitudinal bone growth.

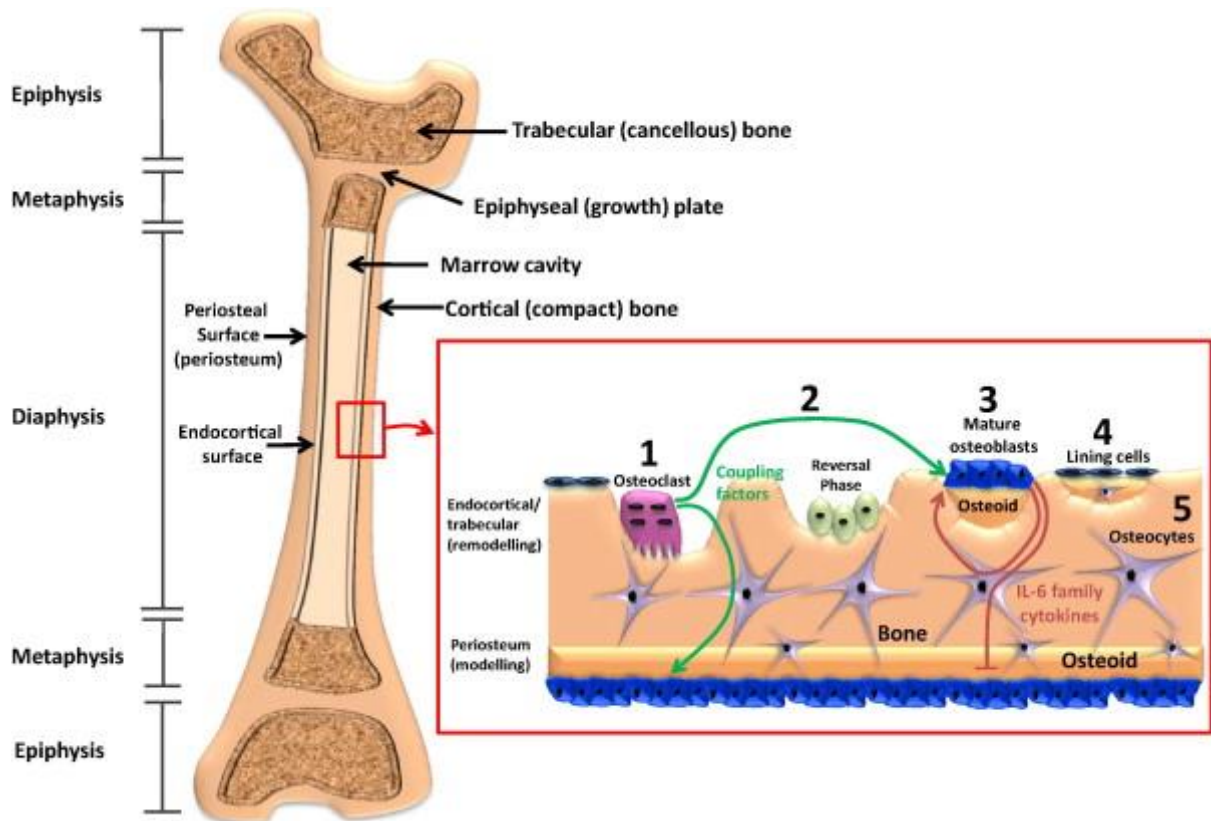


FIG.I.1. Structure of a bone and its remodeling process. The bone structure is formed of cortical (compact bone) and trabecular (cancellous) containing the bone marrow. These two bones are separated by an epiphyseal growth plate. The bone remodeling process is constituted by the remodeling process at the endocortical/trabecular surface, and a modeling at the periosteum surface. This mechanism consists of several steps: 1) The osteoclasts are recruited to the bone surface and activated in order to resorb bone by inducing bone matrix degeneration. These osteoclasts send coupling factors that induce osteoblasts differentiation. 2) Then the premature osteoblasts are recruited to the degenerated bone in the reversal step. 3) The osteoblasts mature and secrete an osteoid (Sims and Vrahnas, 2014).

The prolonged loading on the bones during a person's lifetime induces micro-cracks in the cortical bone and leads to a decrease in bone stiffness. In fact, bone is constantly being resorbed and replaced with new bone in a process called bone remodeling. This process occurs on the periosteum (or periosteal surface), a tissue surrounding the cortical surface of the bones, while the bone remodeling occurs on the trabecular bone and endocortical surface (Sims and Vrahnas, 2014).

Furthermore, several types of cells, called the bone-remodeling units, are known to be involved in this process. First, the osteoclasts, involved in bone resorption and osteoblasts, involved in bone regeneration. The osteoclast cells are derived from the myeloid lineage of the hematopoietic stem cells (HSCs) in a process called osteoclastogenesis, (**FIGI.2.**). The HSCs are present as osteoclast precursor macrophages colony-forming units (CFU-M), which are the

precursor of macrophages and osteoclasts. After activation of the RANKL/RANK signal, which consists of the binding of the RANKL, a nuclear factor- κ B ligand, to the receptor RANK present at the osteoclast surface, the CFU-M are differentiated into mononucleated osteoclasts. These osteoclasts can further fuse to become multinucleated osteoclasts that can degrade the bone by secreting acids, proteases and matrix metalloproteinase (Iaquinta *et al.*, 2019; Kim *et al.*, 2020).

Second, the osteoblasts are derived from the multipotent mesenchymal stem cells (MSCs) in a process called osteoblastogenesis. The committed osteoprogenitor differentiates first to preosteoblast, then they become mature osteoblasts, a process that is associated to the expression of specific transcription factors such as RUNX2 and Osterix. The mature osteoblasts can thus differentiate to lining cells or osteocytes that are the terminally differentiated bone cells in the mineralized bone, or even go through apoptosis to ensure bone turnover (Iaquinta *et al.*, 2019; Kim *et al.*, 2020).

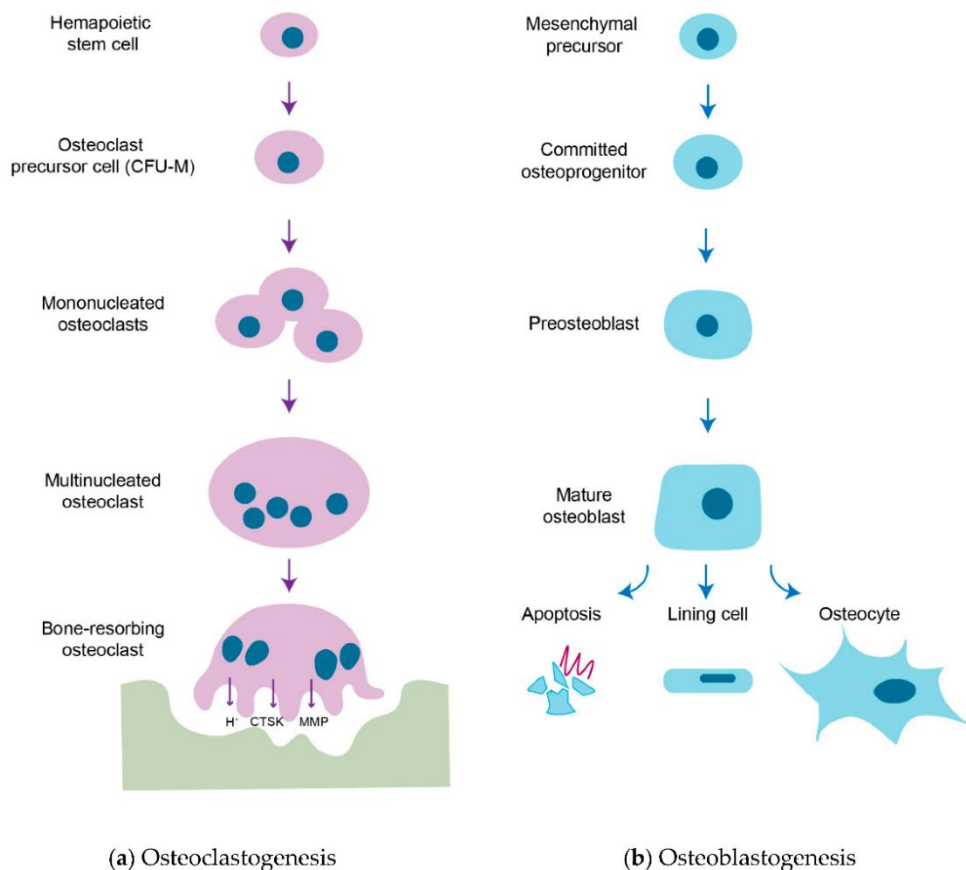


FIG.I.2. The osteoclastogenesis and osteoblastogenesis process. a) The osteoclasts are derived from hematopoietic stem cells. The CFU-M precursors differentiate into mononucleated osteoclasts that can fuse to form multinucleated osteoclasts. The mature osteoclast secretes acids, proteases and matrix metalloproteinase that resorbs the bones by degrading the bone matrix. b) The osteoblasts are derived from the mesenchymal stem cells.

They differentiate from committed osteoprogenitor to preosteoblasts and then become mature osteoblasts. The osteoblasts can then differentiate into osteocytes, lining cells or go through apoptosis (Kim *et al.*, 2020)

Besides, we should mention the presence of other bone marrow cells such as osteomacs, which are resident tissue macrophages, vascular endothelial cells which supply oxygen and nutrients, and removes products of resorption, in addition to lymphocytes T and B which are involved in the crosstalk between the immune and skeletal systems (Kular *et al.*, 2012).

The remodeling mechanism has several steps (**FIG.I.1.B**). First, in the initiation step, osteoclasts are recruited and activated. They resorb bone by degrading the mineralized bone matrix, and release coupling factors such as IGF-1, TGF- β , cardio- trophin-1, sphingosine-1-phosphate, BMP6 and Wnt10b that activate osteoblast differentiation. Second is the reversal phase where the osteoclasts enter into apoptosis, and the premature osteoblasts are recruited to the newly exposed bone surface where they can deposit unmineralized bone matrix known as osteoid. Third, bone is forming again where the osteoblasts are either embedded in the osteoid, or become lining cells or are differentiating into osteocytes that regulate bone mineralization. Finally, in the termination phase, an equal amount of the resorbed bone has been replaced and the remodeling ends (Raggatt and Partridge, 2010; Sims and Vrahnas, 2014). This remodeling process takes about 200 days in the cancellous bone, out of which 150 days are dedicated to bone formation (Kular *et al.*, 2012).

I.A.2. Bone repair

Apart from the physiological bone remodeling, the bones possess the capacity to regenerate after a bone fracture by initiating a cascade of events to ensure an efficient bone repair. Upon bone fracture, an initial inflammatory response occurs and a hematoma characterized by reduced levels of O₂ and pH, and an increased lactate is formed due to the plasma coagulation and platelet exposure to the extravascular environment (**FIG.I.3.A**). The injured tissues are then removed, and secreted stimulatory factors secreted by the different cells of the microenvironment (cells from the bone marrow, the periosteum and from cortical bone); These factors include tumor necrosis factor alpha (TNF- α), bone morphogenetic proteins (BMPs), fibroblast growth factors (FGF) and Wingless-type MMTV integration site family of proteins (Wnt). This step is followed by the formation of a granulated tissue containing progenitor cells that can expand leading to cellular condensation, followed by cell differentiation: first cells differentiate to chondrocytes (**FIG.I.3.B**), and then into osteoblasts, which form a woven bone

with the hypertrophic mineralized chondrocytes (**FIG.I.3.C**). Finally, the bone undergoes cycles of bone remodeling with osteoblasts and osteoclasts to bridge the fracture (Arvidson *et al.*, 2011; Ho-Shui-Ling *et al.*, 2018).

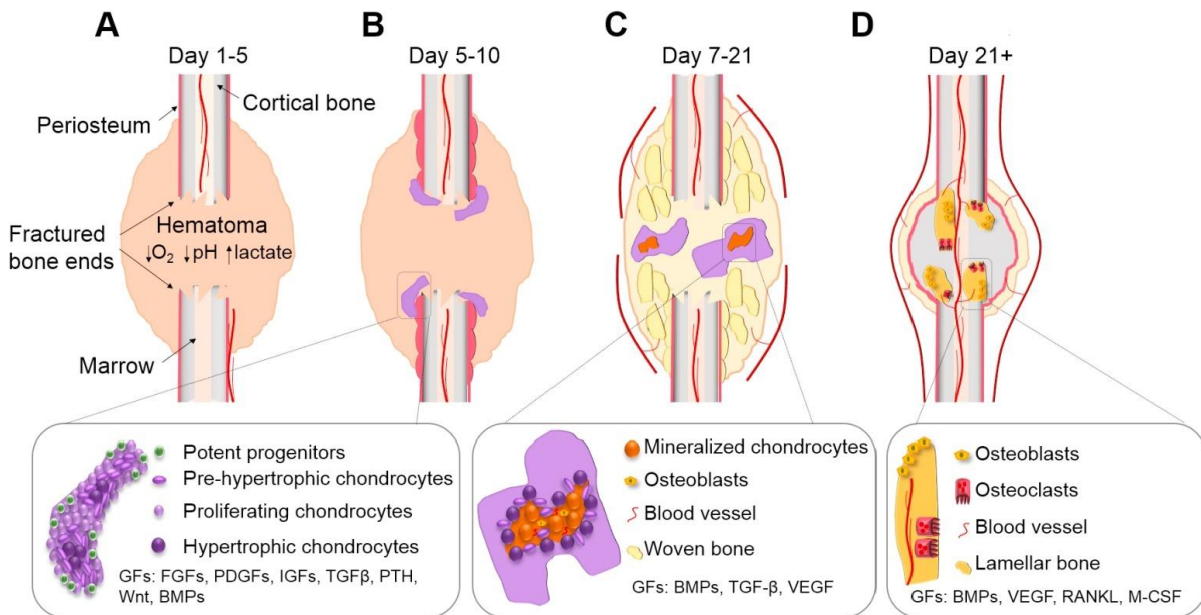


FIG.I.3. Healing process of a bone fracture. The bone healing process consists of different steps: A) After fracture, reduced levels of O_2 and pH are detected, in addition to increased lactate. In this stage, a hematoma forms and inflammatory cells secrete stimulatory factors to recruit progenitor cells. B) Formation of a callus and initiation of chondrogenic differentiation. C) Chondrocytes mineralize the callus and osteoblasts form woven bone. D) Remodeling of the woven bone by osteoclast-osteoblast coupling. The lamellar bone eventually bridges the fracture (Ho-Shui-Ling *et al.*, 2018).

This bone fracture healing process is modulated by several growth factors notably BMPs, TGF- β , Wnt, platelet-derived growth factors (PDGFs) and insulin-like growth factor 1 families, which have a role in recruiting progenitor cells, in the proliferation and differentiation of chondrocytes, osteoblasts and endothelial cells.

I.B. Bone morphogenetic proteins (BMP), transforming growth factors (TGF- β) and their receptors

I.B.1. History of the discovery of BMPs and TGF- β s

The concept of bone regeneration was mentioned repeatedly throughout history, with the first documented notions mentioned by Greek philosophers such as Aristotle and Galen (Odelberg, 2004; Lazzeri *et al.*, 2009). However the first bone regeneration studies scientifically described

were in 1889 by Schede who used blood coagulation to treat wounds, and Senn who based on Schede's results to develop a technique using decalcified bone for osteogenic repairs in dogs (Senn, 1889).

In 1965, Dr. Marshall R. Urist introduced the term "bone morphogenetic proteins (BMPs)". After implanting parts of diaphyseal bone under a muscle pouches of rabbits, rats, mice and guinea pigs, he discovered the presence of a bone auto induction system involving a pool of osteoprogenitor stem cells and small capillaries (Marshall R. Urist, 1965). He then defined the bone-derived protein responsible for the osteogenic embryonic induction in post fetal life as bone morphogenetic protein (BMP) (Urist and Strates, 1971). Studies followed to determine the key steps of their involvement in differentiation and bone formation (Grgurevic, Pecina and Vukicevic, 2017). Afterwards, a research team at the Genetics Institute cloned the first BMPs; BMP-1, BMP-2A and BMP-3 which all demonstrated an ability to induce the formation of cartilage *in vivo*. (Wozney *et al.*, 1989).

Similarly, other groups were working on identifying and purifying secreted growth factors able to transform fibroblasts (Moses, Roberts and Derynck, 2016). De Larco and Todaro first described the partial purification of a partial growth polypeptide that could induce the growth and formation of colonies of normal fibroblasts and murine sarcoma virus-transformed fibroblasts in cell cultures *in vitro* (De Larco and Todaro, 1978). Besides their ability to trigger the formation of cell colonies, these growth factors can bind to epidermal growth factor (EGF) receptors. Later on, purification efforts by (Moses *et al.*, 1981; Roberts *et al.*, 1981), led to the discovery and separation of these transforming polypeptides in two distinct groups called transforming growth factors (TGF). Those, which could bind EGF receptor, were called TGF- α and those, which are needed for colony formation, were called TGF- β (Moses, Roberts and Derynck, 2016).

Afterwards, the identification of the similarities in TGF- β , BMP and other ligand structures, sequences and roles, led to their assembly in a TGF- β superfamily.

I.B. 2. BMP and TGF- β

I.B.2.1. Classification of TGF- β superfamily

The TGF- β superfamily of growth factors consists of more than 33 members in humans, divided into several families notably the activins/inhibins/Müllerian inhibiting substance (MIS) group, the glial cell line-derived neurotrophic factors (GDNFs) group, the BMPs/Growth differentiation factors (GDF) group and the TGF- β group (Heldin and Moustakas, 2016) (**FIG.1**).

First, the activin/inhibin family contains ligands secreted by the placenta, pituitary and gonadotrope cells. These growth factors are formed by two subunits, sharing a common β subunit. The inhibins are present as $\alpha\beta$ heterodimers, while activins are present as $\beta\beta$ homodimers. The β subunit is mainly present as βA or βB forms. Hence, the activin A is a dimer of $\beta A/\beta A$ subunits, and activin B as a dimer of $\beta B/\beta B$, while inhibin A is a dimer of $\alpha/\beta A$ subunits, and inhibin B a dimer of $\alpha/\beta B$ subunits. In addition, other forms of activin such as activin C (βC) and activin E (βE) were discovered in liver, testis and prostate (Gold *et al.*, 2009; Namwanje and Brown, 2016). These growth factors have been described to have several physiological roles in development and homeostasis as well as pathological roles. The activins are mainly involved in the release of the follicle – stimulating hormone by gonatrophic cells, in contrast to inhibins that have an inhibitory effect (Wijayarathna and de Kretser, 2016). These factors are also involved in angiogenesis and osteogenesis (Namwanje and Brown, 2016).

Furthermore, the MIS member which is also produced in Sertoli cells in males and granulosa cells in female (Kim, MacLaughlin and Donahoe, 2014). This growth factor has been described to have a role in the regression of the female reproductive structures in males, as well as in fertility as it is a marker of the ovarian reserve and a protective role during gonadotoxic chemotherapeutics (Grynnerup, Lindhard and Sørensen, 2012; Kano *et al.*, 2017). In addition, the secreted glycoproteins Lefty A and Lefty B are also part of the TGF- β superfamily. They are reported to be regulators of human embryonic stem cells (hESCs) and cell differentiation (Khalkhali-Ellis *et al.*, 2016).

Second, the GDNFs family is composed of GDNF, Neurturin, Artemin and Persephin. They are considered distant members of the TGF- β superfamily, since they only share 20% sequence similarity with other TGF- β members and signal through tyrosine kinase receptors and not with serine/threonine kinase receptors. However, they share noticeable similarity with TGF- $\beta 2$ and BMP-7, and are active in their homodimeric form (Saarma, 2000; Chang, Brown and Matzuk, 2002). GDNFs have a role in neurogenesis as they promote the survival of embryonic dopaminergic neurons and rescues spinal motor neurons in Parkinson disease (Sariola and Saarma, 2003). They also have a role in kidney development and spermatogenesis (Airaksinen and Saarma, 2002).

Third, the BMPs family is formed from 20 ligands (**FIG.I.4**). The homology in the primary amino acid sequences led to the classification of BMPs in different groups: first, the BMP-2/BMP-4 group that have been reported to diverge from a single ancestral gene and share more than 80% homology in their amino acid identity (Goldman, Donley and Christian, 2009).

Second, the BMP-5/BMP-6/BMP-7 (or OP-1)/BMP-8 (or OP-2) (Miyazono, Maeda and Imamura, 2005). Third, the BMP-9/BMP-10 group which have 65% of amino acid homology (David *et al.*, 2007). Fourth, the GDF-1/3 and the GDF-5/6/7 (BMP-12, 13, 14), and GDF9/BMP-15 groups which are also considered members of the BMP family since they have similar functions (Katagiri and Watabe, 2016).

Finally, the two BMP groups often assigned to the activin/inhibin subgroup, BMP-3 (GDF-3) or osteogenin group with GDF-10, which differs remarkably from other members of BMPs and share 80% sequence similarity in their mature region (Cunningham *et al.*, 1995). In addition to the GDF-8/BMP-11 group which are homologs that share 90% of their sequence in their C-terminal signaling domain with the activin/inhibin group (Walker *et al.*, 2017).

Regarding TGF- β , five genes have been discovered, designated TGF- β 1 to TGF- β 5. Although the mammals' three isoforms (TGF- β 1, TGF- β 2, TGF- β 3) present 70% to 80% amino acid homology, they have been described to have distinct expression patterns and therefore have different physiological roles (Gold *et al.*, 2000; Gilbert, Vickaryous and Vilorio-Petit, 2016).

We should also note that BMP-1 possesses procollagen C-proteinase function involved in collagen maturation and does not belong to the TGF- β superfamily (Kessler *et al.*, 1996).

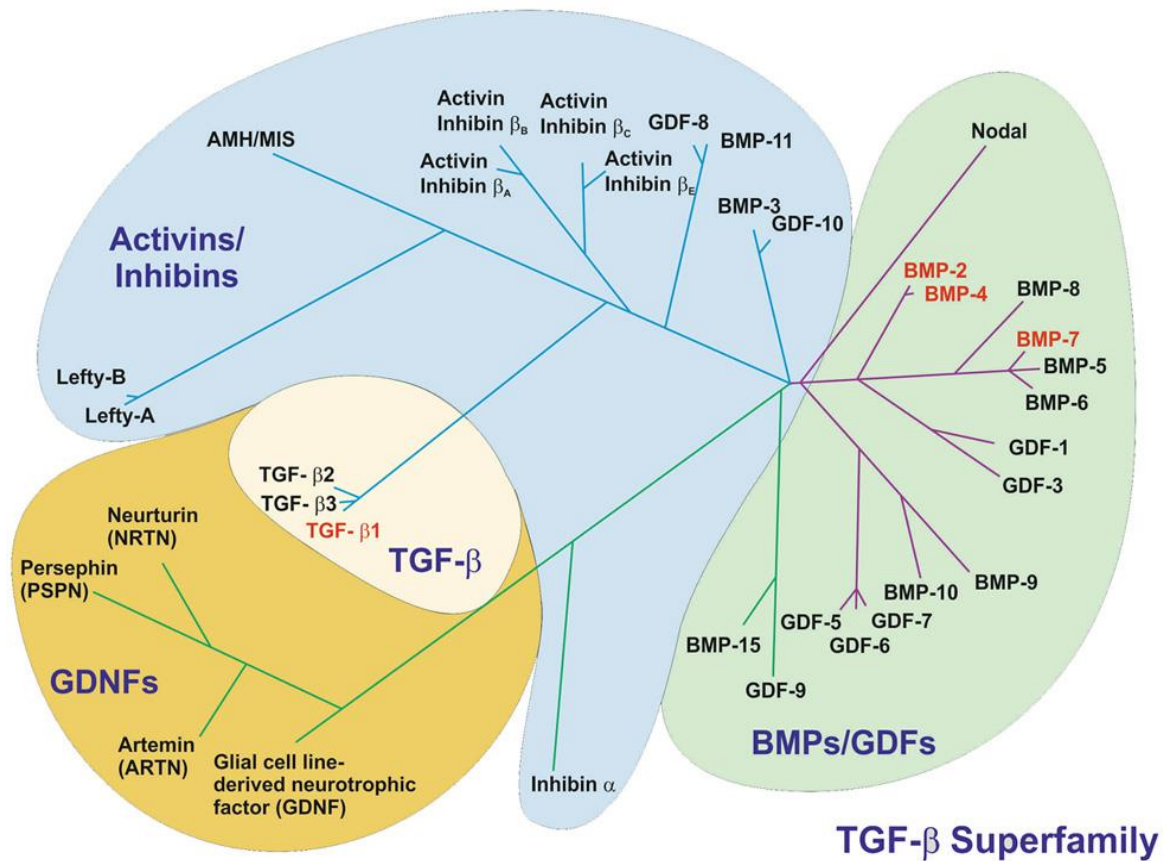


FIG.I.4: Phylogenetic tree of the TGF-β superfamily. This superfamily consists of three major groups, which are: Activin/Inhibins, GDNFs, TGF-β, and BMPs/GDF group (Weiskirchen *et al.*, 2009).

The structure of TGF-β and BMPs and their physiological and pathological roles will be detailed in the next section. We will mainly focus on BMP-2, BMP-4, BMP-7, BMP-9 and TGF-β1 for two major reasons: first, these BMPs have been studied previously in the team (Machillot *et al.*, 2018; Sales *et al.*, 2022). Second, they are among the most studied BMPs in the field, as seen in **FIG.I.5** (Hiepen *et al.*, 2016). Third, TGF-β is the most widely studied member of the TGF-β superfamily.

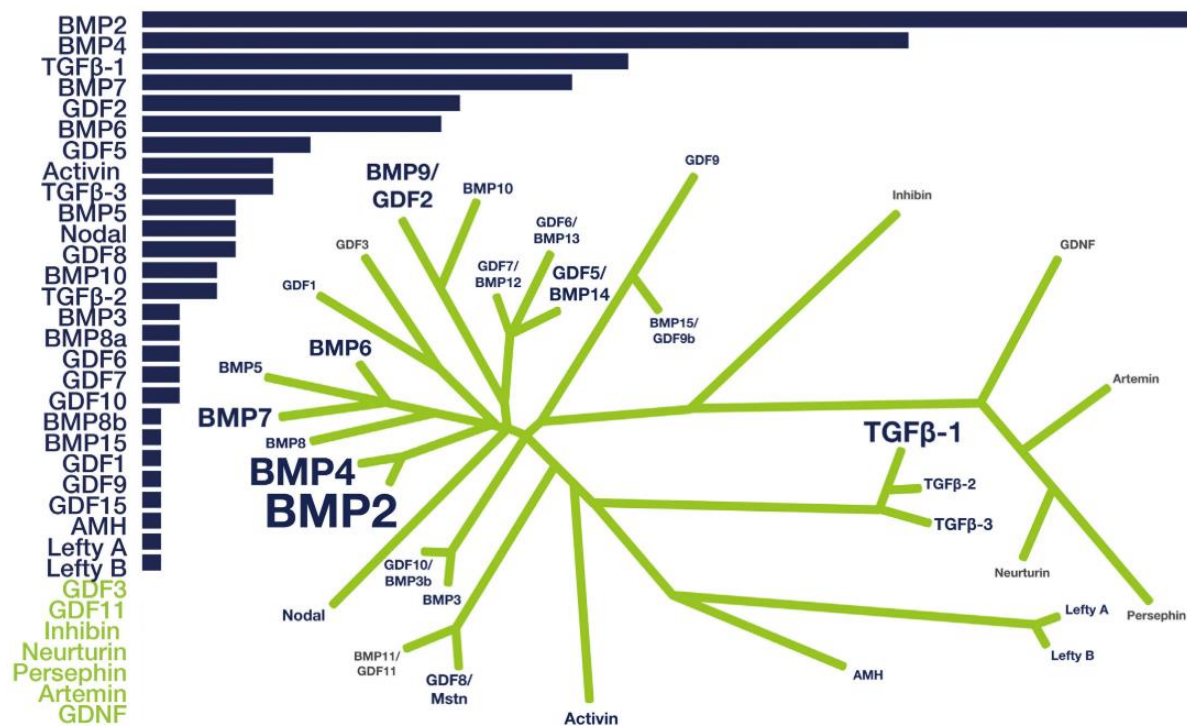


FIG.I.5. Frequency of the mention of the TGF- β superfamily members at the 10th international BMP conference that took place in Berlin in 2014 (Hiepen *et al.*, 2016).

I.B.2.2. Physiological and pathological roles of BMPs and TGF- β s

As their name suggests, BMPs are involved in bone regeneration as they have osteogenic properties and can induce bone formation. Indeed, BMP-2, BMP-4, BMP-6, BMP-7 and BMP-9 have been shown to be osteogenic (Cheng *et al.*, 2003; Kang *et al.*, 2004). BMP-2 was found to be the major growth factor in fracture repair, since mice lacking BMP-2 do not have the ability to repair fractures (Tsuji *et al.*, 2006). Besides, BMP-2 induced the osteogenic differentiation in C2C12 skeletal myoblast (Katagiri *et al.*, 1994), adipose derived mesenchymal stem cells (Knippenberg *et al.*, 2006) as well as bone marrow and umbilical cord mesenchymal stem cells (Marupanthorn *et al.*, 2017). Furthermore, BMP-4 transduction in adipose-derived stromal cells led to their differentiation into osteoblasts *in vitro* and *in vivo* (L. Lin *et al.*, 2006). It also was described to induce bone formation indirectly by inducing the expression of the osteoclastogenesis inhibitory factor in mouse bone-marrow-derived stromal cells (Tazoe *et al.*, 2003). BMP-7 also demonstrated osteogenic activity when used for repairing critically human defects (Geesink, Hoefnagels and Bulstra, 1999). Thus, both BMP-2 and BMP-7 were considered for their use in human spine surgery; BMP-7 initially received authorization in 2003 but is no longer in use since the closure of Olympus Biotech in 2014, while BMP-2 was

approved by the Food and Drug Administration (FDA) in 2003 and is commercialized to repair fractures in humans (Hustedt and Blizzard, 2014).

BMP-6 was reported to induce ectopic bone differentiation when injected in rat muscle *in vivo* (Jane *et al.*, 2002), and differentiation of C2C12 and MC3T3-E1 cells to osteoblasts *in vitro* (Ebisawa *et al.*, 1999), as well as to induce bone differentiation more efficiently than BMP-2 in mesenchymal stem cells (Mizrahi *et al.*, 2013). Interestingly, BMP-9 has also been described to be an osteogenic factor (Kang *et al.*, 2004; Lamplot *et al.*, 2013), although with a different signaling pathway than BMP-2 and BMP-7 (Hue H *et al.*, 2007). We should mention that several BMPs have been found to be essential in embryogenesis and early developmental processes since their knockout result in embryonic lethality or death shortly after birth (Wang *et al.*, 2014).

On the other hand, both of BMP-2 and BMP-4 were shown to have roles in the chondrogenesis of the growth plate *in vitro*, since BMP-2 led to activation in chondrocyte hypertrophy (De Luca *et al.*, 2001) and BMP-4 has a role in chondrocyte maturation (Hatakeyama, Tuan and Shum, 2004). On the other hand, *in vivo*, only BMP-2 was shown to have a crucial role in chondrocyte proliferation and maturation during endochronal bone development (Shu *et al.*, 2011). However, it was also associated with chondrocyte hypertrophy and cartilage degradation in osteoarthritis (Valcourt *et al.*, 2002; Papathanasiou, Malizos and Tsezou, 2012). In contrast, BMP-7 reduces the degradation of articular cartilage (Badlani *et al.*, 2009; Hunter *et al.*, 2010). Furthermore, TGF- β has been described to have a dual role in the pathology of arthritis as the loss of its signaling leads to chondrocyte hypertrophy and therefore cartilage degeneration. Thus, the preservation of articular cartilage can be done by pharmaceutical activation (Wu, Chen and Li, 2016).

In muscles, the BMP signaling pathway has been described to be key in the control of the muscle mass (Sartori *et al.*, 2013). Similar results was also seen with BMP-7 which induced muscle hypertrophy through the Smad signaling (Winbanks *et al.*, 2013).

In the gastrointestinal system, BMP-4 is reported to be upregulated and is involved in the transformation of inflamed esophageal mucosal into Barrett esophagus (BE) disease which consists of having the epithelium of the esophagus replaced by columnar epithelium (Milano *et al.*, 2007; Kestens *et al.*, 2016).

In the cardiovascular system, it is described that several of the TGF- β superfamily ligands are involved in cardiac development and angiogenesis. In fact, BMP-2 and BMP-4 were found to

play an essential role in atrioventricular septation of the heart through an activation of an epithelial-mesenchymal transformation (Jiao *et al.*, 2003; Ma *et al.*, 2005; Rivera-feliciano and Tabin, 2006). While TGF- β has been described to induce angiogenesis and stimulates collagen production by the fibroblasts (Roberts *et al.*, 1986). In addition, all of the three TGF- β are involved in cardiovascular development and hypertrophy of cardiomyocytes, as well as hypertension pathologies (Azhar *et al.*, 2003).

TGF- β 1 is mostly known for its role in fibrosis, a process caused by contractile and secretory myofibroblasts and in which there is accumulation of the extracellular matrix (ECM) components in inflamed tissues that leads to organ dysfunction (Hinz *et al.*, 2007). Fibrosis could affect various organs notably lung, pancreas, liver, skin, heart, kidney and pancreas (Weiskirchen, Weiskirchen and Tacke, 2019). TGF- β regulates the function and phenotype of fibroblast that is transformed to myofibroblasts necessary for tissue repair and the effector cells in fibrosis. In the case of fibrosis, apart from the transformation of mesenchymal stem cells to myofibroblasts, TGF- β stimulates an additional transformation of epithelial cells in a process called epithelial-mesenchymal transition (EMT) (Valcourt *et al.*, 2005; Biernacka, Dobaczewski and Frangogiannis, 2011).

In angiogenesis, it was reported that BMP-2, BMP-4, BMP-7 and BMP-9 have pro- and antiangiogenic roles by either directly regulation functions of endothelial cells or indirectly by influencing angiogenic factors such as vascular endothelial growth factor (VEGF) (Moreno-Miralles, Schisler and Patterson, 2009). Indeed, both of BMP-2 and BMP-4 were shown to be necessary to the proliferation, migration and angiogenesis of human umbilical vein endothelial cells (HUVECs) (Zuo *et al.*, 2016). In contrast, BMP-9 has an anti-angiogenic effect since it was reported to be an inhibitor of angiogenesis and a regulator of vascular tone (David *et al.*, 2008), although a pro-angiogenic effect was seen at low concentrations of BMP-9 (Suzuki *et al.*, 2010). These angiogenic activities are seen in the context of cancer as BMP-2 promote angiogenesis of lung cancer tumour (Langenfeld and Langenfeld, 2004) and BMP-2, BMP-4 and BMP-7 promote chronic myelogenous leukemia (Zylbersztejn *et al.*, 2018).

On the other hand, BMP-9 was found to inhibit the growth of prostate cancer by inducing apoptosis (Ye, Kynaston and Jiang, 2008), as well as breast cancer in a mammary carcinoma model, in addition to being a quiescence factor in mammary tumor growth and lung metastasis (Ouarné *et al.*, 2018). Similarly, TGF- β was also demonstrated to have a dual role in cancer. In normal cells, TGF- β has tumor suppressor properties such as activation of apoptosis and

cytostasis. However, when malignant cells can alter his signaling pathway which leads to a loss of its protective properties and activation of EMT transition and metastasis (Massagué, 2008).

In the urinary system, BMP-4 mutations have been associated with renal dysplasia patients who have a maldevelopment of the renal tissue (Weber *et al.*, 2008). In addition, both BMP-4 and BMP-7 were found to be important for the development of the urethra during embryonic development (Morgan *et al.*, 2003), and BMP-7 has been shown to reduce renal fibrosis (Weiskirchen *et al.*, 2009). Furthermore, BMP-4 and BMP7 mutations have been associated with patients that have developmental eye anomalies such as retinal dystrophy and myopia (Bakrania *et al.*, 2008; Wyatt *et al.*, 2010).

We should note that BMP-6 was reported to promote fertility by playing a role in the response to the luteinizing hormone (Sugiura, Su and Eppig, 2010). In addition, it has an essential role in iron homeostasis since disruption of BMP-6 in mice led to an accumulation of iron in liver, pancreas heart and kidney (Camaschella, 2009; Meynard *et al.*, 2009).

Finally, BMPs have also a role in the adipose tissue, as BMP-2 and BMP-4 were able to induce the differentiation of stem cells into adipocytes (Huang *et al.*, 2009). Moreover, BMP-4 is associated to the differentiation of stem cells to white adipose cells while BMP-7 differentiates them to brown adipose cells (Blázquez-Medela, Jumabay and Boström, 2019).

A summary of the various functions of BMPs are presented in **TABLE.I.1**.

TABLE.I.1. Table summarizing the physiological and pathological roles of A) BMP-2, B) BMP-4, C) BMP-6, BMP-7 and D) BMP-9 and TGF- β 1. The roles of BMPs / TGF- β 1 are classified by BMP and sub-classified by tissue. The physiological roles are presented in black, and the pathological roles in **red**.

A.

Protein	Tissue	Physiological and pathological role	References
BMP-2	Blood vessels	It is necessary for the proliferation, migration and angiogenesis of human umbilical vein endothelial cells	Zuo, W et al, Scientific Reports (2016)
		It promotes angiogenesis of lung cancer tumor and promote chronic myelogenous leukemia	Langenfeld, E & Langenfeld J, Molecular Cancer Research (2004) Zylbersztejn, F et al, Experimental Hematology (2018)
	Bone	It induces osteogenic differentiation in C2C12 adipose derived mesenchymal stem cells as well as bone marrow and umbilical cord mesenchymal stem cells	katagiri, T et al, Journal of Cell Biology (1994) Knippenberg, M et al, Biochemical and Biophysical Research Communications (2006) Marupanthorn, A et al, International Journal of Molecular Medicine (2017)
		It is involved in the differentiation of mesenchymal cells during fracture repair	Tsuji, K. et al, Nature Genetics (2006)
	Cartilage	It activates chondrocytes proliferation and maturation during endochondral bone development	De Luca, F et al, Endocrinology (2001) Shu, B. et al, J cell Sci (2011)
		It induces chondrocyte hypertrophy and cartilage degeneration notably in osteoarthritis	Valcourt, U et al, Journal of Biological Chemistry (2002) Papathanasiou, I et al, Arthritis Research & therapy (2012)
	Fat	It induces the differentiation of stem cells into adipocytes	Huang, H et al, PNAS (2009)
	Heart	It is involved in heart chamber and valve development through an activation of an epithelial-mesenchymal transformation	Feliciano, R., Tabin, CJ, Dev Biol (2006) Ma, L. et al, Development (2005)

B.

BMP-4	Blood vessels	It is necessary for the proliferation, migration and angiogenesis of human umbilical vein endothelial cells	Zuo, W et al, Scientific Reports (2016)
		it promotes chronic myelogenous leukemia	Zylbersztejn, F et al, Experimental Hematology (2018)
	Bone	It induces the expression of osteoclastogenesis inhibitory factor in mouse bone-marrow-derived stromal cells	Tazoe, M et al, Archives of Oral Biology (2003)
		It induces the differentiation of adipose-derived stromal cells into osteoblasts	Lin, L et al, Acta Pharmacologica Sinica (2006)
	Cartilage	It is involved in chondrocytes differentiation and maturation	Hatakeyama, Y et al, Journal of Cellular Biochemistry (2004)
	Esophagus tube	It is involved in the progression of Barrett esophagus by inducing the transformation of normal esophageal squamous cells into columnar cells	Milano, F. et al, Gastroenterology (2007) Kestens, C. et al, PLoS One (2016)
	Eye	It is involved in eye development. Mutations within its sequence was found in patients that have developmental eye anomalies	Bakrania, P et al, American Journal of Human Genetics (2008)
	Fat	It induces the differentiation of stem cells into adipocytes	Huang, H et al, PNAS (2009)
		It induces the differentiation of stem cells to white adipocytes and alters insulin sensitivity	Blázquez-Medela, A et al, Obesity Reviews (2009)
	Heart	It is involved in heart chamber and valve development through activation of an epithelial-mesenchymal transformation	Jiao, K et al, Genes & Development (2003)
Renal	It is involved in the development of the urethra during embryonic development	Morgan, E et al, Development (2003)	
	Its mutations have been associated with renal dysplasia patients who have a maldevelopment of the renal tissue	Weber, S. et al J Am Soc Nephrol (2008)	

C.

BMP-6	Bone	It induces bone differentiation in vivo, and differentiation of C2C12, MC3T3-E1 and MSC to osteoblasts in vitro	Jane, J et al, Molecular therapy (2002) Ebisawa, T et al, Journal of Cell Science (1999) Mizrahi, O et al, gene therapy (2013)
	Liver	It has an essential role in iron homeostasis in the liver	Meynard, D et al, Nature Genetics (2009)
	Uterus	It plays a role in fertility by enabling response to luteinizing hormone	Sugiura, K et al, Biology of Reproduction (2010)
BMP-7	Blood vessels	It promotes chronic myelogenous leukemia	Zylbersztejn, F et al, Experimental Hematology (2018)
	Bone	It demonstrated osteogenic activity when used for repairing critically human defects	Geesink, R et al, Journal of Bone and Joint Surgery (1999)
	Cartilage	It may have a protective role in Osteoarthritis as it reduces the degradation of articular cartilage. Clinical trials are being done to determine its efficiency	Badlani, N. et al, Clinical Orthopaedics and Related Research (2009) Hunter, D.J. et al, BMC Musculoskeletal Disord (2010)
	Eye	It is involved in eye development. Mutations within its sequence was found in patients that have developmental eye anomalies	Wyatt, A et al, Human Mutation (2010)
	Fat	It induces the differentiation of stem cells into adipocytes to brown adipose cells	Blázquez-Medela, A et al, Obesity Reviews (2009)
	Muscle	It induces muscle hypertrophy	Winbanks, C et al, Journal of Cell Biology (2013)
	Renal		It is involved development of the urethra during embryonic development
		It plays a protective role in renal fibrosis	Weiskirchen, R et al, Frontiers in Bioscience (2009)

D.

BMP-9	Breast	It is a quiescence factor in a mammary carcinoma tumor growth and lung metastasis	Ouarné, M et al, Journal of Experimental and Clinical Cancer Research (2018)
	Blood vessels	It is an inhibitor of angiogenesis and a regulator of vascular tone, as well as activator of angiogenesis at low concentrations of BMP-9	David, L et al, Circulation Research (2008) Suzuki, Y et al, Journal of Cell Science (2010)
	Bone	It induces the osteoblastic differentiation of MSCs	Lamplot, J et al, American Journal of Stem Cells (2013)
	Prostate	It inhibits the growth of prostate cancer by inducing apoptosis	Ye, L et al, Molecular Cancer Research (2008)
TGF- β 1	Blood vessels	It induces angiogenesis and stimulates collagen production by the fibroblasts	Roberts, A et al, Proc. Nati. Acad. Sci. (1986)
	Bone	It has a dual role in Arthritis diseases: loss of its signaling in cartilage leads to chondrocyte hypertrophy and cartilage degeneration	Wu, M et al, Bone Research (2016)
	Cartilage	While its activation of its signaling in osteoblasts les to cartilage degeneration	
	Heart	It is involved in cardiovascular development and hypertrophy of cardiomyocytes, as well as hypertension pathologies	Azhar, M et al, Cytokine and Growth Factor Reviews (2003)
		It plays a role in fibrosis by stimulating epithelial-mesenchymal transition	Biernacka, A et al, Growth factors (2011)
	Epithelium	It has a dual role in cancer: tumor suppressor properties such as activation of apoptosis and cytostasis, but when its signal is altered it activates EMT transition and metastasis	Massagué, J, Cell (2008)
It plays a role in fibrosis by stimulating epithelial-mesenchymal transition		Valcourt, U et al, Mol Biol Cell (2005)	

I.B.2.3. Structural characteristics of BMPs and TGF- β s

Members of the TGF- β superfamily are identified by their biological activity as dimeric ligands, and their common structural entity, which is a cysteine knot (Galat, 2011). Indeed, BMPs are described to be active in their dimeric form. Their structure is described as butterfly-shaped dimer formed by two antiparallel β -sheets and four-turn α -helix perpendicular to the strands. This folding structure has been also described as a hand where the helix mimic the wrist, the cysteine-knot the palm and the β -sheets the fingers (**FIG.I.6.A**) (Scheufler, Sebald and Hülsmeier, 1999).

The monomeric structure of BMPs is characterized by the presence of seven cysteine out of which six residues form intracellular disulfide bonds. These residues are oriented in a cysteine-knot structure that is highly conserved between ligands, and whose role is to stabilize the

monomeric structure. While the seventh cysteine residue form an inter-subunit bond and allow the dimerization of the two monomers (**FIG.I.6.B**) (Scheufler, Sebald and Hülsmeier, 1999; Mueller and Nickel, 2012; Vallejo and Rinas, 2013).

On the other hand, the structure of TGF- β also resembles a butterfly-like structure. The monomers of the TGF- β family have nine conserved cysteine with eight residues forming intra-chain bonds to stabilize the core of the structure, and one to form inter-chain disulfide bond with the other monomer (Daopin *et al.*, 1992; Wisotzkey and Newfeld, 2020).

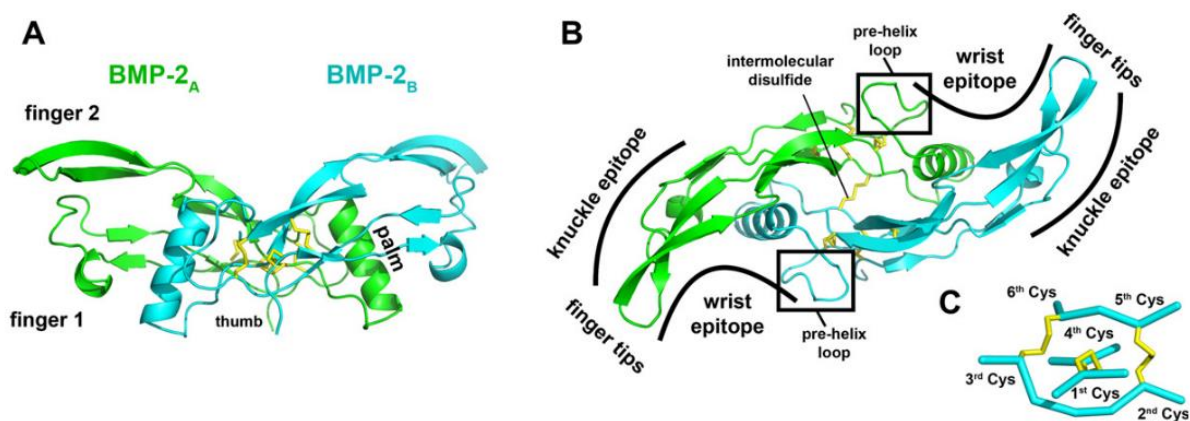


FIG.I.6. Dimeric structure of BMP-2. A) A ribbon presentation with two monomers (BMP-2_A and BMP-2_B). B) A structure of dimeric BMP-2 viewed along the two-fold symmetry axis. C) A close up on the cysteine-knot formed by six cysteine (A disulfide bond between Cys2-Cys5, Cys3-Cys6 and Cys1-Cys4). Adapted from (Mueller and Nickel, 2012).

I.B.2.4. Structures of several BMPs and TGF- β s

In the past decades, the structure of several members of the TGF- β superfamily have been described. These structures share a butterfly-like conformation and a cysteine knot, as well as antiparallel β -sheets and a α -helix almost perpendicular to the strands (Scheufler, Sebald and Hülsmeier, 1999; Brown *et al.*, 2005).

The TGF- β 2 structure was the first structure to be determined (Daopin *et al.*, 1992) in the TGF- β superfamily, followed by TGF- β 1 and TGF- β 3 (**FIG.I.7**). Both of TGF- β 2 and TGF- β 3 share an identical central core with minor differences that could affect the binding to its receptor (Mittl *et al.*, 1996). Then the structure of BMP-7 determined in 1997 by (Griffith *et al.*, 1996) who presented the similarities with the three structures of TGF- β family ligands, notably with

a common polypeptide fold with TGF- β 2, even though they only share limited sequence similarity.

Afterward, the structure of BMP-2 was determined in 1999 by (Scheufler, Sebald and Hülsmeier, 1999) using X-ray crystallography. Its structure showed the presence of glycosylation sites, as well as a pro-knot sequence containing a heparin-binding site that is specific to BMP-2. Furthermore, in comparison to TGF- β 2, the N terminus of BMP-2 and BMP-7 could not be characterized due to disordered structure (Scheufler, Sebald and Hülsmeier, 1999). As for the structure of BMP-4, it has yet not been determined (**FIG.I.7**).

In addition, the structure of BMP-6 was determined and showed a flexibility in the pre-helix loop that is involved in receptor interaction (Saremba *et al.*, 2007). On the other hand, the structure of BMP-9 presented noticeable differences at the level of several amino acids involved in BMP/ BMP receptor interaction, in comparison to BMP-7 and BMP-2, thus justifying the difference in its binding affinities to the BMPR (Brown *et al.*, 2005).

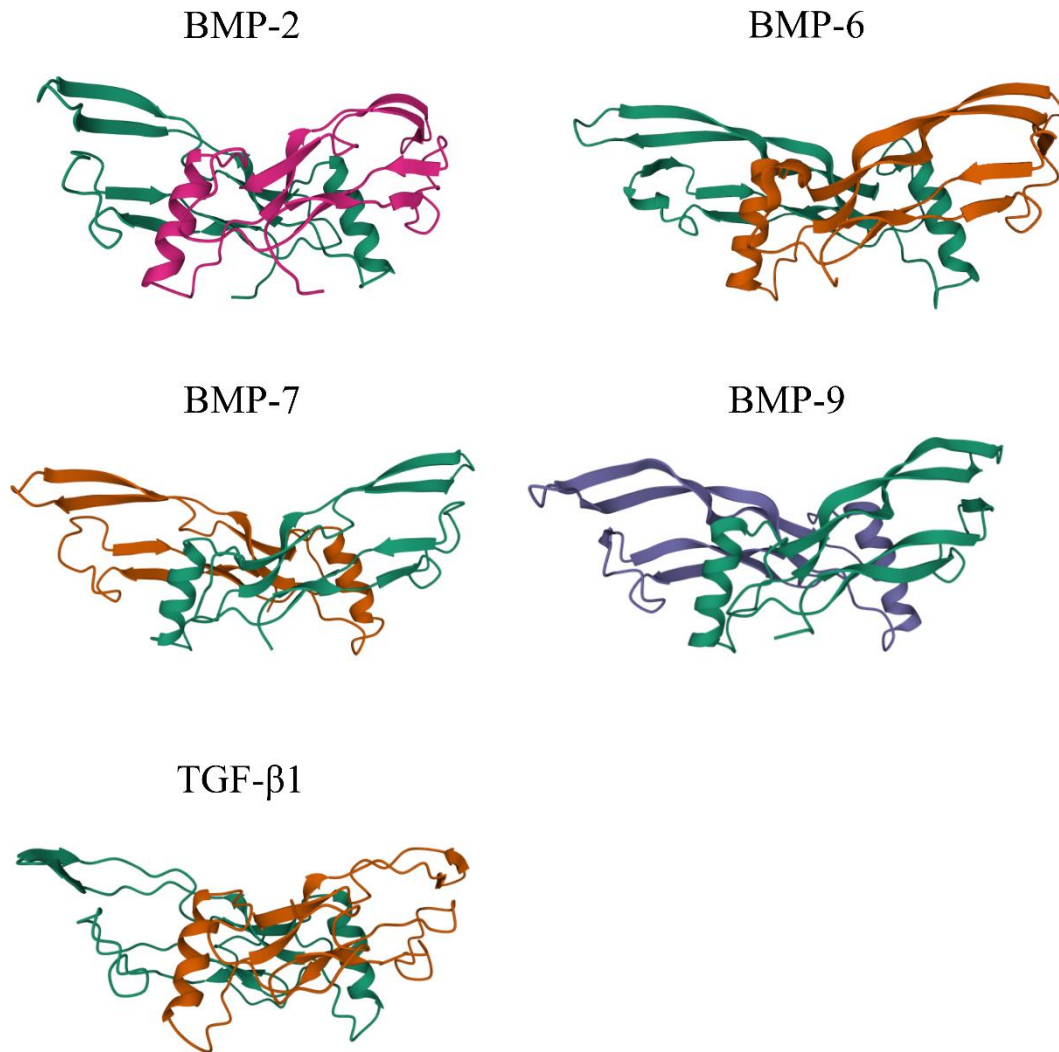


FIG.I.7. 3D structures of several BMPs and TGF-β. Structures of BMP-2 (PDB: 3BMP), BMP-6 (PDB: 2R52), BMP-7 (PDB: 1BMP), BMP-9 (PDB:1ZKZ), TGF-β1 (PDB: 1KLC). The structure of BMP-4 is yet still to be determined.

I.B.2.5. Secretion of BMPs

BMPs are synthesized as peptides formed of an N-terminal signal peptide, a prodomain involved in folding and dimerization, and a carboxy-terminal mature domain (**FIG.I.6**). During synthesis, the precursor of BMP is assembled, folded and cleaved by proprotein convertase. Indeed, in the case of BMP-4, furin cleaves the precursor in two sites: S1 at Arg-X-Arg/lys-Arg presumed to happen in the trans-Golgi network (TGN), which is transported to the post-TGN where the acidic environment renders the S2 site at Arg-X-X-Arg accessible for cleavage (Nelsen and Christian, 2009; Ali and Brazil, 2014). The absence of cleavage at the S2 site, the prodomain-mature complex is degraded by the lysosome (**FIG.I.8**).

We should note that, in the case of BMP-7 and BMP-9, the pro-region remains associated to the mature domain even after secretion and was shown to be biologically active (Brown *et al.*, 2005; Gregory *et al.*, 2005; Bidart *et al.*, 2012).

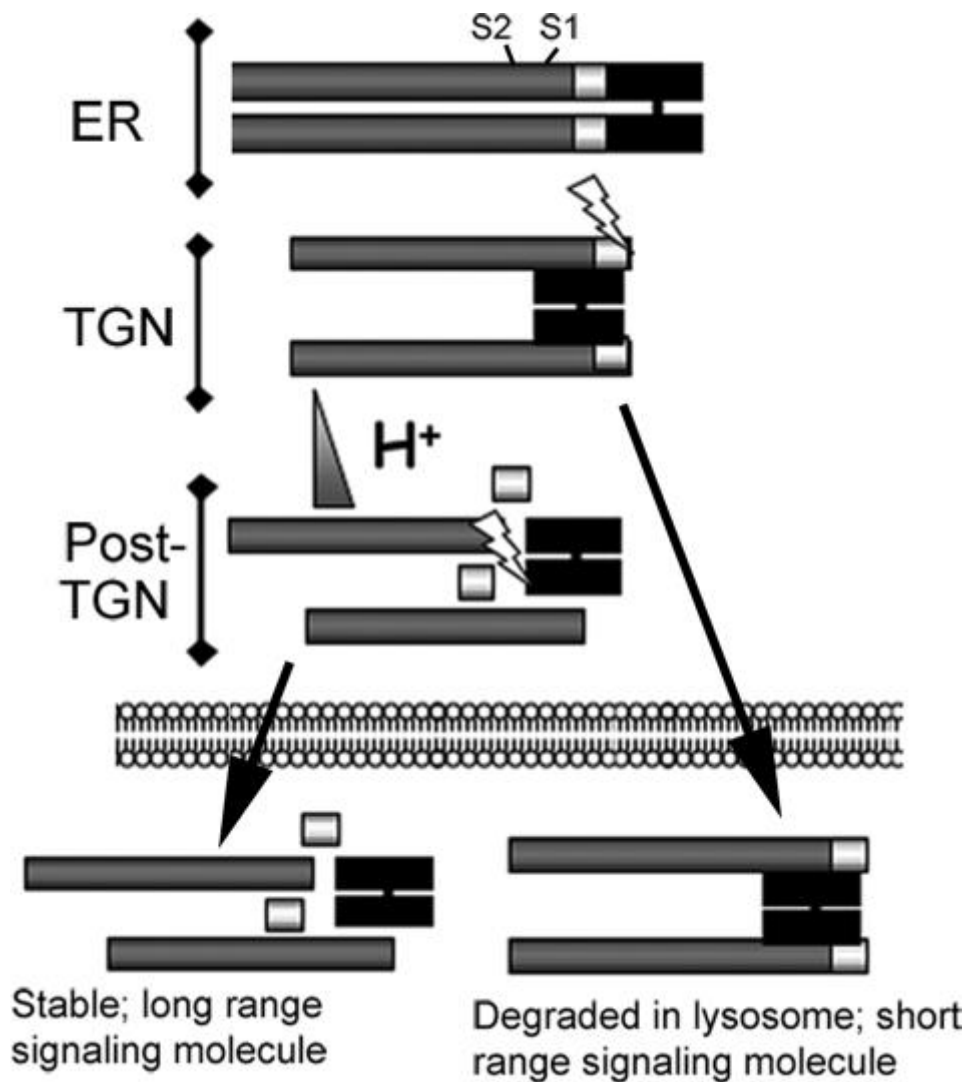


FIG.I.8. Processing of BMP-4. The precursor of BMP-4 is assembled, folded and cleaved in the TGN. The cleavage occurs first at the S1 site and then at the S2 after being trafficked to the post-TGN acid environment that renders the S2 available. After cleavage, the mature BMP is secreted either as stable dimeric protein, or as complex associated with its prodomain that is targeted by lysosomes. The prodomain is marked by light grey and the mature domain in dark grey (Nelsen and Christian, 2009).

I.B.2.6. Secretion of TGF- β

Three different genes encode TGF- β 1, TGF- β 2 and TGF- β 3. *In vivo*, they are synthesized as a TGF- β precursor that is capable of forming dimers. This precursor is subsequently cleaved by furin in the TGN, which leads to the formation of latency-associated peptides (LAP) associated

to the TGF- β peptide. The complex of TGF β -1 homodimer bound with non-covalent interaction to two latency-associated peptides (LAP) is called small latent complex (SLC). In the SLC, the dimeric TGF- β is wrapped by LAP and is inactive. Finally, the SLC is secreted along with latent TGF- β binding protein (LTBP), as an inactive complex. The complex between SLC and LTBP is called the large latent complex (LLC) (Javelaud and Mauviel, 2004; Robertson and Rifkin, 2016; Boguslawska *et al.*, 2019) (**FIG.I.9**). The release of the active TGF- β 1 is described in section I.C.2.

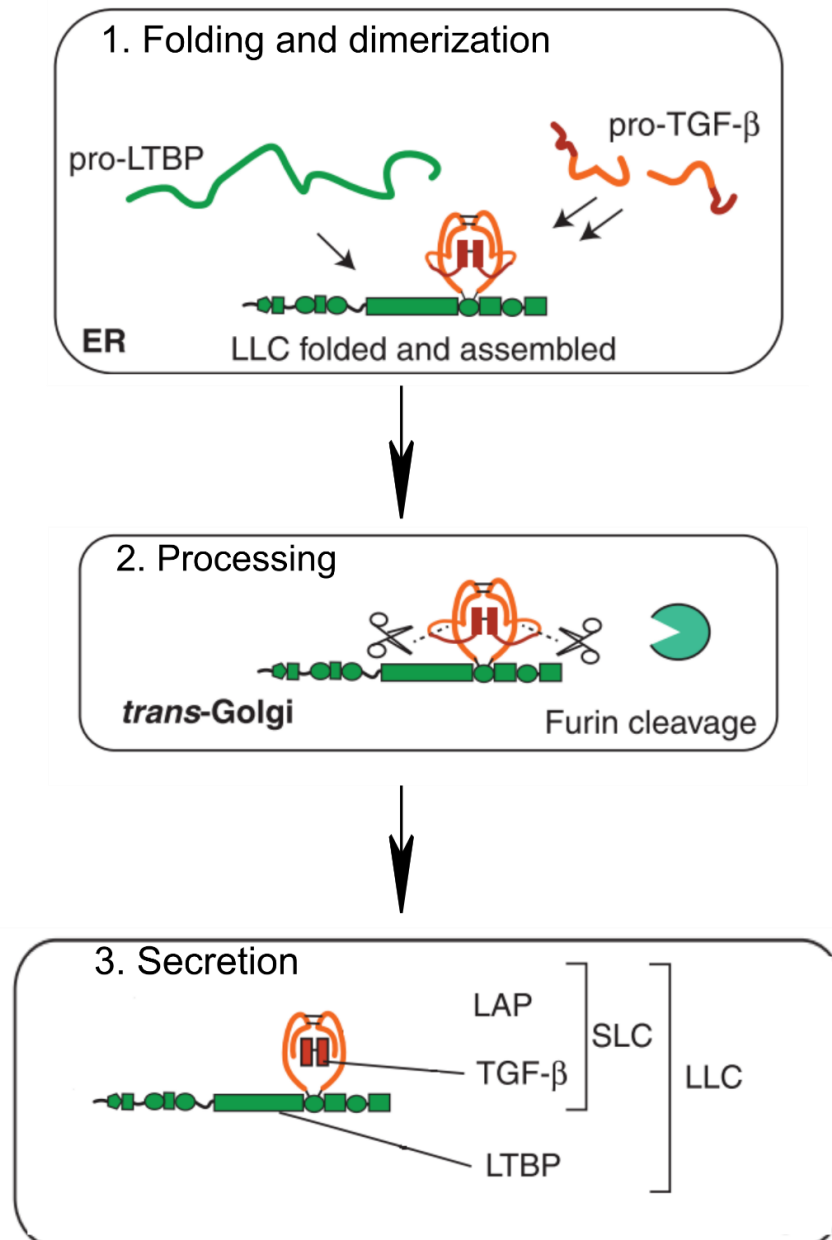


FIG.I.9. Processing of TGF- β . TGF- β is synthesized as a precursor pre-pro-TGF- β 1, which can be dimerized and then cleaved by furin. The cleaved components latency-associated peptides (LAP) along with TGF- β 1 form a small latent complex (SLC), which is secreted with

latent TGF- β binding protein (LTBP). The complex between LTBP and SLC form the large latent complex (LLC). Adapted from (Robertson and Rifkin, 2016).

I.B.3. Type I and type II receptors

I.B.3.1. Classification

BMPs have been reported to bind to two types of receptors, namely type-I and type-II BMPRs. The difference between these receptors can be summarized in their structure and function in signaling, which will be discussed in the following section. Four type-I BMPR known as activin receptor-like kinase 1 (ALK1), ALK2 (or Activin A receptor type I (ACVR1)), ALK3 (or BMPR type IA (BMPR-IA)), ALK6 (or BMPR type IB (BMPR-IB)), and three type-II BMPR termed BMPR-II, activin receptor 2A (ACTR-IIA) and ACTR-IIB were identified (Williams and Bullock, 2018). While TGF- β has three types of receptors (TGF- β R); type I TGF- β R (ALK5) and type II, in addition to type-III TGF- β R, which is a considered as a co-receptor and will be discussed in section I.C.2 (Heldin and Moustakas, 2016).

I.B.3.2. Functional roles of BMPR and TGF- β R

Several mutations of BMPRs have been reported to be associated to several diseases, including musculoskeletal and cardiovascular disorders and cancers (**TABLE.I.2**). For instance ALK1 mutations were found with patients of Hereditary hemorrhagic telangiectasia 2 (HHT2) which is characterized by arteriovenous malformation leading to abnormal development of direct connections between arteries and veins (Johnson *et al.*, 1996; Tillet and Bailly, 2014; Roman and Hinck, 2017).

Furthermore, ALK1 mutations have been shown to lead to a disorder indistinguishable from pulmonary arterial hypertension (PAH), which is characterized by a sustained pulmonary vascular resistance and arterial pressure leading to heart failure (Trembath *et al.*, 2001; Yuan, 2018).

Regarding ALK2, it was linked to Fibrodysplasia Ossificans Progressive (FOP) that is characterized by developmental skeletal defects and heterotopic ossification of muscle and ligaments (Shore *et al.*, 2006; Kaplan *et al.*, 2009). A mutation of ALK2 was also found in Diffuse Intrinsic Pontine Glioma (DIPG), which are rare brain tumors usually occurring in children (Pacifici and Shore, 2016; Kluiver *et al.*, 2020).

ALK3 is another important ALK member: in fact, ALK3 mutations were associated with juvenile Polyposis Syndrome (JPS) characterized by the development of gastrointestinal juvenile polyps and are a predictive risk of gastrointestinal cancer (Howe *et al.*, 2001; Brosens *et al.*, 2011).

Mutations of ALK5 have been linked to Loeys–Dietz syndrome, which is characterized by arterial and aortic aneurysms that could lead to aortic dissection or rupture at early age, as well as an altered craniofacial anatomy (Loeys *et al.*, 2006; MacCarrick *et al.*, 2014). In addition, mutations of TGF- β R were found to be present in colorectal cancer (Ku *et al.*, 2007; Xu and Pasche, 2007).

ALK6 mutations were linked to Brachydactyly type A1 characterized by short and absent tubular bones in the limbs due to bone hypoplasia and malformed interphalangeal joints (Racacho *et al.*, 2015).

Regarding the type II BMPR mutations, it is striking that there are much less known effects. Indeed, BMPR-II mutations were found in >70% of patients with PAH (Machado *et al.*, 2006; Gordon and Blobe, 2008). While ACTR-IIA mutations have been associated to colorectal tumors with microsatellite instability (Jung *et al.*, 2004), while ACTR-IIB has not been clearly reported to be associated to known diseases.

A summary of the pathological roles of BMP and TGF- β receptors is presented in **TABLE.I.2**.

TABLE.I.2. A table summarizing the pathological roles of ALK1, ALK2, ALK3, ALK5, ALK6, BMPR-II and ACTR-IIA. The name of the disease and its phenotype as well as the receptor role are presented.

Receptor	Tissue	Name of the disease	Receptor role	Consequence	References
ALK1	Blood vessels	Hereditary hemorrhagic telangiectasia 2 (HHT2)	Mutations in ALK1 were found in HHT2 patients	Arteriovenous malformation leading to an abnormal formation of vessels in skin and mucosa	Johnson, D. W et al, Nature Genetics (1996) Tillet, E. & Bailly, S, Frontiers in Genetics (2014) Roman, B & Hinck, A., Cell Mol Life Sci (2017)
		Cancer	Expressed in breast tumors	Promotes vasculature and growth of breast tumours. Its pharmaceutical inhibition could be a target to block metastasis	Cunha, S et al, Cancer Research (2015)
ALK2	Lung	Pulmonary arterial hypertension (PAH)	Carriers of ALK1 mutation develop disorder indistinguishable from PAH	A high pulmonary arterial hypertension that causes heart failure	Trembath, R. et al, New England Journal of Medicine (2001) Yuan, S, Pediatrics and Neonatology (2018)
	Brain	Diffuse intrinsic pontine gliomas (DIPGs)	Similar ALK2 mutations to those found in FOP were seen in tumors	A highly aggressive rare tumour that leads to impairment of movements coordination an speech	Pacifici, M. & Shore, E, Cytokine Growth Factor Rev (2016) Kluiver, T. et al, Frontiers in Oncology (2020)
	Muscles and ligaments	Fibrodysplasia Ossificans Progressive (FOP)	Gain of function mutations in ALK2 cause of FOP with R206H mutation (2q23-24) in the GS domain being the most common	Heterotopic ossification of muscle and ligaments	Shore, E. et al, Nature Genetics (2005) Kaplan, F. et al, Human mutation (2009)
ALK3	intestine	Juvenile Polyposis Syndrome (JPS)	Mutations in ALK3 are associated with JPS	Appearance of polyps in gastrointestinal tract and an increase risk of gastrointestinal cancer	Howe, J.R et al, Annals of Surgical Oncology (1998) Howe, J.R et al, Nature Genetics (2001) Brosens, L. et al, World J Gastroenterol (2011)
ALK5	Bones and blood vessels	Loeys–Dietz syndrome	Mutations in ALK5 have been linked to this syndrome	Vascular aneurysm in association with craniofacial and skeletal manifestations	Loeys, B. et al, The New England Journal of Medicine (2006) MacCarrick, G. et al, Genetics in medicine (2014)
	Colon	Colon cancer	Mutations of ALK5 were found in patients with colon cancer	A chronic inflammation due to a suppression of tumor suppressor genes and genes related to DNA repair mechanisms	Ku, J.K et al, cancer letters (2007) Hu, Y. & Pasche, B. Hum Mol Genet (2007)
ALK6	Bones	Brachydactyly type A1	Mutations of ALK6 were found in patients of brachydactyly	Short and malformations of the limbs	Racacho, L. et al, European Journal of Human Genetics (2015)
BMPR-II	Lung	Pulmonary arterial hypertension (PAH)	BMPR-II mutations are found in the majority of patients with PAH	A high pulmonary arterial hypertension that causes heart failure	Machado, R. et al, Hum mutation (2006) Gordon, K & Blöbe, G., Biochimica et Biophysica Acta (2008)
ACTR-IIA	Colon	Colon cancer	ACTR-IIA mutations are frequent in colon cancer with microsatellite instability	A chronic inflammation due to a suppression of tumor suppressor genes and genes related to DNA repair mechanisms	Jung, . Et al, Gastroenterology (2004)

I.B.3.3. Biochemical properties and structural details

TGF- β R and BMPR contain 500-570 amino acids and weight about 55 to 70 kDa. Their structure is formed by several domains: an N-glycosylated cysteine-rich extracellular domain (ECD) with a TGF- β /BMP ligand-binding domain, a single transmembrane region characteristic of type-I receptor containing a highly conserved region with a characteristic “SGSGSG” sequence called the GS domain, and an intracellular domain comprised of serine/threonine kinase domain (Massagué, 1998).

The structures of several type-I and type-II receptors were determined in unbound and bound states to BMPs, in addition to their structure in complex with inhibitors (Greenwald *et al.*, 1999; Mace, Cutfield and Cutfield, 2006; Han *et al.*, 2007; Groppe *et al.*, 2008; Klages *et al.*, 2008; Zuniga *et al.*, 2011; Mahlawat *et al.*, 2012; Agnew *et al.*, 2021)

I.C. BMP and TGF- β signaling

I.C.1. Interactions between BMP/BMPR and TGF- β /TGF- β R

In vivo, it is reported that BMP binds to a variety of type-I and II BMPR. The binding of BMPR to BMPs occurs at two binding epitopes; the wrist epitope which is a large continuous area formed by α -helix that binds type-I BMPR, and a knuckle epitope capable of binding type-II BMPRs (Keller *et al.*, 2004).

After this binding, the constitutively activated type-II BMPR even in the absence of a ligand, induces the activation of the inactive type-I BMPR by phosphorylating its transmembrane kinase domain at the level of the glycine-serine (GS) domain (Wrana *et al.*, 1994; Chen and Weinberg, 1995). Thus, forming a ternary complex of BMP/type-I and type-II BMPR that leads to activation of the signaling pathways (**FIG.I.10**) (Mueller and Nickel, 2012).

Concerning TGF- β R, a similar mechanism was proposed: TGF- β binds the constitutively activated TGF- β R-II, which then leads to the phosphorylation of the TGF- β R-I. The binding of type-I and type-II TGF- β R takes place at the underside part of the “fingers” and “fingertips” in TGF- β (Hinck, 2012). This activation of type-I TGF- β R subsequently activates a signaling pathway (Franzén, Heldin and Miyazono, 1995; Huang and Chen, 2012). We should note the presence of a type-III TGF- β R that has a role in regulating the TGF- β signal, as discussed in section I.C.2.

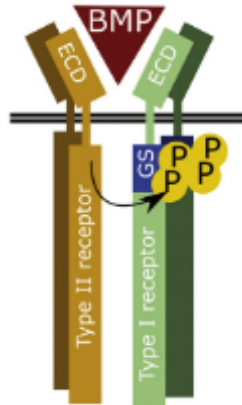


FIG.I.10. Schematic representation of a BMP/type-I and type-II BMPR. In the case of BMP, BMP binds first to type-I BMPR. The formation of this complex leads to the recruitment of type-II BMPR that activates type-I BMPR by phosphorylating its GS domain (Sanchez-Duffhues *et al.*, 2020).

After identifying the interactions of BMPs and TGF- β with their respective receptors, studies focused on studying the specificities of these interactions. With a high number of twelve BMPs, compared to number of receptors, i.e. four type-I BMPRs and three type-II BMPRs, a phenomenon of promiscuity, where a single BMP binds different receptors with distinct affinities, has been described (Mueller and Nickel, 2012).

Later structural studies focused on determining these interactions with protein-protein interaction technique, notably surface plasmon resonance (SPR). BMPs were described to bind to specific BMPRs in agreement to their previous classification into different groups (Ehata *et al.*, 2013). Indeed, both BMP-2 and BMP-4 were described to bind ALK3 and ALK6 at high affinity, while BMP-7 was mainly associated to ALK2, and BMP-9 was reported to bind ALK1 at a high affinity and ALK2 with a lower one (Luo *et al.*, 2010; Ray *et al.*, 2010; Mueller and Nickel, 2012; Williams and Bullock, 2018) (FIG.I.11). Nevertheless, studies did not report critical distinctions in the BMP binding to type-II BMPRs and consisted on describing a similar binding of several BMPs to type-II BMPRs. These observations were described in previous immunoprecipitation and structural studies with different BMP/BMPR couples, and various experimental conditions.

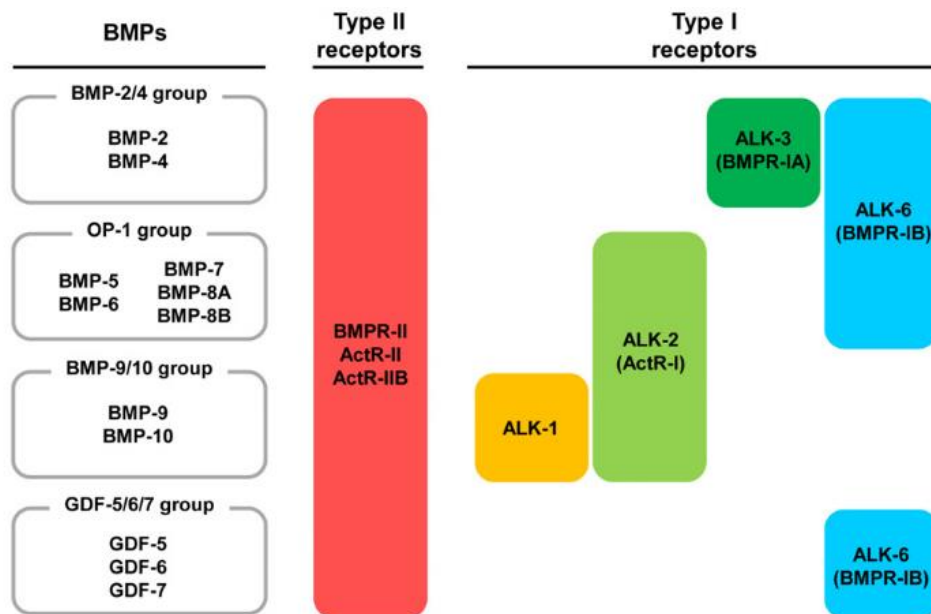


FIG.I.11. Binding couples of BMPs classified in different groups, and their binding s to type-I and type-II BMPRs. The BMP2/BMP4 group bind specifically ALK3 and ALK6, the OP-1 group (containing, BMP-5 BMP-6, BMP-7, BMP-8) bind ALK2, the BMP-/BMP-10 group bind ALK1 and ALK2 and he GDF-5/GDF-6/GDF-7 group bind ALK-6. All BMPs were reported to bind similarly type-II BMPRs without any distinction between these three different receptors. Modified from (Ehata *et al.*, 2013).

In contrast, all three isoforms of TGF- β bind with high affinity to type-III TGF- β R. Similarly, type-II TGF- β R binds TGF- β 1 and TGF- β 3 with high affinity but not TGF- β 2 when expressed alone without other TGF- β R. We should note that type-III TGF- β R was described to facilitate TGF- β binding to type-II TGF- β R. While type-I TGF- β R is reported to not efficiently bind to TGF- β when expressed without type-II TGF- β R (Derynck and Feng, 1997; Massagué, 1998).

Binding mechanisms

BMP and TGF- β can be distinguished based on their binding modes: the first mode of binding described for TGF- β , consists in their binding to type-II TGF- β R which then leads to the recruitment of type-I receptor. The second binding mode, characteristic to BMPs, consists on the binding of BMP to type-I and II BMPRs with different affinities. This binding mode was described as cooperative, where BMP has a higher affinity for BMPRs when expressed together (Massagué, 1998; Nickel *et al.*, 2009) (**FIG.I.12**). This observation led to the discovery of two distinct BMP receptor activation modes. First, the ligand-induced sequential assembly called BMP-induced signaling complex (BISC) where the BMP binds to a high-affinity type-I receptor which then leads to the recruitment of the constitutively active type-II BMPR. Second, the preformed complex (PFC) binding mode where BMPs can bind directly to preformed type-

I/type II BMPR complex (Gilboa *et al.*, 2000; Nohe *et al.*, 2002; Nickel *et al.*, 2009). Interestingly, it was shown that in the case of PFC binding, pSmad 1/5/8 is activated, while the BISC activates Smad-independent pathways such as p38 and MAPK pathways (Nohe *et al.*, 2002). Moreover, the formation of PFC was reported to be transient as it underwent several association/dissociation cycles in the absence of BMP-2, with an increase in heterocomplex fraction number in the presence of BMP-2 (Marom *et al.*, 2011). Nevertheless, further studies are needed to better understand the structural details of BMP's binding to the PFC. We should note that the PFC complexes were also described in the case of TGF- β and investigated for their role in TGF- β signaling (Ehrlich *et al.*, 2012).

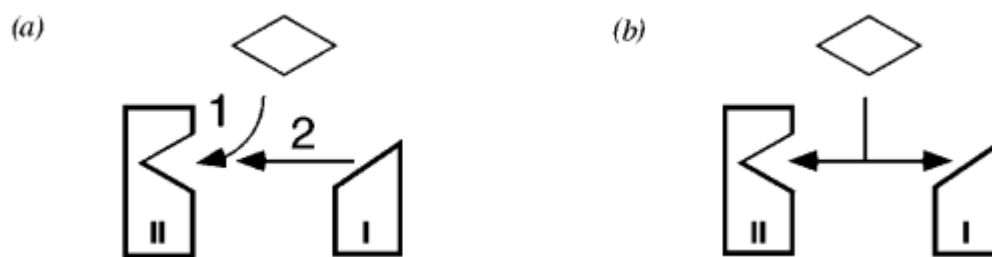


FIG.I.12. Two modes of ligand/receptor binding. a) The first binding mode is characteristic to TGF- β , which first bind type-II receptor and form a complex that leads to the recruitment of type-I receptor. b) The second mode of binding is characteristic to BMP, which is capable of binding type-I and type-II BMPR in the presence of both receptors (Massagué, 1998).

BMP heterodimer

Some studies investigated the process of receptor's homo-dimerization on the surface, and reported the formation of homodimer and heterodimer type-I/type-II BMPR such as ALK3/ALK3, ALK6/ALK6, BMPR-II/BMPR-II as well as ALK3/BMPR-II and ALK6/BMPR-II in the absence of ligand, using immunofluorescence co-patching studies (Gilboa *et al.*, 2000).

Furthermore, the presence of BMP heterodimers such as BMP-2/BMP-7 that can induce ectopic bone formation and play a role during embryonic development (Lyons, Hogan and Robertson, 1995; Kaito *et al.*, 2018). In addition, BMP-7 was found to form heterodimers with BMP-2 and BMP-4 and to have roles during mammalian development (Kim *et al.*, 2019). In an effort to understand the roles of these heterodimers in signaling, researchers generated BMP-2/BMP-6 heterodimer and investigated the alteration of the specific BMPR binding interfaces resulting

in a higher affinity to these receptors (Isaacs *et al.*, 2010). Moreover, a study found that BMP2/7 heterodimers require ALK2/ALK3 heterodimers to be able to signal (Tajer *et al.*, 2021).

Similarly, the presence of TGF- β heterodimers was also described (Cheifetz *et al.*, 1987), and ALK2/ALK5 heterodimers have been reported to be involved in signaling during epithelial-to-mesenchymal transition (Ramachandran *et al.*, 2018). Nevertheless, further studies are needed to better understand the relevance of these heterodimers *in vivo*.

I.C.2. Regulation of the early steps of BMP and TGF- β signaling

BMP and TGF- β are regulated at the cell surface at different levels of their signaling pathway. This regulation ensures control of the effect and timing of BMP signaling notably during developmental processes as seen with the role of BMP in dorsal-ventral patterning in *Drosophila*. These processes are governed by the presence of a gradient of growth factors due to the several regulators (Zakin and De Robertis, 2010).

In the majority of the cases, the BMP and TGF- β -binding proteins impede the ligands from binding to their receptors and reduce their mobility. These regulatory proteins can modulate the ligand signal at different steps. First, during the release and activation of the ligand, second during transportation through the tissues and third, at the level of the membrane during the initiation steps of the biochemical signaling (Umulis, O'Connor and Blair, 2009). We should note that other intracellular regulation mechanisms exists at the level of the signaling pathway, however they will not be addressed in this section.

At the secretion and activation level, the BMP pro-domain is cleaved into signaling and pro-domain fragments. This cleavage is inhibited by cysteine-rich transmembrane BMP regulator 1 (CRIM1), which is a transmembrane protein capable of binding preprotein BMP which leads to a reduction in their processing to maturation, tethering of the proteins to the cell surface and reduction in BMP secretion (Wilkinson *et al.*, 2003).

Similarly, the secreted latent TGF- β is regulated at the cell surface by several proteins depending on the organism, tissue and cell type. Indeed, the TGF- β is secreted from the cell with its prodomain LAP covalently attached. This LAP is also disulfide-linked to LTBP. Thus, the liberation of the active TGF- β from the latent complex occurs either through degradation of the LAP or the LTPB, or through modification of the conformation of the SLC (Massagué, 1998). The association of LTPB to the ECM facilitates TGF- β activation, as the forces exerted by integrins, notably α vb1 and α vb5, can deform the LAP and release TGF- β (Robertson *et al.*,

2015). Apart from integrins, several proteins are responsible of proteolytically cleaving TGF- β from the latent complex: First, the matrix metalloproteinases such as MMP-2, MMP-9 and plasmin which can degrade the ECM and cleave the LTBP or LAP. Similarly, the ECM protein thrombospondin-1 (TSP-1) can interact with LAP. Similarly, thrombospondin-1 (Tsp-1) can release the active TGF- β by binding LAP and changing its conformation (Murphy-Ullrich and Poczatek, 2000). Furthermore, BMP-1 was recently described implicated in TGF- β activation, as it cleaved TSP-1 (Anastasi *et al.*, 2020).

Finally, the change in the pH and reactive oxygen species (ROS) have been shown to change the conformation of TGF- β . The ROS can induce scissions and side group modifications, rendering the LAP inactive. While the change in pH during bone resorption by osteoclasts denaturates LAP, thus liberating TGF- β (Annes, Munger and Rifkin, 2003).

BMPs and TGF- β 's access to the receptors is regulated at the surface of the cells by several modulator proteins that can be classified into two different groups: Diffusible proteins and membrane-associated proteins (**FIG.I.13 and TABLE.I.3**).

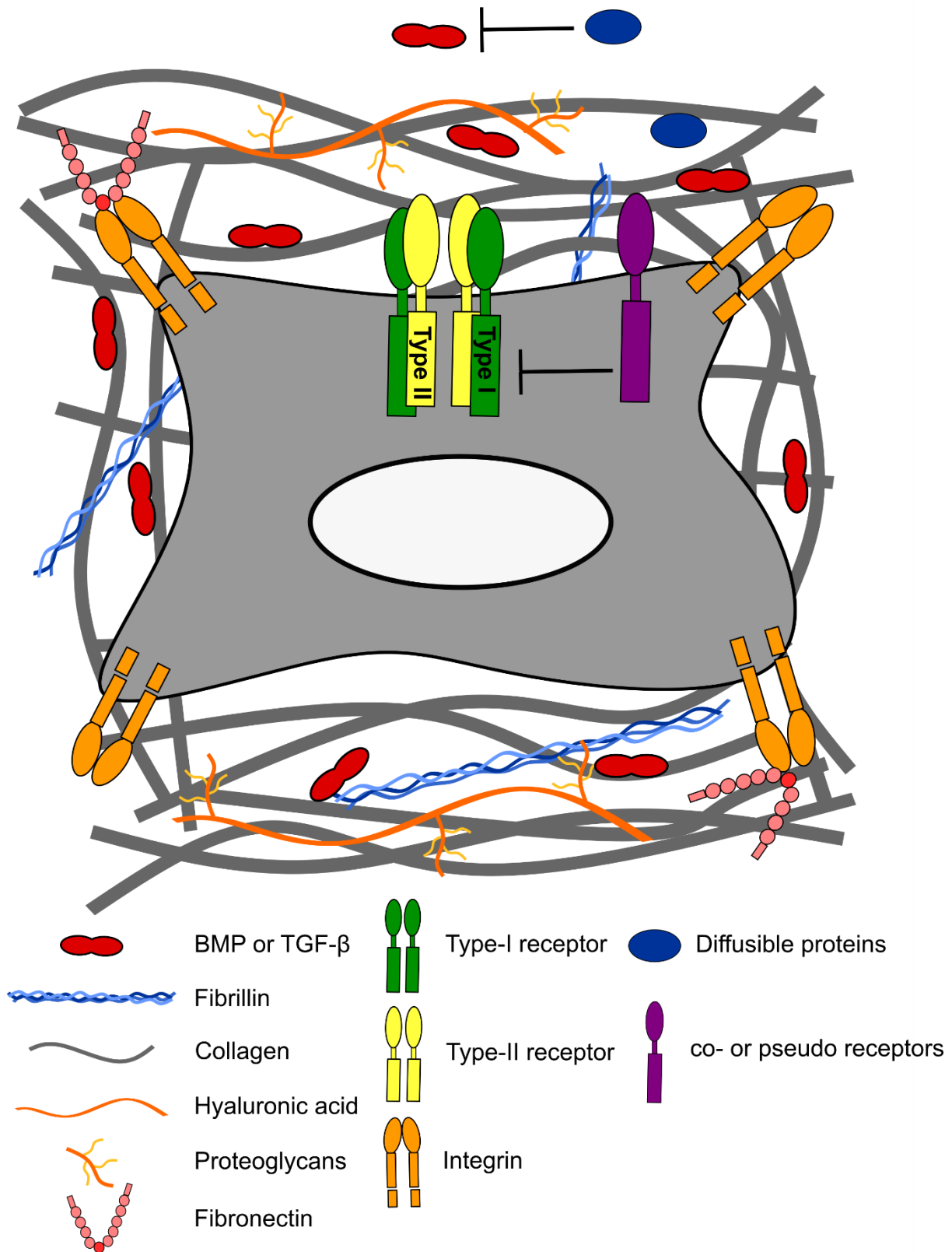


FIG.I.13. Extracellular regulation of BMPs and TGF-β. BMP and TGF-β are regulated by several proteins, notably: A) Diffusible proteins such as Noggin, Chordin, Twisted gastrulation, Follistatin, members of the Dan family, members of the CCN family. These proteins can also bind to the ECM components. B) ECM components such as proteoglycans and hyaluronic acid, as well as fibrillary proteins such as Fibrillin, Collagen and Fibronectin. C) Membrane

associated receptors such as type-III TGF- β R, Endoglin co-receptors as well as BAMBI and DRAGON, pseudo-receptors. We should note that both Endoglin and type-III TGF- β R can also be present as a soluble form. Adapted from (Migliorini *et al.*, 2020).

The BMP antagonists can be classified in different families based on their sequence homology and structural characterizations. We can distinguish six families: Noggin, Chordin, twisted gastrulation (tsg), Follistatin, Dan and cellular communication network (CCN) families (Hinck, Mueller and Springer, 2016).

First, Noggin a protein secreted as homodimer was first discovered in *Xenopus* embryos to have a role in normal dorsal development (Smith and Harland, 1992). It was then reported to bind BMP-4 with high affinity, and block its interaction with BMPR, thus inhibiting its signaling. In this case, the activity of BMP as mesoderm ventralizer is blocked, and the establishment of dorsal mesoderm is promoted (Zimmerman, De Jesús-Escobar and Harland, 1996). Moreover, it was shown that despite Noggin being secreted and diffusible, it binds strongly to heparan sulfate proteoglycans at the cell surface. The bound Noggin can still bind BMP-4 and reduce its signaling thus creating gradients of BMP activity (Paine-Saunders *et al.*, 2002). Noggin has a role in inhibiting BMPs signaling since it was reported to have an N-terminus segment capable of binding BMPs at the binding sites of type-I and II BMPR, thus impeding their binding to BMPR (Groppe *et al.*, 2002). We should note that BMP-9 and BMP-10 are reported to be resistant to Noggin (Lichtner *et al.*, 2013; Wang *et al.*, 2013).

This observation was also observed with another modulator protein Chordin that is secreted at the dorsal side of the embryo. This protein binds BMPs and inhibits their binding to BMPR thus antagonizing the ventral BMP signaling dorsalizing mesoderm and neutralizing ectoderm in embryos (Piccolo *et al.*, 1996; Millet *et al.*, 2001). This inhibition is reversible since Tolloid metalloproteinases cleave chordin at two sites thus liberating BMP (Zakin and De Robertis, 2010).

Furthermore, tsg can bind to both Chordin and BMP, and form a heterocomplex. This protein exerts pro- and anti- BMP signaling, depending on the context, as it enhances chordin activity by blocking the access of BMP to its receptor, yet on the other hand, the complex tsg/chordin/BMP serves as a ligand for Xolloid that cleaves chordin thus activating the BMP signaling (Wills, Harland and Khokha, 2006; Zakin and De Robertis, 2010)

Similarly, Follistatin, is a soluble glycoprotein that has a role in inhibiting pituitary FSH production. This protein has been described to bind mainly Activin, and also BMP although

with a lower affinity, by wrapping around the growth factors, thus inhibiting the binding to their receptor (S. J. Lin *et al.*, 2006).

The Dan family composed of seven known members in mammals also plays a part in modulating the BMP signaling. This family consists of neuroblastoma suppressor of tumorigenicity 1 (Nbl1, also known as Dan and DAND1), Gremlin (Drm also known as DAND2), protein-related to Dan and Cerberus (PDRC), Coco (DAN5), which can sequester BMP. In addition to Sclerostin (SOCT) which antagonizes the wnt pathway by blocking the co-receptor LRP5/6 and inhibits the BMP signaling indirectly (Van Bezooijen *et al.*, 2007; Krause *et al.*, 2010), as well as cerberus (Cer1) and uterine sensitization-associated gene 1 (USAG-1/wise) which are inhibitors of Wnt, BMP and Nodal pathways (Nolan and Thompson, 2014; Li *et al.*, 2021).

Finally, the CCN family composed of cysteine-rich regulatory proteins: CCN1, CCN2, CCN3, CCN4, CCN5 and CCN6. These proteins can bind both BMP and TGF- β ligands as CCN2 enhances TGF- β signaling by acting as a chaperone, while CCN3 inhibits BMP-2 induced osteoblast differentiation (Jia *et al.*, 2021).

On the other hand, the membrane-bound proteins are present in the ECM or at the cell membrane.

The extracellular matrix (ECM) contains molecules that are essential for BMP and TGF- β function, by providing them with binding site and regulating their dose and availability. It is composed of proteoglycans and fibrillary proteins. The proteoglycans are formed by chains of glycosaminoglycans (GAGs) (also known as mucopolysaccharides), covalently linked to a core protein. GAGs have four families: heparin/heparin sulfate (HS), hyaluronic acid (HA), chondroitin/dermatan sulfate (CS/DS) and keratin sulfate.

Previous studies reported the binding of BMPs to several GAGs such as heparin and HS, HA and CS (Billings *et al.*, 2018). The role of these polysaccharides is debated in the literature, as they are described to have a dual role in the BMP signaling. They have been reported to bind BMPs and alter their conformation therefore reducing their affinity to BMPR (Hintze *et al.*, 2014). While, other studies reported a role of GAGs in acting as a co-receptor aiding the formation of the BMPR signaling complex (Kuo, Digman and Lander, 2010). Furthermore, HA was demonstrated to have a role in osteoblastic differentiation by own-regulating BMP-2 antagonists and ERK phosphorylation (Kawano *et al.*, 2011). On the other hand, sulfated HA

derivatives were shown to block the binding of TGF- β 1 to its type-I and II receptor (Koehler *et al.*, 2017).

In addition to proteoglycans, fibrillar proteins such as collagen, fibrillin, fibronectin (FN), elastin and laminin are involved in organ and tissue structure (Frantz, Stewart and Weaver, 2010; Kusindarta and Wihadmadyatami, 2018). They mediate cell adhesion and modulate BMP activity notably by binding to BMPs. Indeed, type-IIA pro-collagen present in cartilage was reported to contain a chordin-like domain that negatively regulate BMP-2 and BMP-4 functions (Migliorini *et al.*, 2020). In addition, collagen IV binds the BMP signaling molecule Dpp in *Drosophila* and exhibit dual role: increasing Dpp signaling in the embryo, and restricting of the signaling in the ovary by sequestering the ligand (Ashe, 2008). Furthermore, fibrillin, self-assembling glycoproteins forming microfibrils structures, control the availability of BMP-2,-4,-7,-10 and TGF- β by binding to their pro-domains. This protein is reported to be a negative reservoir for these ligands (Sengle and Sakai, 2015). In addition, FN is a protein present under two forms: Plasma FN synthesized by the hepatocytes, and cellular FN expressed by various tissues. It is reported that FN binds BMP at a close domain known to interact with integrins, (Martino and Hubbell, 2010; Fourel *et al.*, 2016) , thus providing proximity between integrins and BMPR. Moreover, FN was shown to be critical for the incorporation of latent TGF- β binding proteins to the ECM (Dallas *et al.*, 2005).

Other membrane-bound proteins were also mentioned in the literature. Type-III TGF- β R, also known as betaglycan, is a membrane-anchored proteoglycans capable of binding TGF- β 1, TGF- β 2 and TGF- β 3, as well as BMP-2 and BMP-4. This receptor is present in soluble and membrane-bound forms. It was reported that while the soluble betaglycan is an inhibitor of TGF- β binding to its receptors, the membrane-anchored betaglycan activates TGF- β signaling by presenting it to the type-II/type-I TGF- β R complex (Derynck and Feng, 1997; Nickel, Ten Dijke and Mueller, 2018).

Similarly, the endoglin co-receptor, expressed in vascular endothelial cells, cardiac fibroblasts, hepatic stellate cells as well as mesangial cells, shares a high homology with betaglycan. This protein has an essential role in vascular development, and structural mutations have been associated with hereditary hemorrhagic telangiectasia type I (Tillet and Bailly, 2014). It has been reported that endoglin binds BMP-9/BMP-10 with high affinity and promotes its signaling (David *et al.*, 2007; Lawera *et al.*, 2019). In addition, Endoglin can bind TGF- β 1 and TGF- β 3 and increases its signaling (Meurer *et al.*, 2014).

On the other hand, pseudo-receptors such as BMP and activin membrane-bound inhibitor (BAMBI) have been described to regulate the BMP signaling at the level of the receptors. This transmembrane protein share structural homology with type-I receptors, yet it lacks the intracellular kinase domain (Tramullas *et al.*, 2010). This protein does not bind directly BMP-2 or TGF- β 1, rather it interacts with all of BMPR and TGF- β R, apart from ALK2; Its recruitment to the type-I/type-II TGF- β R complex led to a lower phosphorylation of the type-I receptor with TGF- β 1. It is thus suggested that their role is to inhibit the assembly of the type-I/type-II receptor heterocomplex (Onichtchouk *et al.*, 1999). We should note that BAMBI plays other regulatory roles by having intracellular interactions with several signaling partners such as the co-receptor LRP6 in the Wnt pathway and Smad (Nickel, Ten Dijke and Mueller, 2018).

Similarly, DRAGON (also known as repulsive guidance molecules b (RGMB)), a member of the RGM family, was also mentioned in the literature to be a specific co-receptor for Smad signal with BMPs. This protein lacks a transmembrane domain, yet it can localize on the cell membrane by attaching to a glycosylphosphatidylinositol (GPI) anchor through its C-terminal sequence (Nickel, Ten Dijke and Mueller, 2018). This protein is expressed in several organs such as heart, lung, pancreas, liver and limb cartilage, and most importantly in the central nervous system and have a role in axonal guidance and neural tube closure. They have been reported to compete with type-I BMPR in binding with high affinity BMPs, thus forming type-I BMPR/RGM/BMP complexes. However, this interaction seems to be pH independent as acidification of the membrane could release the type-II BMPR from the RGM complex and thus activates BMP signaling pathways (Mueller, 2015).

Due to the implications of BMP in several pathological processes, some of these natural antagonists are considered as pharmaceutical targets to treat BMP-related diseases (Section I.D.4).

TABLE.I.3. A non-exhaustive list of BMP and TGF- β modulator proteins. A list of modulator proteins binding BMP and TGF- β and their effect on signaling. Adapted from (Umulis, O'Connor and Blair, 2009; Chang, 2016; Ouahoud, Hardwick and Hawinkels, 2020).

Modulator protein	Ligands	Effect on signaling
<u>Diffusible proteins</u>		
Noggin	BMP-2,-4,-7	Inhibits
Chordin	BMP-2,-4,-7	Inhibits
Twisted gastrulation	BMP-2,-4	Inhibits/promotes
Follistatin	BMP-2,-4,-7,-15	Inhibits
Dan	BMP-2,-4	Inhibits
Gremlin	BMP-2,-4, -7	Inhibits
PRDC	BMP-2,-4,-7	Inhibits
Coco	BMP-4	Inhibits
Sclerostin	BMP-2,-4,-5-6,-7	Inhibits
Cerberus	BMP-4,-7	Inhibits
USAG-1	BMP-2,-4,-6,-7	Inhibits
CCN2	BMP-2,-4, TGF- β 1	Inhibits/promotes
CCN3	BMP-2	Inhibits
<u>Membrane-associated proteins</u>		
Proteoglycans	BMPs and TGF- β	Inhibits
Fibrillar proteins	BMPs and TGF- β	Inhibits
TGF β R-III (Betaglycan)	BMP-2,-4,-7, TGF- β -1,-2,-3	Inhibits/Promotes
Endoglin	BMP-9,-10, TGF- β -1,-3	Promotes
BAMBI	BMPR and TGF- β R	Inhibits
DRAGON	Type-I BMPR	Inhibits

I.D. BMP and TGF- β signaling pathways

I.D.1. Smad-dependent signaling pathway

Smad subfamilies

The Smad family was first discovered after the identification of the *Mad* (*mothers against dpp*) gene in *Drosophila*, after its null mutation led to developmental defects in the gut and pupal lethality (Aashaq *et al.*, 2021). In addition, *sma-2*, *sma-3* and *sma-4* genes were identified in *Caenorhabditis elegans* after their mutations lead to similar phenotypes as TGF- β like receptor, *daf4* (Savage *et al.*, 1996).

Studies followed to identify their homologues in murine and humans, and found *sma* and *mad* genes, named thereafter Smads (Aashaq *et al.*, 2021). Subsequently, Smad was described to be part of the TGF- β pathway since its phosphorylated form accumulated in the nucleus after BMP stimulation (Hoodless *et al.*, 1996). The Smad family was discovered and described to be composed of eight members assembled into three groups: First, the receptor-regulated Smads (R-Smads) group composed of Smad 1, Smad 2, Smad 3, Smad 5 and Smad 8 (also called Smad 9) involved in different signaling pathways. Second, the co-mediator (Co-Smads) composed mainly of Smad 4 whose role is to form a complex with the R-Smads and regulate their signaling. Third, the inhibitory Smads group (or anti-Smad) composed of Smad 6 and Smad 7 capable of degrading the receptors or competing with R-Smads for receptor binding (**FIG.I.14**) (Attisano and Lee-Hoeflich, 2001; Aashaq *et al.*, 2021).

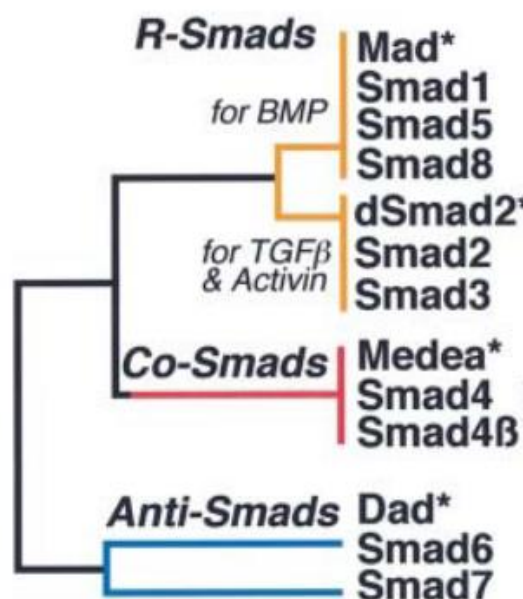


FIG.I.14. The Smad family. A phylogenetic tree of the three Smad subfamilies. The sequence of R-Smad and Co-Smad contain similar N-terminal (MH1) (yellow), a linker region (white)

and C-terminal domains (MH2) (orange), in addition to the receptor phosphorylation sites at the C-terminus of R-Smads. The Anti-Smads contain only the MH2 domain. The triangle is added to identify the alternatively spliced insert in Smad 2. Asterisks (*) are added to indicate the members from *Drosophila*. Modified from (Massague and David, 2000).

Smad structure and activation

The Smad proteins have been described to share common structural domains; First, the mad-homology 1 (MH1) is a conserved domain in R-Smads and Co-Smads and present at the N-terminal. Second, the mad-homology 2 (MH2) domain which is conserved in all Smads and present at the C-terminal. Both of these domains are separated by a linker region, variable in size and sequence, containing MAP-kinase phosphorylation sites which if phosphorylated inhibits translocation of the Smad to the nucleus (**FIG.I.15**) (Massagué, 1998).

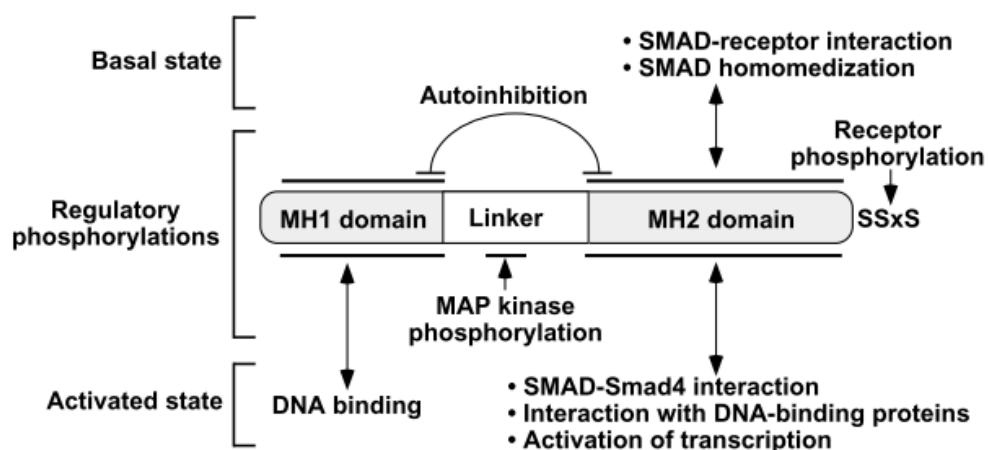


FIG.I.15. Structure of Smad. The Smad structure is formed by two domains: MH1 and MH2. While the MH2 is present in all Smad, the MH1 is only present in R-Smad and Co-Smad. These two domains separated by a linker region, play several roles in the Smad signaling. At the basal state, the MH2 plays a role in Smad-receptor interaction and homodimerization of Smad. At this state, the MH1 and MH2 domains can interact and induce autoinhibition of their respective function. After interaction with the receptors, the R-Smad are phosphorylated at their C-terminal tail on the SSxS motif. After its phosphorylation, the R-Smad can interact with the Co-Smad 4 in order to be translocated to the nucleus. In the nucleus, the MH1 domain can bind the DNA and the MH2 domain interacts with the DNA binding proteins, which leads to the activation of transcription of target genes (Massagué, 1998).

At the basal state, the MH1 and MH2 domains can physically interact and inhibit each other's function. In this state, prior to phosphorylation by the receptors, Smads are monomeric in addition to be able to form oligomers. Indeed, while Smad 2 is mainly present as a monomer,

Smad 4 is capable of forming homotrimers in solution similarly to Smad 3 which formed multiple oligomeric complexes (Jayaraman and Massague, 2000). Likewise, Smad 1 is present mainly as monomer in the unphosphorylated state yet can form transient trimers (Qin *et al.*, 2001).

After ligand (BMP or TGF- β) binding and formation of a type-I/type-II receptor ternary complex, the type-I receptor is phosphorylated in its GS region. The activation of type-I receptor leads to the recruitment and binding of R-Smad to the GS region of the receptor through its MH2 domain with the help of anchor proteins notably Smad anchor for receptor activation (SARA) with Smad 2 and 3, and Endofin with Smad 1/5/8 (FIG.I.16) (Wu *et al.*, 2001; Macias, Martin-Malpartida and Massagué, 2016). The Smad 1, 5 and 9 are usually recruited with receptors associated with the BMP pathway, while Smad 2 and 3 are associated with receptors from the TGF- β pathway (Zou *et al.*, 2021).

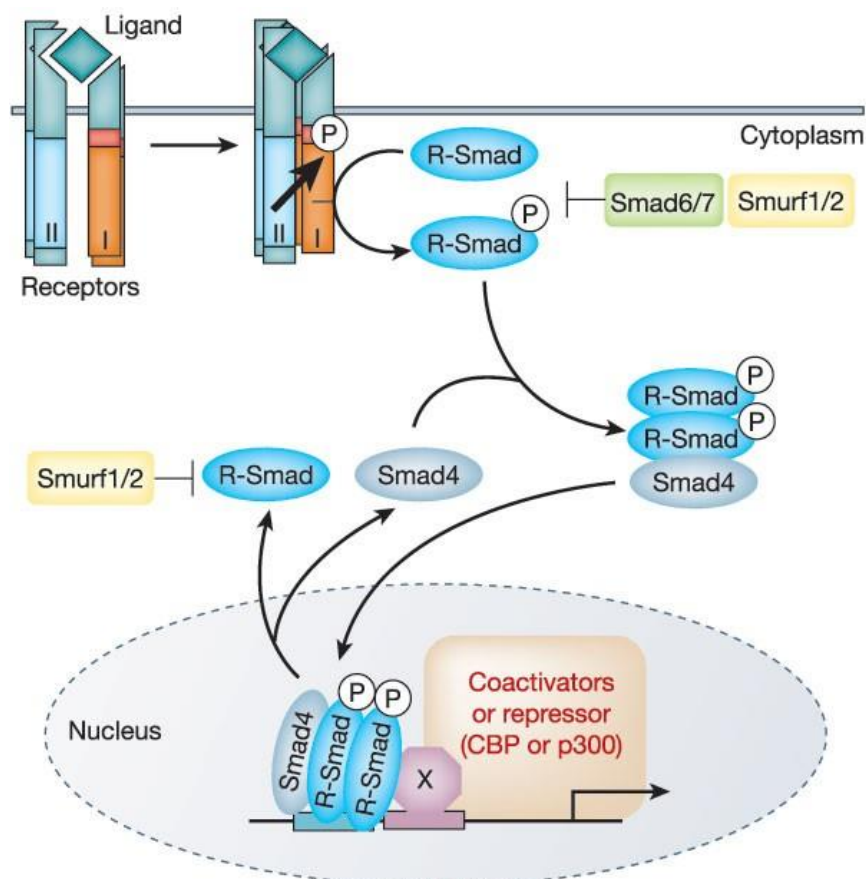


FIG.I.16. A Schematic representation of a Smad dependent pathway. After the formation of a ternary complex with BMP or TGF- β /type I and type II BMPR or TGF- β R, the R-Smad are activated. In the BMP pathway, it is Smad 1/5/9 with are activated while in the TGF- β pathway, it is the Smad 2/3. The R-Smad are translocated to the nucleus with Smad 4 where it can activate its target genes. After a certain time, the R-Smad are exported from the nucleus to

the cytoplasm where they can either be degraded with the help of Smurf 2 or recycled for further use (Derynck and Zhang, 2003).

The highly positive charged basic region next to loop L3 on the surface of MH2 domain of Smad facilitates its binding to the type-I activated receptor. The binding occurs at the level of the phosphorylated GS region which provides binding affinity, while the interaction of the L3 loop of Smad with L45 loop of the receptor provides specificity (Wu *et al.*, 2000; Qin *et al.*, 2001). The binding of Smad to the type-I receptor induces its phosphorylation at the flexible and disoriented C-terminal domain on the serine residues of the SSXS motif as seen for Smad 2 on Ser⁴⁶⁵/Ser⁴⁶⁷ and Ser⁴²³/Ser⁴²⁵ residues (Macias *et al.*, 1996) and Smad 1 on Ser⁴⁶³ and Ser⁴⁶⁵ residues (Kretzschmar *et al.*, 1997; Bruce and Sapkota, 2012).

After phosphorylation, the Smad undergoes a conformational change at the level of its L3 loop and three-helix bundle, which contributes to its dissociation from the receptor kinase domain, and binding to a phosphorylated-C-terminal tail of another active Smad molecule leading to the formation of homotrimers (Qin *et al.*, 2001; Wu *et al.*, 2001). This phosphorylation of Smad also increases the affinity of R-Smad to Smad 4, which form a heterocomplex involving the MH2 domain, that mediates the nuclear translocation in mammalian cells (Abdollah *et al.*, 1997; Souchelnyskyi *et al.*, 1997; Ullah *et al.*, 2018). This complex is usually formed by as a trimer as seen with Smad 3/4 heterotrimers composed of two Smad 3 and one Smad 4 (Chacko *et al.*, 2001; Martin-malpartida *et al.*, 2017).

The Smad heterocomplex is subsequently translocated to the nucleus where it activates several genes.

Inhibitory Smad

This pathway is regulated by inhibitory Smads (I-Smad) such as Smad 6 and Smad 7, which are structurally different than other Smad as they lack a MH1 domain. These I-Smads inhibit the BMP pathway and TGF- β pathways by interacting with the phosphorylated R-Smad through several ways. They can bind to the type-I BMPR, thus preventing the recruitment and phosphorylation of R-Smad, as well as prevent the formation of R-Smad/Smad4 complex. Furthermore, they can bind Smad-ubiquitination-regulatory factor (smurf) such as Smurf1 and Smurf2 and recruit them to the type-I receptor resulting its ubiquitination and degradation. Finally, these I-Smad can recruit the catalytic subunit of protein phosphatase 1 to the receptors to dephosphorylate type-I receptors (**FIG.I.15**) (Derynck and Zhang, 2003; Hill, 2009; Miyazawa and Miyazono, 2017).

Nucleus translocation

Two mechanisms of nucleus translocation have been described for Smad: the karyopherin-dependent pathway and karyopherin-independent pathway.

Proteins are usually transported from the cytoplasm into the nucleus through the nuclear pore complex (NPC). Although small proteins (<20 kDa) can diffuse through the complex, larger proteins require assistance from transport receptors such as karyopherins that can both import and export proteins. The Smad containing a nuclear basic localization signal (NLS) like-sequence present in the MH1 domain binds to an importin α , which in its turn recruit an importin β and form a trimeric import complex that can be transported to the nucleus. In the nucleus, RanGTP binds to the import complex and releases the Smad into the nucleus. On the other hand, during export, the exportins bind Smad, which also contains a nuclear export signal (NES), and RanGTP and transport the complex to the cytoplasm. In the cytoplasm, RanGTP releases the export complex when its GTP is hydrolysed (**FIG.I.17**) (Hill, 2009; Wentz and Rout, 2010).

Furthermore, a karyopherin-independent pathway was also described where direct contacts were observed between domains of Smad and NPC.

In that regards, Smad 1, 3 and 4 were described to translocate to the nucleus by a karyopherin-dependent transport. However, a karyopherin-independent transport was described with Smad 3, and Smad 2 that possesses a non-functional NLS-like motif limiting its binding to importin β 1. It is suggested that the import occurs through the interaction of its MH2 domain (Xu *et al.*, 2002).

The accumulation of Smad 2 and Smad3 proteins in the nucleus was observed after 45 min of ligand stimulation, and was seen to re-localize to the cytoplasm after 4 to 5h, in its unphosphorylated state, indicating the occurrence of a dephosphorylation during nuclear export (Hill, 2009; Wentz and Rout, 2010).

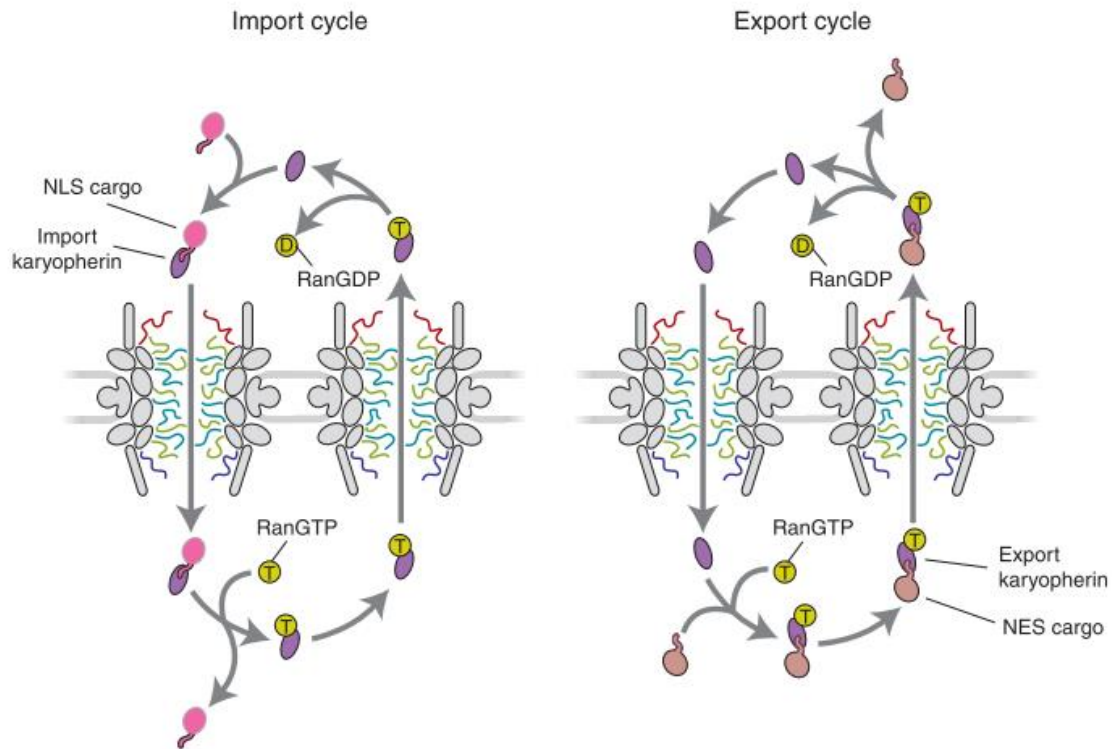


FIG.I.17. karyopherin Import and export of cargo (i.e. Smad). During import, the import karyopherin (**purple**) binds to the molecule or cargo with the NLS sequence (i.e Smad) (**pink**), and transports it through the nuclear pore, where it can be released from the karyopherin thanks to the binding of RanGTP (**yellow**). During export, the RanGTP, the export karyopherin and the cargo with the NES sequence (i.e. Smad) form a complex that is exported through the nuclear pore to the cytoplasm where it can be liberated (Wente and Rout, 2010).

Gene transcription via Smad in bone regeneration

In vivo, all Smads, apart from Smad 2, act as transcription factors that control target genes. They associate with DNA-binding factors and form complexes capable of binding the promoters of target genes with high affinity (Massagué, Seoane and Wotton, 2005; Hill, 2016). These Smad cofactors are grouped in different families, notably FoxH1 (or FAST1), member of the forkhead family, which was first identified in *Xenopus* for its ability to recruit pSmad 2 and 4 (Chen et al., 1997). On the other hand, FOS and Jun, members of AP1 transcription factors family were reported to act with Smad 3 and 4 to activate transcription in response to TGF- β (Zhang, Feng and Derynck, 1998). Furthermore, the Runt-related transcription factor (RUNX) family with its members (Runx1, Runx2 and Runx3) have been described to interact with Smad 2/3 and 4 (Massagué, Seoane and Wotton, 2005).

At the DNA level, the R-Smad and Smad4 recognize a Smad binding element (SBE) present on a double-stranded DNA sequence through their MH1 domain (**FIG.I.14**) (Shi et al., 1998).

Furthermore, we should note that the MH2 domain of Smad also plays an important role in transcription as it demonstrated a transcriptional activation potential. These transcription factors and others play an essential role in induction and repression of several Smad target genes, thus they have been described to have various functional roles notably in early development processes such as skeletal formation (Attisano and Lee-Hoeflich, 2001; Massagué, Seoane and Wotton, 2005).

I.D.2. Smad-independent pathways

Besides the Smad pathway, many studies described that BMP and TGF- β activate Smad-independent pathways, which include the mitogen-activated protein kinase (MAPK) pathways. The MAPK are grouped in three subfamilies: the extracellular signal-regulated kinases (ERK1 and ERK2), the c-Jun N-terminal kinase (JNK1, JNK2 and JNK3), and the p38 MAPKs. These pathways signal through a sequence of several MAP kinase called MAP kinase kinase (MAPKKK), as illustrated in **FIG.I.18** (Derynck and Zhang, 2003).

Several studies in the literature described the activation of these pathways to be Smad-dependent and independent. Indeed, the first MAPKK homolog to be described to activate with BMP is TAK1 (Yamaguchi *et al.*, 1999). Similarly, several studies reported the activation of ERK, p38 and JNK MAPKs by TGF- β in diverse cellular contexts, such as osteoblasts, hepatocytes, endothelial and cancer cells. However, they have been described to have either a rapid or a delayed response, and it is suggested that a delayed response is a result of a crosstalk with Smad. This crosstalk was seen with ERK for example which was shown to phosphorylate the linker region in Smad 1, Smad 2 and Smad 3, which leads to an inhibition of their translocation to the nucleus. Moreover, the R-Smad/Smad 4 complex was also reported to interact with activating protein-1 (AP-1), a transcription factor of the MAPK signaling pathway in the nucleus (Javelaud and Mauviel, 2005).

One of the most described roles for these pathways is their role in tumor progression and metastasis. Indeed, the activation of MAPK pathway by TGF- β is associated with the EMT process, which is characterized by loss of cell polarity, tumor invasion and changes in the actin cytoskeleton (Chapnick *et al.*, 2011). Furthermore, the JNK and p38 MAPK pathways can collaborate with TGF- β to induce apoptosis (Zhang, 2017).

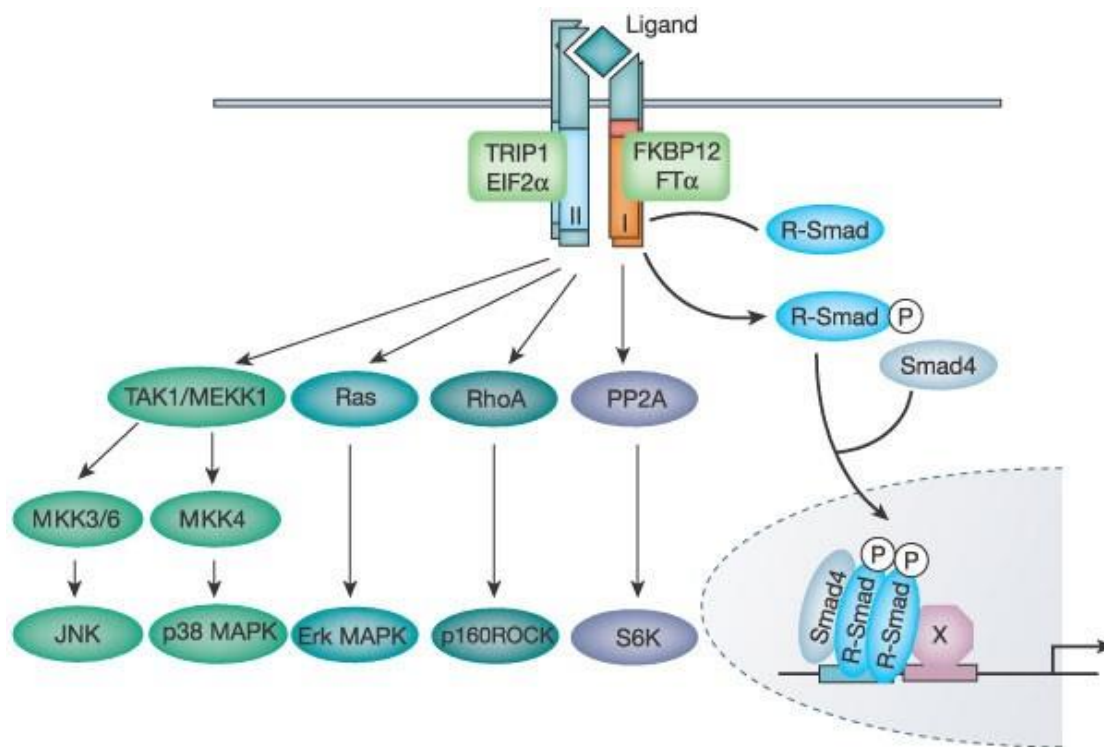


FIG.I.18. A scheme of Smad-dependent and Smad-independent pathways. After ligand (BMP or TGF- β) binding to their receptors and formation of the ternary complex, a cascade of signaling is activated. In Smad-dependent signaling, the R-Smad phosphorylated by the ternary complex of receptors associate to Smad 4 in order to be exported into the nucleus. In Smad-independent pathways, several MAPK can be activated notably TAK1/MEKK1 which activate JNK or p38 MAPK via MKK3/6 and MKK4 respectively. Also, ERK MAPK and p160ROCK pathways can be activated through Ras and RhoA respectively. Finally, PP2A can activate the S6K kinase pathway (Derynck and Zhang, 2003).

I.D.3. BMP-responsive cells

In order to study BMP signaling and BMP-induced cell differentiation, researchers have employed several cellular models, notably: C2C12 skeletal myoblast cells, NIH-3T3 mouse embryonic fibroblasts, and human mesenchymal stem cells (hMSCs).

The C2C12 cells are a skeletal myoblast cell line that is commonly used in the biomedical field. These cells were isolated in the 1970s from adult dystrophic muscles and was shown to proliferate and differentiate *in vitro* (Yaffe and Saxel, 1977). Studies then showed that they can differentiate to osteoblasts, instead of myoblasts, in the presence of BMP-2 by activating a Smad 1/5 pathway (Katagiri *et al.*, 1994; Yamamoto *et al.*, 1997). In addition, the osteogenic differentiation of these cells was investigated by studying the activity of alkaline phosphatase (ALP). It was thus shown that they can differentiate to osteoblasts in the presence of BMP-2,

BMP-4, BMP-6, BMP-7 and BMP-9 (Cheng *et al.*, 2003). Consequently, throughout the past decades, these cells have been established as standard cellular model in the bone field.

We should note that NIH-3T3 cells, mouse embryonic fibroblasts developed in the 1960s, are another mice cell line used in the bone field. They are commonly used in DNA transfection studies, and have been demonstrated to differentiate to chondrogenic, adipogenic and osteogenic lineages (Li *et al.*, 2005; Dastagir *et al.*, 2014).

The hMSCs are isolated and obtained from the bone marrow. These cells were first described as having fibroblast morphology, capable of forming colonies and adhere to cell cultures (Charbord, 2010; Stefanska *et al.*, 2020). Studies demonstrated an osteogenic differentiation of these cells, as evaluated by ALP signaling, in the presence of BMP-2 and BMP-9 (Luther *et al.*, 2011; Sun *et al.*, 2015; Marupanthorn *et al.*, 2017).

I.D.4. Pharmaceutical strategies targeting BMP/TGF- β signaling

As previously mentioned BMPs and BMPRs have several physiological and pathological roles and have been linked to a large number of diseases. Thus, researchers and companies have focused their efforts on discovering and developing drugs to limit the effects of BMPs and TGF- β signaling. Due to the large number of used therapies, we present here some examples of possible therapeutic targets (**FIG.I.19**).

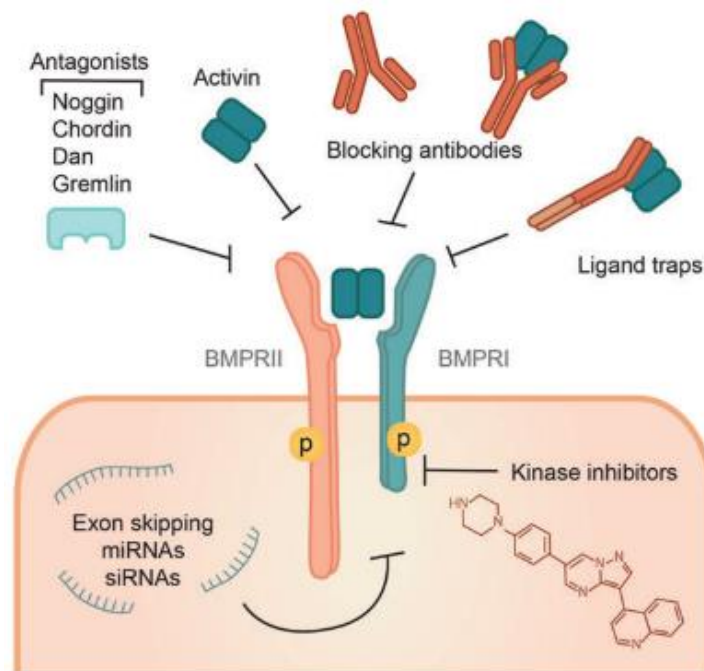


FIG.I.19. A schematic representation of the different types of BMP and TGF- β antagonists that can be used in therapy (Gomez-Puerto *et al.*, 2019).

First, at the ligand/receptor level, some inhibitors have been reported, notably antagonists such as Noggin, Chordin, Dan and Gremlin, as previously mentioned in section I.C.2, have been reported. Furthermore, BMP-specific blocking antibodies and ligand traps such as BMPR-Fc chimeras have been developed. These molecules are capable of binding BMP or TGF- β and hinder their binding to their receptors (Kumar *et al.*, 2021).

Second, at the intracellular level, specific molecules have been synthesized and screened for their abilities to act as ATP kinase inhibitors. These inhibitors are called type-I inhibitors and are the focus of several pharmaceutical companies. They usually consist on binding the ATP-binding pockets of the receptor kinase domain resulting in a displacement of ATP and thus an inhibition of their following signaling (Cohen and Alessi, 2013). Dorsomorphin was the first kinase inhibitor of type-I BMPR identified after a phenotypic screen showed that it blocks ALK2, ALK3 and ALK6 in zebrafish resulting in an inhibition of Smad 1/5/8 signaling and leading to a dorsalization in zebrafish embryos, in contrast to the ventralizing that occurs in the presence of BMP (Yu *et al.*, 2008).

In order to screen for other inhibitors, researchers have synthesized several inhibitor compounds using the same core structure pyrazolo[1,5-a]pyrimidine ring present in Dorsomorphin. An ELISA assay is usually used to observe the inhibition of the BMP-induced phosphorylation of Smad signaling in the presence of these compounds. Then an *in vivo* pharmacokinetics test consisting of compounds administration is carried out, usually in mice. The half-life of the compounds is then measured by observing the plasma concentrations. In this particular study, a derivative inhibitor LDN-193189 was identified to be an improved inhibitor (Cuny *et al.*, 2008).

The chemical structures of some known type-I BMPR inhibitors is presented in **FIG.I.20** (Williams and Bullock, 2018).

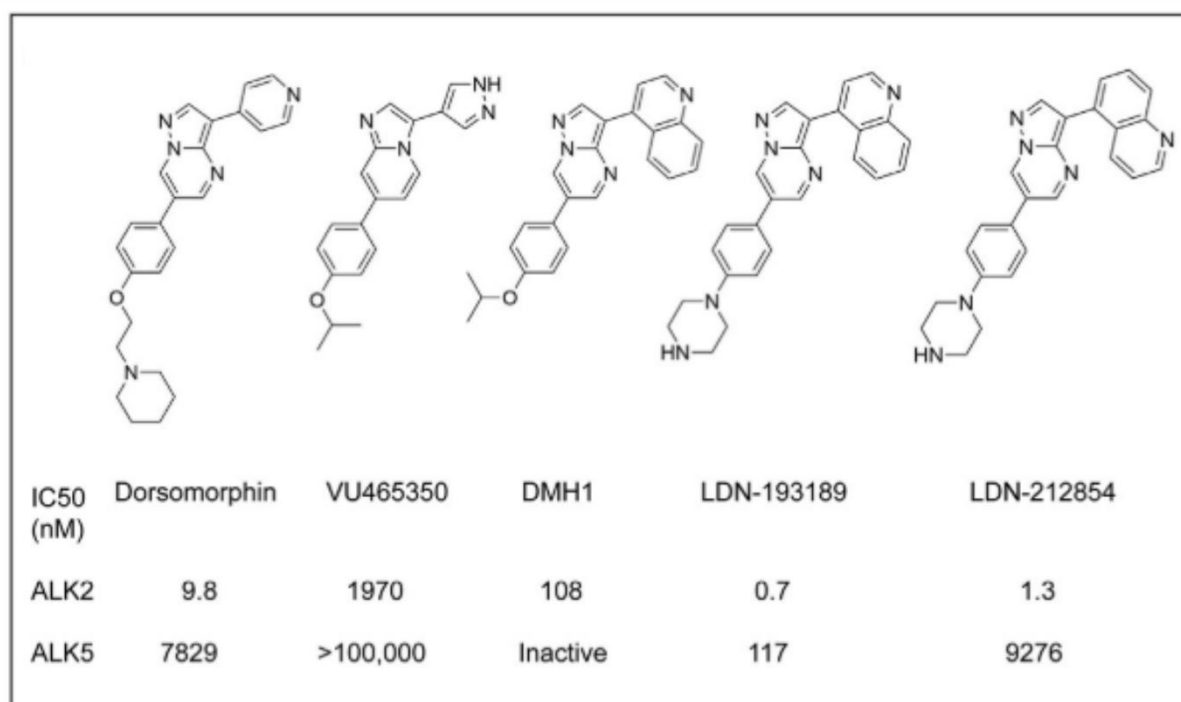


FIG.I.20. Chemical structures of five selected type-I BMPR inhibitors. The inhibitors are derived from the core pyrazolo[1,5-a]pyrimidine scaffold of dorsomorphin. The IC₅₀ of ALK2 and ALK5 with these inhibitors was determined (Williams and Bullock, 2018)

Other studies followed to determine new and improved inhibitors for both BMP and TGF- β receptors. For instance, pharmaceutical companies have determined a library of TGF- β inhibitors for applications in cancer and fibrosis. Their drug screening process includes evaluation of the inhibitory activity by a cell-free *in vitro* assay, usually the kinase Assay with [γ 32P] – ATP or a thermal shift assay. Then cell viability and proliferation assays are performed to determine the toxicity of each compound. In addition, a TGF- β dependent luciferase cellular assay is performed to further evaluate the inhibitory effects of the compounds and determine its half-maximal inhibitory concentration (IC₅₀). Finally, the compounds are occasionally tested for their gene and protein expression by qPCR and Western Blot.

Following these *in vitro* screening, several optimal drugs were selected and tested for toxicity and potency in animals: this is the case for Galunisertib (LY2157299) developed by Eli Lilly and Company, and Vactosertib developed by MedPacto, Inc (Seoul, Korea). After passing these further tests, these drugs can be used in human clinical studies. Indeed, both Galunisertib and Vactosertib were tested in clinical trials. Although, the clinical trials of Galunisertib were stopped in phase 2 in 2020, Vactosertib is still in being studies in phase 2 (Jin *et al.*, 2014; Herbertz *et al.*, 2015; Kim *et al.*, 2021).

We should note that preclinical drug studies have mainly relied two major techniques to study the signaling pathway western blot and bioluminescence (using cells transformed with a luciferase reporter gene). Although these techniques are reliable, they are not well adapted for high-content screening. In addition, they do not allow single cell studies (Badr, 2014; Ghosh *et al.*, 2014).

Third, at the intracellular level, several strategies can also be used to negatively regulate gene expression. We note exon skipping, which consists on using an antisense oligonucleotide that can bind to a mutation site in the pre-messenger RNA thereby blocking the translation of the mutated sequence (Harding *et al.*, 2007). In addition to miRNA that are non-coding RNA molecules capable of recognizing target sequences of RNA in order to induce gene silencing by either mRNA cleavage or translation repression) (MacFarlane and R. Murphy, 2010), as well as siRNAs which can block mRNA translation by cleaving it.

Due to the complexity of the TGF- β superfamily pathway, all these strategies could be studied and developed for future applications as therapeutic tools.

I.E. Biomaterials to study BMPs

I.E.1. Biomaterials to study BMPs

In vivo, as seen above, BMPs are present in the ECM. Indeed, the ECM contains several fibrillary proteins and proteoglycans that can bind BMPs and regulate their bioavailability and activity. Thus, the field of bioengineering has recently been developing several biomaterial models to mimic BMP microenvironments, in order to advance *in vitro* research and also for their use *in vivo* in bone repair. In this part, I will briefly summarize few important results of this flourishing field.

Using engineered materials, several presentation mode of BMPs have been developed for two major aims: i) *in vitro* studies on BMP signaling, ii) *in vivo* studies using BMP-2 to trigger bone regeneration for the repair of bone defects. In this case, the BMPs are associated to various types of materials used as implants (Migliorini *et al.*, 2016).

BMPs can be immobilized at a material surface either covalently (ie permanent bond), or via physical adsorption (ie non-covalent binding). A large number of strategies have been proposed, which are reviewed in (Migliorini *et al.*, 2016). For instance, crosslinking of BMP-2 in polyelectrolyte films (**FIG.I.21.A**), or biotin-streptavidin which is a known non-covalent grafting strategy. This immobilization strategy consists first in coating the surface with biotin

then streptavidin then adding biotinylated-BMP (Migliorini *et al.*, 2016). In one instance, amino-biotinylated BMP was immobilized on poly(methyl methacrylate) coated with streptavidin (**FIG.I.21.B**) (Lagunas *et al.*, 2013). Similarly, other strategies include BMP fused to titanium-binding motives (Kashiwagi, Tsuji and Shiba, 2009).

Moreover, in the design of materials, several studies considered surface patterning of materials in order to control the spatial presentation of BMPs and in a simplified way mimic tissue organization as it is *in vivo* (Hauff *et al.*, 2015; Fitzpatrick *et al.*, 2017). One study developed an active material with micro patterned BMP deposited by inkjet printing on a fibrin-coated glass surface (Phillippi *et al.*, 2008), while a previous work of our team developed mixed micropatterns of BMPs and fibronectin (FN). To this end, we used biomimetic films made of poly(L-lysine) and hyaluronic acid (PLL/HA) as supporting material (Fitzpatrick *et al.*, 2017). Furthermore, using microcontact printing using poly(dimethylsiloxane) stamp, a study developed a fibronectin pattern surface on which a neutrAvidin was used to link biotinylated FN and BMP-2 (Hauff *et al.*, 2015). This surface was shown to activate Smad 1/5 phosphorylation and to inhibit the formation of myotubes by C2C12 skeletal myoblasts (Hauff *et al.*, 2015).

Another strategy to pattern a surface is to use nanoparticles with a size ranging between 150 to 460 nm. These particles are usually used to study the effect of tunable physicochemical properties of a substrate or to determine the effect of surface roughness density on BMP signaling (Migliorini *et al.*, 2016). One study developed a model of PEG layer coated with gold nanoparticle, fabricated with block copolymer micellar nanolithography, on which BMP-2 is immobilized using heterobifunctional linker, 11-mercaptoundecanoyl *N*-hydroxysuccinimide ester (MU-NHS) linker (**FIG.I.21.C**). With each nanoparticle binding one BMP molecule, it is possible to quantify the surface density using atomic force microscopy and therefore do cellular studies by varying BMP-2 density. This model exhibited a delayed but prolonged Smad 1/5/8 phosphorylation in C2C12 cells with BMP-2 (Schwab *et al.*, 2015).

Regarding the non-covalent strategies, several studies have focused on developing materials that contain components of the ECM, notably heparin, hyaluronic acid, and proteins and peptides derived from the ECM proteins, such as Arginine-glycine-aspartic acid (RGD) motif. For instance, heparin-binding peptides and RGD-containing peptides can be presented via a self-assembled monolayer. The peptides can consequently bind the heparin that is complexed to BMPs (Hudalla *et al.*, 2011) (**FIG.I.21.D**). In addition, a titanium implant with a heparin-modified surface was developed, where BMP-2 adsorbed on the surface through electrostatic

interactions between BMP-2 and the negatively charged heparin, and induced osteogenic differentiation of human osteosarcoma MG-63 cell (Kim *et al.*, 2014).

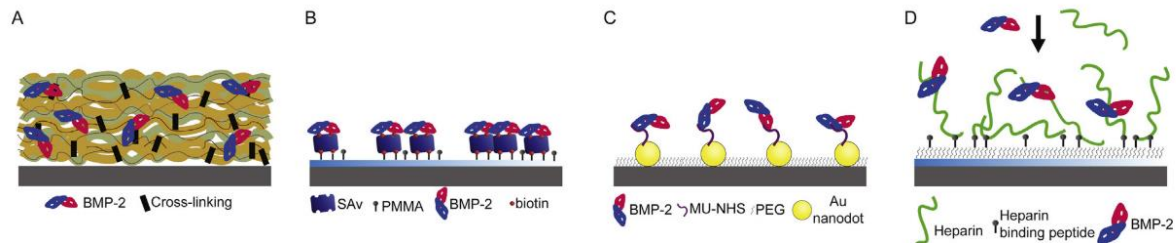


FIG.I.21 Schematic illustration of different strategies used to engineer biomaterial surfaces that present BMPs. A) Physical entrapment of BMP-2 in polyelectrolyte multilayer films. B) Non-covalent immobilization of biotinylated BMP on streptavidin-coated surfaces. C) Grafting of BMP using a MU-NHS linker, on gold nanoparticles produced by block copolymer micellar nanolithography. D) Immobilization on self-assembled monolayer, heparin-bind peptides and RGD peptides that can bind heparin, which consequently is complexed to BMP in solution. Modified from (Migliorini *et al.*, 2016)

These material surfaces are more often used for *in vitro* studies. However, some can also be used for *in vivo* studies. As seen here, the traditional 2D culture on glass does not allow the investigation of the mechanosensitive cell responses, since they are far too stiff. Hence, the development of materials with specific and well-defined physico-chemical properties is still needed since these can be used for fundamental studies *in vitro* aimed at unraveling the biological processes underlying the BMP response.

I.E.2. Development of BMP-containing self-assembled films by our team

In the past two decades, our team has been developing biomimetic polyelectrolytes films to present BMPs in a matrix-bound manner to the cells. This work was initiated more than 20 years ago by forming layer-by-layer films made of PLL and HA named hereafter (PLL/HA) films (**FIG.I.22**) (Picart *et al.*, 2001). The films can be crosslinked with different concentrations of 1-ethyl-3-(3-dimethylaminopropyl) carbodiimide hydrochloride (EDC)/NHS, which creates covalent bonds between carboxylic groups and ammonium groups and thereby also changes the film stiffness (Richert *et al.*, 2004; Schneider *et al.*, 2006). Tuning the concentration of EDC in the crosslinking solution enables to modulate the film stiffness. Later, it was shown that BMP-2 can be loaded efficiently in the films (Crouzier *et al.*, 2009) and be retained in these films due to its direct interaction with hyaluronic acid, as demonstrated by size exclusion chromatography.

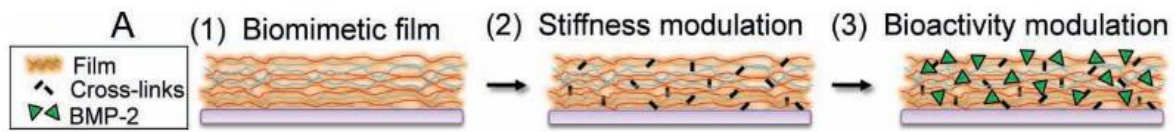


FIG.I.22 Schematics of the preparation of the biomimetic and bioactive polyelectrolyte films. 1) The films are first prepared by depositing polyelectrolytes in a layer-by-layer manner using a robot. 2) Second, the films are crosslinked step using EDC as chemical crosslinker and sulfo-NHS as catalyser. The consequence of film crosslinking is to increase the film stiffness, which has been measured using atomic force microscopy (AFM) nano-indentations. 3) The BMPs are then post-loaded in the films by adapting the physico-chemical conditions (pH, ionic strength), hence rendering them bioactive, more specifically osteo-inductive, meaning that they are able to trigger cell differentiation to bone cell. Adapted from (Crouzier *et al.*, 2011).

The loading of BMP-2 at an initial concentration range of BMP-2 in solution from 1 to 150 $\mu\text{g}/\text{mL}$ showed that 1 hour was sufficient to load BMP at low ionic strength and acidic pH of 3. The release of BMP-2 studied over 7h showed an initial release of BMP-2 over the first 5 hours before reaching a steady state with minimal release up to several days (Crouzier *et al.*, 2009).

The bioactivity of BMP-2 trapped in the film (named hereafter matrix-bound BMP-2) was found to be conserved for up to 12 days, as assessed by doing three cycles of cell plating/replating cultures and quantifying ALP activity. Furthermore, using BMP-2 labeled with rhodamine, it was shown that BMP-2 can diffuse in the films (Crouzier *et al.*, 2009).

Furthermore, the effect of film stiffness on myoblast cell adhesion, proliferation and differentiation was extensively assessed (Kefeng *et al.*, 2008). First, the team studied the effect of film crosslinking-without the presence of adsorbed proteins- on cell adhesion and differentiation. C2C12 skeletal myoblasts were found to anchor and attach with a preference to the highly cross-linked films (i.e. stiff) (EDC concentration at 50 and 100 mg/mL) in comparison to the low cross-linked (i.e.. soft) films (EDC at 5 and 10 mg/mL). In addition, the cross-linking level influenced morphologically myoblast differentiation to myotubes (Kefeng *et al.*, 2008). Then, studies using stiff films (EDC crosslinking at 100 mg/mL) and soft films (EDC crosslinking at 30 mg/mL) containing bBMP-2 were conducted. C2C12 myoblasts were found to differentiate to bone cells on the bBMP-2. Surprisingly, myoblasts were also found to increase cell adhesion and migration, notably on bBMP-2 delivered from soft films, which was quite unexpected (**FIG.I.23**). To note, this effect was more striking for cells culture on bBMP-

2 on soft films than for bBMP-2 on stiff films, where film stiffness was already impacting cell adhesion and migration (Crouzier *et al.*, 2011).

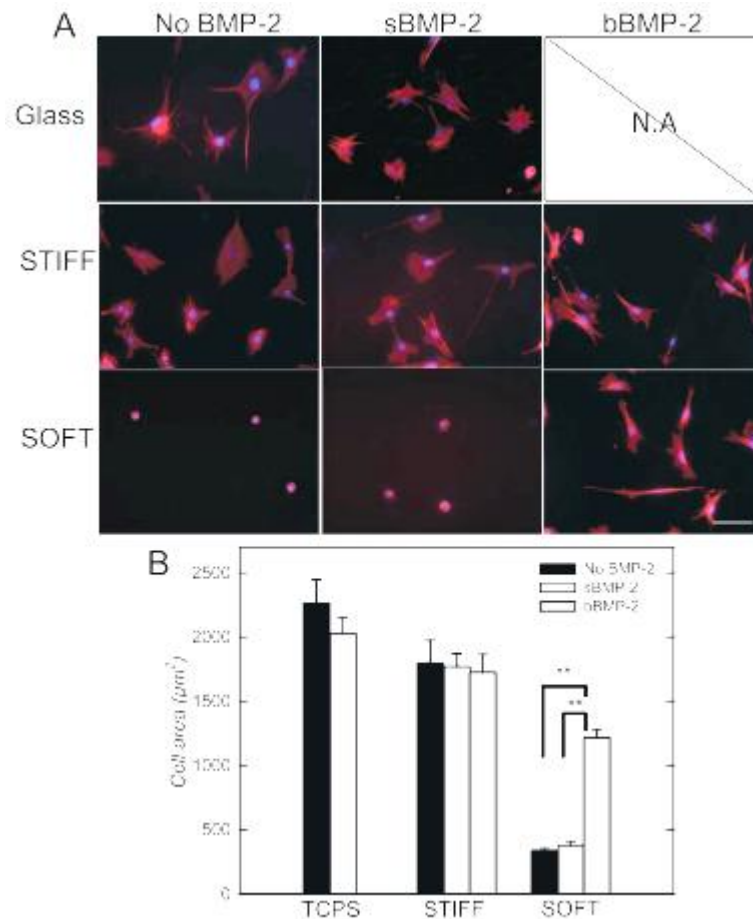


FIG.I.23 Effect of matrix-bound BMP-2 (bBMP-2) on the cell spreading area of C2C12 skeletal myoblasts. The cell morphology was assessed after overnight culture, i.e. 16 h after plating the cells. A) Representative images of cells plated on glass, stiff and soft films in the absence of BMP-2 and in the presence of either soluble BMP-2 (sBMP-2) or bBMP-2. B) Quantification of the cell surface area for the different experimental conditions (Crouzier *et al.*, 2011).

Further studies using these engineered biomimetic thin films were performed in collaboration with the Albiges team at Institute of Advanced Biosciences. Notably, the role of integrins in bBMP-2 mediated cell adhesion was studied in the frame of the PhD thesis by Laure Fourel. It was found that BMP-mediated cell adhesion depends on integrins, notably $\beta 3$ integrin (Fourel *et al.*, 2016). In fact, BMP-2 presented by the films induced the clustering of $\alpha \beta 3$ integrins. Indeed, after binding to fibronectin that is naturally present in the pericellular coat of C2C12 skeletal myoblasts, it was found that $\alpha \beta 3$ integrin is involved in BMP-2-induced cell

spreading. In addition, matrix-bound BMP-2 lead to a faster recruitment of focal adhesion components such as paxillin, in comparison to sBMP-2 (Fourel *et al.*, 2016). Furthermore, the results obtained suggested that the binding of BMP-2 to BMPR activates a $\beta 3$ integrin-dependent cell spreading.

Hence, due to the matrix-bound configuration of BMP-2, the cells were able to bind to the BMP-2 presenting (PLL/HA) films at two anchoring points: first, BMP-2 interacted with fibronectin present at the cell surface, then enabling their binding to the cell surface receptor $\beta 3$ integrin. Second, BMP-2 interaction with BMPR leads to the formation of focal adhesions.

Matrix-bound BMPs were shown to have an effect on cytoskeleton organization and cell spreading, notably when they are presented from soft films (Fourel *et al.*, 2016). In addition, the crosstalk between $\beta 3$ integrin and BMP receptors can only be revealed thanks to the nature of the film, which induces a spatial confinement of the BMP receptors due to the locally high concentration of BMPs in the biomimetic films. Hence, the restricted diffusion of BMPs in the film as well as the increased availability of BMP-2 in close proximity to the cellular receptors, allowed the observation of specific biological processes that was masked in standard cell culture conditions, ie for cells cultured on glass or on tissue culture polystyrene (TCPS). In fact, in a way, these very hard surfaces (glass, polystyrene) are masking the biological effects of the BMPs on cells. In striking contrast, when cells are cultured on soft films, the biological effects of the bBMP-2 can be highlighted and quantified.

To note, generally, engineered biomaterials can provide new solution to study cell signaling and can help to decipher cell-signaling pathways that could not be observed in standard cell culture conditions on glass. The major differences between two presentation mode: matrix-bound BMP-2 and soluble BMPs are presented in **FIG.I.24** (Crouzier *et al.*, 2011).

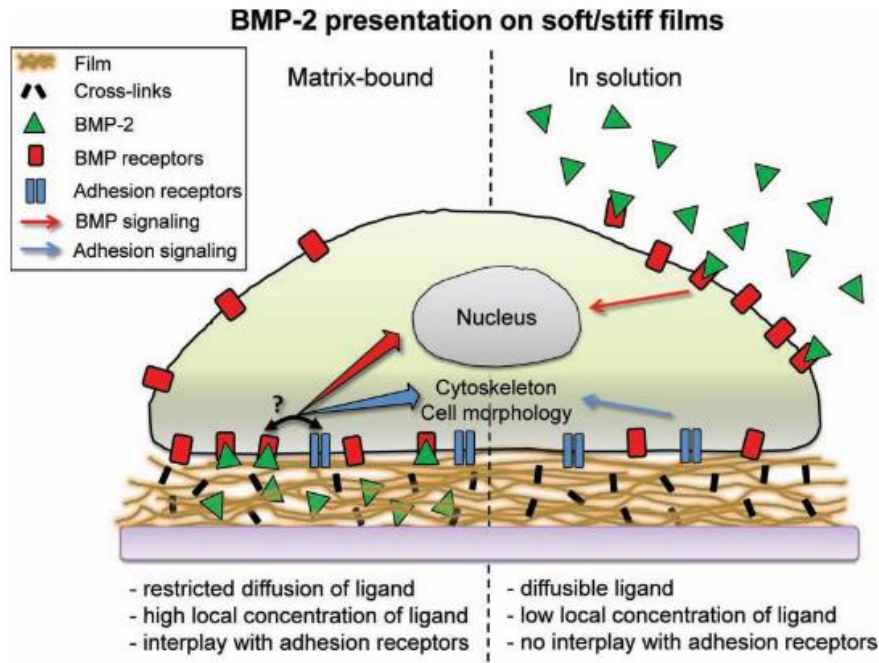


FIG.I.24. Schematic representation of two different BMP-2 presentation modes: matrix-bound (bBMP-2, left hand side) and soluble (sBMP-2, right hand side). The differences between matrix-bound BMP-2 (left) and soluble BMP-2 (right) are presented in terms of i) Diffusion. ii) Concentration of BMP-2 ligand. iii) Interplay with adhesion receptors, which are located at the basal side of the cell, where they adhere (Crouzier *et al.*, 2011).

Technological development made by the team in the past years in the frame of ERC grants, notably the ERC Proof-Of-Concept BioactiveCoatings enable to speed up the film preparation process. Until 2016, the films were always prepared using a dipping robot on 14-mm or 32-mm glass slides. Then, the glass slides had to be transferred inside cell culture microplates. Alternately, the films were deposited manually using a multi-channel pipette directly inside multiple well cell culture plates (Gribova *et al.*, 2013), in order to use plate readers for absorbance, luminescence or fluorescence measurements. This manual process was tedious and time-consuming, as well as amenable to human errors. Hence, the team decided to develop an automated process to build the biomimetic films directly inside the wells of cell culture microplates, in order to perform high-content screening of cellular processes (Machillot *et al.*, 2018). To this end, the team adapted the use of a liquid handling robot to directly deposit the films in a layer-by-layer manner at the bottom of each well of a multiple-well plate. The 96-well plate format is particularly interesting since it can be used to screen multiple conditions in parallel. Besides, a well in a 96-well plate requires much less cells than a well in a 24-well plates, which is particularly interesting when precious cells such as stem cells are to be used. The polyelectrolytes are dispensed using a robotic arm with multiples channels in the wells to

ensure homogeneity of film deposit at the bottom of the well. In addition, a microplate-tilting step was introduced to ensure that the dispensing, rinsing and aspiration steps were done properly without leaving any residual liquid inside the wells.

In addition to the 96-well microplates, the robot was recently optimized for different plates format, notably 6-wells, 12-well, 24-well microplates and in Labtek chambers, hence making it versatile to be used in a large range of cellular assays and imaging methods. Furthermore, different types of plates, with glass or polystyrene bottom have been considered. The script of the robot was optimized for different usage.

The ability to deposit films in cell-culture microplates enables to perform a large set of experiments using cells, especially since the microplates are compatible with all kinds of microplate readers and all sorts of microscopes. As a first proof-of-concept, these biomimetic films prepared by the robot, were consequently used in high content screening of stem cell differentiation (Machillot *et al.*, 2018).

With these technological advances, the team has begun several projects using high-content screening of transcription factors. Recently, the team also begun the development of another type of material notably biomimetic platforms made by self-assembly of streptavidin/biotin, which can additionally present the GAG heparan sulfate (Sefkow-Werner *et al.*, 2020). Another application focuses on the automated film-coating of 3D printed scaffolds to study cancer cell response to controlled microenvironments.

Objectives of the PhD thesis

BMPs play a role in several physiological processes, notably in bone formation. In addition, they are known to be involved in several pathological processes, such as FOP and PAH that involve a dysfunction of the BMP receptors. Thus, it is important to study their biological role *in vivo* as well as understand their signaling pathways. As highlighted above, the BMPs pathway starts with their interaction with BMPR. This interaction have been described to be complex as it is largely regulated by modulator proteins, pseudo and co-receptors. Furthermore, the promiscuous nature of the interaction with BMPR, in addition to the presence of heterocomplex of BMP and BMPs render it more difficult to clearly characterize this step.

Therefore, in the past decades, the BMPs field focused on the development of biomaterial models to investigate their biological processes when presented in a matrix-bound manner to the cells, in order to mimic the matrix-bound BMP present *in vivo*. Several strategies to engineer materials presenting BMPs were developed, consisting of immobilization by chemical binding or by physical adsorption at a material surface. As an example of a BMP-presenting biomaterials, our team developed polyelectrolytes films loaded with BMPs and used them to study the cascade of bone regeneration (Crouzier *et al.*, 2009; Fourel *et al.*, 2016; Sales *et al.*, 2022).

In this context, my thesis work focused on the early steps of bone regeneration, which begins by the interaction at the cell membrane of the BMPs with their BMP receptors. Thus, we first decided to study the binding affinities and kinetic constants of four different BMPs that are among the most important (BMP-2, 4, 6 and 9), with the BMP receptors type I and type II, with five BMP-type I receptors and Three BMP-type II receptors.

In a second step, I made a comparative study of the cell types that are BMP-responsive by characterizing their expression level of BMP receptors and quantifying cell differentiation to bone using simple readouts, notably pSmad and ALP activity.

Finally, in a third step, I contributed to establish a high-content analysis test based on pSmad immuno-fluorescence to compare the effect of different experimental conditions. After optimizing several parameters that affect the immuno-fluorescence level, I performed a proof-of-concept of drug testing on the biomimetic films, using drugs against BMP receptors and TGF- β that are currently in clinical trials.

This PhD manuscript is divided in three main parts, which are explained below and summarized in the schematics (**FIG.I.25**).

- **Chapter III:** This chapter deals with a comparative study of the binding affinities and kinetics constants of BMPs (BMP-2, BMP-4, BMP-7 and BMP-9) with five type-I BMPR (ALK1, ALK2, ALK3, ALK5, ALK6) and three type-II BMPR (BMPR-II, ACTR-IIA, ACTR-IIB) receptors using the bio-layer interferometry (BLI) technique.
- **Chapter IV:** In this chapter, three cellular models, including C2C12 myoblast cells, human periosteum derived stem cells (hPDSCs), and human mesenchymal stem cells (hMSCs) were compared by determining the expression levels of their BMPR and adhesion receptors integrins. A literature study was also conducted to compare their characteristics. In addition, preliminary studies were done using hMSCs to investigate their possible use for drug assays.
- **Chapter V:** An immuno-fluorescence assay was developed to quantify phosphorylated pSmad at high content in single cells using an automated microscope. The experimental conditions (time, culture medium, fixation conditions, and type of plate) were optimized so as to obtain the highest fluorescence intensity level with the lowest background. Then, model drugs were selected among those currently in clinical trials and a proof-of-concept was done for drug testing on glass and on the biomimetic films, using C2C12 myoblasts as BMP-responsive cells.

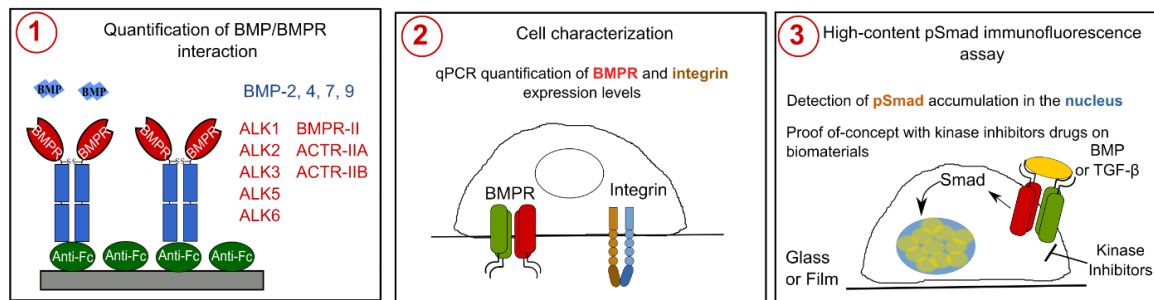
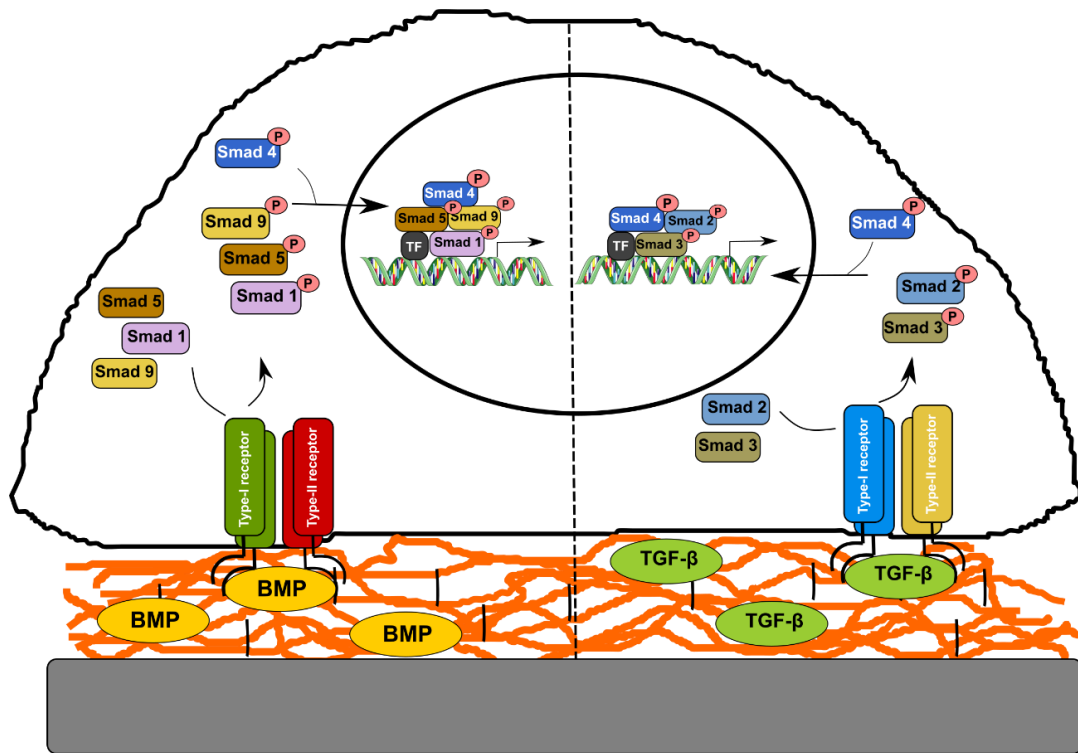


FIG.I.25. Schematic representation of the thesis objectives. 1) Quantification of BMP/BMPR interaction using bio-layer interferometry. 2) Cellular characterization on C2C12, hPDSCs and hMSCs. 3) Development and optimization of high-content pSmad assay and a proof of concept for drug testing on biomaterials with C2C12 was done.

Chapter II:

Materials and Methods

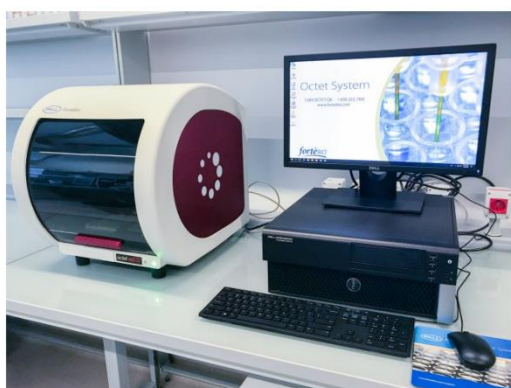
In this chapter, we will review the experimental details and techniques that we have used to carry out our projects.

II.A. BMP/BMPR affinity experiments

II.A.1. Bio-layer interferometry (BLI) kinetic experiments

The bio-layer interferometry is a bimolecular interaction method, label-free optical technique able to characterize protein-protein interactions. It consists of using dip-and-read glass biosensors on which a ligand is immobilized with different strategies (**FIG.II.1**) (Hänel and Gauglitz, 2002; Tobias, 2013; Delis, 2016).

A



B



FIG.II.1 An image of a BLI biosensor and a schematic representation of its tip. A) A picture of an OctetRED96e equipment. B) The glass biosensors are dipped into a 96 wells plate containing different samples and buffers.(Abdiche *et al.*, 2008; Tobias, 2013).

The technique is based on a reflectometry interference spectroscopy (RIfS) which measures the white light's interference caused by the partial reflection at the surface, therefore determining the optical thickness of the layer (Hänel and Gauglitz, 2002). In more details, the BLI technology emits a white light to the tip of the biosensor and then measures its reflected light from two interfaces: the internal reference layer and a layer of immobilized complex on the surface of the biosensors. After the analyte binding, the optical thickness of the biosensor changes, thus shifting the interference pattern (**FIG.II.2**) (Tobias, 2013; Sultana and Lee, 2015).

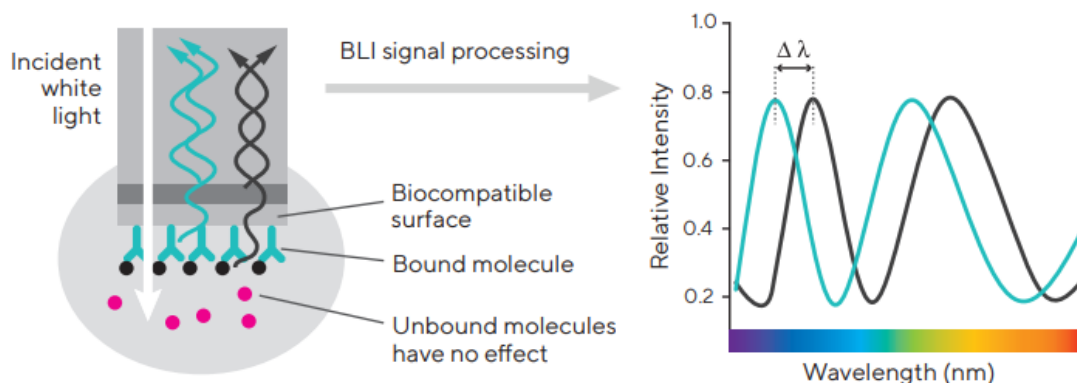


FIG.II.2. A schematic representation of the BLI technology's principle. A white light is emitted to the tips of the biosensor and then it is reflected back to the apparatus from the biocompatible surface and from the surface of the bound molecule. The signal of BLI is processed and the difference between the two wavelengths is measured and translated into kinetic data (Tobias, 2013).

The common immobilization strategies are amine-coupling which allows the functionalization of the surface with EDC/NHS (Johnsson, Löfås and Lindquist, 1991), as well as biotin/streptavidin which creates a strong non-covalent bond of 160 ± 20 pN (Florin, Moy and Gaub, 1994). In addition to antibody/anti-Fc used for protein-antibody interactions measurements, and all of His-tag/Ni-NTA, GST/anti-GST and FLAG/anti-FLAG used for affinity tagged-proteins, with each presenting advantages and disadvantages (Delis, 2016).

In our study, we used an Octet system set up with 96 wells plate that allow parallelization of experiments and the performance of a high throughput studies with large number of samples at a short amount of time (Abdiche *et al.*, 2008) (**FIG.II.1**).

II.A.2. Kinetic analysis of BLI sensograms

We performed the BLI experiments on an OctetRED96e system present on the SPR/ BLI platform at institute of structural Biology in Grenoble. We used an immobilization strategy that consists of the usage of BMPR-Fc chimeras and anti-Fc coated biosensors (**FIG.II.3**).

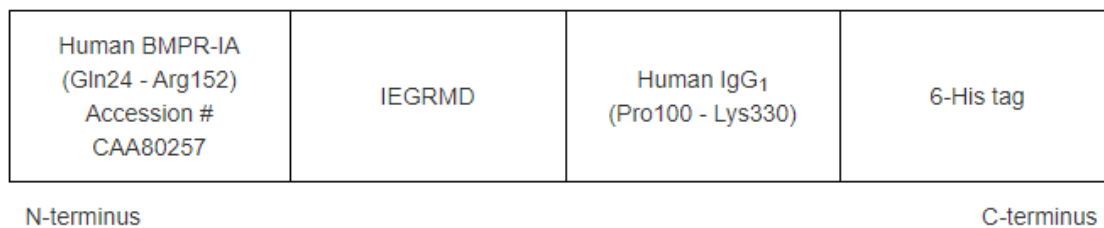


FIG.II.3. An example of BMPR-Fc chimera sequence here ALK3-Fc. The sequence of ALK3-Fc chimera is composed of an ALK3 sequence, followed by a linker region and the Antibody-Fc sequence. Finally, the C-terminus comprises 6-His tag (*Recombinant Human BMPR-IA/ALK-3 Fc Chimera Protein*, no date).

BMPs and BMPR-Fc chimeras were bought from Sigma Aldrich (Missouri, USA) and R&D systems (Minnesota, USA) respectively. The BMPR and BMP samples were both diluted in 20 mM HEPES 150 mM NaCl pH 7.4 with 0.02% Tween 20 analysis buffer. Black 96-well plates were filled with 0.2 mL of each sample and maintained at 25°C with 1000 r.p.m agitation. Before the kinetic experiments, we performed an optimization step where BMPR-Fc diluted at different concentrations were loaded for 200 seconds to reach a spectrum shift between 0.8 and 1.1 nm on the Anti-hIgG biosensors purchased from ForteBio (California, USA) (Now purchased by Sartorius). The association and dissociation steps consisted of 400 seconds steps, followed by a full regeneration of the sensors using 10 mM glycine at pH 1.7 regeneration buffer between each experiments (**FIG.II.4**).

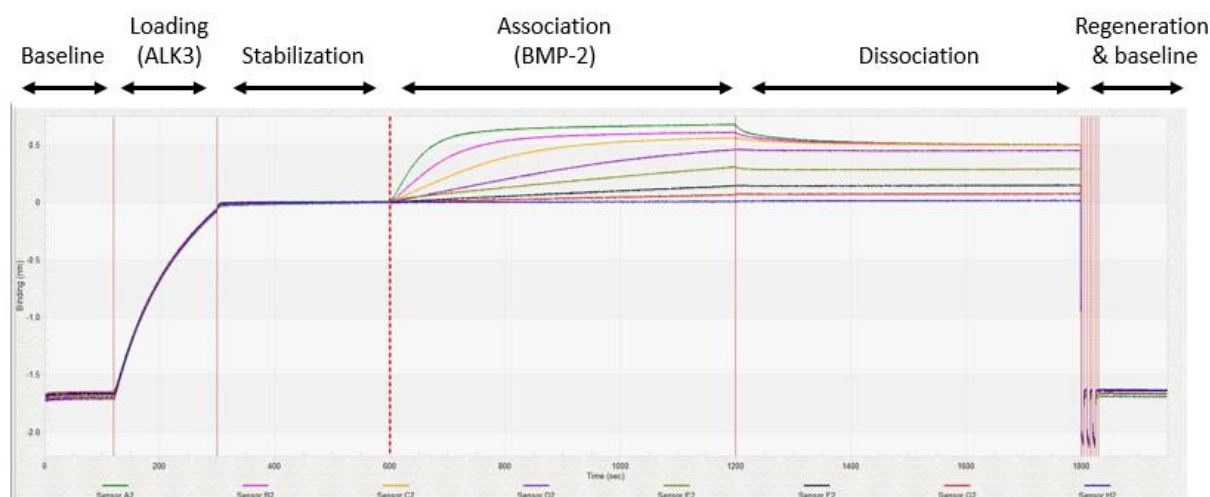


FIG.II.4. An example of a kinetic sensorgram here with ALK3/BMP-2 interaction. The different steps of the sensorgram are the baseline, followed by the loading of the receptor (here ALK3), then a stabilization and an association (here with BMP-2) and dissociation steps. Finally, the sensorgram is regenerated with a final regeneration step.

The kinetic data were fitted using 1:1 Langmuir or 2:1 heterogeneous ligand model and analyzed using the manufacturer software (Data analysis HT v11.1). The kinetic constants such as association constant (k_a) and dissociation constant (k_d) were determined, and affinity constant K_D was deduced from the measured k_d and k_a values using the equation $K_D = k_d/k_a$.

II.A.3. Surface plasmon resonance (SPR) kinetic experiments

The SPR is one of the most used techniques for protein-protein interaction studies. It consists on stimulating a material with high permittivity by an incident light thus resulting in a resonant oscillation of electrons at the interface. The ligands, here BMPR-Fc, were captured on biosensors coated with protein A attached to a monolayer of carboxymethylated dextran on a gold surface. The analyte, here BMP, flows in the microfluidic channel over the functionalized surface and binds to it, thus leading to a change in the resonance angle ($\delta\theta$) of the refracted light (**FIG.II.5**) (**FIG.II.6**). Hence, the change in the refraction is in quantified in resonance units (RU) where 1RU corresponds to 10^{-4} degrees of angle shift (Myszka *et al.*, 1998; Nguyen *et al.*, 2015; Migliorini *et al.*, 2018).

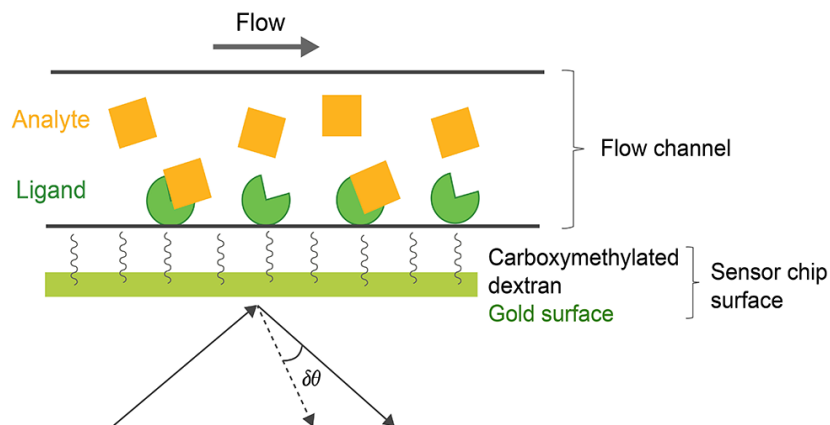


FIG.II.5. A schematic representation of the SPR technology's principle. An incident white light is emitted to the gold surface where the ligand (BMPR) is immobilized to the carboxymethylated dextran. When the analyte (BMP) binds to the BMPR, the refracted light changes leading to a variation in the resonance angle $\delta\theta$ measured in resonance units (RU) (*Principle and Protocol of Surface Plasmon Resonance (SPR)*, 2021).

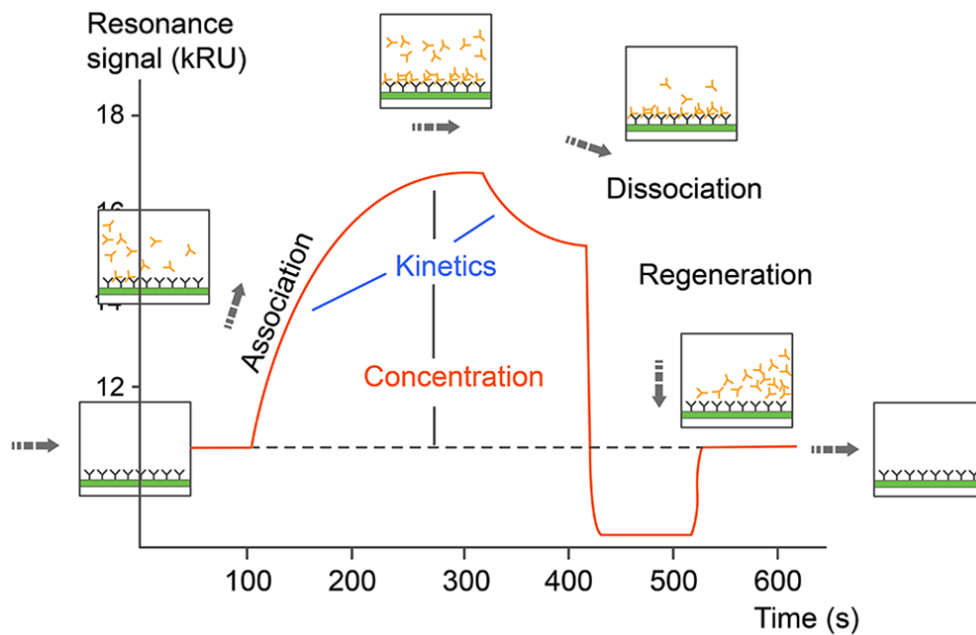


FIG.II.6. An example of an SPR sensorgram. This scheme presents the different steps of SPR, notably the association step with the analyte binding to the immobilized ligand, followed by a dissociation step where the analyte is slowly dissociating from the ligand. Finally, a regeneration step is performed where all the analyte and ligands are removed (*Principle and Protocol of Surface Plasmon Resonance (SPR)*, 2021)

II.A.4. Kinetic analysis of SPR sensorgrams

The SPR kinetics were performed using a Biacore T200 apparatus present on the SPR/BLI platform of institute of structural Biology. The BMPR-Fc and BMPs were both diluted in 20 mM HEPES 150 mM NaCl pH 7.4 with 0.02% Tween 20 analysis buffer. The BMPR-Fc were loaded on the protein-A coated sensors (GE Healthcare Lifesciences) for 100 seconds in order to reach a signal level of 100 RU. We performed association of BMPs and dissociation steps for 300 seconds, followed by full regeneration of the surface by adding glycine regeneration buffer for 30 seconds. The kinetic data were fitted using 1:1 Langmuir model. The association constants k_a and dissociation constants k_d were determined and used to calculate the K_D from the ratio k_d/k_a .

II.B. Preparation of the biomimetic film

II.B.1. Preparation of polyelectrolyte solutions

The biomimetic films developed by the team are made up of several polyelectrolyte multilayers of polycation and polyanion. The used polyelectrolytes are the positively charged poly(ethyleneimine) (PEI) and PLL, as well as the negatively charged sodium hyaluronate (HA) (**FIG.II.7**).

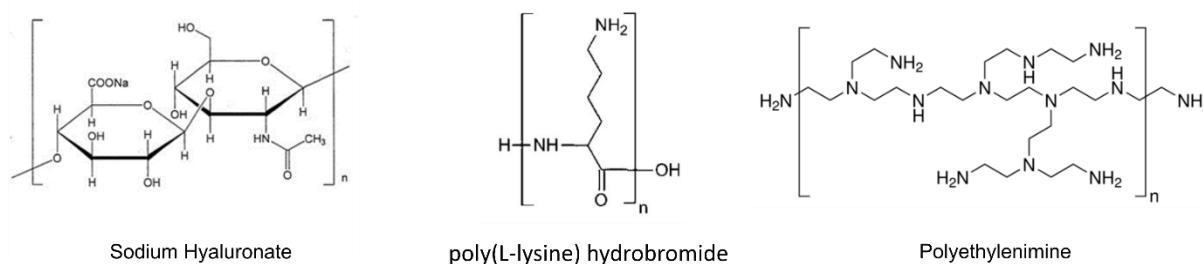


FIG.II.7. The polyelectrolyte formulas are A) Sodium hyaluronate, B) poly(L-lysine) hydrobromide, and C) poly(ethyleneimine).

The polyelectrolyte PEI is in its soluble form stored at room temperature, while HA and PLL are stored at -20 degrees and taken out of the freezer to equilibrate at room temperature for 20 min. Then they are weighed and dissolved with 20 mM HEPES 0.15 mM NaCl pH 7.4 buffer filtered with 0.22 μ m filters. The PEI is prepared at 5 mg/mL, HA at 0,5 mg/mL and PLL at 1 mg/mL.

II.B.2. Film buildup and crosslinking

The biomimetic films are prepared using EVO100 Tecan robot using a custom-made program (Machillot *et al.*, 2018). Several macros and scripts were developed by the team to prepare films in several plate formats such as CELLview, which is a 10 wells plate immobilized on a cover glass bottom, as well as 6, 24 and 96 well plates in glass and plastic formats. The buildup of polyelectrolyte starts with the deposition of a layer of the polycation PEI, followed by two rinses of 0.15 M NaCl pH 6.4 rinsing solution, and a layer of the polyanion HA. This first HA layer is succeeded by 12 cycles of deposit of (PLL/HA) layers intercalated with rinsing steps.

Then a cross-linking step is performed using EDC/Sulfo-NHS to create covalent amide bonds between the free carboxylic and ammonium groups (**FIG.II.8**). This chemical crosslinking has also a consequence of increasing the film stiffness.

EDC crosslinking is performed in acidic solution at pH 5.5. When added, the EDC reacts with carboxyl groups to form active O-acylisourea intermediate (**FIG.II.8.Step 1**). This intermediate then reacts with sulfo-NHS to form NHS-ester intermediates (**FIG.II.8.Step 2**). Afterwards, the the NHS-ester reacts with a primary amine site and form amine derivative (**FIG.II.8.Step 3**). In case the it did not interact with the an amine, the NHS-ester is hydrolyzed, the carboxyls regenerated and the sulfo-NHS released (**FIG.II.8.Step 4**) (Richert *et al.*, 2004).

Thus, adding the sulfo-NHS as catalyzer allows EDC to couple to carboxyl with an improved efficiency and to create stable amine-reactive sulfo-NHS ester, instead of the unstable O-acylisourea intermediate formed in the presence of EDC alone (*Carbodiimide Crosslinker Chemistry*, 2021).

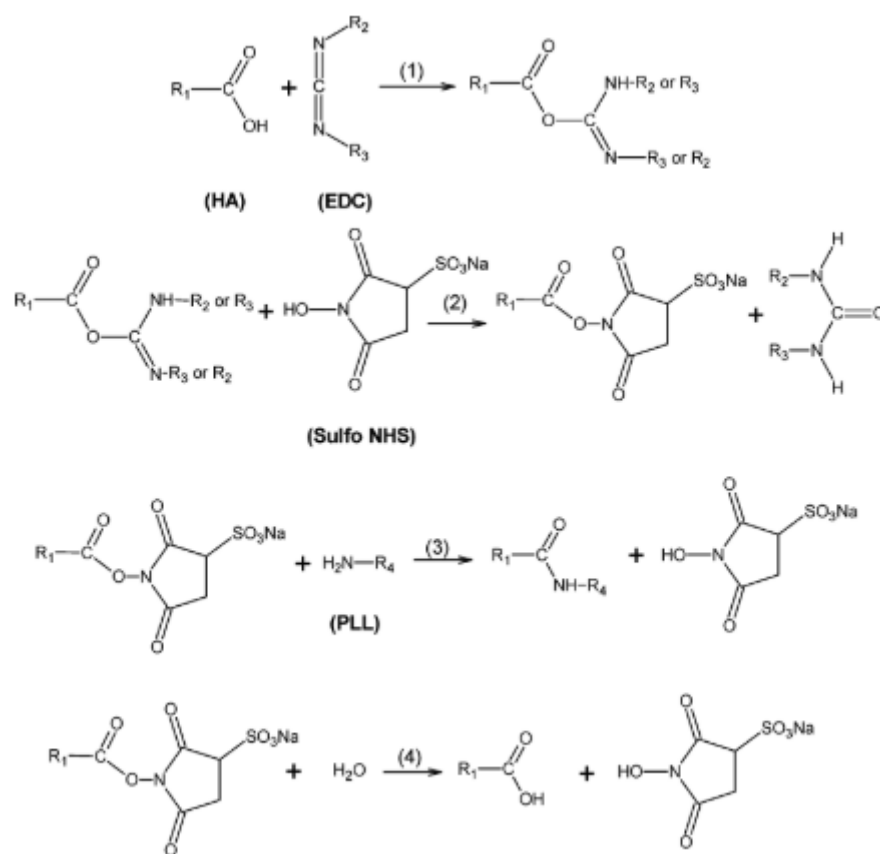


FIG.II.8. Schematic of the EDC and sulfo-NHS crosslinking reaction. EDC crosslinker reacts with the carboxyl group of an amino acid to form the unstable o-Acylisourea intermediate (Step 1). This intermediate then interact sith Sulfo-NHS and form NHS-ester intermediates (Step 2). The NHS-ester intermediate can either interact with the primary amine of PLL and form amine derivative (Step 3),or it is hydrolyzed leading to the regeneration of carboxyls and release of sulfo-NHS (Step 4) (Richert *et al.*, 2004).

The two chemicals are prepared with 0.15 M NaCl at pH 5.5 solution at 11 mg/mL for sulfo-NHS, while EDC concentration can vary from 0 to 100 mg/mL. They are then added to the

prepared films to be incubated overnight for 18h in the fridge at 4°C. The films used were at 70 mg/mL of EDC, named hereafter EDC70.

The next day, 7 washes of 10 min with HEPES 20 mM, NaCl 0,15 M pH 7.4 were performed, followed by quick two rinses of water to get rid of salt before drying it under the hood for at least 1 hour. The films can then be stored in the fridge for future utilization.

II.B.3. Loading of BMP and TGFβ in the film and UV sterilization

In order to functionalize the films, the BMP or TGFβ (Sigma Aldrich (Missouri, USA)) are first diluted at a concentration of 20 µg/mL and 0.75 µg/mL respectively in 1 mM HCl pH 3. They are then added to the film and incubated at 37°C for 2h. The solution containing unbound protein can be kept in order to do a micro Bicinchoninic acid (µBCA) quantification assay. The protein loaded in the films will be named “matrix-bound” BMP or TGF-β, in contrast to the BMP added in solution to the glass condition that will be named “soluble” BMP or TGF-β. The plate is then washed during 6 washes of 10 min in a solution of 150 mM NaCl 20 mM HEPES pH 7.4. Before any usage, the plates containing the films and their covers are sterilized under UV In the cell culture hood for 20 min.

II.B.4. Quantification of bound BMP with Bicinchoninic acid (BCA) assay

The assay with BCA is used to quantify the released quantity of BMP and consequently the bound BMP. The assay comprises two steps; first, it consists of reducing the Cu²⁺ to Cu⁺ with protein, leading to the formation of a blue-colored complex. Second, the BCA reagent, a colorimetric agent, reacts with the copper cation and forms a violet-colored complex that absorbs light at 540 nm (**FIG.II.9**). The signal induced by BCA is measured at 562 nm by a microplate reader Tecan Spark (*BCA Assay and Lowry Assays*, 2021).

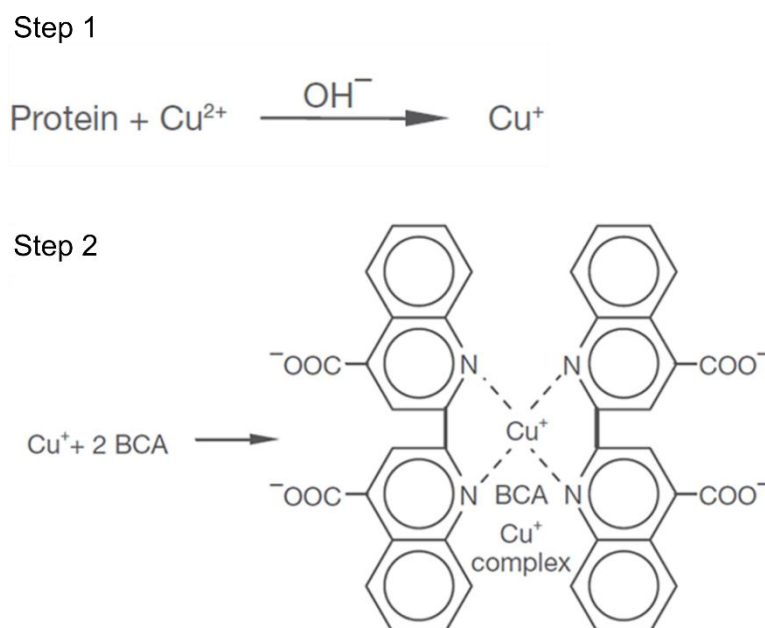


FIG.II.9. BCA assay principle. The assay consists of two steps. First, the copper is reduced with protein. Second, the BCA reagent reacts with Cu^+ cation and forms a purple color that can be measured at 562 nm (*BCA Assay and Lowry Assays*, 2021).

We use a QuantiPro kit from Sigma to do the μBCA assay. The μBCA assay is capable of detecting concentrations of proteins (0.5 to $30\mu\text{g/mL}$), while the standard BCA detects concentrations of 200 to $1000\mu\text{g/mL}$. Since we use low concentrations, the μBCA is more adapted to our experiment. The A and B solutions are mixed at a 1:1 ratio, while the copper is mixed at a ratio of 1:50 with the final volume. The BMP and TGF- β solutions are added to a 96 well plate and mixed with reagent mix. A calibration curve using BCA is also prepared by serial dilution (**FIG.II.10**). The plate is then incubated at 60°C for 60 min in the dark. Finally the absorbance is measured at 562 nm by a Tecan Spark. The quantity of protein released is calculated by dividing the absorbance by the slope (**in FIG.II.10**, it is 0.0092).

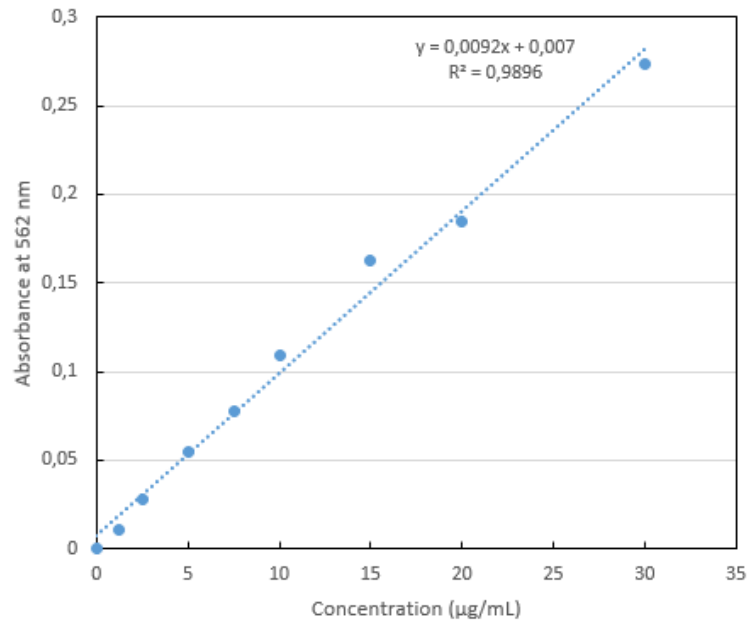


FIG.II.10. A calibration curve with a serial dilution of BCA. A linear regression trend line is drawn based on the different concentrations of BCA, according to the linear equation $y = bx + a$, with b being the slope of the line and a is the intercept where the value of y and x are 0.

II.C. Cell culture

II.C.1. Cell culture

C2C12 mouse myoblasts cells were used in our study since they are a well-acknowledge model for BMP-responsive cells (Katagiri *et al.*, 1994; Gilde *et al.*, 2016). They were bought from ATCC. They are an immortalized mouse cell line capable of proliferating rapidly *in vitro* under high serum conditions, and differentiate into myotubes, precursors of skeletal muscle cells under low serum conditions. The cells were kept in growth medium (GM) made up of Dulbecco's Modified Eagle Medium (DMEM)/Nutrient mixture F12 medium with 10% fetal bovine serum (FBS), 1% of penicillin and streptomycin.

The hMSCs were collected from donors in the French blood bank, and the army hospital. These adult stem cells present in several tissues, can differentiate into multiple tissues such as bone, cartilage, muscle and fat cells, and are responsive to BMP (Dominici *et al.*, 2006). The cells were maintained in GM composed of 89% DMEM with low glucose, 10% FBS, 1% penicillin and streptomycin.

The hPDSCs are gifted from our collaborator Dr. Frank Luyten. As mentioned before, these adult stem cells are obtained from the periosteum, and have demonstrated ability to response to BMP (Ferretti, 2014; Sales *et al.*, 2022)

The cells were cultured in polystyrene 75 cm² flasks in an incubator at 37°C and 5% CO₂, maintained at 60-70% confluence and passed every 2 days in GM.

II.C.2. Cell lysis and study of BMPR expression by quantitative polymerase chain reaction (qPCR)

In order to measure the expression levels of protein a quantification PCR technique was used. The principle consists on using a pair of primers complementary to a sequence of interest that we want to amplify. A single copy can be amplified to up to 10¹¹ copies and are usually detected by a fluorescent reporter dye.

The first step consists on lysing the cultured cells using a RNA lysis buffer to extract the RNA. The lysis buffer contains salts such as guanidine HCl that disrupt H-bonds, hydrophobic interactions and van der Waals forces of proteins, as well as proteinase K that degrade proteins.

The lysate is then transferred into a series of purification columns and centrifugation cycles to remove cellular debris and genomic DNA, followed by a binding solution to bind and isolate RNA. The RNA is quantified by a UV spectrophotometry using the Nanodrop with 1 absorbance at 260 nM corresponding to 40 µg/mL.

After the purification, a step is required to synthesize cDNA from RNA. An iScript reverse transcription (RT) supermix containing: 1) Moloney murine leukemia virus reverse transcriptase (RNaseH⁺) which is a DNA polymerase capable of generating a complementary cDNA strand and degrading the RNA sequence. In addition to 2) RNase inhibitor, 3) dNTPs that provide nucleotides for DNA synthesis, and 4) oligo(dT) and primers that allow the priming of DN synthesis on the polyA of mRNA and non-messenger RNA molecules. The mix is added to the 0.5 µg RNA sample and distributed into tubes with the following program: 5 min at 25°C, 20 min at 46°C for the reverse transcription and 1 min at 95°C to inactivate the reaction.

Afterwards, an amplification of the DNA fragments is performed. Reaction mixtures containing 2x SYBR green and primer mix specific to each interest gene are distributed in 96 well plates. The SYBR Green is a dye that binds to double stranded DNA. The PCR protocol consists of an initial denaturation step for 2 min at 94°C that consist of separating the double-stranded DNA templates. This step is followed by an annealing step where the temperature is lowered to 60°C

and where specific primers bind to target DNA. Then an extension step where DNA polymerase extends the primers by adding nucleotides to form DNA strand, occurs at 72°C. These steps are repeated for 40 cycles to ensure DNA amplification (Garibyan and Avashia, 2013).

When added, the SYBR green do not bind to the single-brand DNA. However, during the annealing step and the binding of primer to the complementary DNA, the SYBR green binds to the newly formed double brand. With each cycle, the SYBR dye then binds to every new copy of double stranded DNA and the fluorescence intensity increases proportionally with the quantity of DNA (**FIG.II.11**) (Cao *et al.*, 2020).

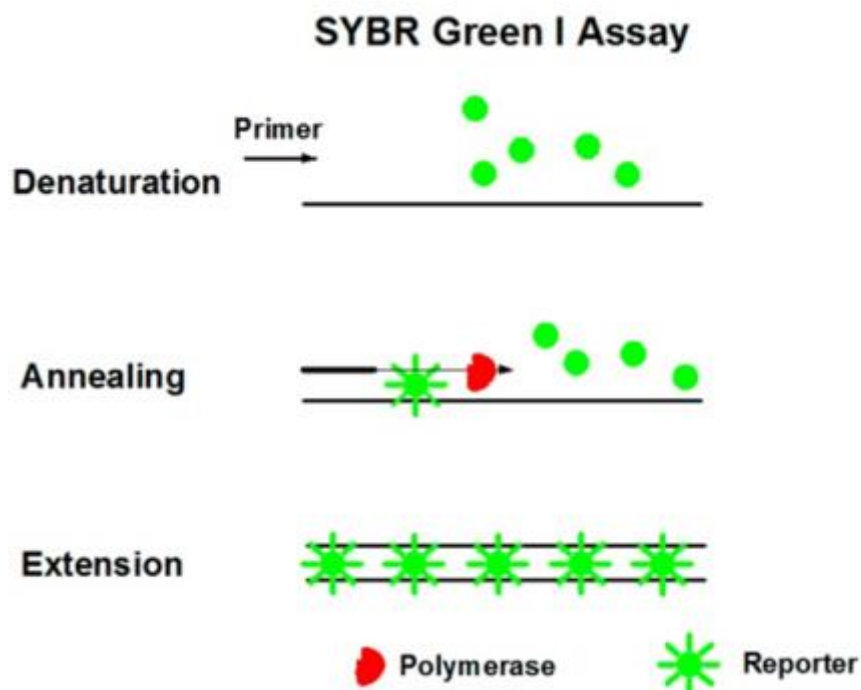


FIG.II.11. SYBR Green dye assay principle. It consists of an initial step of reaction setup where SYBR Green does not bind the single-stranded DNA. Then, SYBR green starts binding to the double stranded sequence of DNA that is binding the primers. Finally, the extension of the double-stranded DNA by the polymerase leads to an increase binding of SYBR green proportionally and therefore and increase in fluorescence can be measured by a thermocycler Modified from (Cao *et al.*, 2020).

At the end of qPCR, we obtain curves similar to this graph with 2 phases: exponential and non-exponential phase (**FIG.II.12**).

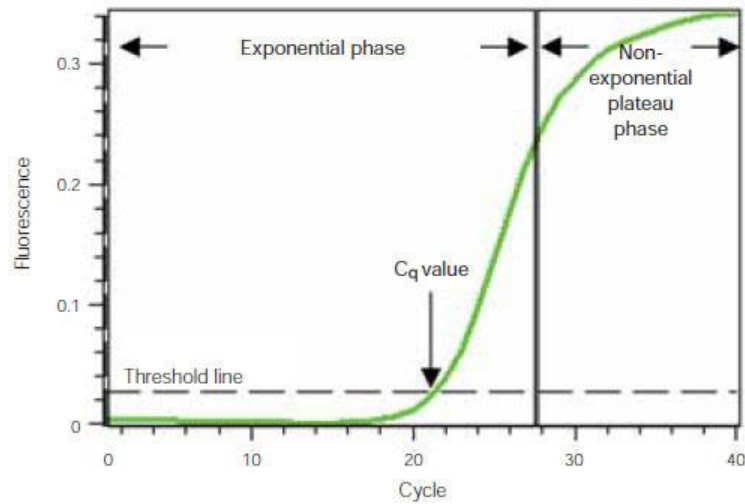


FIG.II.12. qPCR amplification plot. A graph presenting fluorescence versus cycle number. The Cq value is obtained at the intersection of the signal plot with the threshold baseline line (*What is Real-Time PCR (qPCR)?*, 2021).

After fixing the threshold, we obtain Cq values, which represents the cycle number at which the fluorescence of a target gene intersect with the threshold line. The Cq line is dependent of the initial amount of template present at the beginning of the reaction, hence for example, a low Cq indicates a high level of expression of the target gene (Pabinger *et al.*, 2014). Besides, we can quantify of the relative amount of RNA for each gene in each sample using the formula:

$$\text{Relative quantity of RNA} = \frac{E_{ref}^{Cq_{ref,i}}}{E_x^{Cq_{x,i}}}$$

With E_x the efficacy of the primer

$Cq_{x,i}$ the Cq value for the gene x and the sample i

Ref the reference gene chosen for the normalization

After normalization with EF1, PPIA and GUSB housekeeping genes (Table SI.2 from (Sales *et al.*, 2022), we use the formula

$$(\text{Relative quantity of RNA for the gene X, in the sample i}) = \frac{\sqrt[3]{E_{ref1}^{Cq_{ref1,i}} * E_{ref2}^{Cq_{ref2,i}} * E_{ref3}^{Cq_{ref3,i}}}}{E_x^{Cq_{X,i}}}$$

The efficacy of the primers is determined by a standard curve where a qPCR with serial dilutions of cDNA is performed to obtain a Cq versus concentration plot and determine a slope (p). The efficiency E is thus given at $E=10^{-1/p}$ and should be around 2.

II.C.3. Evaluation of pSmad signaling

Principle:

Immunofluorescence is an assay used to detect the presence and placement of target molecules through antibody/ antigen bond technology. The antibodies are usually coupled to fluorescent dyes that allow the visualization of the bound target molecules using a microscope.

The immunofluorescence assays can be performed in direct or indirect configurations. With a direct immunofluorescence, the fluorescent antibody directly binds to the antigen, while the indirect configuration consists on using an unmarked antibody that binds the antigen, as well as a secondary fluorescent antibody that binds the primary antibody (**FIG.II.13**) (Lager, 2020).

In our team, we use indirect immunofluorescence where a mice anti-pSmad 1/5/9 or mice anti-pSmad 2 primary antibody binds to the pSmad in the nucleus and a goat anti mice Alexa fluor + 555 secondary antibody. This strategy has the advantage of being less expensive since the secondary antibody can be used to detect several primary antibodies.

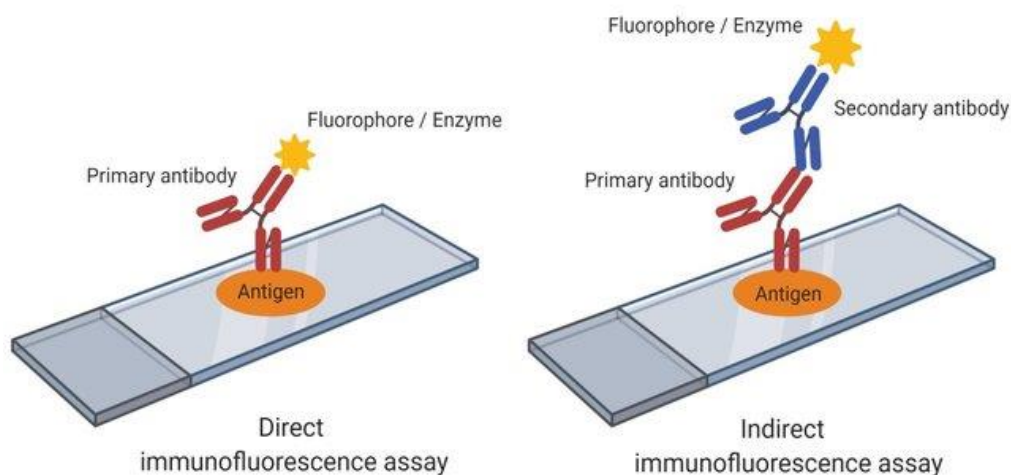


FIG.II.13. Schematics of Immunofluorescence assay. The immunofluorescence assay can be performed in two configurations: direct and indirect configuration. In the direct assay, one fluorescent antibody capable to bind to the antigen is used, while in the indirect assay a primary antibody binding the antigen as well as a fluorescent secondary antibody that binds the primary antibody (Lager, 2020).

Protocol

First, the cells in culture in the 96 wells plate are fixed with paraformaldehyde 3.7% solution (PFA) prepared in PBS, for 20 min under the hood. Depending on the experiment, a pre-fixation step is performed where PFA is added to the wells containing the medium, followed by a fixation step of 15 min. The plates are washed 3 times with PBS and then can be kept in PBS

in the fridge for up to a week, although usually the immunofluorescence experiment is done rapidly.

The first step of immunofluorescence consists on permeabilizing the cells using 0.2% Triton X-100 in PBS for 4 min, followed by 3 washing steps. Then the cells are treated by a blocking solution bovine serum albumin (BSA) to improve sensitivity by improving the signal-to-noise ratio and reducing background interference. After a thorough 3 times washing, the primary antibody diluted at 1/800 in a solution of 1% BSA in PBS, is added to the plates and incubated overnight at 4°C.

In the next day, the plates are washed 3 times for 5 min with PBS and incubated for 1h with secondary antibody diluted at 1/500 at room temperature, in a dark box. Afterwards, three washing steps are necessary followed by either F-actin labelling with Phalloin-Rhodamine, or by direct nucleus labelling. The nucleus labelling step is performed using either Hoechst 33342 diluted 1/2000 in PBS or with DAPI at 1/1000 in PBS with an incubation for 5 min in a dark box. The assay concludes with a three times washing step with PBS.

Data analysis

We do the acquisition of fluorescence images using an in cell analyzer imaging system which allows the automatic detection of samples at high content in multiple-well plates (**FIG.II.14**). The analysis protocol consists on acquiring 16 to 21 fields in each well with a limit of cell counting of 500 or 1000 cells per well, using two fluorescent channels blue for DAPI at 5 ms (acquisition time) and orange for the pSmad at 200 ms.



FIG.II.14. Image of an IN Cell analyzer setup with an acquisition computer (*IN Cell Analyzer High-Content Cellular Analysis System*, 2021).

The consecutive data analysis is carried out with InCarta® program using an analysis protocol with the following parameters: 14 μm a maximum diameter per cell, and 4000 as a max

fluorescence intensity, in order to define a mask on cells. After analysis, we obtain data are presented in excel files with data per cell, field of view or well. We then analyze the data per well by taking the nuclei intensity subtracted from background and do the mean and standard deviation for each condition.

II.C.3.1. Kinetic studies

The pSmad immunofluorescence readout is used for the kinetic studies. Indeed, we performed kinetic studies of both pSmad 2 and pSmad 1/5/9 in order to determine the optimal timing to do the drug experiments.

We initially used 96 well plates and PFA solution to fix the cells. However, since the experiment required fixation at different time points, we observed a reduction in the number of cells remaining in the other wells, indicating cell death. Therefore, we tested other fixing solutions such as methanol and acetone for their ability to fix the cells. As it will be explained in chapter V, each of these solutions presented some advantages and disadvantages. Thus, to surpass the cell dying issue, we used one CELLview plate for each time point and used PFA for fixation.

For each time point, we had film and glass conditions loaded with BMP-2 or TGF- β 1 or controls without any proteins. The loading of the proteins in the films have been previously described, while the glass condition consisted on adding soluble BMP-2 or TGF- β 1 (called sBMP-2 or sTGF- β 1). The bBMP-2 and bTGF- β 1 are used at 20 μ g/mL and 0.75 μ g/mL, while the sBMP-2 and sTGF- β 1 are used at 400 ng/mL and 10 ng/mL respectively.

II.C.3.2. Dose response

In order to determine the optimum concentration for the drug experiments, we did dose response studies where we determined the half-maximal effective concentration (EC50). For the sBMP-2 and sTGF- β 1 experiments, the concentrations range is 1 pg/mL to 10 μ g/mL and 0.001 pg/mL to 1 μ g/mL respectively. The cells were seeded at 10 000 cells/cm². We carried out experiments under 3 conditions: Glass condition at T=0 where the cells are seeded and the proteins are added immediately, Film condition at T=0 where cells are added to the films containing proteins soluble protein, and T=24h where the cells were seeded and the proteins are added after 24h. In the three conditions, the cells were fixed after 1h of protein addition using PFA (**FIG.II.15**).

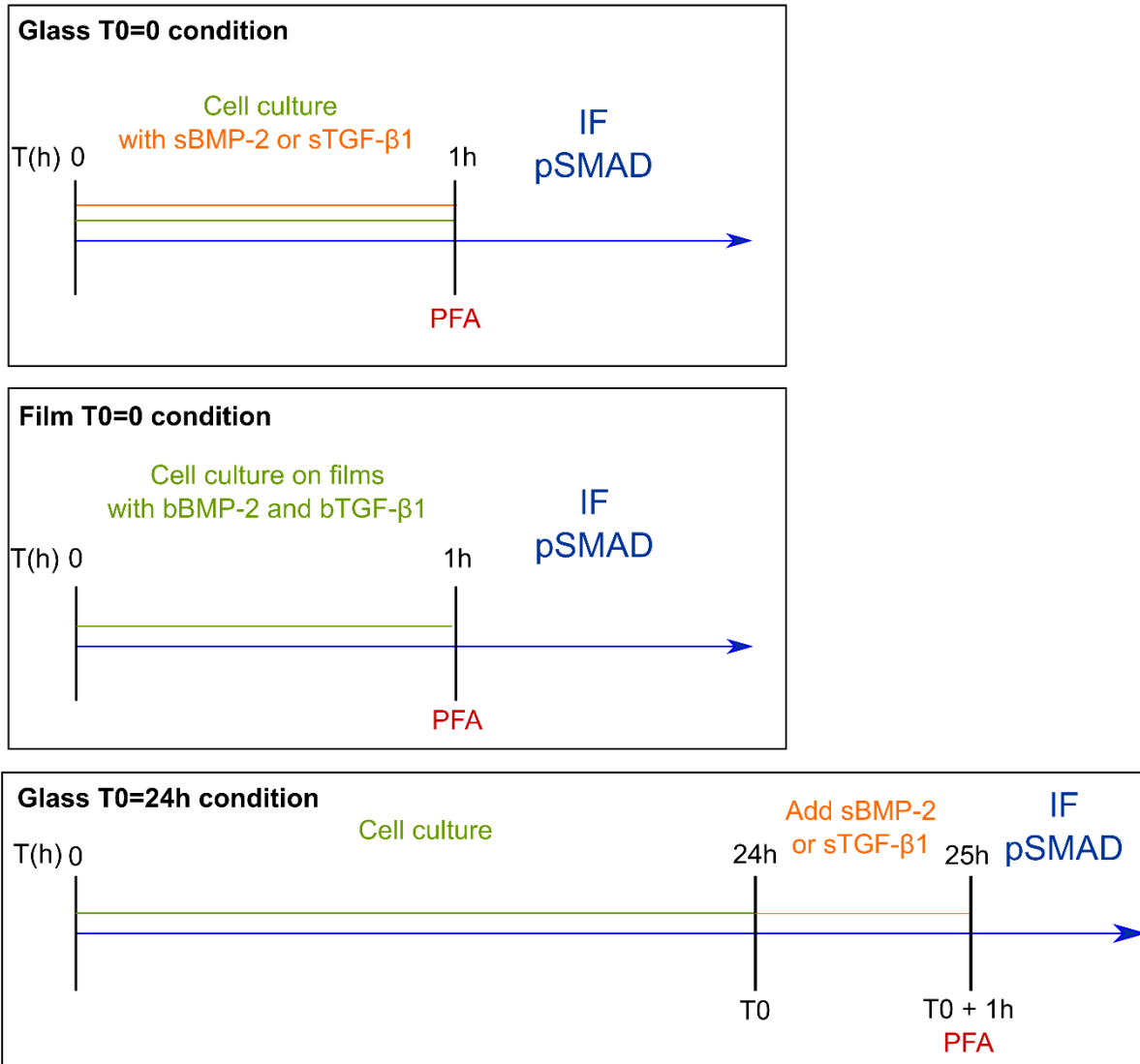


FIG.II.15. Schematics presenting the three experimental conditions of dose response assays. In the film and glass conditions at T=0, the cells were seeded on glass or on the biomimetic films loaded with bBMP-2 and bTGF-β1. The soluble proteins were added simultaneously with cell seeding for the glass condition, followed by a fixation with PFA at 1h. In the glass condition at T=24h, the proteins (BMP-2 and TGF-β1) were added after 24h of cell culture and the cells fixed with PFA after 1h of protein addition. Immunofluorescence assay was performed during the week following the experiment.

The EC50 value is determined by performing a fit using the dose response formula (*Equation: Sigmoidal dose-response*, 2021) with the origin program:

$$Y = \text{Bottom} + \frac{(\text{Top} - \text{Bottom})}{1 + 10^{\text{LogEC50} - x}}$$

With:

- X: BMP or TGF-β concentration

- Y: Measured fluorescence
- Bottom: the y value of the bottom of the curve
- Top: the y value of the top of the curve
- Log EC50: logarithm of EC50

II.C.3.3. Treatment with drug inhibitors against ALK receptors

The drug experiments are performed using BMP-2 at 20 $\mu\text{g/mL}$ for the film condition and 400 $\mu\text{g/mL}$ for the soluble condition, while TGF- β 1 was used at 0.75 $\mu\text{g/mL}$ for the film condition and 10 ng/mL for the soluble condition. We used three known drugs to do these experiments (*LDN-193189 2HCl*, 2021; *Galunisertib*, 2021; *Vactosertib*, 2021) (**FIG.II.16**):

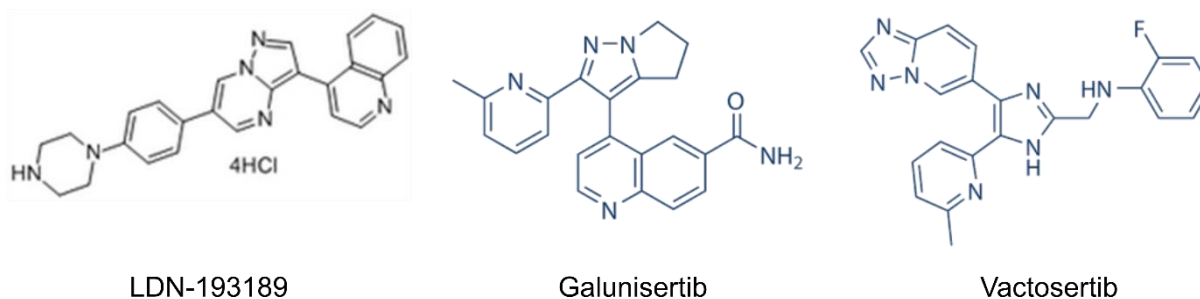


FIG.II.16. Chemical formulas of three ALK inhibitors. The chemical formulas of LDN-193189, Galunisertib and Vactosertib respectively.

LDN-193189 is pyrazoloquinoline analog of Dorsomorphin which inhibits mainly ALK1, ALK2 and ALK3 and ALK6. Their reported IC₅₀ determined by *in vitro* kinase assays, are 0.8, 0.8, 5.3 and 16.7 nM, respectively. This compound can also inhibit ALK4, ALK5 and ALK7 receptors at a concentration of 150 nM (*LDN-193189*, no date).

Galunisertib (LY2157299) is a cancer drug for hepatocellular carcinoma. It is inhibitor of TGF β receptor I (ALK5), developed by Eli Lilly company, although it was discontinued in 2020 due to the company's effort to focus on higher convicting programs. Their reported IC₅₀ is 56 nM determined by a cell-free assay (*Galunisertib (LY2157299)*, no date).

Vactosertib (TEW-7197, EW-7197) is an inhibitor of ALK4/ALK5 TGF- β receptor. Their reported IC₅₀ determined by in a cell-free assay, is 13 nM and 11 nM, respectively. It is currently being studied in phase II (*Vactosertib (TEW-7197)*, no date).

The experiments were performed at T=0 and consisted of seeding the cells and adding the proteins (BMP-2 or TGF- β 1) simultaneously, followed by an addition of drugs, or dimethyl sulfoxide (DMSO) for the control conditions after 15 min. The cells are subsequently fixed at

t=1 hour (**FIG.II.17**). The pSmad quantification is performed using the previously described immunofluorescence assay. We quantified pSmad 1/5/9 with BMP-2, and pSmad 2 with TGF- β 1. The image acquisition is performed as previously described.

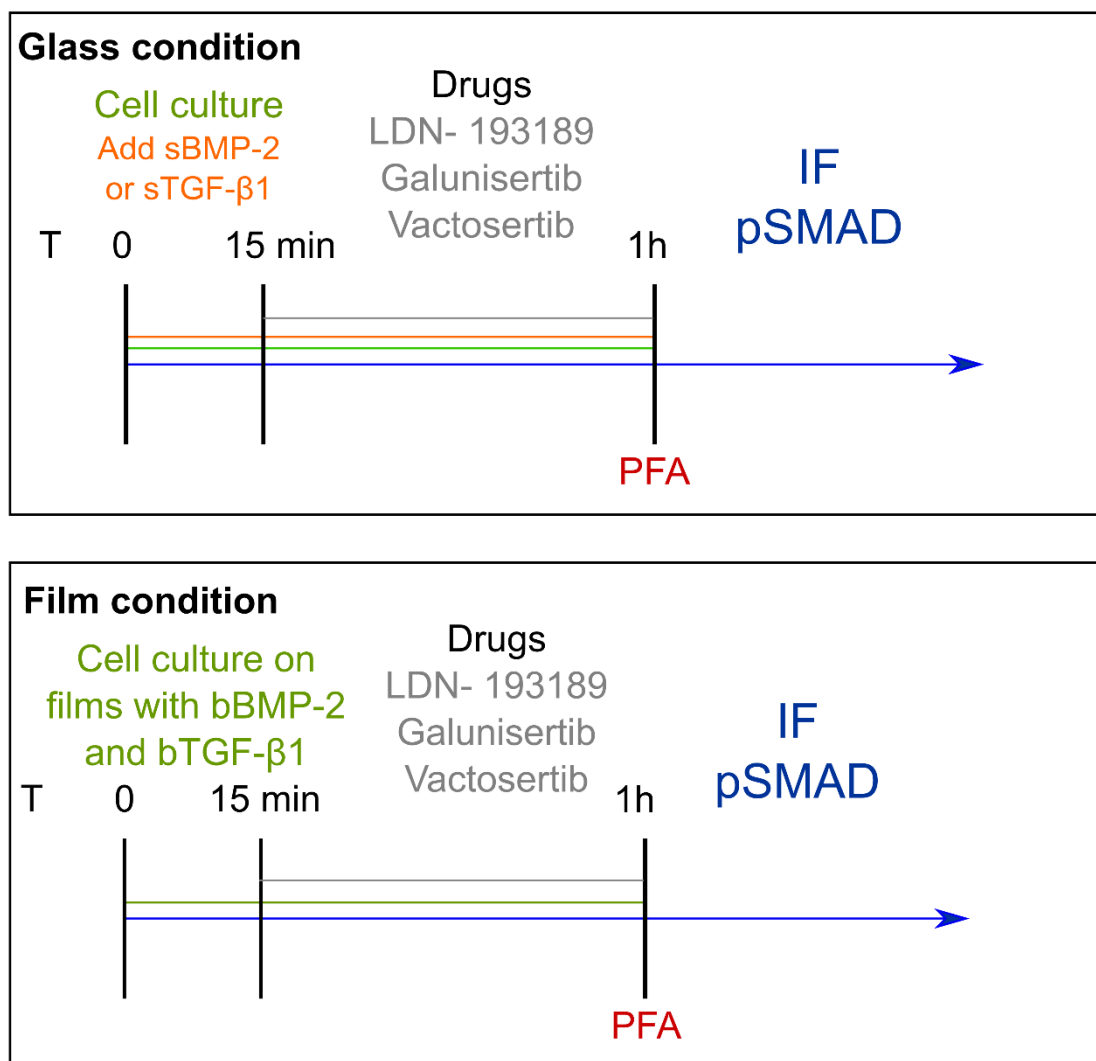


FIG.II.17. Schematics presenting the experimental conditions of drug assay. In the film condition, the cells were seeded on the films containing the matrix-bound BMP or TGF- β . At T=15 min, a serial dilution of one of the three drugs (LDN-193189 or Galunisertib or Vactosertib) is added. At T=1h the cells are fixed using PFA and the pSmad immunofluorescence assay is performed. In the glass conditions, the cells were seeded and the proteins (BMP-2 and TGF- β 1) were added simultaneously. At T=15 min, a serial dilution of one of the three drugs was added to the cells. The cells were fixed with PFA at T=1h and the pSmad immunofluorescence assay is performed.

Chapter III:
**High throughput measurements of bone
morphogenetic protein (BMP)/BMP
receptors interactions using bio-layer
interferometry**

III.1. Article Summary

The aim of this work was to determine the binding affinities of several BMPs with their receptors in similar experimental conditions, in order to compare them. Due to the lack of data in the literature and the variety of used protocols, it was difficult until now to compare the affinity of several BMP/BMPR couples and to better understand the properties of each BMP. First, we did a literature survey to compile all the experiments aimed at quantifying BMP/BMP receptor interactions. We noticed that SPR is the reference technique in the field. Recently, another optical technique, named the biolayer interferometry, has been developed to study protein/ligand interactions using reflectometric interference microscopy (Hänel and Gauglitz, 2002). The principle of this technique is to measure the interference pattern of white light reflected from an internal reference layer and the biomolecular layer.

Thus, we decided to use the bio-layer interferometry technique, which is available at the platform of the Institute of Structural Biology (IBS).

In order to better mimic the BMP/BMP interaction that occur *in vivo*, the experiments were done by immobilizing a commercialized extracellular domain (ECD) of a dimeric BMPR-Fc chimera on the surface of the biosensor and adding a dimer of BMP as analyte. We performed the experiments with four BMP (BMP-2, BMP-4, BMP-7 and BMP-9), five type-I BMP receptors (ALK1, 2, 3, 5, 6) and three type-II BMP receptors (BMPR-II, ACTR-IIA, ACTR-IIB).

With these kinetic experiments, we were able to determine the kinetic constants, such as the association constant (k_a), the dissociation constant (k_d) as well as the binding affinity constant K_D . Through this study, we observed a difference between the characteristics of BMP-2 and BMP-4. Indeed, BMP-2 had a better affinity for both type-I and type-II BMPR compared to BMP-4, notably due to the greater association of BMP-2 to these receptors as also demonstrated by the k_a . In addition, BMP-7 showed a preference for all three type-II BMPR in comparison to type-I BMPR. Moreover, BMP-9 demonstrated a high affinity for ALK1, as previously known in the literature, as well as ALK2 and ALK5 although with lower affinity. It also had a high affinity for type-II BMPRs. It is worth to note that all BMP were able to bind to the TGF- β 1 receptor ALK5, which indicates a possible crosstalk of TGF- β and BMP at the receptor level.

Kinetic studies with both type-I and type-II BMPR were performed to mimic the formation of heterocomplex *in vivo*. Unfortunately, the usage of both receptors did not yield any

improvement in the affinity compared to the binary BMP/BMPR interactions, although this phenomena of cooperativity is described in the literature.

Our results are promising as they reveal specific differences between the various BMPs in binding to the BMPR. Our study provides insights on the interaction of BMP/BMPR and helps with the understanding of their signaling pathway. It also opens the way to future studies using BLI for other receptors and growth factors. They also open the way for future cellular studies notably with ALK5, and receptors in a pathological context.

III.II. Article

High throughput measurements of bone morphogenetic protein (BMP)/BMP receptors interactions using bio-layer interferometry

(Published in Biointerphases journal)

Running title: Quantification of BMP/BMPR interactions

Running Authors: Khodr et al.

Valia Khodr^{1,2}, Paul Machillot^{1,2}, Elisa Migliorini^{1,2}, Jean-Baptiste Reiser³, Catherine Picart^{1,2*}

¹Interdisciplinary Research Institute of Grenoble (IRIG), ERL BRM 5000 (CNRS/UGA/CEA), CEA Grenoble, 17 rue des Martyrs, 38054 Grenoble cedex, France

² CNRS, Grenoble Institute of Technology, LMGP, UMR 5628, 3 Parvis Louis Néel, 38016 Grenoble

³ Institut de Biologie Structurale, UMR 5075, Univ. Grenoble Alpes, CEA, CNRS, IBS, F-38000 Grenoble, France

*Corresponding author: Catherine Picart - E-mail: catherine.picart@cea.fr

Abbreviations

BMP-2, bone morphogenetic protein 2; BMP-4, bone morphogenetic protein 4; BMP-7, bone morphogenetic protein 7; BMP-9, bone morphogenetic protein 9; BMPR, Bone morphogenetic protein receptor; ALK1, Activin receptor-like kinase 1; ALK2, Activin receptor-like kinase 2; ALK3, Activin receptor-like kinase 3; ALK5, Activin receptor-like kinase 5; ALK6, Activin receptor-like kinase 6; ECD, extracellular domain; TGF β , transforming growth factor; TGF β R, transforming growth factor receptor; AMHR-II, Anti-Müllerian hormone receptor II; BLI, Bio-layer interferometry; SPR, Surface plasmon resonance.

Abstract

Bone morphogenetic proteins (BMP) are an important family of growth factors playing a role in a large number of physiological and pathological processes, including bone homeostasis, tissue regeneration and cancers. *In vivo*, BMPs bind successively to both BMP receptors (BMPR) of type I and type II, and a promiscuity has been reported. In this study, we used bio-layer interferometry to perform parallel real-time biosensing and to deduce the kinetic parameters (k_a , k_d) and the equilibrium constant (K_D) for a large range of BMPs/BMPR combinations in similar experimental conditions. We selected four members of the BMP family (BMP-2, 4, 7, 9) known for their physiological relevance and studied their interactions with five type-I BMP receptors (ALK1, 2, 3, 5, 6) and three type-II BMP receptors (BMPR-II, ACTR-IIA, ACTR-IIB). We reveal that BMP-2 and BMP-4 behave differently, especially regarding their kinetic interactions and affinities with the type-II BMPR. We found that BMP-7 has a higher affinity for the type-II BMPR receptor ACTR-IIA and a tenfold lower affinity with the type-I receptors. While BMP-9 has a high and similar affinity for all type-II receptors, it can interact with ALK5 and ALK2, in addition to ALK1. Interestingly, we also found that all BMPs can interact with ALK5. The interaction between BMPs and both type-I and type II receptors in a ternary complex did not reveal further cooperativity. Our work provides a synthetic view of the interactions of these BMPs with their receptors and paves the way for future studies on their cell-type and receptor specific signaling pathways.

I. INTRODUCTION

Bone morphogenetic proteins (BMPs) are members of the transforming growth factor- β (TGF β) superfamily who have been widely studied in view of the numerous physiological and pathological roles [1], [2], including embryogenesis, development, bone homeostasis and regeneration and cancers [3]. The BMP family comprises more than 15 different ligands in humans, which have been grouped into four different subfamilies depending on their functions: BMP-2/4, BMP-5/6/7/8, BMP-9/10 and GDF5-6-7 [3]–[6].

Among these BMPs, BMP-2 is known for its role in morphogenesis, bone regeneration and musculoskeletal disorders [7], [8]. In addition, BMP-4 plays a part in hematopoiesis and leukemia [9] while BMP-7 is involved in inflammation and glucose homeostasis [10]. BMP-9 and 10 have a major role in cardiovascular disease and anemia [11]. Furthermore, BMPs have been also reported to have an increasing role in cancer [12].

BMPs are active in their dimeric form and interact at the cell membrane with two sub-types of specific receptors (BMPR): type-I and type II BMPRs [2], [4], [5], [13]. Seven different type-I receptors (ALK1 to ALK7) and five different type-II receptors (BMPR-II, ACTR-IIA, ACTR-IIB, TGF β R-II and AMHR-II) are reported. BMPR-II, ACTR-IIA, ACTR-IIB associated to binding of all BMPs, while TGF β R-II and AMHR-II are reported to be specific of TGF β ligands and anti-Müllerian hormone respectively, but not BMPs. BMPs have been reported to mostly bind to four receptors [3]: ALK1, ALK2 (also named ACTR-IA), ALK3 (also named BMPR-IA) and ALK6 (also named BMPR-IB). Each of these receptors has important physiological roles. For instance, for the type-I BMPRs, ALK1 is the predominant receptor in endothelial cells and is involved in cardiovascular diseases [11]. ALK2 is an important receptor for bone homeostasis as a mutation in the ALK2 receptor is involved in a rare skeletal disorder named fibrodysplasia ossificans progressiva (FOP) and in a rare pediatric glioblastoma named diffuse intrinsic pontine glioblastoma (DIPG) [14]. ALK3 plays a major role in several cancers, including breast and colorectal cancer [12]. ALK6 plays a role in chronic myeloid leukemia [9], [15]. ALK5 is reported to be a TGF β receptor that is present in mesenchymal stem cells [16]. The three type-II receptors are usually considered to have similar roles in the signaling pathway associated to BMPs [3] but BMPR-II has likely been the most studied. Indeed, it was recently shown to play a protective role for endothelial cells from increased TGF β responses and altered cell mechanics [34].

BMP signaling is initiated by the binding of BMPs to type-I BMPRs with high affinity prompting the constitutively active type-II BMPRs to come in close proximity to the formed complex, and induce the trans-phosphorylation of the glycine/serine-rich region (GS-box) preceding the kinase domain. Thus, leading to the formation of a ternary complex of BMP/type-I BMPR/type-II BMPR [1], [35]–[37]. In this signaling pathway, the high number of BMP ligands (≈ 20) compared to the low number of BMP receptors (four type-I and three type-II receptors) indicates the presence of a promiscuous mechanism in which a given BMP can bind several receptors with distinct binding affinities [6], [38]. Furthermore, it has been reported that high affinity ligands can compete with low affinity ligands for the binding of BMPRs and therefore can antagonize their signaling [39]. The previously described structures of several BMPs (BMP-2 pdb: 3BMP, BMP-7 pdb: 1BMP, BMP-9 pdb: 1ZKZ) lead us to gain insights on the structural differences between them. For example, it was described that most of the residues existing in BMP-2 wrist epitope are invariant or replaced by isofunctional side chains in BMP-7. Similarly, most binding residues in the knuckle region of BMP-2 are invariant in

BMP-7 and BMP-4, suggesting that the specificity is only determined by a small subset of residues[17]. However, the lack of comparative structural studies of the binding sites of BMP and BMPR are needed to better understand the cause of this promiscuous binding. A better knowledge of the detailed binding characteristics of the BMPs to the BMPRs will help to identify the high affinity couples and to gain insight into the initiation of BMP signaling pathways.

The data available from the literature of BMP/BMPR interactions are assembled in Table.1. To date, most of the characterizations of BMP/BMPR interactions have been determined using surface plasmon resonance (SPR), which can be considered as a gold standard in the field. However, the direct comparison of KD for the different BMPs and BMP receptors is difficult since data has been obtained using various experimental conditions (different protein constructs, different immobilization strategies, different buffers, different SPR instruments...), which introduces a large variability in the experimental data. In addition, this data focused on particular BMP/BMPR couples and there is a lack of data for BMP-4 and 9 as well as for ALK1.

Among all the biophysical methods available today to characterize protein-protein interactions, the reflectometric interference spectroscopy (RifS) [40], [41] is a label-free optical method based on white light interferences at layers of sensors . A commercially-available setup known as bio-layer interferometry (BLI) enables to perform parallel real-time binding measurements and characterization of biomolecule interactions. It is increasingly used to study kinetic constants and binding affinities of protein-protein and protein-nucleic acid interactions [41]–[44] and it has only recently begun to be used to study BMP/activin A chimera interactions [23].

In the present study, our aim was to quantify in similar experimental conditions and a large set of BMP/BMPR interactions in a parallel manner, in order to directly compare their kinetic parameters and binding affinities. We decided to focus on four BMPs that are among the most widely studied: BMP-2, BMP-4, BMP-7 and BMP-9 [45]. For the type-I BMP receptors, we considered ALK1, ALK2, ALK3, ALK6 and added ALK5 known as an essential TGF β receptor [46], since it is involved in the signaling of BMP-responsive cells such as mesenchymal stem cells [16]. We studied the three type-II BMP receptors (BMPR-II, ACTR-IIA and ACTR-IIB).

TABLE 1. Literature study of all the KD (nM) of the interactions between couples of BMP and their receptors (type I and type II BMPR). The experiments were usually performed in one of the two configurations: in red, when the BMPR is immobilized and in blue, when the BMP is immobilized. BLI: Bio-layer interferometry, Confo: Conformation, Tech. Technique.

K _D (nM)	Confo.	Tech.	ALK1	ALK2	ALK3	ALK5	ALK6	BMPR-II	ACTR-IIA	ACTR-IIB
BMP-2	BMPR Immobilized	SPR BLI			0,004 – 2,6 [17]– [22] 1.1[23]		2,5–11 [17], [18], [20]–[22] 1.1[23]	45-100 [17], [18], [21] 26.7 [23]	14 - 80 [17]–[19], [21], [24], [25] 52.7 [23]	6 - 36 [18], [19], [21] 8 [23]
	BMP immobilized	SPR	N.D [26]	>400 000 [27]	10 – 330 [21], [26], [27]		95-350 [21], [27]		3800-5400 [25], [27]	
BMP-4	BMPR Immobilized	SPR			0.06 [22]		0.22 [22]			
	BMP immobilized	SPR			1.2 – 47 [28], [29]					
BMP-7	BMPR Immobilized	SPR		>500 [18], [21]	2 – 1680 [18], [19], [21], [22]		0.3 - 9 [18], [21], [22]	25 – 100 [18], [21]	1 – 5.1 [18], [19], [21], [24], [25]	2 – 10 [18], [19], [21]
	BMP immobilized	SPR		55 000 – 143 000 [25], [27]	1900–10 000 [21], [27]		750-1000 [21], [27]		900 – 1700 [25], [27]	
BMP-9	BMPR Immobilized	SPR	<0.008 – 0,045 [30]–[33]					0.6 – 3.3 [30], [31]	6.4 – 42.7 [30], [31]	0.02 – 1.4 [30], [31]
	BMP immobilized	SPR	2 – 45 [26], [33]		N.D [26]					

II. EXPERIMENTAL SECTION

A. Protein and reagents

Apart from BMP-2 which was gifted by Bioventus (North Carolina, USA), BMPs and extracellular domains (ECD) of the BMPR-FC chimeras were bought from Sigma Aldrich (Missouri, USA) and R&D systems (Minnesota, USA) respectively. BMP-2 (Bioventus, North Carolina, USA) and BMP-7 (catalog number: 120-03P) and BMP-9 (catalog number: 120-07) (Peprtech, Rocky Hill, USA) are produced in Chinese hamster ovary (CHO) cells while BMP-4 (Catalog number 120-05ET) was produced in *Escherichia coli* (Peprtech, Rocky Hill, USA). The Anti-hIgG Fc (AHC) capture biosensors were purchased from ForteBio (California, USA), and the SPR protein A coated chips were purchased from GE Healthcare Life Sciences (Illinois,

USA). The buffer was made of 20 mM HEPES at pH 7.4 with 150 mM NaCl (name hereafter HEPES-NaCl) and 0.02% Tween 20 while the regeneration buffer was made of 10 mM glycine at pH 1.7 (named hereafter regeneration buffer). They were all prepared in-house.

B. BLI kinetics interaction experiments

All the BLI experiments were performed using an OctetRED96e apparatus from Pall/FortéBio (California, U.S) and data were recorded with the manufacturer software (Data Acquisition v11.11). All proteins were solubilized following the supplier instruction in Hepes-NaCl buffer. The analysis protocol was adapted from previous studies [23], [30]. In details, prior any capture, the BMPR-Fc samples were first diluted in the Hepes-NaCl buffer. For the association phase, the BMPs were diluted in 2-fold serial dilutions in Hepes-NaCl buffer. 0.2 ml of each sample and buffer were disposed in wells of black 96-well plates (Nunc F96 MicroWell, Thermo Fisher Scientific), maintained at 25°C and agitated at 1000 r.p.m. the whole time. Prior each assay, all biosensors were pre-wetted in 0.2 ml of Hepes-buffer for 10 min, followed by monitored equilibration for 60 or 120 s. Anti-hIgG Fc (AHC) capture biosensors (FortéBio) were loaded with each ligand for 200 s until to reach a spectrum shift between 0.8 and 1.1 nm depending of BMPR-Fc, followed by an additional equilibration step of 60 s or 120 s in Hepes-NaCl buffer. Association phases were monitored during dipping the functionalized biosensors in analyte solutions of different concentrations between 2 and 80 nM for 400 s, and the dissociation phases in the buffer for 400 s. To assess and monitor analyte unspecific binding, blank biosensors were treated with the same procedures but replacing the ligand solutions by analysis buffer. All sensors were fully regenerated between experiments with different BMPRs by dipping for 30s in regeneration buffer. All measurements were performed three times in independent experiments.

Kinetics data were analyzed using the manufacturer software (Data analysis HT v11.1). The “blank” signal from the biosensor in the presence of the Hepes-NaCl buffer was subtracted from the signal obtained from each functionalized biosensor and each analyte concentration. The kinetic signals were then fitted using a global/local method and 1:1 Langmuir or 2:1 heterogeneous ligand model. Affinity constants were calculated from the ratio k_d/k_a values. The reported values are given as mean + SD obtained from three independent experiments.

C. Surface plasmon resonance experiments

All surface plasmon resonance experiments were performed using a Biacore T200 apparatus (GE Healthcare Life Sciences/Biacore, Illinois, U.S) and data were recorded using the manufacturer software (Biacore control software v2.0). All protein samples were solubilized following the supplier instruction in analysis buffer prior any experiment. Prior to capture, the BMPR-Fc samples were first diluted in analysis buffer. For association phase, BMP samples were diluted at concentration between 0.2 and 6.4 nM in 2-fold serial dilutions in the HEPES-NaCl buffer. Sensor chips and system were pre-equilibrated in HEPES-NaCl buffer prior any injection. The protein A sensor chips (GE Healthcare Lifesciences) were loaded by injecting each ligand for 100 s until to reach a signal level between 100 and 120 arbitrary response units (R.U.) depending of BMPR-Fc, followed by an additional equilibration step of several minutes in analysis buffer. Association phases were monitored during injections over the functionalized surfaces of analyte solutions of different concentrations for 300 s, and the dissociation phases of analysis buffer for 300 s. To assess and monitor analyte unspecific binding, blank surfaces were treated with the same procedures but replacing the ligand solutions by analysis buffer. All surfaces were fully regenerated between experiments with different BMPR-Fc by injecting for 30s regeneration buffer. Two independent experiments were performed. Kinetic data were processed with the manufacturer software (Biacore Evaluation software v3.1). Signals from the reference surface were subtracted from the signals obtained from each functionalized ship. Resulting specific kinetics signals were then fitted using the 1:1 Langmuir model. Affinity constants were calculated from the ratio k_d/k_a values. Reported values are obtained by averaging the values obtained from the replicates and reported errors as the standard deviation.

III. RESULTS

We first performed a literature study to gain information on the state-of-the-art regarding BMP/BMPR interactions. Table.1 provides a view of the KD values, which are in the nM range for the highest affinity interactions. S1.Table.1 gives the detailed information obtained from each published study. We first note that all experiments, but one using the commercially-available BLI setup [23], were conducted using SPR with two configurations to perform the experiments: the first configuration consists in immobilizing the BMPs on the sensor chip while the second consists in immobilizing the BMPRs, this second strategy being the most common. In terms of immobilization protocols, we noted that several strategies were proposed, which can be grouped in three major categories (S1.Table.1): i) using biotinylated BMPR coupled to

streptavidin-coated surfaces; ii) using BMPR-Fc captured on anti-Fc coated sensors and iii) direct immobilization of BMPR using an amine coupling strategy.

Looking at the published studies (Table.1 and S1.Table.1), it appears from that for a given BMP/BMPR couple; the range of measured KD can be very broad. These discrepancies likely arise from the differences in experimental details, including immobilization strategies, experimental working conditions, the usage of monomeric BMPR ectodomains and the biochemistry of BMPs itself. Moreover, since BMP-2 and BMP-4 are usually considered to behave similarly [3], several studies were performed only on BMP-2 interaction with type-II BMPRs (BMPR-II, ACTR-IIA and ACTR-IIB) and with type-I BMPR ALK2, but there is no such study for BMP-4. We also noted a unavailability of data for the interactions of BMP-2, 4 and 7 with ALK1 since it was reported to be the major BMP-9 receptor [11]. Lastly, we noticed the absence of data on ALK5 (TGF β R-I) with any of the chosen BMPs, since it was traditionally considered solely as a TGF β receptor [46] but was also shown to be a central point in BMP/TGF β signaling [47].

A. Dimeric state of BMPs and BMPR

The commercially available proteins that we used were produced in CHO for BMP-2, 7 and 9 or in E.coli for BMP-4. The BMPR coupled to Fc fragments (BMPR-Fc) were produced in mouse myeloma NS0 cells, except for ACTR-IIA that was produced in CHO cells. We verified the biochemical state (monomeric or dimeric) of all BMPs and BMPR-Fc by gel electrophoresis in both non-reducing and reducing conditions (S2.Fig.1). The BMPs were mostly dimeric, as expected [6], and migrate at ≈ 26 kDa in non-reducing conditions, and at ≈ 13 kDa in reducing conditions. Since the Fc fragment form dimers, the BMPR chimeras are also present in dimeric state and migrate at 90 and 110 kDa in non-reducing condition and in a monomeric form with a band between 45 and 55 kDa in reducing conditions (S2.Fig.1).

B. Immobilization of BMPR on the biosensor

In vivo, the BMPs are soluble proteins that localize in the extracellular matrix or in blood for BMP-9. They can then be considered to diffuse freely in a 3D space. The BMPRs are trans-membrane proteins that are localized at the cellular membrane and are thus diffusing in a 2D space. For this reason, it is likely that the order of magnitude of the diffusion of BMPR is similar to that of lipids in a membrane ($\approx 1 \mu\text{m}^2/\text{s}$) while that of BMPs is similar to a protein diffusing freely ($\approx 100 \mu\text{m}^2/\text{s}$) [48]. We thus choose to immobilize the BMPRs at the biosensor surface and to adsorb BMPs at their surface to better mimic the *in vivo* situation.

In order to find a protocol applicable to all BMP/BMPR couples, we considered several capture strategies for BMPR immobilization at the biosensor surface. The same previously-published capture methods used for SPR, including biotinylated ligand/streptavidin surface, amine coupling absorption or Fc chimera/anti-human IgG or protein A surfaces were considered (S1.Table.1) [17], [20], [24], [25]. Since all the BMPR-Fc chimeras were commercially-available, and as anti-Fc fragment-coated biosensors are known to more stable than protein A [23], [30], we selected this strategy that consists in immobilizing the BMPR-Fc chimeras, formed by homodimers of BMPRs and an Fc fragment, to the anti-Fc coated biosensor surfaces (Fig.1A and Material and methods). This configuration presents the advantage of immobilizing all of the BMPR homogeneously in one orientation, with their binding site accessible to BMPs.

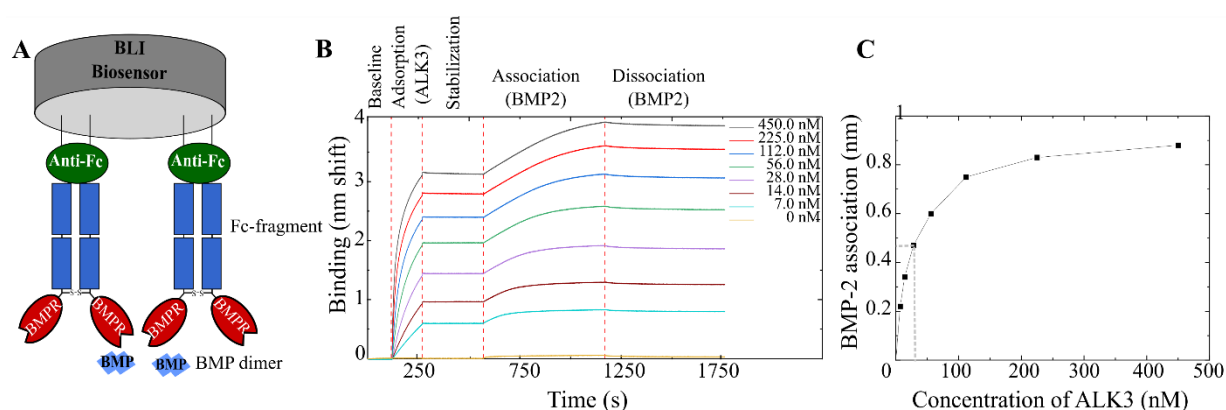


FIGURE 1. Adsorption strategy of BMPR-Fc on the biosensors. **A)** Schematic representation of the adsorption strategy where an anti-Fc-coated biosensor binds the Fc-Receptor chimera. **B)** Preliminary experiment where ALK3 receptor was adsorbed at increasing concentrations (from 7 nM to 450 nM) and set to interact with BMP-2 at a concentration of 5 nM. **C)** The interaction signal of BMP-2 to ALK3 given in nm shift, plotted as a function of ALK3 initial concentration in solution. Data were obtained using OctetRED96e.

In order to determine a suitable adsorption density of the BMPRs on the biosensors, we performed preliminary assays with ALK3 receptor immobilized at increasing densities leading to a signal between 0.5 to 3 nm of spectral shift (nm) after a fixed contact time of 150 s. The functionalized surfaces were then set in contact with BMP-2 at a constant concentration of 5 nM to proceed to BMP-2 adsorption (Fig.1B). From the response at equilibrium vs. ALK3 concentration (Fig.1C), we selected the concentration of ALK3 \approx 28 nM as an optimal immobilization concentration, leading to an association signal of \approx 0.5 nm after 600s, since it

is one of the lowest concentrations before saturation of the binding sites that yields an acceptable signal.

C. Interaction of BMPs with type-I BMPR and type-II BMPR

The kinetic interaction studies were then performed using the same protocol for the four BMPs with BMPRs. All BMPRs were adsorbed at densities corresponding to a spectral shift between 0.8 and 1.1 nm. The BMP concentrations were varied over a large range ranging from 2 nM to 80 nM (Fig.2). Representative experimental curves for BMP-2/ALK3, BMP-9/ALK1, BMP-2/BMPR-II and BMP-7/ACTR-IIA are shown in Fig.2 (respectively panel A-D).

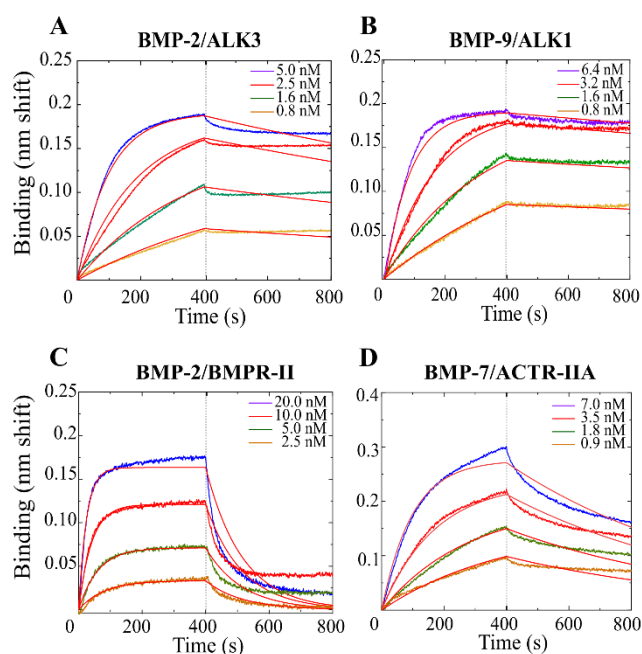


FIGURE 2. Examples of binding kinetics between type-I BMPRs and BMPs. A) BMP-2/ALK3, **B)** BMP-9/ALK1 and between type-II BMP and BMPs, with **C)** BMP-2/BMPR-II and **D)** BMP-7/ACTR-IIA. Data were obtained using OctetRED96e. The 1:1 Langmuir fit was used to fit the experimental data.

To determine the kinetic parameters, the 1:1 Langmuir model binding model has been used. Indeed, it has been shown in structural studies [17], [24], [49] that the BMP/BMP receptor interaction can be considered as bimolecular: It was reported that BMP dimers comprise two distinct pairs of binding sites: one for type-I BMPR, called “the wrist” and the other for type-II BMPR, called “the knuckle”. While the type I interface is a large continuous area formed by residues from both BMP monomers, the interface with type II is composed only of amino-acids from one BMP monomer [5], as seen in the example of BMP-2/ALK3/ACTR-IIA (pdb: 2H64) [50] (Fig.3A). Thus, a one to one binding is expected.

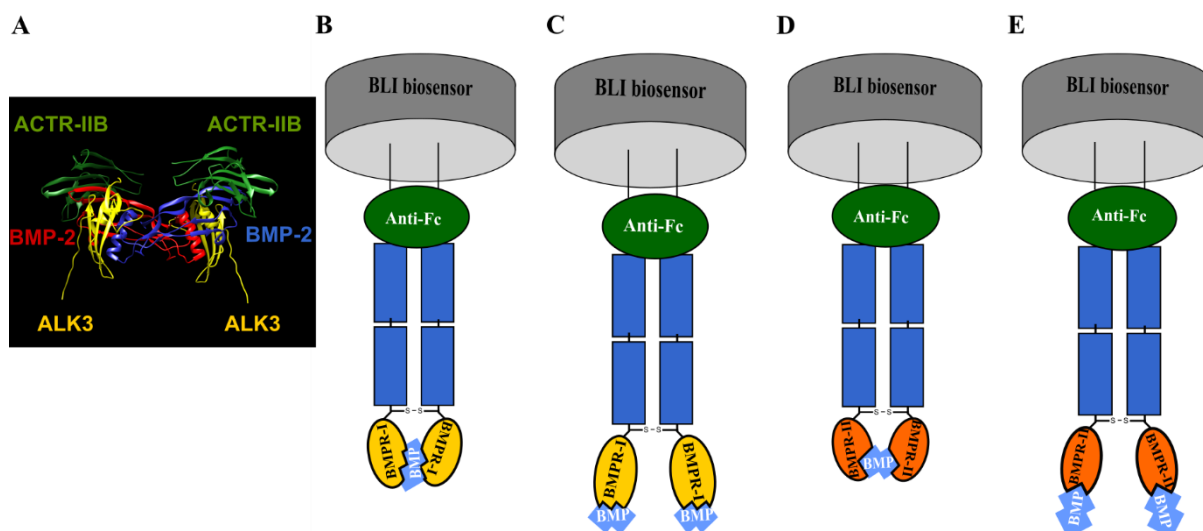


FIGURE 3. A schematic representation of the different binding models in the BLI BMP/BMPR interaction. A) Picture of BMP-2/ALK3/ACTR-IIB ternary complex (PDB:2H64) adapted from Weber, D. et al *BMC struct Biol* 2007 (Weber *et al.*, 2007). B) Association of the two binding sites of BMP dimer to two type-I BMPR. C) Association of one binding site of BMP dimer with one type-I BMPR. D) Association of the two binding sites of BMP with two type-II BMPR. E) Association of one binding site of BMP dimer with type-II BMPR.

In the present case, since the Fc chimera induces a dimerization of the BMPR, two possible binding modes are possible (Fig.3.B-E): one BMP molecule binding to two proximate BMPR binding domains (model B or D) or one BMP molecule binding to one BMPR binding domain (model C or E). Nonetheless, since BMP dimers are fully symmetrical, all binding models may lead to 1:1 binding kinetic. It could be argued that a phenomenon of avidity could be occurring in the Fig.3 B and D, and a more complicated model should be applied. Nevertheless, to be consistent with the literature, we applied the commonly-used 1:1 Langmuir model to fit the experimental data as it has been regularly employed in previous studies, notably in the ones with a Fc adsorption strategy, and in the one using BLI technique to determine kinetics parameters [19], [23], [25], [30]. Furthermore, the R2 values of the fits, presented in S3 table.2 and S4 table.3, are in majority around 0.95 and higher which indicates an acceptable fit.

A fast association was generally observed for all the BMPs interacting with the type-I BMPR, but differences in the dissociation rate are seen. The association constant (k_a) and dissociation constant (k_d) that were extracted from the fit of each interaction curve are presented in Fig.4 as well as S3.table.2 and S4.table.3. BMP-2 and BMP-4 exhibit a high k_a ($\approx 15 \times 10^5 \text{ M}^{-1} \cdot \text{s}^{-1}$ for BMP-2 and $\approx 5 \times 10^5 \text{ M}^{-1} \cdot \text{s}^{-1}$ for BMP-4), and low k_d with both ALK3 and ALK6 ($\approx 0.5 \times 10^{-3} \text{ s}^{-1}$ for BMP-2 and $\approx 1.5 \times 10^{-3} \text{ s}^{-1}$ for BMP-4), indicating a fast association and slow

dissociation to these receptors. Furthermore, BMP-2 associates and dissociates in a similar manner to ALK1, ALK2, ALK5 ($k_a \approx 4 \times 10^5 \text{ M}^{-1} \cdot \text{s}^{-1}$ and $k_d \approx 3 \times 10^{-3} \text{ s}^{-1}$) and to the three type-II BMPRs ($k_a \approx 11 \times 10^5 \text{ M}^{-1} \cdot \text{s}^{-1}$ and $k_d \approx 6 \times 10^{-3} \text{ s}^{-1}$). In comparison to BMP-2, BMP-4 associates more slowly to these receptors.

BMP-7 demonstrates a slow association to all the type-I BMPRs ($\approx 2 \times 10^5 \text{ M}^{-1} \cdot \text{s}^{-1}$), in addition to a slow association ($\approx 6 \times 10^5 \text{ M}^{-1} \cdot \text{s}^{-1}$), and dissociation ($\approx 2 \times 10^{-3} \text{ s}^{-1}$) to type-II BMPRs. Regarding BMP-9, it exhibits a fast association ($15.0 \pm 3.5 \times 10^5 \text{ M}^{-1} \cdot \text{s}^{-1}$) and a very slow dissociation ($0.2 \pm 0.1 \times 10^{-3} \text{ s}^{-1}$) to ALK1 and type-II BMPR ($k_a \approx 20 \times 10^5 \text{ M}^{-1} \cdot \text{s}^{-1}$ and $k_d \approx 3.3 \pm \times 10^{-3} \text{ s}^{-1}$). BMP-9 also presents a slow association and fast dissociation from ALK2 and ALK5 ($k_a \approx 2 \times 10^5 \text{ M}^{-1} \cdot \text{s}^{-1}$ and $k_d \approx 3 \times 10^{-3} \text{ s}^{-1}$), but it does not interact with ALK3 and ALK6.

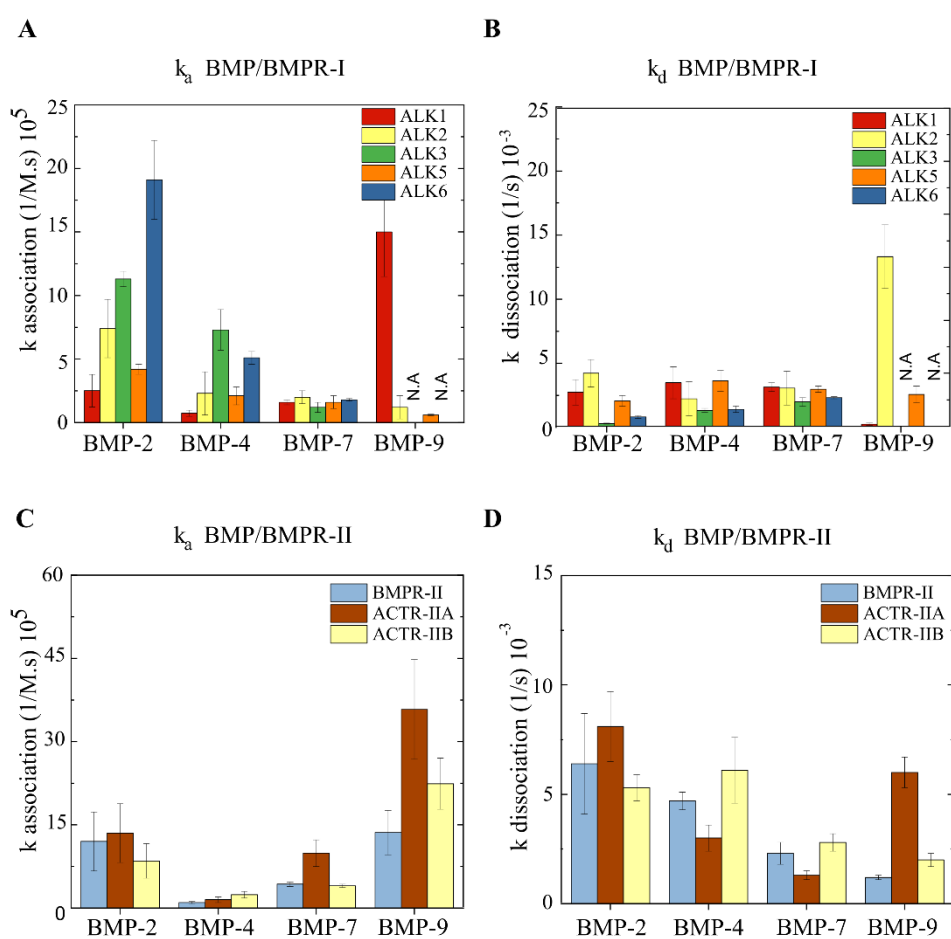


FIGURE 4. Histograms presenting the association constants (k_a) and the dissociation constants (k_d). k_a of **A)** BMP/type-I BMPR and **B)** BMP/type-II BMPR interactions and k_d of **C)** BMP/type-I BMPR and **D)** BMP/type-II BMPR interactions. For BMP-9/ALK3 AND BMP-9/ALK6, the signal was very low (N.A.). The error bars represent the s.d (n=3).

Next, we calculated the equilibrium affinity constant K_D (equal to the ratio of k_d over k_a). BMPs present a generally high affinity to all BMPRs ranging from 133 to 0.2 nM for high affinity interactions. The lowest K_D values are highlighted in dark blue (Table.2).

TABLE 2. Binding affinities (K_D in nM) of BMP/BMPR interactions. Tables summarizing the K_D (nM) of the BMP/BMPR interactions for: A) type I and B) type II receptors, obtained from the kinetic experiments in a conformation where the BMPR is immobilized. The interactions between BMP-9/ALK3 and BMP-9/ALK6 yielded a very low signal (N.A). The high affinity couples are colored in dark blue. The error values represent the s.d (n=3).

A.

BMPR BMP	ALK1	ALK2 (ACTR-I)	ALK3 (BMPR-IA)	ALK5 (TGFβR-I)	ALK6 (BMPR-IB)
BMP-2	13.0 \pm 1.6	7.0 \pm 2.3	0.21 \pm 0.03	5.8 \pm 1.1	0.5 \pm 0.1
BMP-4	55.4 \pm 4.0	10.5 \pm 3.8	1.7 \pm 0.5	21.9 \pm 6.6	3.1 \pm 0.3
BMP-7	23.1 \pm 2.1	18.4 \pm 3.8	19.0 \pm 2.1	22.6 \pm 1.1	15.0 \pm 1.2
BMP-9	0.2 \pm 0.1	133.1 \pm 35.1	N.A	51.0 \pm 18.3	N.A

B.

BMPR BMP	BMPR-II	ACTR-IIA	ACTR-IIB
BMP-2	5.4 \pm 0.8	6.1 \pm 1.2	6.3 \pm 3.4
BMP-4	56.0 \pm 6.0	21.4 \pm 3.7	26.0 \pm 0.5
BMP-7	5.5 \pm 1.2	1.3 \pm 0.3	7.1 \pm 0.7
BMP-9	0.8 \pm 0.2	1.7 \pm 0.1	1.4 \pm 0.4

BMP-2 and BMP-4 have a good binding affinity to both ALK3 and ALK6 since their K_D was < 3 nM (Table.2A). They bind to ALK2 similarly with an affinity of 7.0 ± 2.3 nM for BMP-2 and 10.5 ± 3.8 nM for BMP-4. They also bind to ALK1 and ALK5 but BMP-2 has a ≈ 4 -fold higher affinity to these receptors than BMP-4. Regarding type-II BMPRs, BMP-2 had a similar affinity for both ACTR-IIA and ACTR-IIB (≈ 6 nM) while BMP-4 also interacted with both receptors although with ≈ 4 -fold lower affinity (≈ 23 nM). In addition, BMP-2 has also a 10-fold higher affinity for BMPR-II than BMP-4. We then investigated whether the differences between BMP-2 and BMP-4 may arise from their glycosylation state, since BMP-2 is produced in CHO while BMP-4, being produced in *E-Coli*, is non-glycosylated. We thus compared the interactions of ALK3 with both the glycosylated and non-glycosylated forms of BMP-4 (S5.Fig.2). For the glycosylated form of BMP-4, the increase in the non-specific signal was negligible (≈ 0.02 nm). However, the interactions differed slightly since K_D was 1.32 ± 0.48 nM for the non-glycosylated BMP-4, versus 0.3 ± 0.06 nM for the glycosylated form.

BMP-7 interacts with all type-I BMPRs with similar affinities (≈ 20 nM). In contrast, it has a greater affinity for the three type-II BMPRs as it binds to BMPR-II and ACTR-IIB similarly (≈ 6 nM) and to ACTR-IIA with a 5 to 7-fold higher affinity (1.3 ± 0.3 nM).

Regarding BMP-9, it binds ALK1 with high affinity (0.2 ± 0.1 nM), ALK5 and ALK2 with a much lower affinity (51.0 ± 18.3 nM and 133.1 ± 35.1 nM, respectively). The affinity of BMP-9 for all the three type-II BMPRs is high: 0.8 ± 0.2 nM for BMPR-II, 1.7 ± 0.1 nM for ACTR-IIA and 1.4 ± 0.4 nM for ACTR-IIB. Notably, BMP-9 affinity for BMPR-II is about 2-fold higher in comparison to ACTR-IIA and ACTR-IIB.

Thus, the K_D values indicated that there are notable differences between BMP-2 and BMP-4, a higher affinity of BMP-7 to type-II BMPRs in comparison to type-I BMPR, and a highly selective affinity of BMP-9 for ALK1 as well as to all type-II BMPRs.

In order to compare the BLI technique to SPR (Table.1), we performed SPR kinetic experiments for selected high affinity couples, namely BMP-9/ALK1 and BMP-2 or BMP-4/ALK3 or ALK2. For this purpose, we used commercially available protein A-coated chips and BMPR-Fc chimera as adsorption strategy (Fig.5A). Unfortunately, the BMP-2/ALK3 (S6.Fig.3), BMP-2/ALK2, BMP-4/ALK3 (data not shown) kinetic interaction using this adsorption strategy could not be measured since non-specific binding to the sensor ship was too high and specific binding signal could not be resolved (S6.Fig.3). In contrast, the BMP-9/ALK1 interaction was notable and a K_D of 13.4 pM was obtained. This value is 15-fold lower than obtained by BLI (≈ 200 pM – Fig.5B).

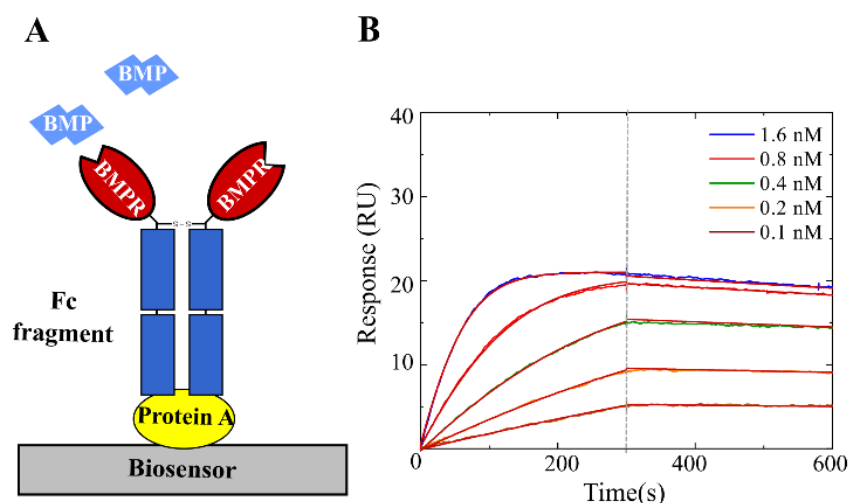
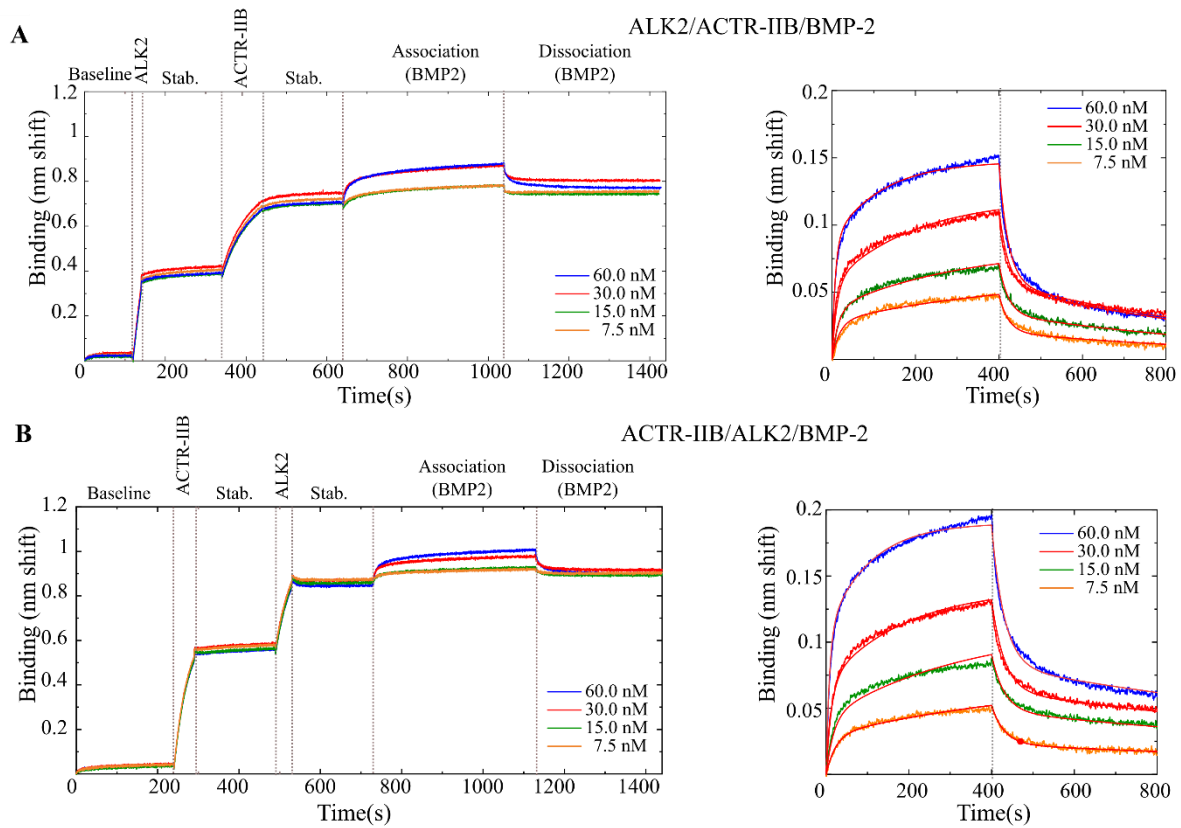


FIGURE 5. SPR study of BMPR/BMP interactions. **A)** A schematic representation of a SPR biosensor surface where the interaction was studied. Protein A was used to immobilize the BMPR Fc fragment. **B)** Example of kinetic experiment for the ALK1/BMP-9 couple showing

the association phase (up to 300s followed by the dissociation phase). The 1:1 Langmuir fit was used to fit the experimental data.

D. Interaction of BMPs with type-I BMPR/ type-II BMPR ternary complex

Next, we decided to investigate the interactions of BMP to type-I/type-II BMPR complexes. In vivo, It is reported that BMPs first bind to the inactive type-I BMPRs thus triggering type-II BMPRs to activate (by phosphorylation) the type-I BMPRs by forming a ternary complex [25], [51]. We studied ALK2 as a type-I BMPR and all three type-II BMPRs with BMP-2, BMP-4 and BMP-7. We chose ALK2 since it is a well-studied receptor involved in several diseases and has a middle range affinity for the BMPs. Our experimental approach consisted in loading sequentially both types of BMP receptors on the biosensor (Fig.6A-B). We performed experiments using two capture strategies. Firstly, ALK2 was loaded, followed by a type-II BMPR and then BMP-2 was set into contact with the functionalized surfaces (Fig.6A). Secondly, a reverse sequence was used in which ACTR-IIB was captured first, followed by ALK2 and then BMP-2 (Fig.6B). The adsorption times were chosen such as to have an equivalent level of adsorption for each receptor, with a total shift being similar to the case of single BMP/BMPR interactions.



	Loading ALK2 (s)	Loading ACTR-IIB (s)	K_D1 (nM)	k_{d1} ($M^{-1}\cdot s^{-1}$) 10^5	k_{d1} (s^{-1}) 10^{-3}	K_D2 (nM)	k_{d2} ($M^{-1}\cdot s^{-1}$) 10^5	k_{d1} (s^{-1}) 10^{-3}
Loading order	First	Second						
ALK2/ACTR-IIB	20	100	46.1±11.5	12.2 ± 3.1	56.2 ± 20.3	14.4 ± 2.3	1.09 ± 0.01	1.6 ± 0.1
Loading order	Second	First						
ACTR-IIB/ALK2	50	40	22.9 ± 1.9	22.2 ± 9.9	50.9 ± 0.3	4.6 ± 0.2	2.3 ± 1.1	1.1 ± 0.5

FIGURE 6. Interaction between the ALK2/ACTR-IIB heterocomplex and BMP-2. Binding was done sequentially: ALK2 or ACTR-IIB first followed by the second receptor and then BMP-2. **A)** First ALK2 or **B)** first ACTR-IIB. The plots on the right panel represent a zoomed view of the association and dissociation steps of the corresponding full sensograms on the left. **C)** Table summarizing the kinetic parameters deduced from the experimental fit to the data. The stab. step refers to stabilization. Data were obtained using OctetRED96e. The 2:1 heterogeneous ligand model was used to fit the experimental data.

To process and fit the kinetic data, we initially applied a 1:1 Langmuir model but the fit was of poor quality (S7.Fig.4). These interactions consist of two different receptors and therefore possess two pairs of two distinct binding sites for type-I and type-II BMPRs. We thus presumed that both types of type-I and type-II receptors bind BMPs separately with different affinities and therefore applied a 2:1 heterogeneous binding model.

The KD in the configuration where ALK2 was immobilized first was 46.1 ± 11.5 nM for the first binding site and 14.4 ± 2.3 for the second. Conversely, when BMPR-II was adsorbed first

the KD1 was 22.9 ± 1.9 nM and KD2 4.6 ± 0.2 nM (Fig.6C). The same experiment was also performed for ALK2/BMPR-II/BMP-7 resulting in a KD of 4.6 ± 0.7 nM and 19.1 ± 6.4 nM for the experiment where ALK2 was adsorbed first, compared to 5.4 ± 0.2 nM and 23.2 ± 0.1 nM for the reverse order. In the case of BMP-7, binding is similar whatever the order of receptor presentation.

The binding affinities for all the experiments where ALK2 is loaded first are summarized in Table.3. Surprisingly, we did not find any improvements in the KD when two receptors are captured on the biosensor surfaces compared to the situation when only one is present. The KD for all of the experiments appear to be higher than the KD of the simple BMP/BMPR interactions, indicating a lower affinity. In more details, the values of the two KD values may be attributed to the values of two different types of binary interaction (BMP/ALK2 or BMP/type-II BMPR), such as the interaction BMP-7/ALK2/BMPR-II where KD1 = 4.6 ± 0.7 nM and KD2 = 19.1 ± 6.4 nM (Table.3), compared to 18.4 ± 3.8 nM for ALK2 and 5.5 ± 1.2 nM for BMPR-II in the binary experiments (Table.2). Nevertheless, this observation was not observed for other interactions. These results suggest the complexity of the interactions occurring on the surface.

TABLE 3. Binding affinities (K_D) (nM) of BMP/BMPR-I/BMPR-II interactions. Table summarizing the K_D1 and K_D2 (nM) of the BMP/BMPR-I/BMPR-II interactions obtained from the kinetic experiments in a conformation where ALK2 and type-II BMPR are loaded sequentially. The error values represent the s.d (n=3).

	ALK2 (ACTR-I)					
K_D (nM)	BMPR-II		ACTR-IIA		ACTR-IIB	
	K_D^1	K_D^2	K_D^1	K_D^2	K_D^1	K_D^2
BMP-2	17.8 ± 7.2	33.0 ± 10.2	31.7 ± 6.5	47.8 ± 4.5	14.4 ± 2.3	46.1 ± 11.4
BMP-4	55.8 ± 17.2	90.7 ± 33.3	14.1 ± 2.5	125.0 ± 20.4	88.7 ± 22.6	103.2 ± 39.0
BMP-7	4.6 ± 0.7	19.1 ± 6.4	7.1 ± 1.8	350.6 ± 12.3	19.1 ± 5.5	60.7 ± 22.9

IV. DISCUSSION

In this study, we performed experiments using the dimeric form of BMPs and BMPRs as confirmed by gel electrophoresis migration analysis (Fig.SI.1). Indeed, some co-immunoprecipitation studies *in vitro* showed that apart from being homodimers, receptors can be heterodimers (i.e ALK2/ALK3 heterodimers), in the presence of BMP [52]. However, the presence of homodimer receptors is regularly described [1], [53]. Thus, our aim in using dimers of BMPs and BMPRs was to mimic utmost the *in vivo* interactions at the cell surface. In that context, we used a simple adsorption strategy involving BMPR-Fc chimera that induces the dimerization of the receptors and presents them, contrary to other adsorption strategies, in a homogeneous manner on the surface with their binding site accessible.

Using BLI, we quantified the binding affinities of the four BMPs with the eight different BMPRs in similar experimental conditions. As we showed with our SPR data, several BMPR/BMP couples (ALK3/BMP-2, ALK3/BMP-4 and ALK2/BMP-2) could not be analyzed by SPR using the same strategy as BLI with protein A coated sensors (S6.Fig.3), while BMP-9/ALK1 was detected (Fig.5). There may be non-specific adsorption of BMP-2 and 4 to protein A. The direct comparison of BLI versus SPR for the high affinity couple ALK1/BMP-9 showed that K_D measured by BLI was 15-fold lower than that measured by SPR (13.4 pM versus 200 pM) (Fig.5). These differences between both techniques may be explained by the physical and chemical differences of the techniques, since the thickness and composition of the sensor layers as well as the adsorption strategies are different. Another aspect to mention is the sensitivity of the method and the stability of the baseline signal, since the dissociation rate measured are sometimes at the limits of the instrument stability. Altogether, our experimental results show that the BLI technique is well adapted, in our study to gain quantitative information on a large range of BMP/BMPR couples.

To date, BMP-4 has barely been studied since it was often considered to exhibit a very close behavior to BMP-2 [5]. Our study first confirmed that both BMP-2 and BMP-4 bind to ALK3 and ALK6 with high affinity (Table.1), as already mentioned in the literature [6], [23]. Additionally, our data reveals notable differences in the binding behaviors of BMP-2 and BMP-4. Indeed, BMP-2 binds to type-I BMPRs with a 3-fold higher affinity than BMP-4 (Table.2). Interestingly, the difference arises mainly from a difference in association rates to the receptors which was faster for BMP-2 than BMP-4, while the dissociation rates were similar (Fig.3). Particularly, the strongest differences were observed for the type-II BMPR, with faster

association rates for BMP-2 for all the three receptors, and faster dissociation rates for BMP-2 solely for BMPR-II and ACTR-IIA.

Our results are in agreement with previously published cellular data highlighting the distinct role of BMP-4 and BMP-2. One study examined their role in chondrocyte proliferation and found that the deletion of BMP-2 gene alone resulted in severe chondrodysplasia while the deletion of BMP-4 led to minor cartilage phenotype [54]. Likewise, in acute myeloid leukemia, a distinct role of BMP-4 versus BMP-2 has been evidenced [55], [56]: BMP-4 solely is involved as it activates a specific signaling pathway promoting immature resistant leukemic cells, which eventually leads to a relapse after treatment [55], [56]. In view of our findings regarding the specific differences between BMP-2 and BMP-4, it will be interesting to further evaluate their specific functions in different cell signaling contexts.

It is also noteworthy that the average binding of BMPs (-2, 4, 7) to ALK2 is in the same range ≈ 7 -20 nM, and with lower affinity to BMP-9 (133 nM). In addition to the lower affinity of BMP-2 for type-II BMPRs compared to type-I BMPRs, we observed faster kinetic constants (k_a , k_d) for type-II BMPRs (Fig.3). This observation was previously reported and assumed to be the reason why BMP-2 and BMP-4 are recruited in a sequential order, with an initial binding to the higher affinity type-I BMPRs [38]. It may be interesting to further study BMP/ALK2 interactions in the context of the R206H mutation, which is associated to Fibrodysplasia Ossificans Progressiva (FOP): this mutation leads to the activation of BMP signaling in the absence of BMP and to an enhanced biochemical signal in the presence of BMP [57].

Our results showed that BMP-7 binds similarly to all ALKs with an affinity of ≈ 20 nM, in agreement with the literature review (Table.1), although the range of previously reported KD was large. With respect to type-II BMPRs, we found that BMP-7 binds with high affinities to the three type-II BMPRs, with a 5-fold higher affinity for ACTR-IIA (Table.2B). A previous study reported that BMP-7 signals through ACTR-IIA [58]. Notably, BMP-7 was also reported to induce chemotaxis in monocytic cells through BMPR-II and ACTR-IIA receptors, but not through ACTR-IIB [53].

Previous studies on BMP-9 have shown that it binds to ALK1 and ALK5 in endothelial cells [59]–[61], and to ALK1 and ALK2 in mesenchymal cells used for osteogenic differentiation [62]. Our data showing that BMP-9 binds ALK1 with a high affinity (0.2 ± 0.1 nM) and ALK2/ALK5 with a lower affinity (133.1 ± 35.1 nM and 51.0 ± 18.3 nM, respectively) (Table.2A) indicated that all these three ALK receptors are important in the signaling of BMP-9. The comparison of the structural data between both complexes BMP-2/ALK3-ECD/ACTR-

2B-ECD and BMP-9/ALK1-ECD/ACTR-2B-ECD shows that ALK1 has a distinct interface with BMP-9, and presents several structural differences, compared to other type-I BMPRs. These structural disparities may well explain the low affinity of ALK1 for all the other BMPs [30], as seen in our data. Regarding the type-II BMPRs, former studies have shown that BMP-9 can bind to all of them [59], [63]. Our results indicated that BMP-9 bound all type-II BMPR with a very high affinity (\square 0.8 to 1.7 nM) and with a slightly higher affinity for BMPR-II (0.8 ± 0.2 nM) (Table.2), in concert with the literature [30], [31] (Table.SI.1).

Interestingly, our results showed that there is a binding of several BMPs to ALK5 (Fig.4 and Table.2A). We observed average affinities of BMP-2 (5.8 ± 1.1 nM), BMP-4 (21.9 ± 6.6 nM) and BMP-7 (22.6 ± 1.1 nM) to ALK5. Although ALK5 was considered to be mainly a TGF β R, our data show that several BMPs can bind to ALK5, which highlights its possible role in the BMP signaling pathway. Indeed, previous data in our team show an expression of ALK5 in BMP responsive cells notably C2C12 skeletal muscle cells and human periosteum derived stem cells [64]. Moreover, it is reported that ALK5 interacts with ALK1 and inhibits BMP signaling mediated by ALK1 in the growth plate of cartilage [65]. Also BMP-2 appeared to induce complex formation between ALK3 and ALK5 in cancer cells [47]. Last but not least, it was shown that different signaling through ALK1 and ALK5 regulate leptin expression in bone-marrow mesenchymal stem cells [16]. Further in vivo studies should aim to unravel a possible crosstalk between TGF β /BMP pathways mediated by ALK5.

While it is simple to connect the affinity studies directly to the downstream signaling pathway, it would be inherently incorrect not to mention other parameters affecting the signaling. Notably, the tempero-spatial expression of BMPs and BMPRs should be considered[66]. Besides, the BMP signaling can be affected by BMP's interaction with modular proteins (i.e Noggin, Gremlin), co-receptors such as Endoglin, which binds BMP-9[67], and extracellular matrix components (i.e fibrillary proteins and proteoglycans)[68]. Nevertheless, our study provides an insight on the first step of the BMP signaling.

The use of a 2:1 heterogeneous ligand model to analyze the ternary complex interactions did not yield any improvement in the binding affinity compared to the bimolecular BMP/BMPR interactions, although such mechanism of cooperativity has been proposed. It was reported that BMP-7 affinity to ALK2 increases in the presence of ACTR-IIA [25], [69]. Nonetheless, our data do not show any cooperativity between both types of BMPRs. This result agrees with the literature since a previous SPR study of BMP-7/ALK3/ACTR-IIA using a BMPR mix similarly reported limitation of the system in observing a cooperativity [21].

V. SUMMARY AND CONCLUSIONS

Our study highlighted the specific differences in BMP/BMPR binding affinities. The results are consistent with the interactions previously reported, nevertheless with our setup we overcame the previously mentioned limitations of studying this BMP/BMPR interaction, by using a similar binding strategy. The findings help us gain insight on the signaling pathways and will guide future BMP signaling studies, with respect to BMP/TGF β crosstalk and to the type of signaling pathway (Smad versus non-Smad) in addition to the specificities of the receptor (type I versus type II). It would also be interesting to further investigate *in vivo* the functional significance of these interactions.

ACKNOWLEDGMENTS

The authors acknowledge Anne Chouquet from the ISBG platform for her help and Marianne Weidenhaupt (INPG) for discussions regarding the immobilization protocol. We are grateful to Sabine Bailly and Corinne Albiges-Rizo for fruitful discussions and advices.

DATA AVAILABILITY

The data that support the findings of this study are available from the corresponding author upon request.

FUNDING AND ADDITIONAL INFORMATION

The study was supported by Agence Nationale de la Recherche (ANR CODECIDE, ANR-17-CE13-022) to C.P and by the Fondation Recherche Medicale (FRM, grant DEQ20170336746) to C.P. VK was supported by a PhD fellowship from Grenoble Institute of Technology. This work used the platforms from Grenoble Instruct-ERIC Center (ISBG: UMS 3518 CNRS-CEA-UGA-EMBL), within the Grenoble Partnership for Structural Biology (PSB), supported by FRISBI (ANR-10-INBS-05-02) and GRAL, financed within the University Grenoble Alpes graduate school (Ecoles Universitaires de Recherche) CBH-EUR-GS (ANR-17-EURE-0003).

REFERENCES

- ¹ C. Sieber, J. Kopf, C. Hiepen, and P. Knaus, *Cytokine Growth Factor Rev.* **20**, 343 (2009).
- ² R.N. Wang, J. Green, Z. Wang, Y. Deng, M. Qiao, M. Peabody, Q. Zhang, J. Ye, Z. Yan, S. Denduluri, O. Idowu, M. Li, C. Shen, A. Hu, R.C. Haydon, R. Kang, J. Mok, M.J. Lee, H.L. Luu, and L.L. Shi, *Genes Dis.* **1**, 87 (2014).
- ³ S. Ehata, Y. Yokoyama, K. Takahashi, and K. Miyazono, *Pathol. Int.* **63**, 287 (2013).
- ⁴ S. Kishigami and Y. Mishina, *Cytokine Growth Factor Rev.* **16**, 265 (2005).
- ⁵ K. Miyazono, Y. Kamiya, and M. Morikawa, *J. Biochem.* **147**, 35 (2010).
- ⁶ T.D. Mueller and J. Nickel, *FEBS Lett.* **586**, 1846 (2012).
- ⁷ Marshall R. Urist, *Class. Pap. Orthop.* 449 (1965).
- ⁸ V.E. Santo, M.E. Gomes, J.F. Mano, and R.L. Reis, *Tissue Eng. - Part B Rev.* **19**, 308 (2013).
- ⁹ C. Busch and H. Wheadon, *Biochem. Soc. Trans.* **47**, 1307 (2019).
- ¹⁰ L. Grgurevic, G.L. Christensen, T.J. Schulz, and S. Vukicevic, *Cytokine Growth Factor Rev.* **27**, 105 (2016).
- ¹¹ and K.D.B. Nicholas W. Morrell, Donald B. Bloch, Peter ten Dijke, Marie-Jose T.H. Goumans, Akiko Hata, Jim Smith, Paul B. Yu, *Physiol. Nat Rev Cardiol Behav.* **13**, 106 (2016).
- ¹² P. Jiramongkolchai, P. Owens, and C.C. Hong, *Biochem. Soc. Trans.* **44**, 1117 (2016).
- ¹³ K. Miyazono, K. Kusanagi, and H. Inoue, *J. Cell. Physiol.* **187**, 265 (2001).
- ¹⁴ D. Carvalho, K.R. Taylor, N.G. Olaciregui, V. Molinari, M. Clarke, A. Mackay, R. Ruddle, A. Henley, M. Valenti, A. Hayes, A.D.H. Brandon, S.A. Eccles, F. Raynaud, A. Boudhar, M. Monje, S. Popov, A.S. Moore, J. Mora, O. Cruz, M. Vinci, P.E. Brennan, A.N. Bullock, A.M. Carcaboso, and C. Jones, *Commun. Biol.* **2**, (2019).
- ¹⁵ F. Zylbersztejn, M. Flores-Violante, T. Voeltzel, F.E. Nicolini, S. Lefort, and V. Maguer-Satta, *Exp. Hematol.* **61**, 36 (2018).
- ¹⁶ M. Zeddou, B. Relic, O. Malaise, E. Charlier, A. Desoroux, Y. Beguin, D. De Seny, and M.G. Malaise, *Stem Cells Dev.* **21**, 1948 (2012).
- ¹⁷ T. Kirsch, J. Nickel, and W. Sebald, *EMBO J.* **19**, 3314 (2000).
- ¹⁸ W. Sebald, J. Nickel, J.L. Zhang, and T. Mueller, *Biol. Chem.* **385**, 697 (2004).
- ¹⁹ G.P. Allendorph, M.J. Isaacs, Y. Kawakami, J.C.I. Belmonte, and S. Choe, *Biochemistry* **46**, 12238 (2007).
- ²⁰ A. Kotzsch, J. Nickel, A. Seher, K. Heinecke, L. Van Geersdaele, T. Herrmann, W. Sebald, T.D. Mueller, L. Van Geersdaele, T. Herrmann, W. Sebald, and T.D. Mueller, *J. Biol. Chem.* **283**, 5876 (2008).
- ²¹ K. Heinecke, A. Seher, W. Schmitz, T.D. Mueller, W. Sebald, and J. Nickel, *BMC Biol.* **7**, 59 (2009).
- ²² K. Yamawaki, Y. Kondo, T. Okada, T. Oshima, M. Kakitani, and K. Tomizuka, *Sci. Rep.* **6**, 3 (2016).
- ²³ H.J. Seeherman, S.P. Berasi, C.T. Brown, R.X. Martinez, Z. Sean Juo, S. Jelinsky, M.J. Cain, J. Grode, K.E. Tumelty, M. Bohner, O. Grinberg, N. Orr, O. Shoseyov, J. Eyckmans, C. Chen,

- P.R. Morales, C.G. Wilson, E.J. Vanderploeg, and J.M. Wozney, *Sci. Transl. Med.* **11**, 1 (2019).
- ²⁴ G.P. Allendorph, W.W. Vale, and S. Choe, *Proc. Natl. Acad. Sci.* **103**, 7643 (2006).
- ²⁵ J. Greenwald, J. Groppe, P. Gray, E. Wiater, W. Kwiatkowski, W. Vale, and S. Choe, *Mol. Cell* **11**, 605 (2003).
- ²⁶ P. Mahlawat, U. Ilangovan, T. Biswas, L.Z. Sun, and A.P. Hinck, *Biochemistry* **51**, 6328 (2012).
- ²⁷ S. Saremba, J. Nickel, A. Seher, A. Kotzsch, W. Sebald, and T.D. Mueller, *FEBS J.* **12**, 172 (2007).
- ²⁸ T. Hatta, H. Konishi, E. Katoh, T. Natsume, N. Ueno, Y. Kobayashi, and T. Yamazaki, *Biopolym. - Pept. Sci. Sect.* **55**, 399 (2000).
- ²⁹ G. Szláma, K. Kondás, M. Trexler, and L. Patthy, *FEBS J.* **277**, 5040 (2010).
- ³⁰ S.A. Townson, E. Martinez-Hackert, C. Greppi, P. Lowden, D. Sako, J. Liu, J.A. Ucran, K. Liharska, K.W. Underwood, J. Sehra, R. Kumar, and A. V. Grinberg, *J. Biol. Chem.* **287**, 27313 (2012).
- ³¹ Y. Kienast, U. Jucknischke, S. Scheiblich, M. Thier, M. De Wouters, A. Haas, C. Lehmann, V. Brand, D. Bernicke, K. Honold, and S. Lorenz, *J. Biol. Chem.* **291**, 3395 (2016).
- ³² R.M. Salmon, J. Guo, J.H. Wood, Z. Tong, J.S. Beech, A. Lawera, M. Yu, D.J. Grainger, J. Reckless, N.W. Morrell, and W. Li, *Nat. Commun.* **11**, 1 (2020).
- ³³ D. Mitchell, E.G. Pobre, A.W. Mulivor, A. V Grinberg, R. Castonguay, T.E. Monnell, N. Solban, J.A. Ucran, R.S. Pearsall, K.W. Underwood, J. Sehra, and R. Kumar, *Mol. Cancer Ther.* 379 (2010).
- ³⁴ C. Hiepen, J. Jatzlau, S. Hildebrandt, B. Kampfrath, M. Goktas, A. Murgai, J.L. Cuellar Camacho, R. Haag, C. Ruppert, G. Sengle, E.A. Cavalcanti-Adam, K.G. Blank, and P. Knaus, *BMP2 Acts as a Gatekeeper to Protect Endothelial Cells from Increased TGF β Responses and Altered Cell Mechanics* (2019).
- ³⁵ J.W. Lowery and V. Rosen, *Physiol. Rev.* **98**, 2431 (2018).
- ³⁶ D. Yadin, P. Knaus, and T.D. Mueller, *Cytokine Growth Factor Rev.* **27**, 13 (2016).
- ³⁷ G. Sanchez-Duffhues, E. Williams, M.J. Goumans, C.H. Heldin, and P. ten Dijke, *Bone* **138**, (2020).
- ³⁸ J. Nickel and T.D. Mueller, *Cells* **8**, 1579 (2019).
- ³⁹ S. Aykul and E. Martinez-hackert, **291**, 10792 (2016).
- ⁴⁰ C. Hänel and G. Gauglitz, *Anal. Bioanal. Chem.* **372**, 91 (2002).
- ⁴¹ G. Gauglitz, *Anal. Bioanal. Chem.* **412**, 3317 (2020).
- ⁴² Y. Abdiche, D. Malashock, A. Pinkerton, and J. Pons, *Anal. Biochem.* **377**, 209 (2008).
- ⁴³ A. Sultana and J.E. Lee, *Curr. Protoc. Protein Sci.* **2015**, 19.25.1 (2015).
- ⁴⁴ D. Frenzel and D. Willbold, *PLoS One* **9**, 1 (2014).
- ⁴⁵ D.O. Wagner, C. Sieber, R. Bhushan, J.H. Börgemann, D. Graf, and P. Knaus, *Sci. Signal.* **3**, (2010).
- ⁴⁶ J. Massagué, *Annu Rev Biochem* **67**, (1998).
- ⁴⁷ A. Holtzhausen, C. Golzio, T. How, Y.H. Lee, W.P. Schiemann, N. Katsanis, and G.C. Blobe,

FASEB J. **28**, 1248 (2014).

⁴⁸ G. Blin, E. Margeat, K. Carvalho, C.A. Royer, C. Roy, and C. Picart, *Biophys. J.* **94**, 1021 (2008).

⁴⁹ M.J. Isaacs, Y. Kawakami, G.P. Allendorph, B.H. Yoon, J.C. Izpisua Belmonte, and S. Choe, *Mol. Endocrinol.* **24**, 1469 (2010).

⁵⁰ D. Weber, A. Kotzsch, J. Nickel, S. Harth, A. Seher, U. Mueller, W. Sebald, and T.D. Mueller, *BMC Struct. Biol.* **7**, 1 (2007).

⁵¹ M. Ehrlich, O. Gutman, P. Knaus, and Y.I. Henis, *FEBS Lett.* **586**, 1885 (2012).

⁵² L. Traeger, I. Gallitz, R. Sekhri, N. Bäumer, T. Kuhlmann, M. Holtkamp, J. Müller, U. Karst, F. Canonne-, M.U. Muckenthaler, D.B. Bloch, A. Olschewski, B. Bartnikas, and A.U. Steinbicker, 127 (2019).

⁵³ J.C. Perron and J. Dodd, *PLoS One* **4**, (2009).

⁵⁴ B. Shu, M. Zhang, R. Xie, M. Wang, H. Jin, W. Hou, D. Tang, S.E. Harris, Y. Mishina, R.J. O'Keefe, M.J. Hilton, Y. Wang, and D. Chen, *J. Cell Sci.* **124**, 3428 (2011).

⁵⁵ T. Voeltzel, M. Flores-Violante, F. Zylbersztejn, S. Lefort, M. Billandon, S. Jeanpierre, S. Joly, G. Fossard, M. Milenkov, F. Mazurier, A. Nehme, A. Belhabri, E. Paubelle, X. Thomas, M. Michallet, F. Louache, F.E. Nicolini, C. Caron de Fromentel, and V. Maguer-Satta, *Cell Death Dis.* **9**, (2018).

⁵⁶ S. Lefort and V. Maguer-Satta, *Biochem. Soc. Trans.* **48**, 411 (2020).

⁵⁷ F.S. Kaplan, P. Seemann, J. Haupt, M. Xu, V.Y. Lounev, M. Mullins, and E.M. Shore, *Methods Enzymol.* **484**, 357 (2010).

⁵⁸ K. Lavery, P. Swain, D. Falb, and M.H. Alaoui-Ismaili, *J. Biol. Chem.* **283**, 20948 (2008).

⁵⁹ M. Scharpfenecker, M. van Dinther, Z. Liu, R.L. van Bezooijen, Q. Zhao, L. Pukac, C.W.G.M. Löwik, and P. ten Dijke, *J. Cell Sci.* **120**, 964 (2007).

⁶⁰ L. David, C. Mallet, S. Mazerbourg, J.J. Feige, and S. Bailly, *Blood* **109**, 1953 (2007).

⁶¹ B.N. Ray, N.Y. Lee, T. How, and G.C. Blobe, *Carcinogenesis* **31**, 435 (2010).

⁶² J. Luo, M. Tang, J. Huang, B.C. He, J.L. Gao, L. Chen, G.W. Zuo, W. Zhang, Q. Luo, Q. Shi, B.Q. Zhang, Y. Bi, X. Luo, W. Jiang, Y. Su, J. Shen, S.H. Kim, E. Huang, Y. Gao, J.Z. Zhou, K. Yang, H.H. Luu, X. Pan, R.C. Haydon, Z.L. Deng, and T.C. He, *J. Biol. Chem.* **285**, 29588 (2010).

⁶³ M.A. Brown, Q. Zhao, K.A. Baker, C. Naik, C. Chen, L. Pukac, M. Singh, T. Tsareva, Y. Parice, A. Mahoney, V. Roschke, I. Sanya, and S. Choe, *J. Biol. Chem.* **280**, 25111 (2005).

⁶⁴ A. Sales, V. Khodr, P. Machillot, L. Chaar, L. Fourel, A. Guevara-Garcia, E. Migliorini, C. Albigès-Rizo, and C. Picart, *Biomaterials*, **281**, 121363 (2022).

⁶⁵ W. Wang, H. Chun, J. Baek, J.E. Sadik, A. Shirazyan, P. Razavi, N. Lopez, and K.M. Lyons, *Proc. Natl. Acad. Sci. U. S. A.* **116**, 15570 (2019).

⁶⁶ K. Miyazono, S. Maeda, and T. Imamura, *Cytokine Growth Factor Rev.* **16**, 251 (2005).

⁶⁷ D.P. Brazil, R.H. Church, S. Surrae, C. Godson, and F. Martin, *Trends Cell Biol.* **25**, 249 (2015).

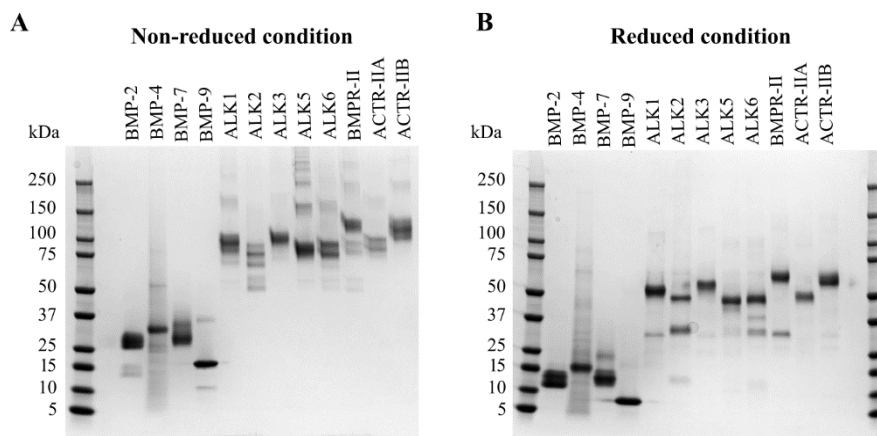
⁶⁸ E. Migliorini, A. Guevara-Garcia, C. Albiges-Rizo, and C. Picart, *Bone* **141**, 115540 (2020).

⁶⁹ W. Sebald and T.D. Mueller, *Trends Biochem. Sci.* **28**, 518 (2003).

Supplementary data:

S1 TABLE 1. Detailed literature study table summarizing the K_D (nM) of the BMP/type-I and type-II BMPR interaction couples. The experiments are usually performed in two different configurations: in red, when the BMP-R is immobilized; in blue when the BMP is immobilized, using SPR and BLI as techniques and different loading strategies. Immo: immobilization, Tech: technique, Ref: reference

K_D	Immo.	Tech.	ALK1	ALK2 (ActR-I)	ALK3 (BMPR-IA)	ALK5 (TGF β R-I)	ALK6 (BMPR-IB)	BMPR-II	ACTR-IIA	ACTR-IIB	Adsorption tech.	Ref.	
BMP-2	BMPR	SPR			1 nM		11 nM	100 nM	50 nM		Biotin/ Streptavidin	Kirsch,T. et al (2000)	
		SPR							38 nM		Amine coupling	Greenwald, J et al (2003)	
		SPR							38 - 80 nM			Amine coupling	Allendorph, G. et al (2006)
		SPR			2.6 nM				47.5 nM	36.1 nM		Amine coupling	Allendorph, G. et al (2007)
		SPR			0.7 nM			2.7 nM				Biotin/ Streptavidin	Kotzsch, A et al (2008)
		SPR			0.8 nM			2.7 nM	45 \pm 20 nM	14 nM	6.3 nM	Biotin/ Streptavidin	Heinecke, K. et al (2009)
	BMP	SPR				3.75 pM		2.48 nM				BMPR-Fc on anti-Fc	Yamawaki, K. et al (2016)
		BLI				1.1 nM		1.1 nM	26.7 nM	52.7 nM	8 nM	BMPR-Fc on anti-Fc	Seeherman, H. et al (2019)
		SPR								5.4 μ M		Amine coupling	Greenwald, J et al (2003)
		SPR		>400 μ M	10 μ M			95 μ M		3.8 μ M		Amine coupling	Saremba, S. et al (2007)
BMP-4	BMPR	SPR			56.4 pM		221 pM				See above	Yamawaki, K. et al (2016)	
		SPR			47 nM						Amine coupling	Hatta, T. et al (2000)	
	BMP	SPR			1.2 - 9.6 nM						Amine coupling	Szlama, G et al (2010)	
BMP-7	BMPR	SPR							1.2 nM		See above	Greenwald, J et al (2003)	
		SPR							1 nM		See above	Allendorph, G. et al (2006)	
		SPR			1680 nM				3.49 nM	7.72 nM		See above	Allendorph, G. et al (2007)
		SPR		> 500 nM	58 nM		9 nM	25 nM	5.1 nM	6.5 nM		See above	Heinecke, K. et al (2009)
		SPR			1.95 nM		268 pM					See above	Yamawaki, K. et al (2016)
	BMP	SPR		143 μ M						1.7 μ M		See above	Greenwald, J et al (2003)
		SPR		55 μ M	10 μ M		1 μ M		0.9 μ M			See above	Saremba, S. et al (2007)
BMP-9	BMPR	SPR	0,57 nM								Amine coupling	Mitchell, D. et al (2010)	
		SPR	45 pM					630 pM	6.43 nM	21.7 pM	BMPR-Fc on anti-Fc	Townson, S. et al (2012)	
		SPR	<8 pM					3.3 nM	42.7 nM	1.4 nM	BMPR-Fc on anti-Fc	Kienast, Y. (2016)	
	BMP	SPR	71.6 pM (monomer) / 48.1 pM (dimer)									Amine coupling	Salmon, R. (2020)
		SPR	2 nM									See above	Mitchell, D. et al (2010)
		SPR	20 - 45 nM (monomer)/ 2-3 nM (dimer)		N.D							See above	Mahlawat, P. et al (2012)



S2 FIGURE 1. Image of a gel electrophoresis showing all the used BMPs, ALKs and type-II BMPR. The proteins were tested in A) non-reducing and B) reducing conditions.

S3 TABLE 2. Detailed kinetic tables indicating the K_D (nM), k_a ($M^{-1}.s^{-1}$), k_d (s^{-1}) and R^2 of the BMP/type-I BMPR interactions. The error values represent s.d (n=3).

BMP	ALK1				ALK2 (ACTR-I)			
	kinetic KD	k_a (1/M.s) (10^5)	k_{dis} (1/s) (10^{-3})	R^2	kinetic KD	k_a (1/M.s) (10^5)	k_{dis} (1/s) (10^{-3})	R^2
BMP-2	13.0 ± 1.6	2.5 ± 1.3	3.2 ± 1.2	0.94 ± 0.02	7.0 ± 2.3	7.4 ± 2.3	5.0 ± 1.3	0.93 ± 0.01
BMP-4	55.4 ± 4.0	0.74 ± 0.24	4.1 ± 1.5	0.95 ± 0.002	10.5 ± 3.8	2.3 ± 1.7	2.6 ± 1.6	0.92 ± 0.04
BMP-7	23.1 ± 2.1	1.6 ± 0.2	3.7 ± 0.4	0.95 ± 0.02	18.4 ± 2.4	2.0 ± 0.5	3.6 ± 0.2	0.96 ± 0.04
BMP-9	0.17 ± 0.08	15.0 ± 3.5	0.2 ± 0.1	0.99 ± 0.01	133.1 ± 35.1	1.2 ± 0.9	16 ± 3	0.93 ± 0.02

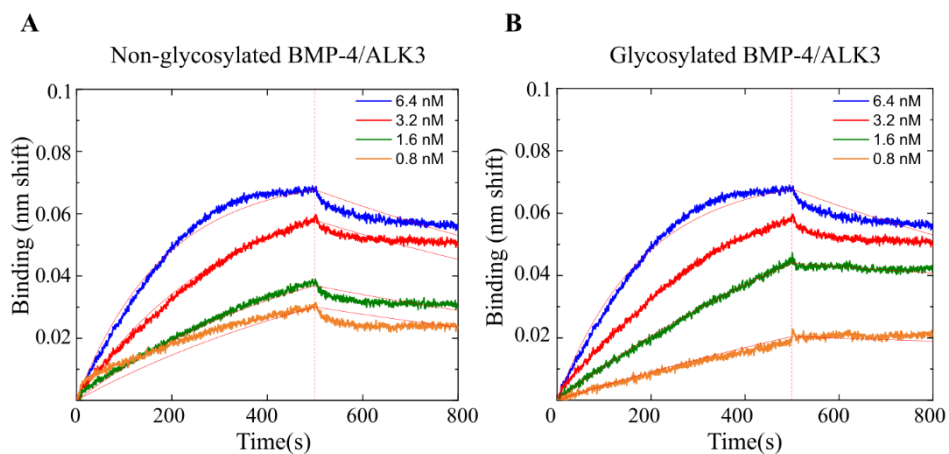
BMP	ALK3 (BMP-R-IA)				ALK5 (TGFβR-I)			
	kinetic KD	k_a (1/M.s) (10^5)	k_{dis} (1/s) (10^{-3})	R^2	kinetic KD	k_a (1/M.s) (10^5)	k_{dis} (1/s) (10^{-3})	R^2
BMP-2	0.21 ± 0.03	11.3 ± 0.6	0.26 ± 0.05	0.99 ± 0.003	5.8 ± 1.1	4.2 ± 0.4	2.4 ± 0.5	0.95 ± 0.03
BMP-4	1.7 ± 0.5	7.3 ± 1.6	1.5 ± 0.2	0.97 ± 0.03	21.9 ± 6.6	2.05 ± 0.7	4.3 ± 1.0	0.94 ± 0.02
BMP-7	19.0 ± 2.1	1.2 ± 0.4	2.3 ± 0.4	0.96 ± 0.02	22.6 ± 1.1	1.6 ± 0.5	3.5 ± 0.3	0.96 ± 0.03
BMP-9	Very low signal	Very low signal	Very low signal	Very low signal	51 ± 18.3	0.6 ± 0.06	3.0 ± 0.8	0.94 ± 0.004

BMP	ALK6 (BMPR-IB)			
	kinetic KD	k_a (1/M.s) (10^5)	k_{dis} (1/s) (10^{-3})	R^2
BMP-2	0.5 ± 0.1	19.1 ± 3.5	0.9 ± 0.1	0.96 ± 0.02
BMP-4	3.0 ± 0.3	5.1 ± 0.5	1.6 ± 0.3	0.95 ± 0.04
BMP-7	14.5 ± 1.2	1.8 ± 0.1	2.7 ± 0.1	0.98 ± 0.005
BMP-9	Very low signal	Very low signal	Very low signal	Very low signal

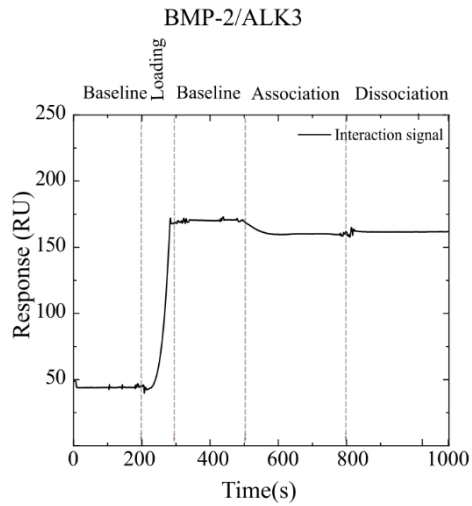
S4 TABLE 3. Detailed kinetic tables indicating the K_D (nM), k_a ($M^{-1}.s^{-1}$), k_d (s^{-1}) and R^2 of the BMP/type-II BMPR interactions. The error values represent s.d (n=3).

BMP	BMPR-II				ACTR-IIA			
	kinetic K_D	k_a ($1/M.s$) (10^5)	k_d ($1/s$) (10^{-3})	R^2	kinetic K_D	k_a ($1/M.s$) (10^5)	k_d ($1/s$) (10^{-3})	R^2
BMP-2	5.4 ± 0.8	12 ± 5.3	6.4 ± 2.3	0.96 ± 0.03	6.08 ± 1.2	13.5 ± 5.8	8.1 ± 1.6	0.95 ± 0.01
BMP-4	56.0 ± 6.0	0.9 ± 0.2	4.8 ± 0.4	0.96 ± 0.01	21.4 ± 3.7	1.5 ± 0.5	3.2 ± 0.6	0.97 ± 0.01
BMP-7	5.5 ± 1.2	4.3 ± 0.4	2.3 ± 0.5	0.99 ± 0.01	1.3 ± 0.3	9.9 ± 2.4	1.3 ± 0.2	0.98 ± 0.01
BMP-9	0.8 ± 0.2	13.6 ± 4.0	1.2 ± 0.1	0.99 ± 0.43	1.7 ± 0.1	35.8 ± 9.1	6.0 ± 0.7	0.93 ± 0.03

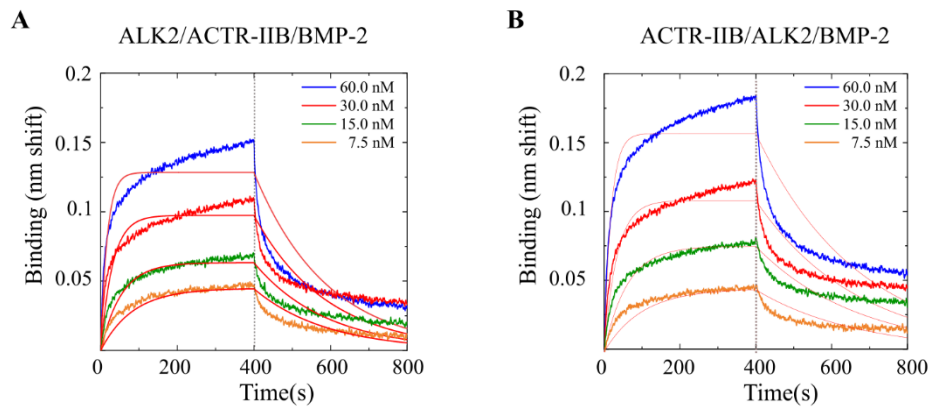
BMP	ACTR-IIB			
	kinetic K_D	k_a ($1/M.s$) (10^5)	k_d ($1/s$) (10^{-3})	R^2
BMP-2	6.3 ± 3.4	8.5 ± 3.1	5.3 ± 0.6	0.94 ± 0.01
BMP-4	26.0 ± 0.5	2.4 ± 0.6	6.1 ± 1.5	0.95 ± 0.02
BMP-7	7.1 ± 0.7	4.0 ± 0.3	2.8 ± 0.4	0.99 ± 0.01
BMP-9	1.4 ± 0.4	22.4 ± 4.6	2.6 ± 0.3	0.95 ± 0.04



S5 FIGURE 2. Binding kinetics between non-glycosylated and glycosylated BMP-4 with ALK3. A) non-glycosylated BMP-4 and B) glycosylated BMP-4. The 1:1 Langmuir fit was used to fit the experimental data.



S6 FIGURE 3. SPR binding curve for BMP-2/ALK3. The association signal was undetectable and even slightly decreased after background subtraction, showing that the interaction was not detectable.



S7 FIGURE 4. BLI binding kinetics of BMP-2 with ALK2 and ACTR-IIB in two confirmations using 1:1 fit. A) ALK2/ACTR-IIB/BMP-2 with ALK2 loaded first and B) ACTR-IIB/ALK2/BMP-2 with ACTR-IIB loaded first. The data were analyzed using a 1:1 fit.

Chapter IV:
**Differential bioactivity of four BMP-family
members as function of biomaterial stiffness**

IV.1. Article Summary

The aim of this work is to study the combined effects of biomaterial stiffness (ie (PLL/HA film crosslinking) and matrix-bound presentation of four major BMPs BMP-2, BMP-4, BMP-7 and BMP-9, on the early differentiation and on cell adhesion.

Indeed, we previously reported the role of BMPs in cell differentiation, cytoskeleton organization, cell spreading and migration (Fourel *et al.*, 2016). In addition, BMP signaling has already been associated with mechanotransduction pathways in bone involving ECM components such as integrins, and therefore sensitive to matrix stiffness (Kopf *et al.*, 2014).

Previous studies in the team have demonstrated the effect of BMP-2 on early cell spreading, adhesion and migration *in vitro* using biomimetic films (Crouzier *et al.*, 2011): this occurs thanks to a crosstalk with the integrin adhesion receptors, notably $\beta 3$ integrin (Fourel *et al.*, 2016). In addition, *in vivo*, it was possible to repair critical-sized bone defects using an polymeric implantable material coated with the biomimetic films loaded with BMP-2 (Bouyer *et al.*, 2016). The preparation of the biomimetic polyelectrolyte films has been automated using a liquid handling robot and was optimized to be done in 96-well microplates (Machillot *et al.*, 2018). Hence, the biomimetic films are now compatible with high-content cellular studies and can be done on a large number of experimental conditions.

In this work, we studied four BMPs (BMP-2, BMP-4, BMP-7 and BMP-9) presented in a matrix-bound manner to evaluate cell adhesion and differentiation of C2C12 skeletal myoblasts and human periosteum-derived stem cells (hPDSCs), known to be BMP-responsive cells. We first seeded the cells on rigid (≈ 400 kPa) and soft films (≈ 200 kPa) loaded with increasing concentrations of bBMPs. After 4 or 5 hours, the cells were fixed and the number of adherent cells and cell spreading areas were quantified. Second, we evaluated early stem cell differentiation to bone by studying: the phosphorylation and nuclear translocation of two Smad members: Smad 1/5/9 that is a hallmark of BMP signalling and Smad 2 that is a hallmark of TGF β signaling, and the expression of alkaline phosphatase, which is rather recognized as being part of the non-classical pathway. In a second part, we investigated the involvement of BMP receptors and integrins in the cell adhesive response by studying their expression level in C2C12 myoblasts and hPDSCs using quantitative PCR. We identified the specific role of each BMP receptor and of β integrins by performing small interfering RNA (siRNA) studies. Similarly, cell adhesion and spreading as well as Smad and ALP signaling were analyzed to determine the role of each receptor.

It is the first time that a comparative study is done on the effect of four BMPs on cell adhesion, spreading and signaling in a stiffness-dependent manner. The results showed that all four BMPs play a role in cellular adhesion and spreading notably on rigid films. Similarly, all of the four BMPs were able to induce Smad and ALP signaling, with various intensities. Interestingly, ALK3 was shown to play an important role in cell adhesion and spreading for all BMPs, and ALK5 was shown to be mechano-sensitive for cell spreading. Finally, all three β 1, β 3 and β 5 integrins played a role in cell adhesion and spreading, while their role in osteogenic differentiation appears to be cell-type and context-dependent. We conclude that the type-I BMPR and integrins are involved in BMP-dependent cell adhesion and spreading, while the type-II BMPR are playing a major role in cell differentiation, followed by type-I BMPR and integrins.

Since the majority of this work was done by the postdoctoral researcher Dr. Adrià Sales, I will only present here the part of the experiments I participated and the results relevant to my PhD project. For more information and in-depth results, the complete article is presented in the Annex of this thesis.

In this work, I did a cellular characterization of C2C12 and hPDSCs by quantifying the levels of BMPR and integrin expression levels using quantitative PCR. Hence, in this chapter, I will be presenting the cellular characterization results, in addition to some preliminary data with MSCs, as well as some selected results of the mentioned article (Sales *et al.*, 2022) that are relevant to this thesis.

IV.2. Cellular characterization

For the cellular characterization studies, we analyzed using qPCR the expression levels of the following type I BMP receptors: ALK1, ALK2, ALK3, ALK4, ALK5 and ALK6 and type II BMP receptors: BMPR-II, ACTR-IIA, ACTR-IIB in C2C12 and hPDSCs. In addition, we also studied the expression of three integrin receptors, β 1, β 3 and β 5 integrins (**FIG.IV.1**). We also studied hMSCS (**FIG.IV.2**) (unpublished results) although these cells were not selected for the BMP-dependent cellular differentiation in bones.

We showed that ALK2, ALK3 and ALK5 mRNA transcripts are present at high level in C2C12 cells, while ALK1, ALK4 and ALK6 were expressed to a much lower extent. In addition, BMPR-II and ACTR-IIA were detected while ACTR-IIB was expressed at a lower level. Regarding integrins, β 1 integrin was the most highly expressed followed by β 5 and β 3 integrins (**FIG.IV.1.A**).

Similarly, the hPDSCs showed mRNA expression of the similar BMPR and integrins as C2C12, although with a lower quantification level (**FIG.IV.1.B**). The expression levels of C2C12 were compared to an *in silico* screening performed using RNA sequencing data from UCSC genome browser (Encode database), presented in **Fig. SI 11** of the article. We also presented in this article, the summary table for the binding affinities that characterize the BMP/BMPR interactions (**Fig. IV.1.C**).

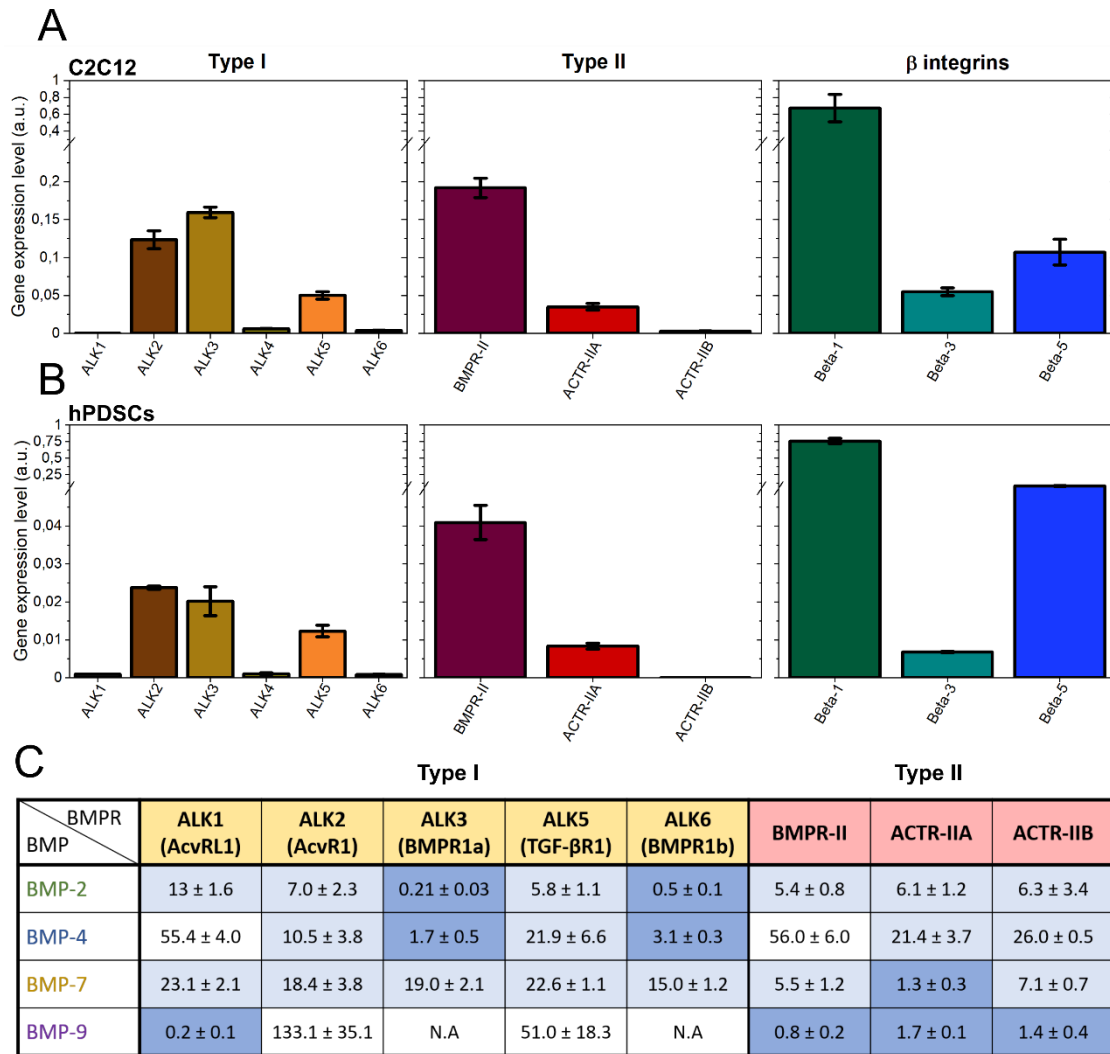


Fig. IV.1. Relative gene expression analysis of type I, type II BMP receptors and β -integrins. Data corresponding to (a) C2C12 cells and to (b) hPDSCs. The gene expression was analyzed by qPCR and it was normalized to the expression of EF1, PPIA and GUSB genes. Data are represented as mean \pm SEM of three independent experiments. (c) Table of the affinity constants (K_d in nM) of the type I and II BMP receptors with the four selected BMPs. Data was obtained from kinetic experiments performed by bio-layer interferometry (BLI), from the work of Khodr *et al.* (Valia Khodr, Paul Machillot, Elisa Migliorini, Jean-Baptiste Reiser, 2020). The highest affinity couples ($K_d < 5$ nM) are highlighted in dark blue, those with an affinity in the range from 5 to 25 nM are in light blue. N.A means no measurable interaction. Values are given as mean \pm SD of three independent experiments.

Comparably, MSCs demonstrated expression of the similar BMPR and integrins as C2C12 and hPDSCs with ALK2, ALK3, ALK5, BMPR-II and ACTR-IIA, as well as β 1 and β 5 (FIG.IV.2). The expression levels of BMPR and adhesion receptors in MSCs appear comparable to those of hPDSCs.

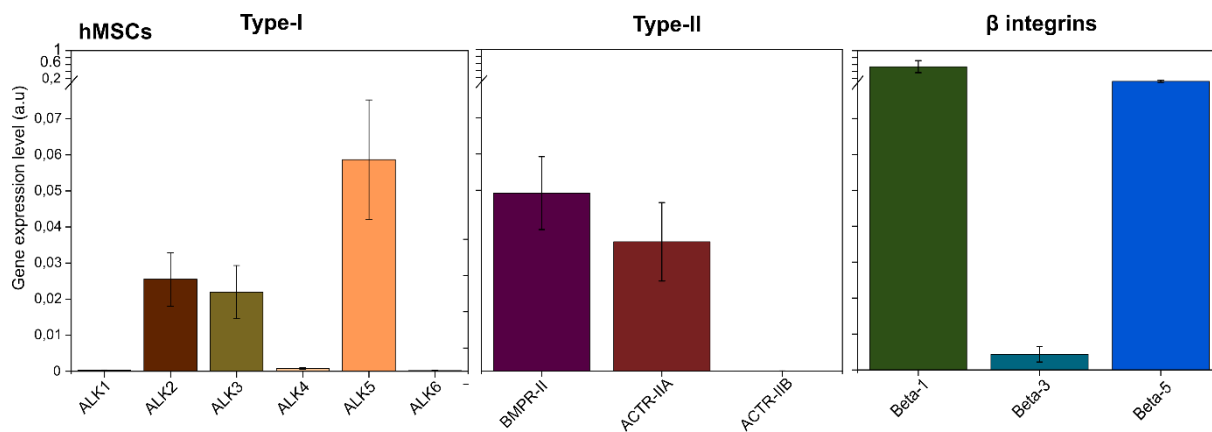


FIG.IV.2. Fig. IV.1. Relative gene expression analysis of type I, type II BMP receptors and β -integrins. Data corresponding to hMSCs. The gene expression was analyzed by qPCR and it was normalized to the expression of EF1, PPIA and GUSB genes. Data are represented as mean \pm SEM of three independent experiments.

To better determine the properties of each used cellular models, we did a synthesis of the described characteristics in the literature (**Table.IV.1**).

TABLE.IV.1. Table summarizing the characteristics, advantages and disadvantages of C2C12 skeletal muscle cells, human mesenchymal stem cells (hMSCs) and human periosteum-derived stem cells (hPDSCs).

	Cell types used in the team		
	C2C12 Skeletal myoblasts	Mesenchymal stem cells (MSC)	Periosteum-derived stem cells (hPDSCs)
<u>Organism</u>	Mouse	Human	Human
<u>Cell type</u>	Myoblast	Stem cells (Bone marrow or umbilical cord)	Periosteum
<u>Source</u>	Commercially available	Center of Blood Transfusion and Centre de Recherche des Armées INSERM	Courtesy of Dr. Frank Luyten lab.
<u>Advantages</u>	<ul style="list-style-type: none"> - Differentiate into chondrocyte, adipocyte - BMP responsive - Robust - Easy to use - Fast cell response (proliferation & differentiation) 	<ul style="list-style-type: none"> - Differentiate into osteoblasts, adipocytes, chondrocyte - Used in cell therapy → Applicative research 	<ul style="list-style-type: none"> - Can adhere and proliferate when cultured on the matrix-bound BMP - Fast cell response
<u>Disadvantages</u>	<ul style="list-style-type: none"> - Mouse cells - Not stem cells 	<ul style="list-style-type: none"> - Heterogeneous extraction protocols - Precious to obtain 	<ul style="list-style-type: none"> - Less known

The C2C12 skeletal myoblast cell line is abundantly used in bone research since they are robust, easy-to-use and give reproducible results. These cells are capable of differentiating into chondrocyte, adipocyte and osteocytes thus they are regularly used to do preliminary studies (Katagiri *et al.*, 1994; Manabe *et al.*, 2012; Gilde *et al.*, 2016). Due to these properties, these cells have been used in the team for several years to study their bone differentiation in BMP and stiffness dependent manner (Kefeng *et al.*, 2008).

The hMSCs are human cells obtained mainly from the bone marrow, and less abundantly from other tissues such as umbilical cord, blood, teeth, muscle and adipose tissues (Hmadcha *et al.*, 2020). Due to the diversity of their extraction sources, the Mesenchymal and Tissue Stem Cell Committee of the International Society for Cellular Therapy defined three criteria to be able to name cells MSCs: First, they must be able to adhere to plastic when grown *in vitro*. Second, they need to express CD73, CD90, and CD105 surface antigens and lack the expression of CD45, CD34, CD14 or CD11b, CD79 α or CD19 and HLA-DR. Third, they must be able to differentiate into adipocytes, chondrocytes and osteoblasts (Dominici *et al.*, 2006). Due to their capacity to migrate to injured tissues and promote tissue regeneration, these cells started to be used in clinical applications for bone and cartilage, cardiovascular, autoimmune and liver diseases (Kim and Cho, 2013). However, their usage is still limited and controversial as functional heterogeneity was observed for cells extracted from different tissue sources and donors. Thus, further studies are needed to better characterize these cells before their universal usage in clinical studies (Phinney, 2012). Due to their usage in therapies, these cells were initially considered in our team to be used in the drug assays experiments.

However, an ALP assay demonstrated issues with the negative and positive controls (FIG.IV.3), since they showed a donor-dependent heterogeneity and reproducibility issues. In addition, it was not easy to have a continuous supply, since this was related to the patients (Center of Blood Transfusion and Centre de Recherche des Armées INSERM).

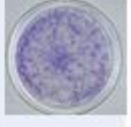
Donor	Negative controls		Positive controls		Triplicates	
	Media	Asc Ac + BGP	BMP-2	Dex	MEM	DMEM
19 MEL	OK 	OK 	OK 	No 		
CSM074	No 	No 	OK 	OK 		
CSM026	No 	No 	OK 	OK 		

FIG.IV.3. ALP assay on MSCs cells obtained from three different donors. The ALP assay showed issues with negative and positive controls as ALP was detected even in the absence of BMP-2 (Media condition). The Asc Ac, Dex and BGP refer to ascorbic acid, dexamethasone and β -glycerolphosphate respectively. This work was done by Laura Clauzier.

For all these reasons, the C2C12 myoblasts were later on chosen to do the drug assays (**Chapter V**).

IV.3. Role of BMPR in adhesion, spreading and signaling

In this part, we also used hPDSCs, obtained from the periosteum, a tissue enclosing the surface of bones. They have been reported to be easily isolated and expanded by usage of similar surface markers as MSCs, although further efforts are needed to identify markers that could separate them from fibroblasts (Ferretti, 2014; Roberts *et al.*, 2015). They have been also shown to adhere and proliferate when cultured on matrix-bound BMP, as well as presenting a fast cell-response (Sales *et al.*, 2022). They remain an adequate cell model to study osteogenesis, although still not very known in the field. These cells are kindly provided by the team of Professor Luyten, an expert of this field, from Leuven.

The work consisted on first studying the effect of the four BMPs (BMP-2, BMP-4, BMP-7 and BMP-9) on cellular adhesion and differentiation in a stiffness-dependent manner (**Article in Annex**). Then we performed the silencing of type-I and type-II BMP receptors and analyzed cellular adhesion and spreading with matrix-bound BMP-2, BMP-4, BMP-7 and BMP-9 presented via soft or rigid biomimetic films after 5h or 4h respectively (**FIG.IV.5**). In addition, we quantified the pSmad 1/5/9, pSmad 2 and ALP signaling (**FIG.IV.6**) (Sales *et al.*, 2022).

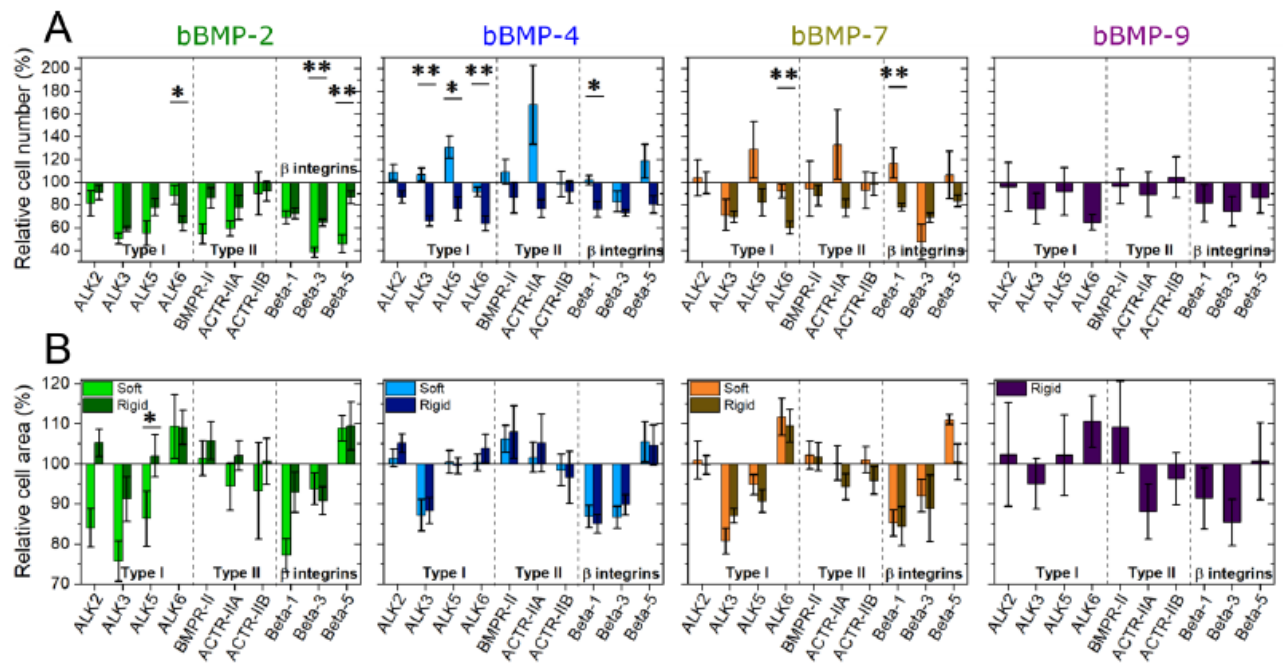


FIG.IV.5. Effect of BMP receptor and β chain integrin silencing on cell adhesion and spreading. We first measured A) the relative cell number by mm², and B) the relative cell area in comparison to the scrambled siRNA, after performing transcription with siRNA against BMP receptor type I (ALK2, ALK3, ALK5, ALK6), BMP receptor type II (BMPR-II, ACTR-IIA, ACTR-IIB) and β chain integrins (β 1, β 3, β 5) and plated on soft (light color) and rigid (dark color) films with bBMPs for 5 or 4 h, respectively. This work was done by Adrià Sales.

The results show that ALK3 and ACTR-IIA have a role on adhesion, as they are stiffness-dependent with bBMP-4, while ALK6 induces adhesion only on rigid films. Furthermore, ALK5 is involved in mechano-sensitive cell adhesion with bBMP-4 and BMP-7. On the other hand ALK2 is mechano-sensitive for cell spreading with bBMP-2 (**FIG.IV.5**).

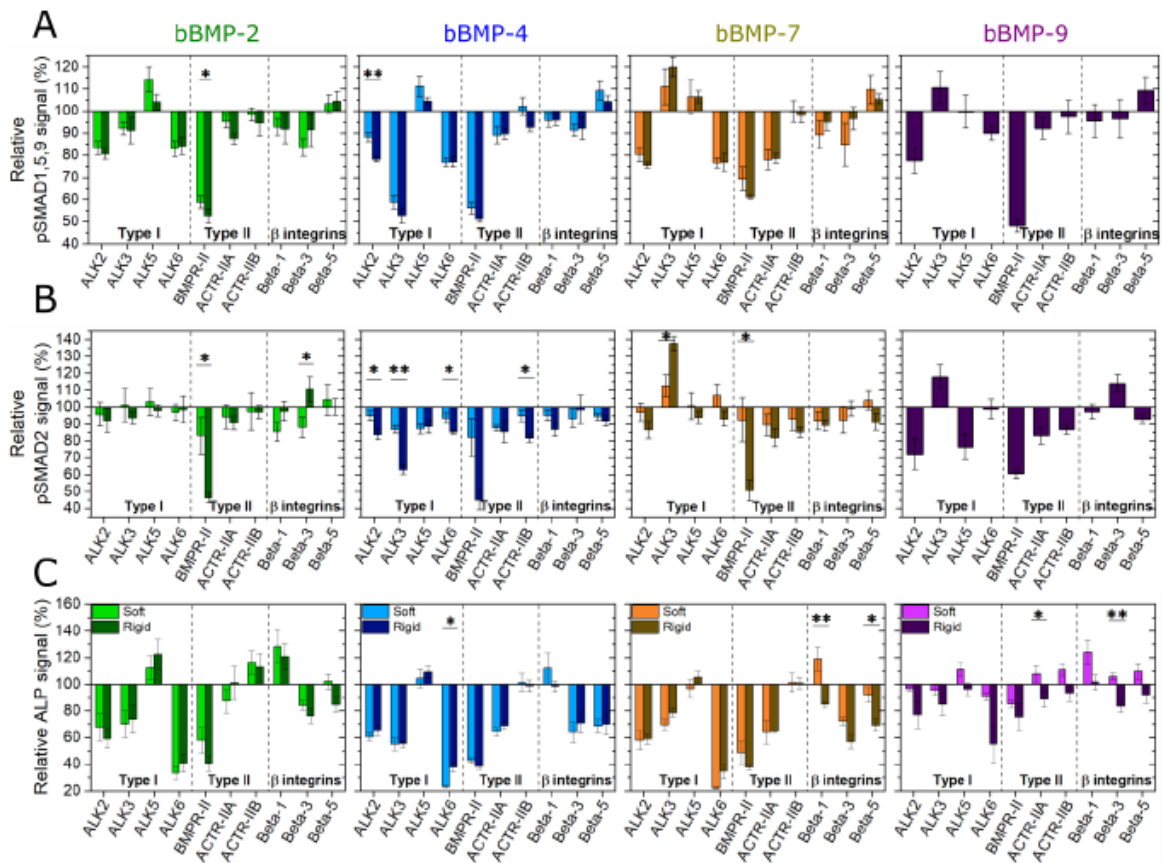


FIG.IV.6. Effect of BMP receptor and β chain integrin silencing on early cell differentiation to bone. Quantification of A) pSmad 1/5/9 signal, B) pSmad 2 signal and C) ALP activity after performing transcription with siRNA against BMP receptor type I (ALK2, ALK3, ALK5, ALK6), BMP receptor type II (BMPR-II, ACTR-IIA, ACTR-IIB) and β chain integrins (β 1, β 3, β 5) and plated on soft (light color) and rigid (dark color) films with bBMPs for 5 or 4 h, respectively. This work was done by Adrià Sales.

The results also show an important role for all BMPs in a non-specific manner. In addition, differences in the role of BMPR in Smad signaling with BMP-4, since ALK5, ALK6, and most importantly ALK3 play an activator role in Smad 2 signaling. These results were not observed with BMP-2. On the other hand, BMPR-II and ACTR-IIA were shown to have activator roles as they demonstrated the highest activation of the pSmad 1/5/9, Smad 2 pathways with BMP-7, in comparison to other receptors (**FIG.IV.6**).

These results show the specific roles of each BMP receptor in cellular adhesion and spreading as well as in bone differentiation.

References

- Bouyer, M. *et al.* (2016) 'Surface delivery of tunable doses of BMP-2 from an adaptable polymeric scaffold induces volumetric bone regeneration', *Biomaterials*, 104(0), pp. 168–181. doi: 10.1016/j.biomaterials.2016.06.001.
- Crouzier, T. *et al.* (2011) 'Presentation of BMP-2 from a soft biopolymeric film unveils its activity on cell adhesion and migration', *Advanced Materials*, 23(12), pp. 111–118. doi: 10.1002/adma.201004637.
- Dominici, M. *et al.* (2006) 'Minimal criteria for defining multipotent mesenchymal stromal cells. The International Society for Cellular Therapy position statement', *Cytotherapy*. Elsevier, 8(4), pp. 315–317. doi: 10.1080/14653240600855905.
- Ferretti, C. (2014) 'Periosteum derived stem cells for regenerative medicine proposals: Boosting current knowledge', *World Journal of Stem Cells*, 6(3), p. 266. doi: 10.4252/wjsc.v6.i3.266.
- Fourel, L. *et al.* (2016) ' β 3 integrin-mediated spreading induced by matrix-bound BMP-2 controls Smad signaling in a stiffness-independent manner', *Journal of Cell Biology*, 212(6), pp. 693–706. doi: 10.1083/jcb.201508018.
- Gilde, F. *et al.* (2016) 'Stiffness-dependent cellular internalization of matrix-bound BMP-2 and its relation to Smad and non-Smad signaling', *Acta Biomaterialia*, 46, pp. 55–67. doi: 10.1016/j.actbio.2016.09.014.
- Hmadcha, A. *et al.* (2020) 'Therapeutic Potential of Mesenchymal Stem Cells for Cancer Therapy', *Frontiers in Bioengineering and Biotechnology*, 8(February), pp. 1–13. doi: 10.3389/fbioe.2020.00043.
- Katagiri, T. *et al.* (1994) 'Bone morphogenetic protein-2 converts the differentiation pathway of C2C12 myoblasts into the osteoblast lineage', *Journal of Cell Biology*, 127(6 I), pp. 1755–1766. doi: 10.1083/jcb.127.6.1755.
- Kefeng, R. *et al.* (2008) 'Polyelectrolyte multilayer films of controlled stiffness modulate myoblast cells differentiation', *Adv Funct Mater*, 18(9), pp. 1378–1389. doi: 10.1002/adfm.200701297.Polyelectrolyte.
- Kim, N. and Cho, S.-G. (2013) 'Clinical applications of mesenchymal stem cells', *korean J iIntern Med*, 28, pp. 387–402. doi: 10.1016/B978-0-08-102680-9.00005-6.
- Kopf, J. *et al.* (2014) 'BMP growth factor signaling in a biomechanical context', *BioFactors*, 40(2), pp. 171–187. doi: 10.1002/biof.1137.
- Machillot, P. *et al.* (2018) 'Automated Buildup of Biomimetic Films in Cell Culture Microplates for High-Throughput Screening of Cellular Behaviors', *Advanced Materials*, 30(27), pp. 1–8. doi: 10.1002/adma.201801097.
- Manabe, Y. *et al.* (2012) 'Characterization of an Acute Muscle Contraction Model Using Cultured C2C12 Myotubes', *PLoS ONE*, 7(12). doi: 10.1371/journal.pone.0052592.
- Phinney, D. G. (2012) 'Functional heterogeneity of mesenchymal stem cells: Implications for cell therapy', *Journal of Cellular Biochemistry*, 113(9), pp. 2806–2812. doi: 10.1002/jcb.24166.
- Roberts, S. J. *et al.* (2015) 'Uncovering the periosteum for skeletal regeneration: The stem cell that lies beneath', *Bone*. Elsevier Inc., 70, pp. 10–18. doi: 10.1016/j.bone.2014.08.007.
- Sales, A. *et al.* (2022) 'Differential bioactivity of four BMP-family members as function of

biomaterial stiffness', *Biomaterials*, 281. doi: 10.1016/j.biomaterials.2022.121363.

Valia Khodr, Paul Machillot, Elisa Migliorini, Jean-Baptiste Reiser, C. P. (2020) 'High throughput measurements of BMP/BMP receptors interactions using bio-layer interferometry', *BioRxiv*. doi: <https://doi.org/10.1101/2020.10.20.348060>.

Chapter V:
**Development of an automated high-content
screening immunofluorescence assay of
pSmad quantification: proof-of-concept
with drugs inhibiting the BMP and TGF β
pathways**

V.I. Article Summary

The canonical pSmad pathway, activated by members of the TGF- β and BMP families, is considered to be a major hallmark of cell differentiation toward the bone lineage. Indeed, the interaction of BMP or TGF- β with their receptors activate the pSmad 1/5/9 or pSmad 2/3, which then leads to their translocation to the nucleus to regulate the expression of target genes.

This signaling pathway is usually studied by common molecular biology techniques such as western blot and bioluminescence luciferase assay. Although very specific, these methods present several limitations, notably the fact that they solely enable the quantification of an average signal a cell population. Here, we established a new method to quantify pSmad in an automated manner using high-content analysis of pSmad immunofluorescence (IF) at the single cell level. We used the BMP-responsive cell line C1C12 skeletal myoblasts in view of their fast and easy-to-follow response. Such IF-based method enables to study heterogeneous cell population and to detect potential differences between cell populations.

Our first objective was to optimize the conditions of the test, including experimental set-up and the conditions for image acquisition and analysis. To do so, we used commonly available cell culture plates made of glass, which is the best surface for optical imaging. We found the experimental conditions that are compatible with a kinetic analysis of pSmad activity. To validate the test, we did a proof-of-concept for two drug inhibitors that are already used in clinical trial and used two types of cell culture surfaces: glass and the biomimetic films loaded with BMP-2. We selected LDN-193189, an ALK2 kinase inhibitor and two ALK5 kinase inhibitors Galunisertib and Vactosertib, and first determined their half maximal inhibitory concentration IC₅₀ values. The Z-factor, a measure of the quality of the experiment, was also calculated. Our results show that the fluorescence signal is comparable for both glass and the biomimetic films in all of the dose-response, kinetic and drug experiments. Thus indicating the robustness and reproducibility of this pSmad assay. This optimized test may be used in other cellular contexts on biomimetic films loaded with a wide range of ECM proteins and growth factors.

V.II. Article

Development of an automated high-content screening immunofluorescence assay of pSmad quantification: proof-of-concept with drugs inhibiting the BMP and TGF β pathways

(In preparation)

Valia Khodr^{1,2,*#}, Laura Clauzier^{1,2,*}, Paul Machillot^{1,2}, Adrià Sales^{1,2}, Elisa Migliorini^{1,2}, Catherine Picart^{1,2*#}

¹Interdisciplinary Research Institute of Grenoble (IRIG), ERL BRM 5000 (CNRS/UGA/CEA), CEA Grenoble, 17 rue des Martyrs, 38054 Grenoble cedex, France

² CNRS, Grenoble Institute of Technology, LMGP, UMR 5628, 3 Parvis Louis Néel, 38016 Grenoble

* Co-first authors

co-corresponding authors: Catherine Picart, Valia Khodr

E-mail: catherine.picart@cea.fr

Keywords: High-content screening, Immunofluorescence, BMP, BMPR, drugs, biomaterials

Abstract

Bone morphogenetic proteins (BMPs) and transforming growth factors (TGF- β) are members of the transforming growth factors superfamily, known for their role in several physiological and pathological processes. These factors are known to bind *in vivo* to BMP and TGF- β receptors respectively, and activate a pSmad signaling pathway. This pathway is generally studied with western blot and luciferase bioluminescence assay, which presents some limitations. Hence, in our work we developed and optimized a high-content immunofluorescence assay to study the pSmad pathway on glass as well as on the biomaterials by overcoming the technical challenges raised by image acquisition and analysis. Furthermore, with this assay, we show here a proof-of concept for drug testing on glass and on the biomimetic films using drug inhibitors of the BMP receptor and of the TGF- β receptors. .

Introduction

The transforming growth (TGF- β) superfamily is a large group of structurally related growth factors (GF) grouped into different families, notably the bone morphogenetic (BMP) and TGF- β families. These GF have been reported to have various physiological roles in development and organ regeneration ((Mueller and Nickel, 2012). They have been described to signal *in vivo*, by binding to a ternary complex of type-I and type-II BMP or TGF- β receptor (called BMPR and TGF- β R respectively), which then activates a cascade of signaling pathways such as the canonical Smad pathway and other Smad-independent pathways. In the Smad pathway, the ternary complex of GF and receptors activates Smad 1/5/9 with BMP-2, and the Smad 2/3 with TGF- β , by undergoing a carboxy-terminal phosphorylation from the type-I receptor (Derynck and Zhang, 2003). The phosphorylated Smad then accumulates in the nucleus and induce the transcription of several regulation genes (Hill, 2009).

The fact that the pSmad signaling is activated by BMP that has a major osteogenic role *in vivo* and *in vitro*, led to the consideration of Smad as an essential marker of early bone regeneration (Song, Estrada and Lyons, 2009). Consequently, this pathway was extensively studied by the standard molecular techniques such as western blot and bioluminescence luciferase. The western blot technique has the advantage of having a high sensitivity of the pictogram order, and being selective in binding specific target antibody in the presence of heterogeneous mixture of several proteins (Ghosh *et al.*, 2014). Similarly the bioluminescence luciferase technique is characterized with a high sensitivity (Thorne, Inglese and Auld, 2010). However, these techniques have limitations in terms of their need for optimization steps, variation of signal quantification, in addition to the limitation of samples number in the case of western blot. Most importantly, these techniques measure the signal average across a population of cells (Badr, 2014; Ghosh *et al.*, 2014). On the other hand, the immunofluorescence technique is generally used for visualization purposes, since the quantification in experiments with several conditions is usually a tedious and lengthy task. However, this technique have the advantage of being compartment-specific and quantitative at a single cell level. This characteristic could be particularly interesting in detecting phenotypic changes that affect subpopulation of cells (Feng *et al.*, 2009; Altschuler and Wu, 2010).

The BMP and TGF- β Smad signaling is studied extensively, due to its association with several diseases such as Fibrodysplasia ossificans progressive, Barret esophagus, leukemia and fibrosis (Wang *et al.*, 2014). Thus, pharmaceutical companies have been focusing on the discovery of new target molecules that can modulate their signaling, in an effort to develop new therapies.

The modulation of BMP and TGF- β signaling can be done at different steps of their signaling, however it is mainly the receptor kinase inhibitors that have been developed (Hong and Yu, 2009). Thus, our aim was first to develop a high-content screening assay to quantify pSmad intensity on the standard glass condition. In addition, we applied this assay to the polylysine/hyaluronic acid (PLL/HA) polyelectrolytes biomimetic films previously developed in the team (Picart *et al.*, 2001; Machillot *et al.*, 2018), and optimized it to arise above the difficulties of doing cellular studies on biomaterials (Appel *et al.*, 2013). Indeed, performing drug screening on biomaterials is not common, yet it has been recently applied to develop a human breast cancer model and hence investigate the effect of extracellular matrix in inducing drug resistance (Schwartz *et al.*, 2017). In that context, drug tests on biomaterials could reveal notable processes that could be masked on glass surfaces. Here, we show here a proof-of-concept with the receptor-kinase inhibitor drugs LDN-193189, inhibitor of ALK2, as well as Galunisertib and Vactosertib, inhibitors of ALK5, on glass and biomaterials using our pSmad assay. In this setting, we used C2C12 skeletal myoblasts that have become the reference cell models in studying bone regeneration since they have the ability to shift their differentiation from myoblasts to osteoblasts in the presence of BMPs (Katagiri *et al.*, 1994).

Materials & Methods

Materials and reagents: Poly(ethylene imine) (PEI) and Poly(L-lysine) hydrobromide (PLL) were purchased from Sigma-Aldrich (St Quentin Fallavier, France), and Sodium Hyaluronate (HA) from Lifecore medical (USA). Paraformaldehyde (PFA), methanol and acetone were purchased from Sigma Aldrich (Missouri, USA). The rinsing solutions 0.15 M NaCl pH 6.4 and pH 5.5, as well as 1 mM HCL pH 3.7 and 0,15 M NaCl 20 mM HEPES pH 7.4 were all prepared in house. BMP-2 were bought from Bioventus (France) and TGF- β 1 from peprotech (France). LDN-193189, Galunisertib and Vactosertib were obtained from Selleckchem (USA). The glass (ref: 655891) and TCPS (ref: 655986) 96-well cell culture microplates as well as the cellview cell culture 10-well plates (ref: 543979) were purchased from Greiner bio-one (Germany). The 4',6-diamidino-2-phenylindole (DAPI) was acquired from Invitrogen, Thermofisher Scientific, France and trihydrate trichlorhydrate de 2'-[4-éthoxyphényl]-5-[4-méthyl-1-pipérazinyl]-2,5'-bi-1H-benzimidazole (Hoechst 33342) anti-pSmad 1/5/9 (ref: 13820S) and anti-pSmad 2 (ref: 18338S) antibodies were obtained from Cell signaling. The

secondary antibody conjugated to Alexa555 or Alexa488 were purchased from Invitrogen, Thermofisher Scientific (France).

Film preparation: The films were prepared as previously described using a modified robot-liquid handling robot (TECAN Freedom EVO® 100, Tecan France, Lyon) in 96-well cell culture microplates with a layer-by-layer deposition of PLL and HA polyelectrolytes (Picart *et al.*, 2001; Machillot *et al.*, 2018). They were then crosslinked with 1-Ethyl-3-(3-Dimethylamino-propyl)Carbodiimide (EDC) at a concentration of 70 mg/mL and N-Hydrosulfosuccinimide sodium salt (Sulfo-NHS) at a concentration of 11 mg/mL. The films were rinsed with a solution of HEPES NaCl at pH 7, as previously described (Richert *et al.*, 2004). The bound BMP-2, hereby called bBMP-2, and bound TGF- β , called bTGF- β 1, were then loaded in a solution of HCl at a concentration of 20 μ g/mL and 0.75 μ g/mL respectively, for 2 h at 37°C, followed by six washes with an HEPES NaCl pH 7 solution. Before usage, the films were sterilized by UV for 30 min.

Cell culture: C2C12 skeletal myoblasts cells, obtained from the American Type Culture Collection, ATCC, were cultured in 1:1 Dulbecco's Modified Eagle Medium (DMEM):Ham's F12 medium (Gibco, Life Technologies, France) supplemented with 10% fetal bovine serum in an incubator at 37°C and 5% CO₂. The cells were cultured up to passage 12 to do the cellular assays. They were then seeded at a density of 10 000 cells/cm² in each well.

Dose response and kinetic studies: The dose response assays at T₀=24h consisted of using a range of concentrations of 0.001 pg/mL to 100 ng/mL for sBMP-2, and 0.001 to 1000 ng/mL for sTGF- β 1. For the T₀=0 conditions, we used a concentration range of 0.001 pg/mL to 1000 ng/mL of BMP-2 and TGF- β 1 on film and glass, with a volume of 50 μ L and 200 μ L per well respectively. In both cases, the cells were exposed to the proteins for 1h. After quantification of pSmad values, the EC₅₀ values were obtained by performing a non-linear dose-response fit on Origin. The kinetic studies consisted on using 400 ng/mL of BMP-2 and TGF- β 1 for the soluble conditions, and 20 μ g/mL for BMP-2 and 0.75 μ g/mL for TGF- β 1 in the bound conditions.

Kinetics and drug assay: These assays consisted on seeding the cells with either sBMP-2 or sTGF- β 1 at a concentration of 400 ng/mL and 10 ng/mL respectively, on glass microplates, or with the bBMP-2 and bTGF- β 1 at a concentration of 20 μ g/mL and 0.75 μ g/mL respectively, on the biomimetic films. In the kinetic assay, the cells were fixed at different time intervals ranging from 15 min until 3 days. While the drug assay consisted on adding the drug, after 15 min of protein exposure, at a concentration range of 0.1 pM to 0.1 μ M for LDN-193189 and 10

pM to 10 μ M M for galunisertib and vactosetib, After 45 min of drug addition, the cells were fixed with PFA. The IC50 values were obtained by performing a non-linear dose-response fit with origin software with the equation $y=A1 + \frac{A2-A1}{1+10^{(Logx0-x)p}}$, with A1 being the highest value, A2 the lowest, and p the hill slope.

Immunofluorescence assay: The cells were fixed with 4% PFA, and stained with 4',6-diamidino-2-phenylindole (DAPI) or Hoechst 33342 for the nuclear staining. The pSmad was stained by using a 1/800 dilution of anti-pSmad antibody, and a secondary antibody conjugated to either Alexa Fluor 488 or Alexa Fluor 555 diluted at 1:500 in BSA 3% w/v in PBS.

Image acquisition: The images were acquired using In Cell GE INCA 2500 imaging system (General Electrics Healthcare, France) with a 20X objective. Similar exposure times were applied for both pSmad 1/5/9 and pSmad 2. 16 to 21 images distributed over each well were acquired and at least 500 cells were analyzed per well. For image analysis, the InCarta® software (General Electrics Healthcare, USA) was used to automatically segment nuclei and cells, and to quantify the nuclear pSmad signal intensity.

Data analysis: The raw intensity data were normalized by the maximum signal measured, and transformed into a percentage of Smad signaling where the background signal corresponds to 0% response. Reported pSmad intensity values are obtained by averaging the values obtained from at least 2 biological replicates, and 3 technical replicates for each experiment. The reported errors are presented as the standard deviation.

Results and discussion

Immunofluorescence pSmad assay and image analysis

In this study, we developed and optimized a high-content screening immunofluorescence assay to quantify the translocation of Smad to the nucleus, first on glass as cell culture substrate, then on the biomimetic film coating. We started by optimizing the experimental conditions, notably cell culture, image acquisition and subsequent analysis to be compatible with both our biomimetic films and the standard glass condition used for imaging (Rodriguez-Hernandez *et al.*, 2014). For simplicity, sBMP-2 and sTGF- β 1 designations will be used to indicate the soluble proteins used on glass surfaces, while bBMP-2 and bTGF- β 1 will be used to designate the matrix-bound proteins loaded in the biomimetic films.

We first performed a dose response assay with sBMP-2 and sTGF- β 1 on 96 wells glass microplates, with C2C12 after 24h of cellular adhesion, as shown in **FIG.1.A**. This condition will be named hereafter T0=24h. Then, after adding sBMP-2 and sTGF- β 1 for 1h, the cells were fixed and analyzed for pSmad 1/5/9 nuclear detection with BMP-2, and pSmad 2 with TGF- β 1, using an immunofluorescence assay.

In an immuno-fluorescence assay, a cell fixation step is essential. In the frame of a kinetic experiment, the cells are ideally fixed at different time points to have images throughout the experiment. Hence, we first optimized the experimental conditions since using the 4% Paraformaldehyde (PFA) commonly-used fixation protocol, we observed toxicity effects. To address this problem, we performed a BMP-2 dose response and compared different methods for cell fixation: 4% PFA, 95% methanol and 40 mM citrate/ 60% acetone (**SI.FIG.1**). We performed an immunofluorescence assay to observe pSmad 1/5/9 signal for both the 4% PFA and 95% methanol in comparison to citrate/acetate (**SI.FIG.1.A**). Then in order to determine in which conditions they could be used, we looked at different parameters, including: i) the possibility to do kinetics on the same plate, ii) the number of adhered cells and cell spreading, iii) the need for a permeabilization step, iv) the possibility to perform an alkaline phosphatase (ALP) staining that is considered an early marker of differentiation in bone cells (Katagiri *et al.*, 1994) (**SI.FIG.1.B**). Overall, we observed that the citrate/acetate solution is not compatible with a pSmad staining, as also seen with the lower Smad intensity level. On the other hand, 95% methanol showed a compatibility with a pSmad staining and did not need a permeabilization step, although it affected the actin staining. Thus, we conclude that both PFA and methanol can be used to study psmad signaling depending on the desired readout.

Moreover, we compared the effect of two different fluorescent antibody: Alexa488 and Alexa555, as well as two supports (glass or tissue culture polystyrene (TCPS)) on pSmad fluorescence intensity (**SI.FIG.2.A-B**). We analyzed the pSmad 1/5/9 signaling with BMP-2 at 400 ng/mL, after 1h of cell culture. We observed a higher pSmad intensity (**SI.FIG.2.A**) and a lower background intensity (**SI.FIG.2.B**) levels with the Alexa555 in comparison to Alexa488. Moreover, the background intensity was lower on the glass plates, which were chosen for their image clarity. Furthermore, we investigated the effect of the dilution level of antibody used during immunofluorescence. We thus used five dilutions of pSmad 1/5/9 primary antibody and two dilutions of Alexa 555 secondary antibody and (**SI.FIG.2.C**). While we observed negligible differences in secondary antibody, the concentration of the different dilutions of primary antibody affected the signal levels. Therefore, we selected a 1/800 dilution of primary antibody

and a 1/500 of secondary antibody as optimal dilutions, to perform the immunofluorescence test.

For the image acquisition analysis, we used an automated imaging system (In Cell analyzer) adapted for high-content screening, as described in the materials and methods section. The raw image of the nuclei was used to set a threshold in order to remove the background fluorescence. This analysis generates a mask image that can be subtracted afterwards from the raw image of Smad staining, hence creating an image showing the Smad staining only present in the nucleus (**FIG.1.B**). The nuclear intensity can then be quantified with either InCarta® , which is the commercialized program of In Cell analyzer, or can be alternatively analyzed using the widely-used image analysis software ImageJ.

A dose-response assay was performed with different concentrations of BMP-2 (**FIG.1.C-D**). As seen in **FIG.1.C**, the pSmad 1/5/9 co-localized with the Hoechst staining in the nucleus, with a low staining in the cytoplasm at both high concentrations of BMP (10^4 ng/mL) as well as the control condition, without BMP-2. The pSmad intensity in the nucleus was subsequently quantified and the half-maximal effective concentration (EC50) calculated, after performing a non-linear dose-response fit (**FIG.1.D**). The EC50 was determined to be 0.92 ± 0.06 ng/mL for sBMP-2 (equivalent to 0.2 ± 0.01 ng, when expressed in absolute mass) and 0.12 ± 0.01 ng/mL (corresponding to 0.02 ± 0.002 ng) for sTGF- β 1.

These values are consistent with the literature data since a study reported the EC50 values, calculated using an AlphaLisa test in C2C12 to be 0.9 ± 0.1 ng/mL for BMP-2 and 0.052 ± 0.002 ng/mL for TGF- β 1 (Hammers *et al.*, 2017). In addition, other studies determined using luciferase assay, the EC50 of BMP-4 to be 0.3 ng/mL in human cervical carcinoma cells (Vrijens *et al.*, 2013), and 2.4 ng/mL in human embryonic kidney cells (HEK293) (Grimley *et al.*, 2019). If compared to BMP-4, the values of EC50 for BMP-2 seems comparable to the literature.

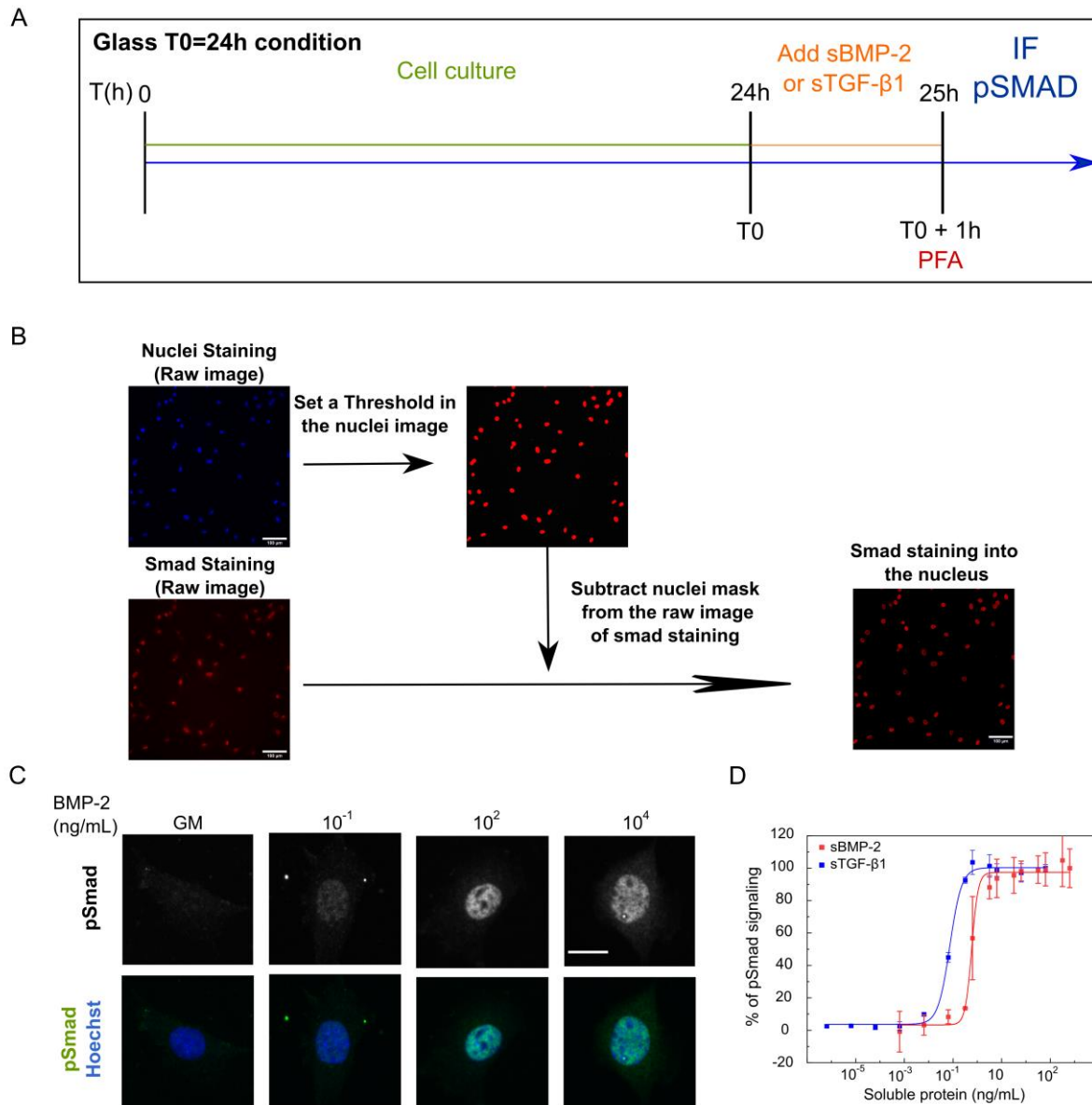


FIG.1. A dose-response immunofluorescence assay for pSmad nuclear translocation. A dose response assay was performed. A) The experiment consisted on seeding the cells and then adding sBMP-2 and TGF- β 1 at a concentration of 10^{-6} to 10^3 ng/mL. After 1h of protein stimulation, the C2C12 cells were fixed with an immunofluorescence assay using Hoechst and pSmad 1/5/9 or pSmad 2 antibody. B) The acquisition was done with an automated inCell analyzer system. The image analysis consisted on first setting a threshold on the raw image of the nuclei, which then creates a mask image that could be subtracted from the raw image of pSmad staining. The resulting image presents then the Smad staining in the nucleus. Scale bar =100 μ m. C) Cellular images of the dose-response assay with BMP-2, with pSmad 1/5/9 and nuclei staining. Scale bar= 26 μ m. D) The dose response curves with BMP-2 and TGF- β 1.

pSmad phosphorylation kinetics with BMP-2 and TGF- β 1

After defining the optimal experimental parameters, we examined the kinetics of pSmad signaling with BMP-2 and TGF- β 1 on both glass and film with the aim of defining the optimal time-window to perform the drug experiments. We first performed a kinetic test in standard conditions, where C2C12 cells adhered for 24 h on glass plate before adding sBMP-2. The cells were then fixed at different time points from 0 to 8h, as shown in **SI.FIG.3**.

Then, we did the kinetic experiments for cells cultured on glass plate with sBMP-2 and sTGF- β 1, and for cells cultured on the biomimetic films with bBMP-2 and bTGF- β 1. The cells were fixed at different time points ranging from 30 min up to 3 days (**FIG.2.A-B**). An effect of cell toxicity was observed when wells of the same 96 wells microplate were fixed with PFA at different time points. The usage of methanol solved the issue of toxicity, yet led to lower signal intensity than PFA. Thus, we used 10 wells CellView microplates for each time point and used PFA to fix cells in the 96 wells microplate.

The result of the kinetics in the three experimental conditions show the presence of a first high pSmad intensity peak at 30 min, followed by a gradual decrease of the pSmad nuclear signal. Notably, the pSmad 1/5/9 signal with BMP-2 in T0=0 showed a sustained signal of 40% up to 8h (**FIG.2.A**), before returning to basal levels at 48h, in comparison to pSmad 2 with TGF- β that showed a return to basal levels at 24h (**FIG.2.B**).

These results are compatible with the literature as kinetic studies of BMP-2 done by western blot showed the presence of a pSmad 1/5/8 signal after 30 min with a sustained signal up to 180 min on different types of biomaterials (Rath *et al.*, 2011; Schwab *et al.*, 2015; Migliorini *et al.*, 2017). Similarly, studies with TGF- β 1 in different cell models showed the activation of pSmad 2 signaling after 30 min of TGF- β 1 addition, and up to 8h in continuous ligand stimulation (Garamszegi *et al.*, 2010; Zi *et al.*, 2011).

The presence of a sustained signal may be explained by the mechanism of Smad regulation of import and export to/from the nucleus. Indeed, it was reported that smad 3 possess an NLS-like sequence in the MH1 domain, capable of binding a karyopherin (the importing β 1) and hence induce its import to the nucleus (Xiao, Liu and Lodish, 2000). In contrast, smad 2 seemed to be by directly interacting with the nucleoporins to translocate to the nucleus (Xiao *et al.*, 2001).

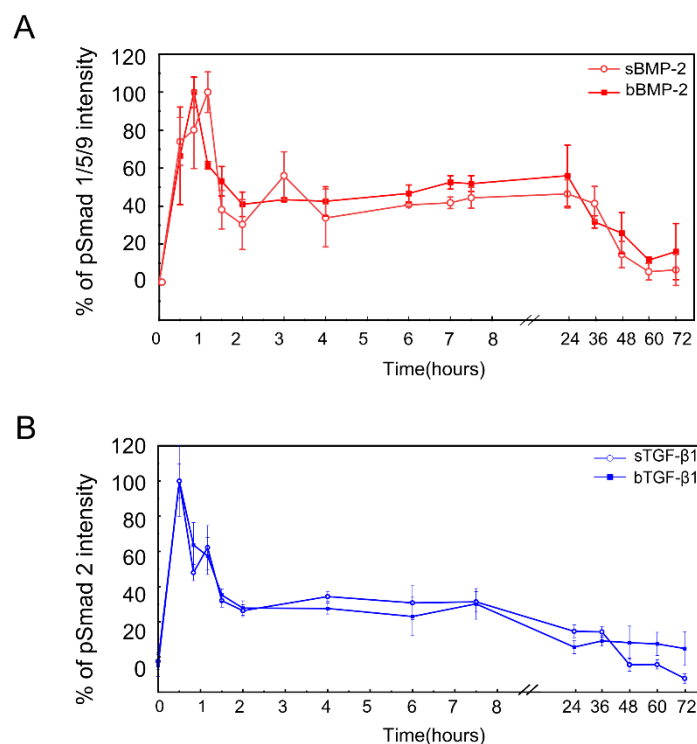


FIG.2. Kinetic study of pSmad phosphorylation in C12C12 skeletal myoblasts in the presence of soluble and matrix-bound BMP-2 and TGF-β1. Data points corresponding to the cell experiments on glass are represented with an empty circle, while those on the biomimetic films are represented with a filled rectangle. A) A kinetic graph of pSmad 1/5/9 after 1h of C2C12 cell exposure to BMP-2 on glass and film. B) A kinetic graph of pSmad 2 after 1h of C2C12 cell exposure to TGF-β1 on glass and film.

Since we observed an initial peak from 30 min to 1h30 for both proteins in the glass and film conditions, we chose 1h as an optimal time for the future experiments using drugs.

Test of BMP receptor drug inhibitors for cells cultured on glass and on biomaterials

After optimizing the time conditions, we performed dose-response assays with soluble and matrix-bound proteins to determine the optimal concentration for the drug experiments. For the film condition, we seeded the C2C12 cells directly on the biomimetic films loaded with bBMP-2 and bTGF-β1, and on the glass condition supplemented with sBMP-2 or sTGF-β1 simultaneously as described in **FIG.3.A**. After quantification of Smad intensity (**FIG.3.B-C**), we determined the EC50 values, which were similar for the glass and film conditions. The values of EC50 on glass are 120 ± 47 ng/mL (corresponding to 24.0 ± 9.4 ng) for sBMP-2, and 0.5 ± 0.16 ng/mL (equivalent to 0.1 ± 0.03 ng) for sTGF-β1. As for the film, the EC50 values were determined to be 288 ± 20 ng/mL (equivalent to 14.4 ± 1.0 ng) for bBMP-2, and 8 ± 2

ng/mL (corresponding to 0.4 ± 0.1 ng) for bTGF- β 1. We note that the EC₅₀ value of sBMP-2 when cell seeding and the protein is added simultaneously (**FIG.3.B-C**) are higher than the EC₅₀ value of sBMP-2 and sTGF- β 1 when cell have adhered to 24h (0.2 ± 0.01 ng and 0.02 ± 0.002 ng, respectively) (**FIG.1.A**).

These values are in agreement with previous studies where the adhesion of C2C12 on the biomimetic films with bBMP-2 was studied (Fourel *et al.*, 2016). They showed that the presentation of the usage of biomimetic films and presenting BMP in a matrix-bound manner leads to a crosstalk between the BMPR and integrins that are responsible for the adhesion. They also showed that the cascade of events starts with BMP-2 binding to BMPR followed by integrin activation, before the Smad signaling (Fourel *et al.*, 2016). We can thus hypothesize that the added BMP-2 when the cells have not yet adhered, are used in focal adhesion formation to ensure adhesion, in addition to BMPR to activate pSmad signaling. We can also assume that a similar process involving integrin occurs when cells are seeded on glass. Hence, the adhesion process could explain the need for a higher quantity of protein when cells have not yet adhered in comparison to when the cells have already adhered.

After characterizing the cellular response to BMP-2 and TGF- β 1 on biomaterials, we chose suitable concentrations higher than the EC₅₀ values to do the drug experiments. We selected LDN-193189, one of the first discovered kinase inhibitor of ALK2 (Cuny *et al.*, 2008), in addition to two ALK5 kinase inhibitors currently being developed in clinical trials for cancer: Galunisertib, which was stopped at phase 2 of clinical trials by the sponsor company, and Vactosertib which are currently in phase 2 (Wick *et al.*, 2020; Kim *et al.*, 2021). The experiments were performed as shown in **FIG.3.D**. The drugs were added for 45 min, followed by cell fixation. After quantification of the Smad signal, we were able to determine the half-maximal inhibitory concentration (IC₅₀). The results showed similar curves and IC₅₀ values for both the film and glass conditions (**FIG.3.E**). The LDN-193189's IC₅₀ is determined at 3.0 ± 0.03 nM and 2.7 ± 0.2 nM for glass and film respectively. While the IC₅₀ of Galunisertib are 1276 ± 79 nM and 1587 ± 552 nM, and Vactosertib are 85 ± 12 nM and 118 ± 21 nM for glass and film respectively.

The data in the literature for the exact IC₅₀ varies, as it is cellular and assay dependent. For instance, the manufacturer's reported IC₅₀ values are 0.8 nM, 56 nM and 11 nM for LDN-193189, Galunisertib and Vactosertib respectively using *in vitro* kinase assays, commonly used in drug development, which consists on measuring the kinase activity by determining the amount of radioactive ATP transferred to the substrate (Jia *et al.*, 2008; Vactosertib, 2021;

Galunisertib, 2021; *LDN-193189*, no date). Furthermore, a study of pSmad 1/5/9 signaling inhibition with BMP-4 and LDN-193189 determined its IC₅₀ to be 4.9 nM (Cuny *et al.*, 2008). On the other hand, other studies have reported the IC₅₀ of Galunisertib at 50 to 430 nM depending on the used assay (Yingling *et al.*, 2018). Nevertheless, in our work the values of IC₅₀ are similar for both film and glass conditions with the three drugs, indicating the robustness of the immunofluorescence assay and its application in different models.

In order to determine the stability of our assay in performing high-throughput screens, we carried out a Z' factor experiment, where LDN-193189 was added at a concentration of 100 nM and BMP-2 at 2 µg/mL and 400 ng/mL for the film and glass respectively. The study demonstrated a Z' factor of 0.3 for glass and 0.6 for film. Since an acceptable assay has a Z' factor around and higher than 0.5, we show here that our pSmad assay is adapted for high-content drug assays on both glass and biomaterials.

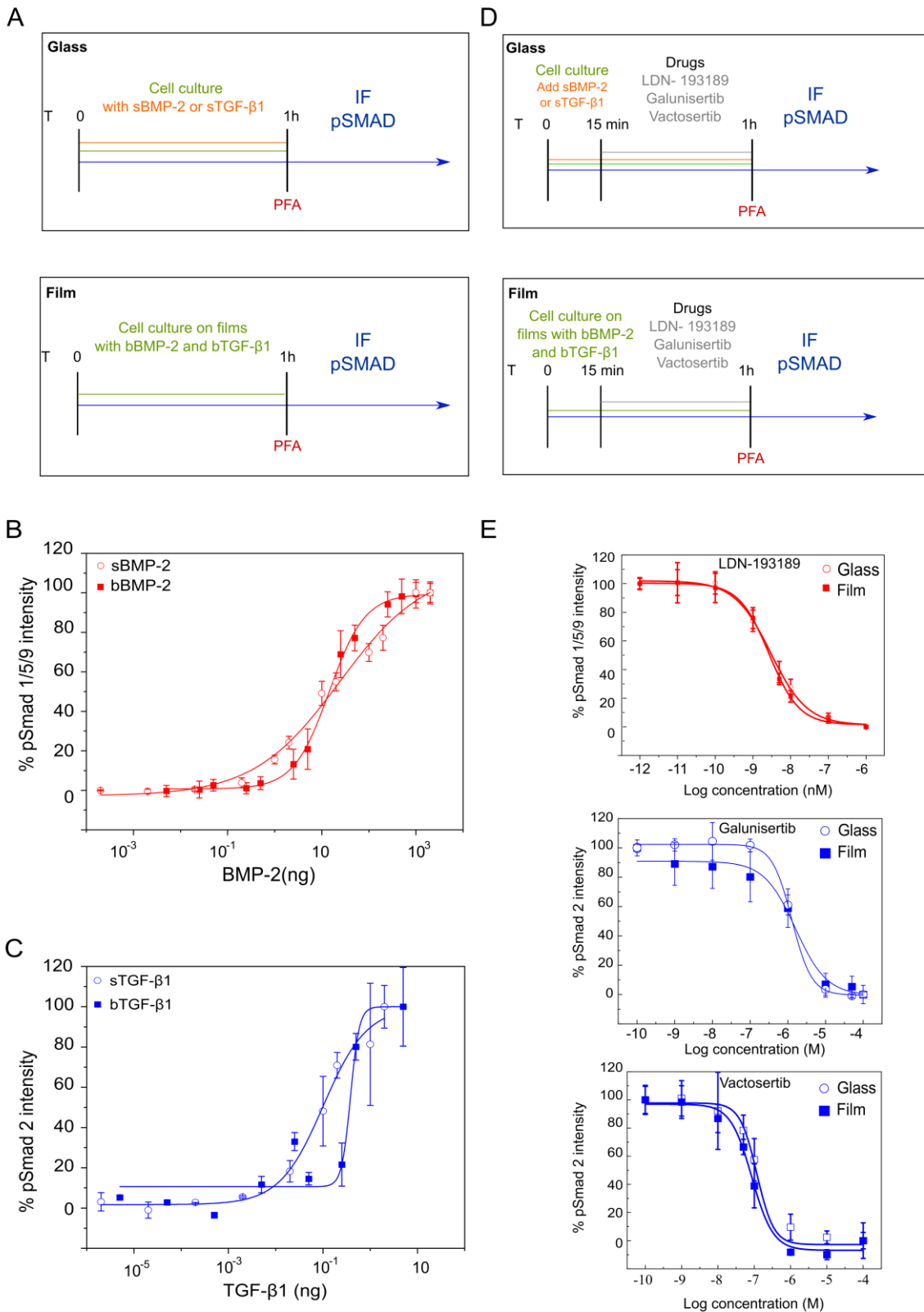


FIG.3. ALK inhibitor drug assay with BMP-2 and TGF- β 1. A) Schematics of the experimental protocol of the dose-response tests on glass and biomaterials with BMP-2 and TGF- β 1. B) A Dose response test with bBMP-2 and sBMP-2 on film and glass respectively

with C2C12 cells. C) A Dose response test with bTGF- β 1 and sTGF- β 1 on film and glass respectively with C2C12 cells. D) Schematics of the experimental protocol of the drug tests on glass and biomaterials with BMP-2 and TGF- β 1. E) Drug assay of LDN-193189 with BMP-2, and Galunisertib and Vactosertib with TGF- β 1 with C2C12 cells on glass and film.

We note that in order to validate that our IC50 are not BMP concentration-dependent, we performed a drug assay with LDN-193189 and several concentrations of BMP-2 and showed that the pSmad intensity is independent of the BMP-2 concentration (**SI.FIG.4-A**). This result is explained with the action mode of the inhibitors that inhibit the BMP and TGF- β signaling at the level of the receptors. In addition, we tested the effect of DMSO on the fluorescence intensity of Smad 1/5/9 and Smad 2/3 (**SI.FIG.4-B-C**). We did not observe any effect on the Smad intensity signal for levels of DMSO up to 1%, which was the maximal concentration used in our assay, while 2% and 5% levels showed an important increase in Smad signaling.

The similarity in IC50 values between the film and glass indicates that the film is comparable to the glass condition, which is commonly used as reference for *in vitro* drug testing. From our study, we can conclude that this optimized pSmad test is adapted to do high content drug screening on bioactive materials, similarly to the standard glass condition. These results further show the possibility of future studies on biomaterials to investigate pathologies in a biomechanical context by modifying the biomimetics films' stiffness.

Conclusion

In this work, we present a high-content immunofluorescence assay to study the pSmad pathway on glass and biomaterials. We show the optimization of the classic protocol to overcome the limitations of doing certain tests such as the kinetic tests on protein-loaded biomaterials. We also demonstrate a proof-of-concept of pSmad activity-based drugs assay on biomaterials. This assay may thus be further used on the biomimetic films containing other ECM proteins or growth factors.

Acknowledgments

The authors thank Marie-Odile Fauvarque, Emmanuelle Soleilhac and Catherine Pillet for fruitful discussions and advices, notably regarding the drug assay experiments. We are also grateful to Sabine Bailly for her feedback and recommendations.

Data availability

The data that support the findings of this study are available from the corresponding author upon request.

Funding and additional information

The study was supported by the Agence Nationale de la Recherche (ANR CODECIDE, ANR-17-CE13-022), and Institut Universitaire de France (IUF) to C.P. In addition to the European Research Council (ERC) under FP7 programm (ERC Biomim GA259370), the ERC POC Bioactive coatings (GA 692924) and by the Fondation Recherche Medicale (FRM, grant DEQ20170336746) to C.P. V.K. was supported by a PhD. fellowship from Grenoble Institute of Technology.

References

- Altschuler, S. J. and Wu, L. F. (2010) ‘Cellular Heterogeneity: Do Differences Make a Difference?’, *Cell*, 141(4), pp. 559–563. doi: 10.1016/j.cell.2010.04.033.
- Appel, A. A. *et al.* (2013) ‘Imaging challenges in biomaterials and tissue engineering’, *Biomaterials*, 34(28), pp. 6615–6630. doi: 10.1016/j.biomaterials.2013.05.033.
- Badr, C. E. (2014) ‘Bioluminescent Imaging’, *Methods in Molecular Biology*, 1098. doi: 10.1007/978-1-62703-718-1.
- Cuny, G. D. *et al.* (2008) ‘Structure-activity relationship study of bone morphogenetic protein (BMP) signaling inhibitors’, *Bioorg Med Chem Lett*, 18(15), pp. 4388–4392. doi: 10.1016/j.bmcl.2008.06.052. Structure-activity.
- Derynck, R. and Zhang, Y. E. (2003) ‘Smad-dependent and Smad-independent pathways in TGF-beta family signalling.’, *Nature*, 425(6958), pp. 577–584. doi: 10.1038/nature02006.
- Feng, Y. *et al.* (2009) ‘Multi-parameter phenotypic profiling: Using cellular effects to characterize small-molecule compounds’, *Nature Reviews Drug Discovery*. Nature Publishing Group, 8(7), pp. 567–578. doi: 10.1038/nrd2876.
- Fouriel, L. *et al.* (2016) ‘ β 3 integrin-mediated spreading induced by matrix-bound BMP-2 controls Smad signaling in a stiffness-independent manner’, *Journal of Cell Biology*, 212(6), pp. 693–706. doi: 10.1083/jcb.201508018.
- Galunisertib* (2021). Available at: <https://www.selleckchem.com/products/ly2157299.html>.
- Garamszegi, N. *et al.* (2010) ‘Extracellular matrix-induced transforming growth factor- β receptor signaling dynamics’, *Oncogene*. Nature Publishing Group, 29, pp. 2368–2380. doi: 10.1038/onc.2009.514.
- Ghosh, R. *et al.* (2014) ‘The necessity of and strategies for improving confidence in the accuracy of western blots’, *Expert Rev Proteomics*, 11(5), pp. 549–560. doi:

10.1586/14789450.2014.939635.The.

Grimley, E. *et al.* (2019) ‘High-throughput screens for agonists of bone morphogenetic protein (BMP) signaling identify potent benzoxazole compounds’, *Journal of Biological Chemistry*, p. jbc.RA118.006817. doi: 10.1074/jbc.ra118.006817.

Hammers, D. W. *et al.* (2017) ‘Supraphysiological levels of GDF 11 induce striated muscle atrophy’, *EMBO Molecular Medicine*, 9(4), pp. 531–544. doi: 10.15252/emmm.201607231.

Hill, C. S. (2009) ‘Nucleocytoplasmic shuttling of Smad proteins’, *Cell Research*, 19(1), pp. 36–46. doi: 10.1038/cr.2008.325.

Hong, C. C. and Yu, P. B. (2009) ‘Applications of small molecule BMP inhibitors in physiology and disease’, *Cytokine and Growth Factor Reviews*, 20(5–6), pp. 409–418. doi: 10.1016/j.cytogfr.2009.10.021.

Jia, Y. *et al.* (2008) ‘Current In Vitro Kinase Assay Technologies: The Quest for a Universal Format’, *Current Drug Discovery Technologies*, 5(1), pp. 59–69. doi: 10.2174/157016308783769414.

Katagiri, T. *et al.* (1994) ‘Bone morphogenetic protein-2 converts the differentiation pathway of C2C12 myoblasts into the osteoblast lineage’, *Journal of Cell Biology*, 127(6 I), pp. 1755–1766. doi: 10.1083/jcb.127.6.1755.

Kim, B. G. *et al.* (2021) ‘Novel therapies emerging in oncology to target the TGF- β pathway’, *Journal of Hematology and Oncology*. BioMed Central, 14(1), pp. 1–20. doi: 10.1186/s13045-021-01053-x.

LDN-193189 (no date) 2021. Available at: <https://www.selleckchem.com/products/ldn193189.html>.

Machillot, P. *et al.* (2018) ‘Automated Buildup of Biomimetic Films in Cell Culture Microplates for High-Throughput Screening of Cellular Behaviors’, *Advanced Materials*, 30(27), pp. 1–8. doi: 10.1002/adma.201801097.

Mueller, T. D. and Nickel, J. (2012) ‘Promiscuity and specificity in BMP receptor activation’, *FEBS Letters*, 586(14), pp. 1846–1859. doi: 10.1016/j.febslet.2012.02.043.

Picart, C. *et al.* (2001) ‘Buildup mechanism for poly(L-lysine)/hyaluronic acid films onto a solid surface’, *Langmuir*, 17(23), pp. 7414–7424. doi: 10.1021/la010848g.

Rath, B. *et al.* (2011) ‘Biomechanical forces exert anabolic effects on osteoblasts by activation of SMAD 1 / 5 / 8 through type 1 BMP receptor’, *Biorheology*, 48, pp. 37–48. doi: 10.3233/BIR-2011-0580.

Richert, L. *et al.* (2004) ‘Improvement of stability and cell adhesion properties of polyelectrolyte multilayer films by chemical cross-linking’, *Biomacromolecules*, 5(2), pp. 284–294. doi: 10.1021/bm0342281.

Rodriguez-Hernandez, C. O. *et al.* (2014) ‘Cell Culture: History, Development and Prospects’, *International Journal of Current Research and Academic Review*, 2(12), pp. 188–200.

Schwab, E. H. *et al.* (2015) ‘Nanoscale control of surface immobilized BMP-2: Toward a quantitative assessment of BMP-mediated signaling events’, *Nano Letters*, 15(3), pp. 1526–1534. doi: 10.1021/acs.nanolett.5b00315.

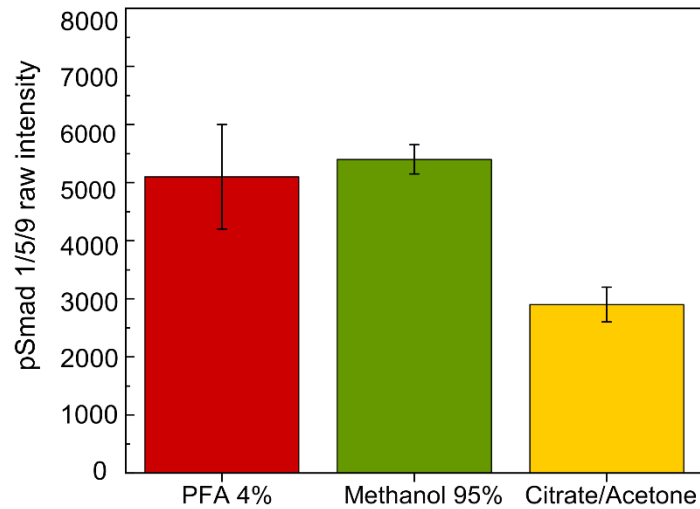
Schwartz, A. D. *et al.* (2018) ‘Mechanisms of Drug Resistance’, 9(12), pp. 912–924. doi: 10.1039/c7ib00128b.A.

Song, B., Estrada, K. D. and Lyons, K. M. (2009) ‘Smad Signaling in Skeletal Development

- and Regeneration Buer', *Cytokine Growth Factor Rev*, 20(5–6), pp. 379–388. doi: 10.1016/j.cytogfr.2009.10.010.Smad.
- Thorne, N., Inglese, J. and Auld, D. (2010) 'Illuminating insights into firefly luciferase and other bioluminescent reporters used in chemical biology', *Chem Biol.*, 17(6), pp. 646–657. doi: 10.1016/j.chembiol.2010.05.012.Illuminating.
- Vactosertib* (2021). Available at: <https://www.selleckchem.com/products/ew-7197.html>.
- Vrijens, K. *et al.* (2013) 'Identification of Small Molecule Activators of BMP Signaling', *PLoS ONE*, 8(3). doi: 10.1371/journal.pone.0059045.
- Wang, R. N. *et al.* (2014) 'Bone Morphogenetic Protein (BMP) signaling in development and human diseases', *Genes and Diseases*. Elsevier Ltd, 1(1), pp. 87–105. doi: 10.1016/j.gendis.2014.07.005.
- Wick, A. *et al.* (2020) 'Phase 1b/2a study of galunisertib, a small molecule inhibitor of transforming growth factor-beta receptor I, in combination with standard temozolomide-based radiochemotherapy in patients with newly diagnosed malignant glioma', *Investigational New Drugs*, 38(5), pp. 1570–1579. doi: 10.1007/s10637-020-00910-9.
- Xiao, Z. *et al.* (2001) 'Nucleocytoplasmic Shuttling of Smad1 Conferred by Its Nuclear Localization and Nuclear Export Signals', *Journal of Biological Chemistry*. © 2001 ASBMB. Currently published by Elsevier Inc; originally published by American Society for Biochemistry and Molecular Biology., 276(42), pp. 39404–39410. doi: 10.1074/jbc.M103117200.
- Xiao, Z., Liu, X. and Lodish, H. F. (2000) 'Accelerated Publication: Importin β mediates nuclear translocation of Smad 3', *Journal of Biological Chemistry*. © 2000 ASBMB. Currently published by Elsevier Inc; originally published by American Society for Biochemistry and Molecular Biology., 275(31), pp. 23425–23428. doi: 10.1074/jbc.C000345200.
- Yingling, J. M. *et al.* (2018) 'Preclinical assessment of galunisertib monohydrate), a first-in-class transforming growth factor- β receptor type I inhibitor', 9(6), pp. 6659–6677.
- Zi, Z. *et al.* (2011) 'Quantitative analysis of transient and sustained transforming growth factor- β signaling dynamics', *Molecular Systems Biology*. Nature Publishing Group, 7(492), pp. 1–12. doi: 10.1038/msb.2011.22.

Supplementary data:

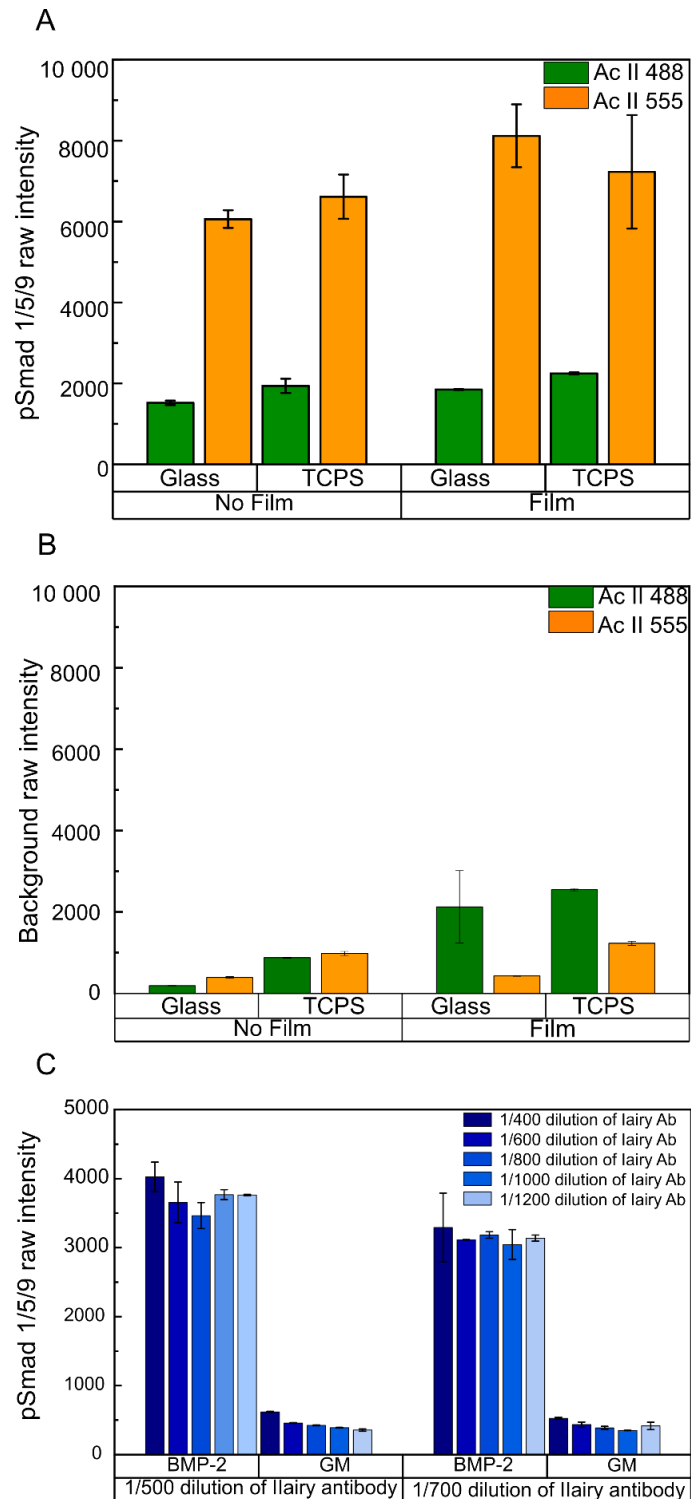
A



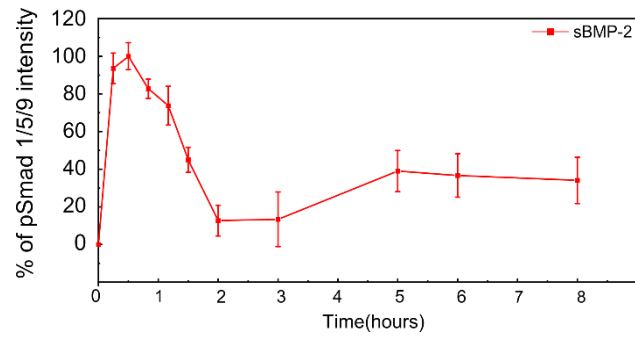
B

	PFA	Methanol	Citrate Acetone
Kinetic on same plate	✗	✓	✓
Adhesion (Cell number)	✓	✓	✓
Spreading (Actin staining)	✓	✗	✓
pSmad1/5/9 staining	✓	✓	✗
Permeabilization step	required	not required	not required
ALP staining	✓	✓	✓

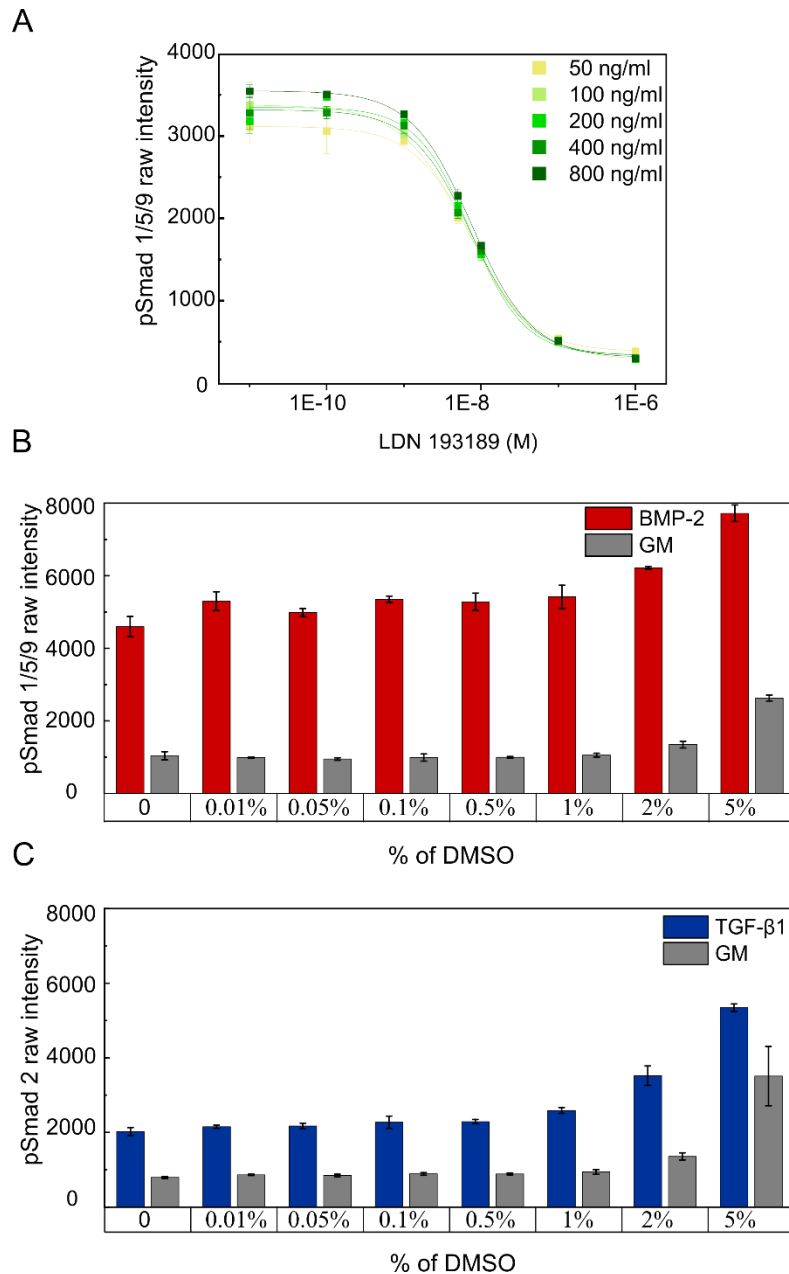
SI.FIG.1. Comparison of different solutions of cell fixation. A) Quantification of pSmad 1/5/9 signal in a dose-response test with BMP-2, after cell fixation with either 4% PFA, 95% Methanol and 40 mM Citrate/60% Acetone. B) A table summarizing the different characteristics of the fixation solutions.



SI.FIG.2. Optimization of antibody and plates usage. A) The pSmad 1/5/9 intensity was measured with the secondary antibody Alexa488 and Alexa55 on film and no film conditions, on glass and TCPS. B) The background intensity was measured with the secondary antibody Alexa488 and Alexa55 on film and no film conditions, on glass and TCPS. C) The pSmad 1/5/9 intensity was measured with 1/400, 1/600, 1/800, 1/1000 and 1/1200 dilutions of pSmad 1/5/9 primary antibody, as well as with 1/500 and 1/700 dilutions with the secondary Alexa555 antibody, in the presence and absence of BMP-2.



SI.FIG.3. A kinetic study of pSmad 1/5/9 translocation to the nucleus with sBMP-2 after 24h of C2C12 cell adhesion on glass support.



SI.FIG.4. Drug experiments control tests. A) A drug test was performed with LDN-193189 and different concentrations of BMP-2 (50 ng/mL, 100 ng/mL, 200 ng/mL, 400 ng/mL and 800 ng/mL). B) The pSmad 1/5/9 raw signal was measured in the presence and absence of BMP-2 with different percentage of DMSO. C) The pSmad 2 raw signal was measured in the presence and absence of TGF-β1 with different percentage of DMSO.

Chapter VI:
General discussion

As mentioned above, bone regeneration is highly regulated by growth factors such as BMPs that can stimulate the differentiation and expansion of stem cells capable of forming new bone tissue. Current bone regeneration therapies are using BMPs or materials to repair bone fractures. On the other hand, several proteins involved in the BMP signaling pathway have been associated with pathologies and diseases, such as mutation of ALK2 for FOP disease, as well as BMPR-II and Smad 9 for PAH (Kaplan *et al.*, 2009; Lijiang and Chung, 2017). Thus, it is imperative to better understand the signaling pathways of BMPs to not only ensure their correct usage *in vivo*, but also to develop therapies to diseases related to the BMP-pathway.

In this thesis, we focused on studying the early steps of bone regeneration involving ligands of the TGF- β superfamily. We therefore investigated the first step of the BMP pathway consisting of the interaction of BMPs with their receptors, in addition to the activation of the Smad-dependent pathway by BMP and TGF- β and Smad 1/5/9 and Smad 2 translocation to the nucleus. During this project, we established and optimized several tools and techniques. These tools may be used by other teams in other projects, since they are easily transposable.

I. Determining BMP/BMPR interaction using BLI

1. BLI as a technique

In this study, we used the BLI technique, which was only recently beginning to be used in the BMP field (Seeherman *et al.*, 2019). In fact, the reference technique in the field is the SPR that is usually used with a common adsorption strategy consisting of immobilizing the BMPR by amine coupling to the surface and adding BMP as analyte. Although several studies reported the success of this strategy, it is a non-specific coupling strategy (Kortt *et al.*, 1997). Here, we used an adsorption strategy consisting of BMPR-Fc chimeras and anti-Fc coated surfaces that allows the presentation of BMPR in one orientation in a way, so that the binding site is always accessible.

Furthermore, we chose the BLI technique instead of SPR since it allows the measurement of several concentrations in parallel, which makes it compatible to do protein/protein interaction for a large numbers of protein couples. To note, we could not measure the interactions of BMP-2 and BMP-4 with BMPR using SPR with the adsorption strategy of BMPR-Fc chimeras and protein A coated surfaces, which further justify the need to use BLI for our experiments. We compared the two techniques SPR and BLI and measured the K_D of ALK1/BMP-9. We found a much lower K_D by SPR in comparison to BLI (13.4 pM versus 200 pM). The 20-fold

difference is most likely due to the specific characteristics of each technique and differences in their sensitivity. For comparison, the SPR sensitivity is reported to be in the order of μM - pM , while the BLI has a range of 1 mM - 10 pM (Sultana and Lee, 2015) .

2. Effect on signaling

With the discovery of the BMP and BMPR families, a phenomenon of promiscuity in BMP binding was described. In that context, we studied the interaction of BMP with their BMPR using BLI in similar experimental conditions, thus providing insights on the BMP/BMPR combinations.

Our BLI results highlight differences in the binding properties of BMP-2 and BMP-4 to BMPR. We show that they bind ALK3, ALK6 and ALK2 with a similar binding affinity, yet BMP-2 binds ALK1, ALK5 and most importantly type-II BMPR with a much higher affinity than BMP-4. These differences in affinities are associated to a higher association rates for BMP-2 in comparison to BMP-4, although they showed similar K_d . These results may appear surprising having in mind that BMP-2 and BMP-4 share more than 80% of sequence homology. Since the 3D structure of BMP-4 is not known yet, we suppose that BMP-4 may present structural differences in the binding sites notably for type-II BMPR that renders its association to these receptors slower than BMP-2.

These differences between BMP-2 and BMP-4 were also observed in the second manuscript at the signaling level (Sales *et al.*, 2022) (Article shown in Annexes). In this work, we performed the silencing of type-I and type-II BMP receptors and quantified the pSmad 1/5/9 and pSmad 2 using matrix-bound BMP-2, BMP-4, BMP-7 and BMP-9 presented via soft or rigid biomimetic films (results presented in chapter IV). Regarding BMP-4, a role of ALK3, ALK5 and ALK6 was found for pSmad 1/5/9 signaling in a stiffness-independent manner, while for pSmad 2, ALK3 had the most important role in stiffness-dependent manner: its role was more important on stiff films than on soft films. This result was not observed with BMP-2, for which ALK2 and ALK6 have a major stiffness-independent role on pSmad 1/5/9 while they have no significant role on pSMAD2.

On the other hand, BMPR-II has an important role, whatever the bBMP, in a stiffness-independent for pSmad 1/5/9 and stiffness-dependent for pSmad 2. ACTR-IIA has also a major role, notably in response to bBMP-7 but also to bBMP-4, for the two readouts pSmad 1/5/9 and ALP but not for pSmad 2. This result is coherent with BMP-7 binding with a high affinity to both BMPR-II, ACTR-IIA. Here, ACTR-IIB has only a minor role.

a. Distinct functional roles of BMPs

Although functional roles are much more complex than just measuring a direct effect of BMP/BMPR interactions, since other regulations are coming into play (e.g. ECM regulation of BMPs), several studies reported functional differences between BMP-2 and BMP-4. This is coherent with what we showed in chapter III that they bind differently to BMPR. Indeed, one study examined their role in chondrocyte proliferation and found that the deletion of BMP-2 gene alone resulted in severe chondrodysplasia while the deletion of BMP-4 led to minor cartilage phenotype (Shu *et al.*, 2011). Furthermore, In acute myeloid leukemia, a distinct role of BMP-4 versus BMP-2 has been evidenced (Voeltzel *et al.*, 2018; Lefort and Maguer-Satta, 2020): Only BMP-4 is involved as its binding to ALK3 then activates $\Delta Np73/NANOG$ (Voeltzel *et al.*, 2018; Lefort and Maguer-Satta, 2020). In addition, It has been demonstrated that BMP-4 has a distinct role in stimulating hematopoietic stem cell proliferation, differentiation and homing (Bhatia *et al.*, 1999; Khurana *et al.*, 2013).

Regarding BMP-7, our results showed that it binds with high affinities to the three type-II BMPRs, with a 5-fold higher affinity for ACTR-IIA. This result is in concert with a previous study reported that BMP-7 signals mainly through ACTR-IIA (Lavery *et al.*, 2008). Notably, BMP-7 was also reported to induce chemotaxis in monocytic cells through BMPR-II and ACTR-IIA receptors, but not via ACTR-IIB (Perron and Dodd, 2009).

b. BMP combination signaling

The promiscuity in receptors has been suggested to occur during organ development, where a high number of BMPs and low numbers of receptors are expressed in a highly confined spaced (Aberg, Wozney and Thesleff, 1997; Keyes *et al.*, 2003; Mueller and Nickel, 2012). Considering, the overlapping spatiotemporal distribution of several BMP ligands and the promiscuity of BMP/BMPR interaction, the cells seem to receive signals encoded by a combination of BMPs (Antebi *et al.*, 2017).

The determination of preferred interactions between BMP/BMPRs is essential to decipher the signaling pathways, notably since the phenomenon of promiscuity has been linked to the activation of distinct signaling pathways. As an example, ACTR-IIB have been described to have dual role in embryogenesis as it activated dorsalization of zebrafish embryos and dorsal and ventro-lateral mesoderm in blastula stage embryos (Nagaso *et al.*, 1999). It is suggested that the difference in ACTR-IIB signaling is related to the activation of distinct signaling pathways due to the recruitment of specific type-I receptors notably ALK3 with BMP-2 and

BMP-4 and TARAM-A (closely related to the mammalian receptor ALK4) with Activin A (Nagaso *et al.*, 1999).

c. Ligand binding competition

Furthermore, a binding competition phenomenon have been reported to have an essential physiological role, and to play a role in several pathologies.

The specificity of Smad signaling (Smad 1/5/9 and Smad 2) after ligand binding competition was addressed in a study, where they looked into the binding competition of Activin, BMP-2, BMP-7 and BMP-9 to type-II BMPR and analyzed the Smad pathway using a luciferase assay. The study showed that Activin A can antagonize BMP-2 and BMP-7 signaling by binding with a higher affinity ($K_D= 43 \text{ pM}$) to the ACTR-IIA compared to BMPs, and therefore inhibit the Smad 1/5/8 pathway and activate the Smad 2/3 (**FIG.VI.2**) (Aykul and Martinez-hackert, 2016).

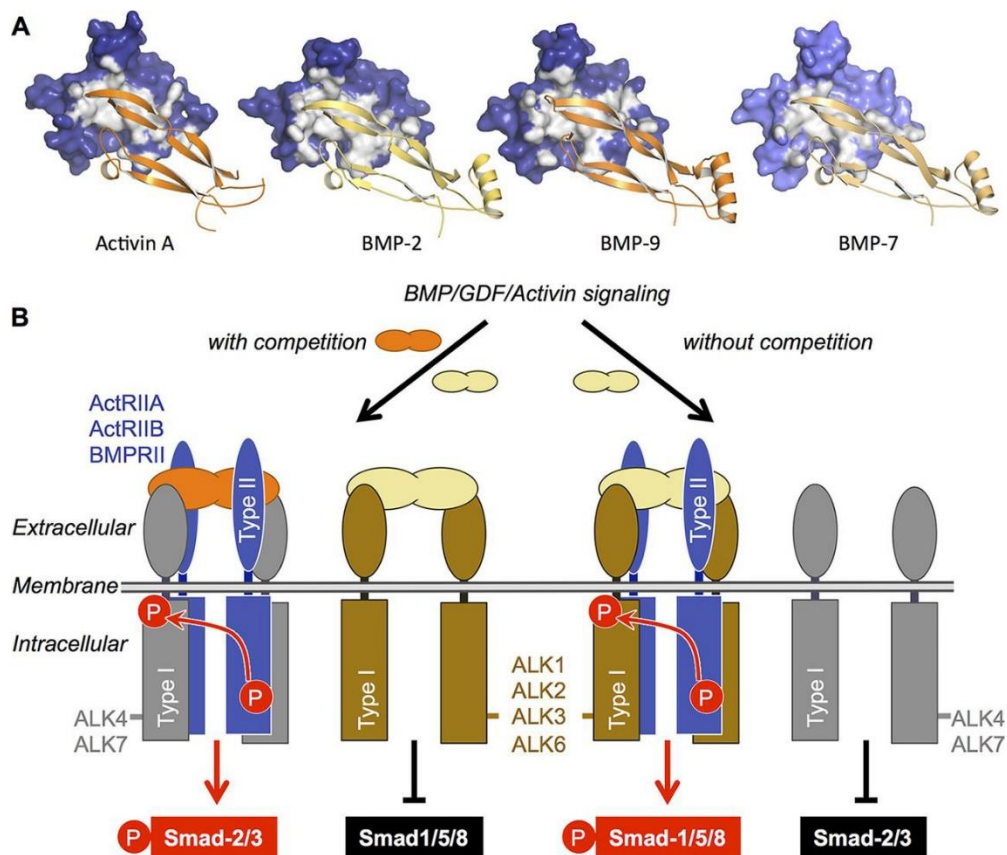


FIG.VI.2. Schematic of ligand binding competition between Activin A, BMP-2, BMP-9 and BMP-7. (Aykul and Martinez-hackert, 2016)

These specificities in signaling have been described in the literature as dependent on type-I receptors that were grouped into Smad 1/5/9 or Smad 2/3 activating receptors. The activation of distinct R-Smad is dependent on the specificities of the L45 loop of the activated type-I BMPR. Indeed, up to date, the type-I BMPR was associated in three categories based on the similarities in their L45 loop amino acid sequence: notably ALK3/ALK6 and ALK1/ALK2 activating Smad 1/5/9 while ALK4/ALK5/ALK7 are activating Smad 2/3 (Fujii *et al.*, 1999; Zou *et al.*, 2021).

Although this knowledge is considered a dogma in the field, it is important to note that some studies reported the activation of Smad 2/3 pathway by ALK3 in gonadotrope-like cells (Wang *et al.*, 2014). Furthermore, the activation of Smad 2 pathway was described by ALK5/ALK3 heterocomplex to regulate dorsoventral axis specification in zebrafish, and activation of Smad 3 by ALK7/ALK6 heterocomplex to regulate cancer cell invasion with BMP-2 (Holtzhausen *et al.*, 2014). Moreover, a study reported the activation of Smad 1/5 pathway by ALK5 with TGF- β in mammary epithelial cells through a L45 loop-dependent mechanism (Liu *et al.*, 2009).

However, we note that no previous study has investigated the stiffness-dependent role of ALK receptors. Here, we reveal that, depending on the bBMPs and on the readout signal (either pSmad 1/5/9, pSmad 2 or ALP), there are some stiffness-dependent responses of ALK receptors: ALK2 and ALK6 are stiffness-independent, while ALK3 and ALK5 can be stiffness-dependent depending on the BMP.

All of these studies indicate the complexity of the interaction of the BMP/BMPR interaction and the effect it has on the signaling pathways. Therefore, it is necessary to determine BMP/BMPR interaction couples to gain insights on the specificity of the activated signals.

3. Crosstalk between the BMP and TGF- β pathway

Indication of a crosstalk between the BMP and TGF- β pathway is revealed via ALK5, which we showed to be an activator of Smad 2 with BMP-9 and to a lower extent for BMP-4 (Chapter IV). This observation is consistent with the BLI results showing that BMP-9 can bind ALK5, although with a low affinity. In fact, our results showed unexpectedly that all BMPs (BMP-2, BMP-4, BMP-7, BMP-9) can bind to ALK5, which was so far considered to be solely a TGF- β receptor.

This crosstalk between the BMP and TGF- β have been previously described in endothelial cells since ALK5 induced the recruitment of ALK1 to the ALK5/TGF β R-II heterocomplex in the presence of TGF- β . In that context, the activation by TGF- β of the ALK5/Smad 2/3 pathway

leads to an inhibition of migration and proliferation while the activation of ALK1/Smad1/5 results in increased migration and proliferation of endothelial cells (**FIG.VI.3**). The formation of a complex ALK1/ALK5/TGF β R-II inhibited Smad 2 and activated Smad 1/5 pathway, which resulted in opposite biological effects from those of ALK5 alone (Goumans *et al.*, 2003).

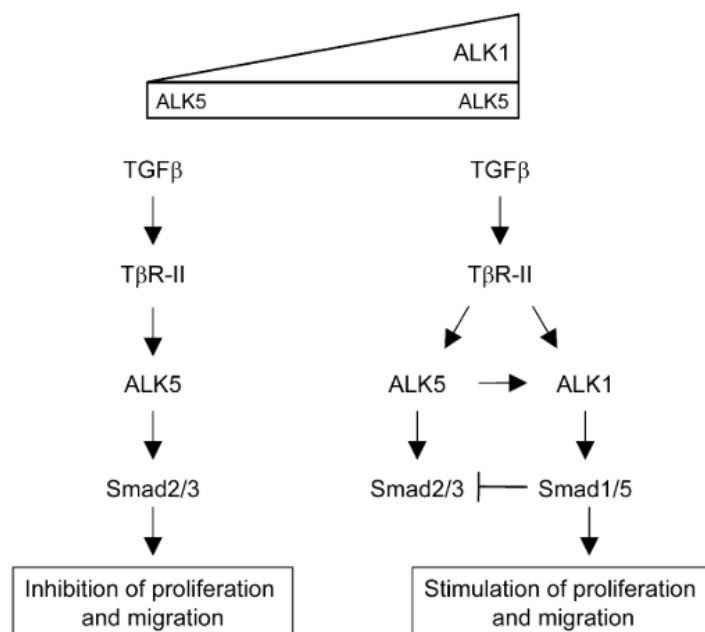


FIG.VI.3. Schematic Model for Activation of TGF- β /BMP crosstalk in endothelial cells (Goumans *et al.*, 2003)

This activation of Smad 1/5 pathway by TGF- β was also seen in endothelial cells lacking BMPR-II. In this case, when BMPR-II is present, the circulating BMP-9 and BMP-10 bind the ALK1/BMPR-II complex and BMP-6 binds ALK2/BMPR-II complex thus inducing the activation of the Smad 1/5 pathway. In the absence of BMPR-II, the ALK1 or ALK2 receptors are recruited to the ALK5/TGF β R-II heterocomplex and become activated by TGF- β (Hiepen *et al.*, 2019). Crosstalk between these two pathways was also reported in cartilage as ALK5 associates with ALK1 and inhibits the activation of its BMP signaling in the growth plate. The loss of ALK5 results in a gain of function of ALK1 in cartilage with BMP-9 (Wang *et al.*, 2019).

4. BMP/BMPR interaction limitations

Here, we showed that BLI provides precise affinity measurements. However, one should keep in mind that these measurements are done *in vitro* in well-defined and simplified conditions.

Thus, one should be careful regarding their relevance for *in vivo* signaling, especially since other factors can come into play. First, the spatio-temporal expression of both BMPs and their receptors is a key aspect that needs to be taken into account: in fact, there is a specific combination of ligands and receptors in a specific cell at a given time, and at a given place *in vivo* (Miyazono, Maeda and Imamura, 2005). Second, the presence of a specific environment of modulator proteins, notably co-receptors and components of the ECM can regulate BMP signaling. For instance, the presence of heparan sulfate, a glycosaminoglycan, was recently found to have a role on the cell response to matrix-bound BMPs (Sefkow-Werner *et al.*, 2020). In this case, two different ligands may induce distinct signals even if they have similar receptor assembly (Migliorini *et al.*, 2020). Finally, the ligand-receptor kinetics and lifetimes could affect the phosphorylation level of the cytoplasmic receptor kinase domains, which could encode ligand-specific signals (Mueller and Nickel, 2012).

II. Drug screening on biomaterials

Modulation of the BMP and TGF- β signaling at the receptor level

In this project, we performed drug assays on C2C12 myoblasts in the usual working conditions, eg a glass surface, and compared them for assays performed on the biomimetic polyelectrolyte films previously developed in our team. In fact, *in vitro*, preclinical trials are usually performed on a 2D glass slides or culture plates made of plastic, in view of the simplicity and established culture protocols. However, these cell culture substrates are very stiff and as such, are not fully representative of the cell microenvironment (Cukierman *et al.*, 2001). In addition, the bioactive proteins (BMP and TGF- β) are added in solution to the cells, similarly to the drugs. Here, we used a biomimetic film presenting BMP and TGF- β in a matrix-bound manner to mimic the presentation of BMPs by the ECM.

Recently, 2D and 3D biomaterial models have been developed to study anticancer drug resistance and to perform drug screening (Schwartz *et al.*, 2017; Nii, Makino and Tabata, 2020). Since our goal was to do high-content drug assay, we developed an immunofluorescence-based assay of pSmad activity, considering that Smad is an essential marker of early bone regeneration (Song, Estrada and Lyons, 2009). The immunofluorescence assay is an alternative to the standard molecular techniques, which are western blot and bioluminescence assays using transformed C2C12 cells. It presents several advantages: i) the

possibility to study cells at the single-cell level and not as average cell population ii) its sensitivity and rapid application, iii) specific location in comparison to the other techniques that measure an averaged signal across a cell population (Badr, 2014; Ghosh et al., 2014).

The pSmad assay was then optimized to surpass the challenges of performing kinetic and drug experiments on biomaterials. Using this assay, we successfully quantified pSmad intensity and observed similar results for cells plated on the biomimetic films than for cells cultured on glass substrates. However, responses to TGF- β 1 seems to be more sensitive on biomaterials in comparison to glass. The three drugs that we used were already developed in clinical trials; LDN-193189 a kinase inhibitor of ALK2 as well as Galunisertib and Vactosertib kinase inhibitors of ALK5. The dose response and drug assays showed similar values of EC50 and IC50 indicating the robustness of the immunofluorescence assay. Furthermore, a Z' factor experiment, which assess the quality of the screening assay, showed the compatibility of our material to be used in high-content studies.

Since these drugs inhibit the signaling at the intracellular level of the cells, the effect of presenting BMP in a matrix-bound manner did not influence the IC50 values on biomaterials in comparison to glass. As a previous study in the team determined a crosstalk between β 3 integrin and BMPR thanks to the use of biomaterials (Fourel *et al.*, 2016), we believe that the use of antagonists with a different action mode, inhibiting the BMP signaling at the extracellular level, could reveal differences in the drug inhibition, in comparison to glass surfaces.

Chapter VII:

Conclusions and Perspectives

I. Conclusions

In this thesis, we investigated the early steps of bone regeneration by studying the BMP signaling, first at the level of receptor by performing a quantification of the BMP/BMPR interaction using the BLI technique. Second, on a cellular level, by developing and optimizing a high-content screening assay to quantify Smad present in the nucleus on glass support. This assay was then optimized and applied on the biomimetic films, to do a proof-of-concept with drugs inhibiting the BMP and TGF- β pathways.

1. Quantification of the BMP/BMPR interaction

In the first part of this work, we focused on the BMP/BMPR interaction which was previously described in the literature to be rather complex. Using similar experimental conditions, we quantified these interactions at the molecular scale. Notably, we revealed differences between BMP-2 and BMP-4 since BMP-2 demonstrated a higher association and binding affinities to type-I and II BMPR. Our study showed for the first time differences in the binding affinities of these BMPs to their receptors. In addition, BMP-7 showed a clear preference to all the BMP type II receptors. Furthermore, BMP-9 did not only bind to ALK1, but it also binds to ALK2 and ALK5, which highlights the importance of these two receptors in BMP-9 signaling. An unexpected finding was that all these four BMPs bind to ALK5, which is known to be a type ITGF- β receptor. These data along with the observation that BMP-9 and ALK5 are involved in pSmad signaling (Sales *et al.*, 2022) suggest that there may be a crosstalk between the TGF- β and the BMP pathways.

Additionally, this work evidenced that the bio-layer interferometry technique is a user-friendly technique for protein-protein interaction studies. Furthermore, our loading strategy with anti-Fc coated surfaces and BMPR-Fc chimeras represents an example of a straightforward and successful and loading strategy, in comparison to the commonly used non-specific amine coupling strategy (Kortt *et al.*, 1997). The methodology we developed in this work may thus be easily translated to other research topics with different ligands and receptors.

2. Modulation of the BMP and TGF- β signaling at the receptor level

As mentioned above, BMPs are involved in a large number of diseases, either directly or being involved in their signaling pathways. In view of their implications in several diseases, many strategies have been developed to modulate BMP signaling. To this end, we developed a high-

content pSmad assay and performed drug assays on biomimetic polyelectrolyte films made of hyaluronic acid and poly(L-lysine) to better mimic the cell environment in the *in vitro* studies.

With our results, we demonstrated the robustness and quality of the screening assay to be used in high-content studies. These results are promising for two major reasons: first, they establish a new high-content screening analysis based on pSmad IF and second, they provide the first proof of concept that drug assay can be done on biomimetic films.

Overall, our work provides a glimpse on the early steps of bone regeneration. Despite the complexity of the BMP and TGF- β signaling, our results can help decipher the specificities of BMP/BMPR couples. On one hand, the BMP/BMPR interaction results opens the door for future cellular studies to decipher the specific signaling pathways. On the other hand, we present a high-content pSmad assay that can be used to study the TGF- β superfamily ligands in different contexts. We provide here the necessary tissue engineering tools for future in depth studies of BMP/BMPR interaction and its modulation.

II. Perspectives

Considering the different parts of this thesis, several questions may be addressed in future research projects. Besides, the technical developments and knowledge may be applied to other biomaterial models.

1. Protein/protein interaction studies

In this thesis, we presented a successful loading strategy and protocol with the BLI technique. In that regards, we can utilize this knowledge to perform other protein/protein interactions. For example, it would be interesting to determine the binding affinities of i) heterodimers of BMPs with BMPR, considering that heterodimers of BMPs have been described *in vivo* to have stronger bone induction ability than homodimers (Kaito *et al.*, 2018). ii) Mutated BMPR involved in diseases could be studied to examine if the BMP/BMPR interaction is altered in pathological conditions. iii) The interaction of BMP with components of the ECM such as fibronectin can be also quantified, iv) the role of inhibitors such as noggin and gremlin. These results would provide new insights into the signaling mechanisms by BMPs and their interactions with ECM components.

2. Cellular studies

The obtained results with BLI open the way for further cellular studies in order to understand the BMP-dependent differences in a cellular context *in vitro*. In addition, molecular studies of BMP-2 and BMP-4 are needed to better understand and reveal their biochemical and structural differences, as well as the effect of these differences on their binding affinities. The distinct role of BMP-2 and BMP-4 may be further studied in a cellular context, such as cartilage (Shu *et al.*, 2011), leukemic cells (Zylbersztejn *et al.*, 2018) and intrapulmonary endothelial cells (Anderson *et al.*, 2010).

Furthermore, the role of ALK5 with BMPs needs to be further investigated, especially since it can bind to the four BMPs. Indeed, the implication of ALK5 in the BMP pathway has recently been observed in our recent cellular studies (Sales *et al.*, 2022): ALK5 plays a role in cell adhesion and spreading: it has an activator role in cellular adhesion and spreading, an inhibitor role on the pSmad 1/5/9 pathway, and an activator role pSmad 2. This was notable with BMP-9 (Sales *et al.*, 2022). Since similar crosstalks between TGF- β and BMP pathways have been already evidenced in endothelial (Hiepen *et al.*, 2019) and cartilage cells (Wang *et al.*, 2019), it would be interesting to investigate this crosstalk in bone cells

3. Technical optimization of a high-content immunofluorescence assay

In a pathological model

The new immunofluorescence assay we developed may be used to pSmad signaling in other cellular models. For instance, studying the role of BMP-9 and BMP-10 in endothelial cells in the context of HHT disease (Cunha *et al.*, 2017). Alternately, pulmonary smooth muscle cells may be used to study PAH disease, which is characterized by an enhanced BMP-6 and BMP-7 signaling (Yu *et al.*, 2005).

On biomaterials of controlled stiffness

It would be also useful to develop a fibrosis cellular model on our biomimetic films of controlled stiffness, since myofibroblast activity was shown to be stiffness-dependent with a high fibrotic activity on stiff surfaces (Balestrini *et al.*, 2012). Our films with a controlled elastic modulus (Schneider *et al.*, 2006) may represent a new physiologically-relevant cell model to study fibrosis, in comparison to cells that are currently cultured on plastic (Hinz, 2015). Thus, Smad 2 signaling with TGF- β may be studied in a stiffness-dependent manner. Moreover, the

effect of TGF- β on fibrosis can be investigated using long-term markers such as collagen production and α -smooth muscle actin expression (Biernacka, Dobaczewski and Frangogiannis, 2011; Organ *et al.*, 2019). In addition, our new assay maybe be used in different context to study Smad-independent pathways involved fibrosis, such as JNK pathway in pulmonary fibrosis, or Ras/MEK/ERK in other diseases such as Sclerosis (Finnsen, Almadani and Philip, 2020).

Drug screening of new ALK inhibitors

BMP-6, another BMP that we did not include in our study, has been reported to regulate iron homeostasis through Smad pathway by increasing the expression of the iron regulatory hormone hepcidin responsible for iron absorption (Pietrangelo *et al.*, 2006; Andriopoulos *et al.*, 2009; Meynard *et al.*, 2009). It would be interesting to apply our high-content pSmad assay to investigate hepaocytes response to BMP-6. In these cells, the transmembrane serine protease Matriptase-2 (MT2) is an inhibitor of the pSmad 1/5/8 pathway. In fact, patients with iron-refractory iron-deficiency anemia (IRIDA) have mutations in the gene encoding MT2, and as a consequence, there is an upregulation of transcription of hepcidin gene, leading to anemia. It was already shown that LJ000328, an inhibitor of ALK2 and ALK3 can improve microcytic anemia by reducing hepcidin expression (Belot *et al.*, 2020). Our pSmad assay may thus be used to do high-content quantification of pSmad to test the effect of new drug inhibitors.

References

- Aashaq, S. *et al.* (2021) 'TGF- β signaling: A recap of SMAD-independent and SMAD-dependent pathways', *Journal of Cellular Physiology*, (March), pp. 1–27. doi: 10.1002/jcp.30529.
- Abdiche, Y. *et al.* (2008) 'Determining kinetics and affinities of protein interactions using a parallel real-time label-free biosensor, the Octet', *Analytical Biochemistry*, 377(2), pp. 209–217. doi: <https://doi.org/10.1016/j.ab.2008.03.035>.
- Abdollah, S. *et al.* (1997) 'T β RI phosphorylation of Smad2 on Ser465 and Ser467 is required for Smad2-Smad4 complex formation and signaling', *Journal of Biological Chemistry*, 272(44), pp. 27678–27685. doi: 10.1074/jbc.272.44.27678.
- Aberg, T., Wozney, J. and Thesleff, I. (1997) 'Expression patterns of bone morphogenetic proteins (Bmps) in the developing mouse tooth suggest roles in morphogenesis and cell differentiation', *Developmental Dynamics*, 210(4), pp. 383–396. doi: 10.1002/(SICI)1097-0177(199712)210:4<383::AID-AJA3>3.0.CO;2-C.
- Agnew, C. *et al.* (2021) 'Structural basis for ALK2/BMP2 receptor complex signaling through kinase domain oligomerization', *Nature Communications*. Springer US, 12(1). doi: 10.1038/s41467-021-25248-5.
- Airaksinen, M. S. and Saarma, M. (2002) 'The GDNF family: Signalling, biological functions and therapeutic value', *Nature Reviews Neuroscience*, 3(5), pp. 383–394. doi: 10.1038/nrn812.
- Ali, I. H. A. and Brazil, D. P. (2014) 'Bone morphogenetic proteins and their antagonists: Current and emerging clinical uses', *British Journal of Pharmacology*, 171(15), pp. 3620–3632. doi: 10.1111/bph.12724.
- Anastasi, C. *et al.* (2020) 'BMP-1 disrupts cell adhesion and enhances TGF- β 2 activation through cleavage of the matricellular protein thrombospondin-1', *Science Signaling*, 13(639), p. eaba3880. doi: 10.1126/scisignal.aba3880.
- Anderson, L. *et al.* (2010) 'Bmp2 and Bmp4 exert opposing effects in hypoxic pulmonary hypertension', *Am J Physiol Regul Integr Comp Physiol* 298, 298, pp. 833–842. doi: 10.1152/ajpregu.00534.2009.
- Andriopoulos, B. *et al.* (2009) 'BMP-6 is a key endogenous regulator of hepcidin expression and iron metabolism', *Nature Genetics*, 41(4), pp. 482–487. doi: 10.1038/ng.335.BMP-6.
- Annes, J. P., Munger, J. S. and Rifkin, D. B. (2003) 'Making sense of latent TGF β activation', *Journal of Cell Science*, 116(2), pp. 217–224. doi: 10.1242/jcs.00229.
- Antebi, Y. E. *et al.* (2017) 'Combinatorial Signal Perception in the BMP Pathway', *Cell*. Elsevier Inc., 170(6), pp. 1184–1196.e24. doi: 10.1016/j.cell.2017.08.015.
- Arvidson, K. *et al.* (2011) 'Bone regeneration and stem cells', *Journal of Cellular and Molecular Medicine*, 15(4), pp. 718–746. doi: 10.1111/j.1582-4934.2010.01224.x.
- Ashe, H. L. (2008) 'Type IV collagens and Dpp positive and negative regulators of signaling', *Fly*, 2(6), pp. 313–315. doi: 10.1038/nature07214.
- Attisano, L. and Lee-Hoeflich, S. T. (2001) 'Protein family review The Smads', *Genome Biology*, 2(8), pp. 3010.1-3010.8.
- Augat, P. and Schorlemmer, S. (2006) 'The role of cortical bone and its microstructure in bone strength', *Age and Ageing*, 35(SUPPL.2), pp. 27–31. doi: 10.1093/ageing/afl081.

- Aykul, S. and Martinez-hackert, E. (2016) 'Transforming Growth Factor- Family Ligands Can Function as Antagonists by Competing for Type II Receptor Binding', *Journal of Biological Chemistry*, 291(20), pp. 10792–10804. doi: 10.1074/jbc.M115.713487.
- Azhar, M. *et al.* (2003) 'Transforming growth factor beta in cardiovascular development and function', *Cytokine and Growth Factor Reviews*, 14(5), pp. 391–407. doi: 10.1016/S1359-6101(03)00044-3.
- Badlani, N. *et al.* (2009) 'Use of Bone Morphogenic Protein-7 as a Treatment for Osteoarthritis', *Clinical Orthopaedics and Related Research*®, 467(12), pp. 3221–3229. doi: 10.1007/s11999-008-0569-9.
- Badr, C. E. (2014) 'Bioluminescent Imaging', *Methods in Molecular Biology*, 1098. doi: 10.1007/978-1-62703-718-1.
- Bakrania, P. *et al.* (2008) 'Mutations in BMP4 Cause Eye, Brain, and Digit Developmental Anomalies: Overlap between the BMP4 and Hedgehog Signaling Pathways', *American Journal of Human Genetics*, 82(2), pp. 304–319. doi: 10.1016/j.ajhg.2007.09.023.
- Balestrini, J. L. *et al.* (2012) 'The mechanical memory of lung myofibroblasts', *Integrative Biology*, 4(4), pp. 410–421. doi: 10.1039/c2ib00149g.
- BCA Assay and Lowry Assays (2021). Available at: <https://www.thermofisher.com/fr/fr/home/life-science/protein-biology/protein-assays-analysis/protein-assays/bca-protein-assays.html>.
- Belot, A. *et al.* (2020) 'LJ000328, a novel ALK2/3 kinase inhibitor, represses hepcidin and significantly improves the phenotype of IRIDA', *Haematologica*, 105(8), pp. e385–e388.
- Van Bezooijen, R. L. *et al.* (2007) 'Wnt but not BMP signaling is involved in the inhibitory action of sclerostin on BMP-stimulated bone formation', *Journal of Bone and Mineral Research*, 22(1), pp. 19–28. doi: 10.1359/jbmr.061002.
- Bhatia, M. *et al.* (1999) 'Bone morphogenetic proteins regulate the developmental program of human hematopoietic stem cells', *Journal of Experimental Medicine*, 189(7), pp. 1139–1147. doi: 10.1084/jem.189.7.1139.
- Bidart, M. *et al.* (2012) 'BMP9 is produced by hepatocytes and circulates mainly in an active mature form complexed to its prodomain', *Cellular and Molecular Life Sciences*, 69(2), pp. 313–324. doi: 10.1007/s00018-011-0751-1.
- Biernacka, A., Dobaczewski, M. and Frangogiannis, N. G. (2011) 'TGF- β signaling in fibrosis', *Growth factors*, 29(5), pp. 196–202. doi: 10.3109/08977194.2011.595714.TGF-.
- Billings, P. C. *et al.* (2018) 'Domains with highest heparan sulfate-binding affinity reside at opposite ends in BMP2/4 versus BMP5/6/7: Implications for function', *Journal of Biological Chemistry*. © 2018 Billings *et al.*, 293(37), pp. 14371–14383. doi: 10.1074/jbc.RA118.003191.
- Blázquez-Medela, A. M., Jumabay, M. and Boström, K. I. (2019) 'Beyond the bone: Bone morphogenetic protein signaling in adipose tissue', *Obesity Reviews*, (November 2018), pp. 1–11. doi: 10.1111/obr.12822.
- Boguslawska, J. *et al.* (2019) 'TGF- β and microRNA Interplay in Genitourinary Cancers', *Cells*, 8(1619).
- Brosens, L. A. A. *et al.* (2011) 'Juvenile polyposis syndrome', *World J Gastroenterol* 2011, 17(44), pp. 4839–4844. doi: 10.3748/wjg.v17.i44.4839.

- Brown, M. A. *et al.* (2005) 'Crystal structure of BMP-9 and functional interactions with pro-region and receptors', *Journal of Biological Chemistry*. © 2005 ASBMB. Currently published by Elsevier Inc; originally published by American Society for Biochemistry and Molecular Biology., 280(26), pp. 25111–25118. doi: 10.1074/jbc.M503328200.
- Bruce, D. L. and Sapkota, G. P. (2012) 'Phosphatases in SMAD regulation', *FEBS Letters*. Federation of European Biochemical Societies, 586(14), pp. 1897–1905. doi: 10.1016/j.febslet.2012.02.001.
- Camaschella, C. (2009) 'BMP6 orchestrates iron metabolism', *Nature Genetics*, 41(4), pp. 386–388.
- Cao, Y. *et al.* (2020) 'Digital PCR as an Emerging Tool for Monitoring of Microbial Biodegradation', *Molecules*, 25(706).
- Carbodiimide Crosslinker Chemistry* (2021). Available at: <https://www.thermofisher.com/fr/fr/home/life-science/protein-biology/protein-biology-learning-center/protein-biology-resource-library/pierce-protein-methods/carbodiimide-crosslinker-chemistry.html>.
- Chacko, B. M. *et al.* (2001) 'The L3 loop and C-terminal phosphorylation jointly define Smad protein trimerization', *Nature Structural Biology*, 8(3), pp. 248–253. doi: 10.1038/84995.
- Chai, Y. C. *et al.* (2012) 'Current views on calcium phosphate osteogenicity and the translation into effective bone regeneration strategies', *Acta Biomaterialia*. Acta Materialia Inc., 8(11), pp. 3876–3887. doi: 10.1016/j.actbio.2012.07.002.
- Chang, C. (2016) 'Agonists and antagonists of TGF- β family ligands', *Cold Spring Harbor Perspectives in Biology*, 8(8), pp. 1–51. doi: 10.1101/cshperspect.a021923.
- Chang, H., Brown, C. W. and Matzuk, M. M. (2002) 'Genetic analysis of the mammalian transforming growth factor- β superfamily', *Endocrine Reviews*, 23(6), pp. 787–823. doi: 10.1210/er.2002-0003.
- Chapnick, D. A. *et al.* (2011) 'Partners in crime: The TGF β and MAPK pathways in cancer progression', *Cell and Bioscience*. BioMed Central Ltd, 1(1), p. 42. doi: 10.1186/2045-3701-1-42.
- Charbord, P. (2010) 'Bone marrow mesenchymal stem cells: Historical overview and concepts', *Human Gene Therapy*, 21(9), pp. 1045–1056. doi: 10.1089/hum.2010.115.
- Cheifetz, S. *et al.* (1987) 'The transforming growth factor- β system, a complex pattern of cross-reactive ligands and receptors', *Cell*, 48(3), pp. 409–415. doi: 10.1016/0092-8674(87)90192-9.
- Chen, F. and Weinberg, R. A. (1995) 'Biochemical evidence for the autophosphorylation and transphosphorylation of transforming growth factor β receptor kinases', *Proceedings of the National Academy of Sciences of the United States of America*, 92(5), pp. 1565–1569. doi: 10.1073/pnas.92.5.1565.
- Chen, X. *et al.* (1997) 'Smad4 and FAST-1 in the assembly of activin-responsive factor', *Nature*, 389(September), pp. 85–89.
- Cheng, H. *et al.* (2003) 'Osteogenic Activity of the Fourteen Types of Human Bone Morphogenetic Proteins (BMPs)', *JBJS*, 85(8). Available at: https://journals.lww.com/jbjsjournal/Fulltext/2003/08000/Osteogenic_Activity_of_the_Fourteen_Types_of_Human.17.aspx.
- Clarke, B. (2008) 'Normal bone anatomy and physiology', *Clinical journal of the American Society of Nephrology : CJASN*, 3 Suppl 3(Suppl 3). doi: 10.2215/CJN.04151206.

- Cohen, P. and Alessi, D. R. (2013) 'Kinase Drug Discovery – What 's Next in the Field?', *ACS Chemical Biology*, 8(1), pp. 96–104. doi: 10.1021/cb300610s.Kinase.
- Crouzier, T. *et al.* (2009) 'Layer-by-layer films as a biomimetic reservoir for rhBMP-2 delivery: Controlled differentiation of myoblasts to osteoblasts', *Small*, 5(5), pp. 598–608. doi: 10.1002/sml.200800804.
- Crouzier, T. *et al.* (2011) 'Presentation of BMP-2 from a soft biopolymeric film unveils its activity on cell adhesion and migration', *Advanced Materials*, 23(12), pp. 111–118. doi: 10.1002/adma.201004637.
- Cukierman, E. *et al.* (2001) 'Taking cell-matrix adhesions to the third dimension', *Science*, 294(5547), pp. 1708–1712. doi: 10.1126/science.1064829.
- Cunha, S. I. *et al.* (2017) 'Deregulated TGF- β /BMP Signaling in Vascular Malformations', *Circulation Research*, 121, pp. 981–999. doi: 10.1161/CIRCRESAHA.117.309930.
- Cunningham, N. S. *et al.* (1995) 'Growth/Differentiation Factor-10: A New Member of the Transforming Growth Factor- β Superfamily Related to Bone Morphogenetic Protein-3', *Growth Factors*. Taylor & Francis, 12(2), pp. 99–109. doi: 10.3109/08977199509028956.
- Cuny, G. D. *et al.* (2008) 'Structure-activity relationship study of bone morphogenetic protein (BMP) signaling inhibitors', *Bioorg Med Chem Lett*, 18(15), pp. 4388–4392. doi: 10.1016/j.bmcl.2008.06.052.Structure-activity.
- Dallas, S. L. *et al.* (2005) 'Fibronectin regulates latent transforming growth factor- β (TGF β) by controlling matrix assembly of latent TGF β -binding protein-1', *Journal of Biological Chemistry*, 280(19), pp. 18871–18880. doi: 10.1074/jbc.M410762200.
- Daopin, S. *et al.* (1992) 'Crystal structure of transforming growth factor- β 2: An unusual fold for the superfamily', *Science*, 257(5068), pp. 369–373. doi: 10.1126/science.1631557.
- Dastagir, K. *et al.* (2014) 'Murine Embryonic Fibroblast Cell Lines Differentiate into Three Mesenchymal Lineages to Different Extents: New Models to Investigate Differentiation Processes', *CELLULAR REPROGRAMMING*, 16(4). doi: 10.1089/cell.2014.0005.
- David, L. *et al.* (2007) 'Identification of BMP9 and BMP10 as functional activators of the orphan activin receptor-like kinase 1 (ALK1) in endothelial cells', *Blood*, 109(5), pp. 1953–1961. doi: 10.1182/blood-2006-07-034124.
- David, L. *et al.* (2008) 'Bone morphogenetic protein-9 is a circulating vascular quiescence factor', *Circulation Research*, 102(8), pp. 914–922. doi: 10.1161/CIRCRESAHA.107.165530.
- Delis, B. (2016) 'Bio-layer interferometry : méthode d ' intérêt dans les procédés de fabrication et pour le contrôle des préparations hospitalières à base d ' anticorps monoclonaux thérapeutiques Benjamin Delis To cite this version : HAL Id : dumas-01264904'.
- Derynck, R. and Feng, X. (1997) 'TGF- β receptor signaling', *Biochimica et Biophysica Acta*, 1333. Available at: papers2://publication/uuid/CA824BC9-C628-4A16-9487-24C4C2021AD7.
- Derynck, R. and Zhang, Y. E. (2003) 'Smad-dependent and Smad-independent pathways in TGF-beta family signalling.', *Nature*, 425(6958), pp. 577–584. doi: 10.1038/nature02006.
- Dominici, M. *et al.* (2006) 'Minimal criteria for defining multipotent mesenchymal stromal cells. The International Society for Cellular Therapy position statement', *Cytotherapy*. Elsevier, 8(4), pp. 315–317. doi: 10.1080/14653240600855905.
- Ebisawa, T. *et al.* (1999) 'Characterization of bone morphogenetic protein-6 signaling

pathways in osteoblast differentiation', *Journal of Cell Science*, 112(20), pp. 3519–3527.

Ehata, S. *et al.* (2013) 'Bi-directional roles of bone morphogenetic proteins in cancer: Another molecular Jekyll and Hyde?', *Pathology International*, 63(6), pp. 287–296. doi: 10.1111/pin.12067.

Ehrlich, M. *et al.* (2012) 'Oligomeric interactions of TGF- β and BMP receptors', *FEBS Letters*. Federation of European Biochemical Societies, 586(14), pp. 1885–1896. doi: 10.1016/j.febslet.2012.01.040.

Equation: Sigmoidal dose-response (2021). Available at: https://www.graphpad.com/guides/prism/latest/curve-fitting/reg_classic_dr.htm.

Ferretti, C. (2014) 'Periosteum derived stem cells for regenerative medicine proposals: Boosting current knowledge', *World Journal of Stem Cells*, 6(3), p. 266. doi: 10.4252/wjsc.v6.i3.266.

Finnson, K. W., Almadani, Y. and Philip, A. (2020) 'Non-canonical (non-SMAD2/3) TGF- β signaling in fibrosis: Mechanisms and targets', *Seminars in Cell and Developmental Biology*. Elsevier, 101(November 2019), pp. 115–122. doi: 10.1016/j.semcdb.2019.11.013.

Fitzpatrick, V. *et al.* (2017) 'Signal mingle: Micropatterns of BMP-2 and fibronectin on soft biopolymeric films regulate myoblast shape and SMAD signaling', *Scientific Reports*. Nature Publishing Group, 7(May 2016), pp. 1–11. doi: 10.1038/srep41479.

Florin, E.-L., Moy, V. T. and Gaub, H. E. (1994) 'Adhesion Forces Between Individual Ligand-Receptor Pairs', *Science*, 264(5157), pp. 415–417. doi: 10.1126/science.8153628.

Fourel, L. *et al.* (2016) ' β 3 integrin-mediated spreading induced by matrix-bound BMP-2 controls Smad signaling in a stiffness-independent manner', *Journal of Cell Biology*, 212(6), pp. 693–706. doi: 10.1083/jcb.201508018.

Frantz, C., Stewart, K. M. and Weaver, V. M. (2010) 'The extracellular matrix at a glance', *Journal of Cell Science*, 123(24), pp. 4195–4200. doi: 10.1242/jcs.023820.

Franzén, P., Heldin, C. H. and Miyazono, K. (1995) 'The GS domain of the transforming growth factor- β type-i receptor is important in signal transduction', *Biochemical and Biophysical Research Communications*, pp. 682–689. doi: 10.1006/bbrc.1995.1241.

Fujii, M. *et al.* (1999) 'Roles of bone morphogenetic protein type I receptors and Smad proteins in osteoblast and chondroblast differentiation', *Molecular Biology of the Cell*, 10(11), pp. 3801–3813. doi: 10.1091/mbc.10.11.3801.

Galat, A. (2011) 'Common structural traits for cystine knot domain of the TGF β superfamily of proteins and three-fingered ectodomain of their cellular receptors', *Cellular and Molecular Life Sciences*, 68(20), pp. 3437–3451. doi: 10.1007/s00018-011-0643-4.

Galunisertib (2021). Available at: <https://www.selleckchem.com/products/ly2157299.html>.

Galunisertib (LY2157299) (no date). Available at: <https://www.selleckchem.com/products/ly2157299.html>.

Garibyan, L. and Avashia, N. (2013) 'Research Techniques Made Simple: Polymerase Chain Reaction (PCR)', *J Invest Dermatol*, 133(3). doi: 10.1038/jid.2013.1.Research.

Geesink, R. G. T., Hoefnagels, N. H. M. and Bulstra, S. K. (1999) 'Osteogenic activity of OP-1 bone morphogenetic protein (BMP-7) in a human fibular defect', *Journal of Bone and Joint Surgery*, 81(4), pp. 710–718. doi: 10.1302/0301-620X.81B4.9311.

Ghosh, R. *et al.* (2014) 'The necessity of and strategies for improving confidence in the

- accuracy of western blots', *Expert Rev Proteomics*, 11(5), pp. 549–560. doi: 10.1586/14789450.2014.939635.The.
- Gilbert, R. W. D., Vickaryous, M. K. and Vilorio-Petit, A. M. (2016) 'Signalling by transforming growth factor beta isoforms in wound healing and tissue regeneration', *Journal of Developmental Biology*, 4(2). doi: 10.3390/jdb4020021.
- Gilboa, L. *et al.* (2000) 'Bone Morphogenetic Protein Receptor Complexes on the Surface of Live Cells : A New Oligomerization Mode for Serine / Threonine Kinase Receptors', *Molecular Biology of the cell*, 11(March), pp. 1023–1035.
- Gilde, F. *et al.* (2016) 'Stiffness-dependent cellular internalization of matrix-bound BMP-2 and its relation to Smad and non-Smad signaling', *Acta Biomaterialia*, 46, pp. 55–67. doi: 10.1016/j.actbio.2016.09.014.
- Gold, E. *et al.* (2009) 'Activin C antagonizes activin A in vitro and overexpression leads to pathologies in vivo', *American Journal of Pathology*, 174(1), pp. 184–195. doi: 10.2353/ajpath.2009.080296.
- Gold, L. I. *et al.* (2000) 'TGF- β isoforms are differentially expressed in increasing malignant grades of HaCaT keratinocytes, suggesting separate roles in skin carcinogenesis', *Journal of Pathology*, 190(5), pp. 579–588. doi: 10.1002/(SICI)1096-9896(200004)190:5<579::AID-PATH548>3.0.CO;2-I.
- Goldman, D. C., Donley, N. and Christian, J. L. (2009) 'Genetic interaction between Bmp2 and Bmp4 reveals shared functions during multiple aspects of mouse organogenesis', *Mechanisms of Development*, 126(3–4), pp. 117–127. doi: 10.1016/j.mod.2008.11.008.
- Gomez-Puerto, M. C. *et al.* (2019) 'Bone morphogenetic protein receptor signal transduction in human disease', *Journal of Pathology*, 247(1), pp. 9–20. doi: 10.1002/path.5170.
- Gordon, K. J. and Blobe, G. C. (2008) 'Role of transforming growth factor- β superfamily signaling pathways in human disease', *Biochimica et Biophysica Acta*, 1782(4), pp. 197–228. doi: 10.1016/j.bbadis.2008.01.006.
- Goumans, M. J. *et al.* (2003) 'Activin receptor-like kinase (ALK)1 is an antagonistic mediator of lateral TGF β /ALK5 signaling', *Molecular Cell*, 12(4), pp. 817–828. doi: 10.1016/S1097-2765(03)00386-1.
- Greenwald, J. *et al.* (1999) 'Three-finger toxin fold for the extracellular ligand-binding domain of the type II activin receptor serine kinase', *Nature Structural Biology*, 6(1), pp. 18–22. doi: 10.1038/4887.
- Gregory, K. E. *et al.* (2005) 'The prodomain of BMP-7 targets the BMP-7 complex to the extracellular matrix', *Journal of Biological Chemistry*, 280(30), pp. 27970–27980. doi: 10.1074/jbc.M504270200.
- Grgurevic, L., Pecina, M. and Vukicevic, S. (2017) 'Marshall R. Urist and the discovery of bone morphogenetic proteins', *International Orthopaedics*. *International Orthopaedics*, 41(5), pp. 1065–1069. doi: 10.1007/s00264-017-3402-9.
- Gribova, V. *et al.* (2013) 'Europe PMC Funders Group Effect of RGD-functionalization and stiffness modulation of polyelectrolyte multilayer films on muscle cell differentiation', *Acta Biomaterialia*, 9(5), pp. 6468–6480. doi: 10.1016/j.actbio.2012.12.015.Effect.
- Griffith, D. L. *et al.* (1996) 'Three-dimensional structure of recombinant human osteogenic protein 1: Structural paradigm for the transforming growth factor 13 superfamily (x-ray crystallography/protein structure/bone morphogenetic protein/cystine knot/receptor binding

model)', *Biophysics*, 93(January), pp. 878–883.

Groppe, J. *et al.* (2002) 'Structural basis of BMP signalling inhibition by the cystine knot protein Noggin', *Nature*, 420(6916), pp. 636–642. doi: 10.1038/nature01245.

Grynnerup, A. G. A., Lindhard, A. and Sørensen, S. (2012) 'The role of anti-Müllerian hormone in female fertility and infertility - An overview', *Acta Obstetrica et Gynecologica Scandinavica*, 91(11), pp. 1252–1260. doi: 10.1111/j.1600-0412.2012.01471.x.

Han, S. *et al.* (2007) 'Crystal structure of activin receptor type IIB kinase domain from human at 2.0 Å resolution', *Protein Science*, 16(10), pp. 2272–2277. doi: 10.1110/ps.073068407.

Hänel, C. and Gauglitz, G. (2002) 'Comparison of reflectometric interference spectroscopy with other instruments for label-free optical detection', *Analytical and Bioanalytical Chemistry*, 372(1), pp. 91–100. doi: 10.1007/s00216-001-1197-3.

Harding, P. L. *et al.* (2007) 'The influence of antisense oligonucleotide length on dystrophin exon skipping', *Molecular Therapy*. The American Society of Gene Therapy, 15(1), pp. 157–166. doi: 10.1038/sj.mt.6300006.

Hatakeyama, Y., Tuan, R. S. and Shum, L. (2004) 'Distinct functions of BMP4 and GDF5 in the regulation of chondrogenesis', *Journal of Cellular Biochemistry*, 91(6), pp. 1204–1217. doi: 10.1002/jcb.20019.

Hauff, K. *et al.* (2015) 'Matrix-immobilized BMP-2 on microcontact printed fibronectin as an in vitro tool to study BMP-mediated signaling and cell migration', *Frontiers in Bioengineering and Biotechnology*, 3(MAY), pp. 1–13. doi: 10.3389/fbioe.2015.00062.

Heldin, C. H. and Moustakas, A. (2016) 'Signaling receptors for TGF- β family members', *Cold Spring Harbor Perspectives in Biology*, 8(8), pp. 1–34. doi: 10.1101/cshperspect.a022053.

Herbertz, S. *et al.* (2015) 'Clinical development of galunisertib (LY2157299 monohydrate), a small molecule inhibitor of transforming growth factor-beta signaling pathway', *Drug Design, Development and Therapy*, pp. 4479–4499.

Hiepen, C. *et al.* (2016) 'Actions from head to toe: An update on Bone/Body Morphogenetic Proteins in health and disease', *Cytokine and Growth Factor Reviews*, 27, pp. 1–11. doi: 10.1016/j.cytogfr.2015.12.006.

Hiepen, C. *et al.* (2019) *BMPR2 acts as a gatekeeper to protect endothelial cells from increased TGF β responses and altered cell mechanics*, *PLoS Biology*. doi: 10.1371/journal.pbio.3000557.

Hill, C. S. (2009) 'Nucleocytoplasmic shuttling of Smad proteins', *Cell Research*, 19(1), pp. 36–46. doi: 10.1038/cr.2008.325.

Hill, C. S. (2016) 'Transcriptional Control by the SMADs', *Cold Spring Harb Perspect Biol*, 8.

Hinck, A. P. (2012) 'Structural studies of the TGF- β s and their receptors - Insights into evolution of the TGF- β superfamily', *FEBS Letters*. Federation of European Biochemical Societies, 586(14), pp. 1860–1870. doi: 10.1016/j.febslet.2012.05.028.

Hinck, A. P., Mueller, T. D. and Springer, T. A. (2016) 'Structural biology and evolution of the TGF- β family', *Cold Spring Harbor Perspectives in Biology*, 8(12). doi: 10.1101/cshperspect.a022103.

Hintze, V. *et al.* (2014) 'Sulfated glycosaminoglycans exploit the conformational plasticity of bone morphogenetic protein-2 (BMP-2) and alter the interaction profile with its receptor', *Biomacromolecules*, 15(8), pp. 3083–3092. doi: 10.1021/bm5006855.

- Hinz, B. *et al.* (2007) 'The Myofibroblast One Function, Multiple Origins', *The American Journal of Pathology*, 170(6), pp. 1807–1816. doi: 10.2353/ajpath.2007.070112.
- Hinz, B. (2015) 'The extracellular matrix and transforming growth factor- β 1: Tale of a strained relationship', *Matrix Biology*. Elsevier B.V., 47, pp. 54–65. doi: 10.1016/j.matbio.2015.05.006.
- Ho-Shui-Ling, A. *et al.* (2018) 'Bone regeneration strategies: Engineered scaffolds, bioactive molecules and stem cells current stage and future perspectives', *Biomaterials*. Elsevier Ltd, 180, pp. 143–162. doi: 10.1016/j.biomaterials.2018.07.017.
- Holtzhausen, A. *et al.* (2014) 'Novel bone morphogenetic protein signaling through Smad2 and Smad3 to regulate cancer progression and development', *FASEB Journal*, 28(3), pp. 1248–1267. doi: 10.1096/fj.13-239178.
- Hoodless, P. A. *et al.* (1996) 'MADR1, a MAD-related protein that functions in BMP2 signaling pathways', *Cell*, 85(4), pp. 489–500. doi: 10.1016/S0092-8674(00)81250-7.
- Howe, J. R. *et al.* (2001) 'Germline mutations of the gene encoding bone morphogenetic protein receptor 1A in juvenile polyposis', *nature genetics*, 28(june), pp. 184–187.
- Huang, F. and Chen, Y. (2012) 'Regulation of Cell Adhesion Activity', *Cell & Bioscience*, 2(9).
- Huang, H. *et al.* (2009) 'BMP signaling pathway is required for commitment of C3H10T1/2 pluripotent stem cells to the adipocyte lineage', *Proceedings of the National Academy of Sciences of the United States of America*, 106(31), pp. 12670–12675. doi: 10.1073/pnas.0906266106.
- Hudalla, G. *et al.* (2011) 'Harnessing endogenous growth factor activity modulates stem cell behavior', *Integr Biol*, 3(8), pp. 832–842. doi: 10.1039/c1ib00021g.Harnessing.
- Hue H, L. *et al.* (2007) 'Distinct Roles of Bone Morphogenetic Proteins in Osteogenic Differentiation of Mesenchymal Stem Cells', *Journal of Orthopaedic Research*, 65(12), pp. 354–359. doi: 10.1002/jor.
- Hunter, D. J. *et al.* (2010) 'Phase 1 safety and tolerability study of BMP-7 in symptomatic knee osteoarthritis', *BMC Musculoskeletal Disorders*. BioMed Central Ltd, 11(1), p. 232. doi: 10.1186/1471-2474-11-232.
- Hustedt, J. W. and Blizzard, D. J. (2014) 'The controversy surrounding bone morphogenetic proteins in the spine: A review of current research', *Yale Journal of Biology and Medicine*, 87(4), pp. 549–561.
- Iaquinta, M. R. *et al.* (2019) 'Adult Stem Cells for Bone Regeneration and Repair', *Frontiers in Cell and Developmental Biology*, 7(November), pp. 1–15. doi: 10.3389/fcell.2019.00268.
- IN Cell Analyzer High-Content Cellular Analysis System* (2021). Available at: <https://www.cytivalifesciences.co.kr/wp-content/uploads/2016/08/IN-Cell-Analyzer-High-Content-Cellular-Analysis-System-28-9937-79AB.pdf>.
- Isaacs, M. J. *et al.* (2010) 'Bone morphogenetic protein-2 and -6 heterodimer illustrates the nature of ligand-receptor assembly', *Molecular Endocrinology*, 24(7), pp. 1469–1477. doi: 10.1210/me.2009-0496.
- Jane, J. A. *et al.* (2002) 'Ectopic osteogenesis using adenoviral bone morphogenetic protein (BMP)-4 and BMP-6 gene transfer', *Molecular Therapy*. American Society for Gene Therapy, 6(4), pp. 464–470. doi: 10.1006/mthe.2002.0691.
- Javelaud, D. and Mauviel, A. (2004) 'Mammalian transforming growth factor- β s: Smad signaling and physio-pathological roles', *International Journal of Biochemistry and Cell*

Biology, 36(7), pp. 1161–1165. doi: 10.1016/S1357-2725(03)00255-3.

Javelaud, D. and Mauviel, A. (2005) ‘Crosstalk mechanisms between the mitogen-activated protein kinase pathways and Smad signaling downstream of TGF- β : Implications for carcinogenesis’, *Oncogene*, 24(37), pp. 5742–5750. doi: 10.1038/sj.onc.1208928.

Jayaraman, L. and Massague, J. (2000) ‘Distinct Oligomeric States of SMAD Proteins in the Transforming Growth Factor- β Pathway *’, *Journal of Biological Chemistry*, 275(52), pp. 40710–40717. doi: 10.1074/jbc.M005799200.

Jia, Q. *et al.* (2021) ‘CCN Family Proteins in Cancer: Insight Into Their Structures and Coordination Role in Tumor Microenvironment’, *Frontiers in Genetics*, 12(March), pp. 1–13. doi: 10.3389/fgene.2021.649387.

Jiao, K. *et al.* (2003) ‘An essential role of Bmp4 in the atrioventricular septation of the mouse heart’, *GENES & DEVELOPMENT*, 17, pp. 2362–2367. doi: 10.1101/gad.1124803.malities.

Jin, C. H. *et al.* (2014) ‘Discovery of N-((4-([1,2,4]Triazolo[1,5-a]pyridin-6-yl)-5-(6-methylpyridin-2-yl)-1H-imidazol-2-yl)methyl)-2-fluoroaniline (EW-7197): A Highly Potent, Selective, and Orally Bioavailable Inhibitor of TGF- β Type I Receptor Kinase as Cancer Immunotherapeutic’, *Journa of medicinal chemistry*, 57, pp. 4213–4238.

Johnson, D. W. *et al.* (1996) ‘Mutations in the activin receptor–like kinase 1 gene in hereditary haemorrhagic telangiectasia type 2’, *Nature Genetics*, 13(2), pp. 189–195. doi: 10.1038/ng0696-189.

Johnsson, B., Löfås, S. and Lindquist, G. (1991) ‘Immobilization of proteins to a carboxymethyl-dextran-modified gold surface for biospecific interaction analysis in surface plasmon resonance sensors’, *Analytical Biochemistry*, 198(2), pp. 268–277. doi: 10.1016/0003-2697(91)90424-R.

Jung, B. *et al.* (2004) ‘Loss of activin receptor type 2 protein expression in microsatellite unstable colon cancers’, *Gastroenterology*, 126(3), pp. 64–659. doi: <https://doi.org/10.1053/j.gastro.2004.01.008>.

Kaito, T. *et al.* (2018) ‘BMP-2/7 heterodimer strongly induces bone regeneration in the absence of increased soft tissue inflammation’, *Spine Journal*. Elsevier Inc., 18(1), pp. 139–146. doi: 10.1016/j.spinee.2017.07.171.

Kang, Q. *et al.* (2004) ‘Characterization of the distinct orthotopic bone-forming activity of 14 BMPs using recombinant adenovirus-mediated gene delivery’, *Gene Therapy*, 11(17), pp. 1312–1320. doi: 10.1038/sj.gt.3302298.

Kano, M. *et al.* (2017) ‘AMH/MIS as a contraceptive that protects the ovarian reserve during chemotherapy’, *Proceedings of the National Academy of Sciences of the United States of America*, 114(9), pp. E1688–E1697. doi: 10.1073/pnas.1620729114.

Kaplan, F. S. *et al.* (2009) ‘Classic and atypical fibrodysplasia ossificans progressiva (FOP) phenotypes are caused by mutations in the bone morphogenetic protein (BMP) type I receptor ACVR1’, *Human Mutation*, 30(3), pp. 379–390. doi: 10.1002/humu.20868.

Kashiwagi, K., Tsuji, T. and Shiba, K. (2009) ‘Directional BMP-2 for functionalization of titanium surfaces’, *Biomaterials*. Elsevier Ltd, 30(6), pp. 1166–1175. doi: 10.1016/j.biomaterials.2008.10.040.

Katagiri, T. *et al.* (1994) ‘Bone morphogenetic protein-2 converts the differentiation pathway of C2C12 myoblasts into the osteoblast lineage’, *Journal of Cell Biology*, 127(6 I), pp. 1755–1766. doi: 10.1083/jcb.127.6.1755.

- Katagiri, T. and Watabe, T. (2016) 'Bone morphogenetic proteins', *Cold Spring Harbor Perspectives in Biology*, 8(6). doi: 10.1101/cshperspect.a021899.
- Kawano, M. *et al.* (2011) 'Mechanism involved in enhancement of osteoblast differentiation by hyaluronic acid', *Biochemical and Biophysical Research Communications*. Elsevier Inc., 405(4), pp. 575–580. doi: 10.1016/j.bbrc.2011.01.071.
- Kefeng, R. *et al.* (2008) 'Polyelectrolyte multilayer films of controlled stiffness modulate myoblast cells differentiation', *Adv Funct Mater*, 18(9), pp. 1378–1389. doi: 10.1002/adfm.200701297.Polyelectrolyte.
- Keller, S. *et al.* (2004) 'Molecular recognition of BMP-2 and BMP receptor IA', *Nature Structural and Molecular Biology*, 11(5), pp. 481–488. doi: 10.1038/nsmb756.
- Kessler, E. *et al.* (1996) 'Bone morphogenetic protein-1: The type I procollagen C-proteinase', *Science*, 271(5247), pp. 360–362. doi: 10.1126/science.271.5247.360.
- Kestens, C. *et al.* (2016) 'BMP4 signaling is able to induce an epithelial-mesenchymal transition-like phenotype in Barrett's esophagus and esophageal adenocarcinoma through induction of SNAIL2', *PLoS ONE*, 11(5), pp. 1–14. doi: 10.1371/journal.pone.0155754.
- Keyes, W. M. *et al.* (2003) 'Expression and function of bone morphogenetic proteins in the development of the embryonic endocardial cushions', *Anatomy and Embryology*, 207(2), pp. 135–147. doi: 10.1007/s00429-003-0337-2.
- Khalkhali-Ellis, Z. *et al.* (2016) 'Lefty Glycoproteins in Human Embryonic Stem Cells: Extracellular Delivery Route and Posttranslational Modification in Differentiation', *Stem Cells and Development*, 25(21), pp. 1681–1690. doi: 10.1089/scd.2016.0081.
- Khodr, V. *et al.* (2021) 'High-throughput measurements of bone morphogenetic protein/bone morphogenetic protein receptor interactions using biolayer interferometry', *Biointerphases*. American Vacuum Society, 16(3), p. 031001. doi: 10.1116/6.0000926.
- Khurana, S. *et al.* (2013) 'A novel role of BMP4 in adult hematopoietic stem and progenitor cell homing via Smad independent regulation of integrin- α 4 expression', *Blood*, 121(5), pp. 781–790. doi: 10.1182/blood-2012-07-446443.
- Kim, B. G. *et al.* (2021) 'Novel therapies emerging in oncology to target the TGF- β pathway', *Journal of Hematology and Oncology*. BioMed Central, 14(1), pp. 1–20. doi: 10.1186/s13045-021-01053-x.
- Kim, H. S. *et al.* (2019) 'BMP7 functions predominantly as a heterodimer with BMP2 or BMP4 during mammalian embryogenesis', *eLife*, 8, pp. 1–22. doi: 10.7554/eLife.48872.
- Kim, J. H., MacLaughlin, D. T. and Donahoe, P. K. (2014) 'Müllerian inhibiting substance/anti-Müllerian hormone: A novel treatment for gynecologic tumors', *Obstetrics & Gynecology Science*, 57(5), p. 343. doi: 10.5468/ogs.2014.57.5.343.
- Kim, J. M. *et al.* (2020) 'Osteoblast-Osteoclast Communication and Bone Homeostasis', *Cells*, 9(9), pp. 1–14. doi: 10.3390/cells9092073.
- Kim, Sung Eun *et al.* (2014) 'Improving osteoblast functions and bone formation upon BMP-2 immobilization on titanium modified with heparin', *Carbohydrate Polymers*. Elsevier Ltd., 114, pp. 123–132. doi: 10.1016/j.carbpol.2014.08.005.
- Klages, J. *et al.* (2008) 'The solution structure of BMPR-IA reveals a local disorder-to-order transition upon BMP-2 binding', *Biochemistry*, 47(46), pp. 11930–11939. doi: 10.1021/bi801059j.

- Kluiser, T. A. *et al.* (2020) ‘Invaders Exposed: Understanding and Targeting Tumor Cell Invasion in Diffuse Intrinsic Pontine Glioma’, *Frontiers in Oncology*, 10(February), pp. 1–13. doi: 10.3389/fonc.2020.00092.
- Knippenberg, M. *et al.* (2006) ‘Osteogenesis versus chondrogenesis by BMP-2 and BMP-7 in adipose stem cells’, *Biochemical and Biophysical Research Communications*, 342(3), pp. 902–908. doi: 10.1016/j.bbrc.2006.02.052.
- Koehler, L. *et al.* (2017) ‘Sulfated Hyaluronan Derivatives Modulate TGF- β 1:Receptor Complex Formation: Possible Consequences for TGF- β 1 Signaling’, *Scientific Reports*, 7(1), pp. 1–11. doi: 10.1038/s41598-017-01264-8.
- Kortt, A. A. *et al.* (1997) ‘Nonspecific amine immobilization of ligand can be a potential source of error in BIAcore binding experiments and may reduce binding affinities’, *Analytical Biochemistry*, 253(1), pp. 103–111. doi: 10.1006/abio.1997.2333.
- Krause, C. *et al.* (2010) ‘Distinct modes of inhibition by Sclerostin on bone morphogenetic protein and Wnt signaling pathways’, *Journal of Biological Chemistry*, 285(53), pp. 41614–41626. doi: 10.1074/jbc.M110.153890.
- Kretzschmar, M. *et al.* (1997) ‘The TGF- β family mediator Smad1 is phosphorylated directly and activated functionally by the BMP receptor kinase’, *Genes and Development*, 11, pp. 984–995.
- Ku, J. L. *et al.* (2007) ‘Genetic alterations of the TGF- β signaling pathway in colorectal cancer cell lines: A novel mutation in Smad3 associated with the inactivation of TGF- β -induced transcriptional activation’, *Cancer Letters*, 247(2), pp. 283–292. doi: 10.1016/j.canlet.2006.05.008.
- Kular, J. *et al.* (2012) ‘An overview of the regulation of bone remodelling at the cellular level’, *Clinical Biochemistry*. The Canadian Society of Clinical Chemists, 45(12), pp. 863–873. doi: 10.1016/j.clinbiochem.2012.03.021.
- Kumar, R. *et al.* (2021) ‘Functionally diverse heteromeric traps for ligands of the transforming growth factor- β superfamily’, *Scientific Reports*. Nature Publishing Group UK, 11(1), pp. 1–16. doi: 10.1038/s41598-021-97203-9.
- Kuo, W. J., Digman, M. A. and Lander, A. D. (2010) ‘Heparan sulfate acts as a bone morphogenetic protein coreceptor by facilitating ligand-induced receptor hetero-oligomerization’, *Molecular Biology of the Cell*, 21(22), pp. 4028–4041. doi: 10.1091/mbc.E10-04-0348.
- Kusindarta, D. L. and Wihadmadyatami, H. (2018) ‘The Role of Extracellular Matrix in Tissue Regeneration’, *Tissue Regeneration*, pp. 1–18. doi: 10.5772/intechopen.75728.
- Lager, M. (2020) *Molecular and serological tools for clinical diagnostics of Lyme borreliosis—can the laboratory analysis be improved?* Available at: <https://books.google.de/books?hl=de&lr=&id=bLgKEAAQBAJ&oi=fnd&pg=PP7&dq=Cytokines+Immunoassay+%22human+risk%22+OR+Incidence+OR+%22product+risk%22+OR+Interference+OR+%22cross+reactivity%22+OR+accident+OR+malfun+OR+aggravation+OR+hazard+%22clinical+di.>
- Lagunas, A. *et al.* (2013) ‘Continuous bone morphogenetic protein-2 gradients for concentration effect studies on C2C12 osteogenic fate’, *Nanomedicine: Nanotechnology, Biology, and Medicine*. Elsevier Inc., 9(5), pp. 694–701. doi: 10.1016/j.nano.2012.12.002.
- Lamplot, J. D. *et al.* (2013) ‘BMP9 signaling in stem cell differentiation and osteogenesis’, *American Journal of Stem Cells*, 2(1), pp. 1–21.

- Langenfeld, E. M. and Langenfeld, J. (2004) 'Bone Morphogenetic Protein-2 Stimulates Angiogenesis in Developing Tumors', *Molecular Cancer Research*, 2(March), pp. 141–149.
- De Larco, J. E. and Todaro, G. J. (1978) 'Growth factors from murine sarcoma virus-transformed cells', *Proceedings of the National Academy of Sciences of the United States of America*, 75(8), pp. 4001–4005. doi: 10.1073/pnas.75.8.4001.
- Lavery, K. *et al.* (2008) 'BMP-2/4 and BMP-6/7 differentially utilize cell surface receptors to induce osteoblastic differentiation of human bone marrow-derived mesenchymal stem cells', *Journal of Biological Chemistry*, 283(30), pp. 20948–20958. doi: 10.1074/jbc.M800850200.
- Lawera, A. *et al.* (2019) 'Role of soluble endoglin in BMP9 signaling', *Proceedings of the National Academy of Sciences of the United States of America*, 116(36), pp. 17800–17808. doi: 10.1073/pnas.1816661116.
- Lazzeri, D. *et al.* (2009) 'Bone regeneration and periosteoplasty: A 250-year-long history', *Cleft Palate-Craniofacial Journal*, 46(6), pp. 621–628. doi: 10.1597/08-085.1.
- LDN-193189 (no date) 2021. Available at: <https://www.selleckchem.com/products/ldn193189.html>.
- LDN-193189 2HCl (2021). Available at: https://www.selleck.eu/products/ldn-193189-2hcl.html?gclid=CjwKCAjwgviIBhBkEiwA10D2j8WCILDZ8_bZUBWidRc7Rx5qE7x1fAfXEsg4V4Wk4FrzIWbRj2zIhoCNbMQAvD_BwE.
- Lefort, S. and Maguer-Satta, V. (2020) 'Targeting BMP signaling in the bone marrow microenvironment of myeloid leukemia', *Biochemical Society transactions*, 48(2), pp. 411–418. doi: 10.1042/BST20190223.
- Li, G. *et al.* (2005) 'Differential Effect of BMP4 on NIH/3T3 and C2C12 Cells: Implications for Endochondral Bone Formation', *JOURNAL OF BONE AND MINERAL RESEARCH*, 20(9), pp. 1611–1623. doi: 10.1359/JBMR.050513.
- Li, X. *et al.* (2021) 'Uterine Sensitization-Associated Gene-1 in the Progression of Kidney Diseases', *Journal of Immunology Research*, 2021. doi: 10.1155/2021/9752139.
- Lichtner, B. *et al.* (2013) 'BMP10 as a potent inducer of trophoblast differentiation in human embryonic and induced pluripotent stem cells', *Biomaterials*. Elsevier Ltd, 34(38), pp. 9789–9802. doi: 10.1016/j.biomaterials.2013.08.084.
- Lin, L. *et al.* (2006) 'Rat adipose-derived stromal cells expressing BMP4 induce ectopic bone formation in vitro and in vivo', *Acta Pharmacologica Sinica*, 27(12), pp. 1608–1615. doi: 10.1111/j.1745-7254.2006.00449.x.
- Lin, S. J. *et al.* (2006) 'The structural basis of TGF- β , bone morphogenetic protein, and activin ligand binding', *Reproduction*, 132(2), pp. 179–190. doi: 10.1530/rep.1.01072.
- Liu, I. M. *et al.* (2009) 'TGF β -stimulated Smad1/5 phosphorylation requires the ALK5 L45 loop and mediates the pro-migratory TGF β switch', *EMBO Journal*, 28(2), pp. 88–98. doi: 10.1038/emboj.2008.266.
- Loeys, B. L. *et al.* (2006) 'Aneurysm Syndromes Caused by Mutations in the TGF- β Receptor', *New England Journal of Medicine*, 355(8), pp. 788–798. doi: 10.1056/nejmoa055695.
- De Luca, F. *et al.* (2001) 'Regulation of growth plate chondrogenesis by bone morphogenetic protein-2', *Endocrinology*, 142(1), pp. 430–436. doi: 10.1210/endo.142.1.7901.
- Luo, J. *et al.* (2010) 'TGF β /BMP type I receptors ALK1 and ALK2 are essential for BMP9-induced osteogenic signaling in mesenchymal stem cells', *Journal of Biological Chemistry*,

285(38), pp. 29588–29598. doi: 10.1074/jbc.M110.130518.

Luther, G. *et al.* (2011) ‘BMP-9 Induced Osteogenic Differentiation of Mesenchymal Stem Cells: Molecular Mechanism and Therapeutic Potential’, *Current Gene Therapy*, 11(3), pp. 229–240. doi: 10.2174/156652311795684777.

Lyons, K. M., Hogan, B. L. M. and Robertson, E. J. (1995) ‘Colocalization of BMP 7 and BMP 2 RNAs suggests that these factors cooperatively mediate tissue interactions during murine development’, *Mechanisms of Development*, 50(1), pp. 71–83. doi: 10.1016/0925-4773(94)00326-I.

Ma, L. *et al.* (2005) ‘Bmp2 is essential for cardiac cushion epithelial-mesenchymal transition and myocardial patterning’, *Development*, 132, pp. 5601–5611. doi: 10.1242/dev.02156.

MacCarrick, G. *et al.* (2014) ‘Loeys-Dietz syndrome: A primer for diagnosis and management’, *Genetics in Medicine*, 16(8), pp. 576–587. doi: 10.1038/gim.2014.11.

Mace, P. D., Cutfield, J. F. and Cutfield, S. M. (2006) ‘High resolution structures of the bone morphogenetic protein type II receptor in two crystal forms: Implications for ligand binding’, *Biochemical and Biophysical Research Communications*, 351(4), pp. 831–838. doi: 10.1016/j.bbrc.2006.10.109.

MacFarlane, L.-A. and R. Murphy, P. (2010) ‘MicroRNA: Biogenesis, Function and Role in Cancer’, *Current Genomics*, 11(7), pp. 537–561. doi: 10.2174/138920210793175895.

Machado, R. D. *et al.* (2006) ‘Mutations of the TGF- β Type II Receptor BMPR2 in Pulmonary Arterial Hypertension’, *Hum Mutation*, 27(2), pp. 121–132. doi: 10.1002/humu.

Machillot, P. *et al.* (2018) ‘Automated Buildup of Biomimetic Films in Cell Culture Microplates for High-Throughput Screening of Cellular Behaviors’, *Advanced Materials*, 30(27), pp. 1–8. doi: 10.1002/adma.201801097.

Macias, M. *et al.* (1996) ‘MADR2 Is a Substrate of the TGF β Receptor and Its Phosphorylation Is Required for Nuclear Accumulation and Signaling’, *Cell*, 87, pp. 1215–1224. doi: 10.1016/S0092-8674(00)81817-6.

Macias, M. J., Martin-Malpartida, P. and Massagué, J. (2016) ‘Structural determinants of SMAD function in TGF- β signaling’, *Trends Biochem Sci*, 40(6), pp. 296–308. doi: 10.1016/j.tibs.2015.03.012.Structural.

Mahlawat, P. *et al.* (2012) ‘Structure of the Alk1 extracellular domain and characterization of its bone morphogenetic protein (BMP) binding properties’, *Biochemistry*, 51(32), pp. 6328–6341. doi: 10.1021/bi300942x.

Marom, B. *et al.* (2011) ‘Formation of stable homomeric and transient heteromeric bone morphogenetic protein (BMP) receptor complexes regulates smad protein signaling’, *Journal of Biological Chemistry*, 286(22), pp. 19287–19296. doi: 10.1074/jbc.M110.210377.

Marshall R. Urist (1965) ‘Bone: Formation by autoinduction’, *Classic Papers in Orthopaedics*, pp. 449–451. doi: 10.1007/978-1-4471-5451-8_114.

Martin-malpartida, P. *et al.* (2017) ‘Structural basis for genome wide recognition of 5- bp GC motifs by SMAD transcription factors’, *Nature Communications*. Springer US, 8, pp. 1–15. doi: 10.1038/s41467-017-02054-6.

Martino, M. M. and Hubbell, J. A. (2010) ‘The 12th-14th type III repeats of fibronectin function as a highly promiscuous growth factor-binding domain’, *FASEB Journal*, 24(12), pp. 4711–4721. doi: 10.1096/fj.09-151282.

- Marupanthorn, A. *et al.* (2017) 'Bone morphogenetic protein-2 enhances the osteogenic differentiation capacity of mesenchymal stromal cells derived from human bone marrow and umbilical cord', *International Journal of Molecular Medicine*, 39(3), pp. 654–662. doi: 10.3892/ijmm.2017.2872.
- Massagué, J. (1998) 'TGF- β SIGNAL TRANSDUCTION', *Annu rev biochem*, 67. doi: 10.1016/S0167-5699(97)01197-3.
- Massagué, J. (2008) 'TGF β in Cancer.pdf', *Cell*, 134(2), pp. 215–230. doi: 10.1016/j.cell.2008.07.001.TGF.
- Massague, J. and David, W. (2000) 'Transcriptional control by the TGF-beta/Smad signaling system', *The EMBO Journal*, 19(8), pp. 1745–1754. doi: 10.1093/emboj/19.8.1745.
- Massagué, J., Seoane, J. and Wotton, D. (2005) 'Smad transcription factors', *Genes and Development*, pp. 2783–2810. doi: 10.1101/gad.1350705.embryo.
- Meurer, S. K. *et al.* (2014) 'Endoglin in liver fibrogenesis: Bridging basic science and clinical practice.', *World journal of biological chemistry*, 5(2), pp. 180–203. doi: 10.4331/wjbc.v5.i2.180.
- Meynard, D. *et al.* (2009) 'Lack of the bone morphogenetic protein BMP6 induces massive iron overload', *Nature Genetics*, 41(4), pp. 478–481. doi: 10.1038/ng.320.
- Migliorini, E. *et al.* (2016) 'Tuning cellular responses to BMP-2 with material surfaces', *Cytokine and Growth Factor Reviews*. Elsevier Ltd, 27, pp. 43–54. doi: 10.1016/j.cytogfr.2015.11.008.
- Migliorini, E. *et al.* (2018) 'Practical guide to characterize biomolecule adsorption on solid surfaces (Review)', *Biointerphases*, 303. doi: 10.1116/1.5045122.
- Migliorini, E. *et al.* (2020) 'Learning from BMPs and their biophysical extracellular matrix microenvironment for biomaterial design', *Bone*, 141, p. 115540. doi: <https://doi.org/10.1016/j.bone.2020.115540>.
- Milano, F. *et al.* (2007) 'Bone Morphogenetic Protein 4 Expressed in Esophagitis Induces a Columnar Phenotype in Esophageal Squamous Cells', *Gastroenterology*, 132(7), pp. 2412–2421. doi: 10.1053/j.gastro.2007.03.026.
- Millet, C. *et al.* (2001) 'The human chordin gene encodes several differentially expressed spliced variants with distinct BMP opposing activities', *Mechanisms of Development*, 106(1–2), pp. 85–96. doi: 10.1016/S0925-4773(01)00423-3.
- Mittl, P. R. E. *et al.* (1996) 'The crystal structure of TGF- β 3 and comparison to TGF- β 2: Implications for receptor binding', *Protein Science*, 5(7), pp. 1261–1271. doi: 10.1002/pro.5560050705.
- Miyazawa, K. and Miyazono, K. (2017) 'Regulation of TGF- β family signaling by inhibitory smads', *Cold Spring Harbor Perspectives in Biology*, 9(3), pp. 1–25. doi: 10.1101/cshperspect.a022095.
- Miyazono, K., Maeda, S. and Imamura, T. (2005) 'BMP receptor signaling: Transcriptional targets, regulation of signals, and signaling cross-talk', *Cytokine and Growth Factor Reviews*, 16(3 SPEC. ISS.), pp. 251–263. doi: 10.1016/j.cytogfr.2005.01.009.
- Mizrahi, O. *et al.* (2013) 'BMP-6 is more efficient in bone formation than BMP-2 when overexpressed in mesenchymal stem cells', *Gene Therapy*, 20(4), pp. 370–377. doi: 10.1038/gt.2012.45.

- Moreno-Miralles, I., Schisler, J. C. and Patterson, C. (2009) 'New insights into bone morphogenetic protein signaling: Focus on angiogenesis', *Current Opinion in Hematology*, 16(3), pp. 195–201. doi: 10.1097/MOH.0b013e32832a07d6.
- Morgan, E. A. *et al.* (2003) 'Loss of Bmp7 and Fgf8 signaling in Hoxa13-mutant mice causes hypospadias', *Development*, 130, pp. 3095–3109. doi: 10.1242/dev.00530.
- Moses, H. L. *et al.* (1981) 'Transforming Growth Factor Production by Chemically Transformed Cells', *Cancer Research*, 41(7), pp. 2842–2848.
- Moses, H. L., Roberts, A. B. and Derynck, R. (2016) 'The discovery and early days of TGF- β : A historical perspective', *Cold Spring Harbor Perspectives in Biology*, 8(7). doi: 10.1101/cshperspect.a021865.
- Mueller, T. D. (2015) 'RGM co-receptors add complexity to BMP signaling', *Nature Structural and Molecular Biology*. Nature Publishing Group, 22(6), pp. 439–440. doi: 10.1038/nsmb.3037.
- Mueller, T. D. and Nickel, J. (2012) 'Promiscuity and specificity in BMP receptor activation', *FEBS Letters*, 586(14), pp. 1846–1859. doi: 10.1016/j.febslet.2012.02.043.
- Murphy-Ullrich, J. E. and Poczatek, M. (2000) 'Activation of latent TGF- β by thrombospondin-1: Mechanisms and physiology', *Cytokine and Growth Factor Reviews*, 11(1–2), pp. 59–69. doi: 10.1016/S1359-6101(99)00029-5.
- Myszka, D. G. *et al.* (1998) 'Extending the range of rate constants available from BIACORE: Interpreting mass transport-influenced binding data', *Biophysical Journal*, 75(2), pp. 583–594. doi: 10.1016/S0006-3495(98)77549-6.
- Nagaso, H. *et al.* (1999) 'Dual specificity of activin type II receptor ActRIIb in dorso-ventral patterning during zebrafish embryogenesis', *Development Growth and Differentiation*, 41(2), pp. 119–133. doi: 10.1046/j.1440-169X.1999.00418.x.
- Namwanje, M. and Brown, C. W. (2016) 'Activins and Inhibins: Roles in Development, Physiology, and Disease', *Cold Spring Harb Perspect Biol.*, 8(7), pp. 1–55.
- Nelsen, S. M. and Christian, J. L. (2009) 'Site-specific cleavage of BMP4 by furin, PC6, and PC7', *Journal of Biological Chemistry*, 284(40), pp. 27157–27166. doi: 10.1074/jbc.M109.028506.
- Nguyen, H. H. *et al.* (2015) 'Surface Plasmon Resonance: A Versatile Technique for Biosensor Applications', *Sensors*, 15, pp. 10481–10510. doi: 10.3390/s150510481.
- Nickel, J. *et al.* (2009) 'Intricacies of BMP receptor assembly', *Cytokine and Growth Factor Reviews*, 20(5–6), pp. 367–377. doi: 10.1016/j.cytogfr.2009.10.022.
- Nickel, J., Ten Dijke, P. and Mueller, T. D. (2018) 'TGF- β family co-receptor function and signaling', *Acta Biochimica et Biophysica Sinica*, 50(1), pp. 12–36. doi: 10.1093/abbs/gmx126.
- Nii, T., Makino, K. and Tabata, Y. (2020) 'Three-dimensional culture system of cancer cells combined with biomaterials for drug screening', *Cancers*, 12(10), pp. 1–24. doi: 10.3390/cancers12102754.
- Nohe, A. *et al.* (2002) 'The mode of bone morphogenetic protein (BMP) receptor oligomerization determines different BMP-2 signaling pathways', *Journal of Biological Chemistry*, 277(7), pp. 5330–5338. doi: 10.1074/jbc.M102750200.
- Nolan, K. and Thompson, T. B. (2014) 'The DAN family: Modulators of TGF- β signaling and beyond', *Protein Science*, 23(8), pp. 999–1012. doi: 10.1002/pro.2485.

- Odelberg, S. J. (2004) 'Unraveling the molecular basis for regenerative cellular plasticity', *PLoS Biology*, 2(8), pp. 2–5. doi: 10.1371/journal.pbio.0020232.
- Onichtchouk, D. *et al.* (1999) 'Silencing of TGF- β signalling by the pseudoreceptor BAMBI', *Nature*, 401(6752), pp. 480–485. doi: 10.1038/46794.
- Organ, L. A. *et al.* (2019) 'Biomarkers of collagen synthesis predict progression in the PROFILE idiopathic pulmonary fibrosis cohort', *Respiratory Research*. *Respiratory Research*, 20(1), pp. 1–10. doi: 10.1186/s12931-019-1118-7.
- Ouahoud, S., Hardwick, J. C. H. and Hawinkels, L. J. A. C. (2020) 'Extracellular bmp antagonists, multifaceted orchestrators in the tumor and its microenvironment', *International Journal of Molecular Sciences*, 21(11), pp. 1–16. doi: 10.3390/ijms21113888.
- Ouarné, M. *et al.* (2018) 'BMP9, but not BMP10, acts as a quiescence factor on tumor growth, vessel normalization and metastasis in a mouse model of breast cancer', *Journal of Experimental and Clinical Cancer Research*. *Journal of Experimental & Clinical Cancer Research*, 37(1), pp. 1–12. doi: 10.1186/s13046-018-0885-1.
- Pabinger, S. *et al.* (2014) 'Biomolecular Detection and Quantification A survey of tools for the analysis of quantitative PCR (qPCR) data', *Biomolecular Detection and Quantification*. Elsevier GmbH, 1(1), pp. 23–33. doi: 10.1016/j.bdq.2014.08.002.
- Pacifici, M. and Shore, E. M. (2016) 'Common mutations in ALK2/ACVR1, a multi-faceted receptor, have roles in distinct pediatric musculoskeletal and neural orphan disorders', *Cytokine Growth Factor Rev*, 27, pp. 93–104. doi: 10.1016/j.physbeh.2017.03.040.
- Paine-Saunders, S. *et al.* (2002) 'Heparan sulfate proteoglycans retain Noggin at the cell surface. A potential mechanism for shaping bone morphogenetic protein gradients', *Journal of Biological Chemistry*. © 2002 ASBMB. Currently published by Elsevier Inc; originally published by American Society for Biochemistry and Molecular Biology., 277(3), pp. 2089–2096. doi: 10.1074/jbc.M109151200.
- Papathanasiou, I., Malizos, K. N. and Tsezou, A. (2012) 'Bone morphogenetic protein-2-induced Wnt/ β -catenin signaling pathway activation through enhanced low-density-lipoprotein receptor-related protein 5 catabolic activity contributes to hypertrophy in osteoarthritic chondrocytes', *Arthritis Research and Therapy*, 14(2), pp. 1–14. doi: 10.1186/ar3805.
- Perron, J. C. and Dodd, J. (2009) 'ActRIIA and BMPRII type II BMP receptor subunits selectively required for Smad4-independent BMP7-evoked chemotaxis', *PLoS ONE*, 4(12). doi: 10.1371/journal.pone.0008198.
- Phillippi, J. A. *et al.* (2008) 'Microenvironments Engineered by Inkjet Bioprinting Spatially Direct Adult Stem Cells Toward Muscle- and Bone-Like Subpopulations', *Stem Cells*, 26(1), pp. 127–134. doi: 10.1634/stemcells.2007-0520.
- Picart, C. *et al.* (2001) 'Buildup mechanism for poly(L-lysine)/hyaluronic acid films onto a solid surface', *Langmuir*, 17(23), pp. 7414–7424. doi: 10.1021/la010848g.
- Piccolo, S. *et al.* (1996) 'Dorsoventral Patterning in Xenopus: Inhibition of Ventral Signals by Direct Binding of Chordin to BMP-4', *Cell*, 86(4), pp. 589–598.
- Pietrangelo, A. *et al.* (2006) 'Juvenile hemochromatosis', 45, pp. 892–894. doi: 10.1016/j.jhep.2006.09.003.
- Principle and Protocol of Surface Plasmon Resonance (SPR)* (2021) *creative-biomart*. Available at: <https://www.creativebiomart.net/resource/principle-protocol-principle-and-protocol-of-surface-plasmon-resonance-spr-361.htm>.

- Qin, B. Y. *et al.* (2001) 'Structural Basis of Smad1 Activation by Receptor Kinase Phosphorylation', *molecular Cell*, 8, pp. 1303–1312.
- Racacho, L. *et al.* (2015) 'Two novel disease-causing variants in BMPR1B are associated with brachydactyly type A1', *European Journal of Human Genetics*. Nature Publishing Group, 23(12), pp. 1640–1645. doi: 10.1038/ejhg.2015.38.
- Raggatt, L. J. and Partridge, N. C. (2010) 'Cellular and molecular mechanisms of bone remodeling', *Journal of Biological Chemistry*. © 2010 ASBMB. Currently published by Elsevier Inc; originally published by American Society for Biochemistry and Molecular Biology., 285(33), pp. 25103–25108. doi: 10.1074/jbc.R109.041087.
- Ramachandran, A. *et al.* (2018) 'TGF- β uses a novel mode of receptor activation to phosphorylate SMAD1/5 and induce epithelial-to-mesenchymal transition', *eLife*, 7, pp. 1–29. doi: 10.7554/eLife.31756.
- Ray, B. N. *et al.* (2010) 'ALK5 phosphorylation of the endoglin cytoplasmic domain regulates Smad1/5/8 signaling and endothelial cell migration', *Carcinogenesis*, 31(3), pp. 435–441. doi: 10.1093/carcin/bgp327.
- Recombinant Human BMPR-IA/ALK-3 Fc Chimera Protein* (no date). Available at: https://www.rndsystems.com/products/recombinant-human-bmpr-ia-alk-3-fc-chimera-protein_315-br.
- Richert, L. *et al.* (2004) 'Improvement of stability and cell adhesion properties of polyelectrolyte multilayer films by chemical cross-linking', *Biomacromolecules*, 5(2), pp. 284–294. doi: 10.1021/bm0342281.
- Rivera-feliciano, J. and Tabin, C. J. (2006) 'Bmp2 instructs cardiac progenitors to form the heart-valve-inducing field', *Developmental Biology*, 295, pp. 580–588. doi: 10.1016/j.ydbio.2006.03.043.
- Roberts, A. B. *et al.* (1981) 'New class of transforming growth factors potentiated by epidermal growth factor: Isolation from non-neoplastic tissues', *Proceedings of the National Academy of Sciences of the United States of America*, 78(9 II), pp. 5339–5343. doi: 10.1073/pnas.78.9.5339.
- Roberts, A. B. *et al.* (1986) 'Transforming growth factor type , 8 : Rapid induction of fibrosis and angiogenesis in vivo and stimulation of collagen formation in vitro', *Proc. Nati. Acad. Sci.*, 83(June), pp. 4167–4171.
- Robertson, I. B. *et al.* (2015) 'Latent TGF- β -binding proteins', *Matrix Biology*. Elsevier B.V., 47, pp. 44–53. doi: 10.1016/j.matbio.2015.05.005.
- Robertson, I. B. and Rifkin, D. B. (2016) 'Regulation of the bioavailability of TGF- β and TGF- β -related proteins', *Cold Spring Harbor Perspectives in Biology*, 8(6). doi: 10.1101/cshperspect.a021907.
- Roman, B. L. and Hinck, A. P. (2017) 'ALK1 signaling in development and disease: new paradigms', *Cellular and Molecular Life Sciences*, 74(24), pp. 4539–4560. doi: 10.1007/s00018-017-2636-4.
- Saarma, M. (2000) 'GDNF - a stranger in the TGF- b superfamily ?', *Eur. J. Biochem.*, 267, pp. 6968–6971.
- Sales, A. *et al.* (2022) 'Differential bioactivity of four BMP-family members as function of biomaterial stiffness', *Biomaterials*, 281. doi: 10.1016/j.biomaterials.2022.121363
- Sanchez-Duffhues, G. *et al.* (2020) 'Bone morphogenetic protein receptors: Structure, function and targeting by selective small molecule kinase inhibitors', *Bone*, 138(April). doi:

10.1016/j.bone.2020.115472.

Saremba, S. *et al.* (2007) 'Type I receptor binding of bone morphogenetic protein 6 is dependent on N-glycosylation of the ligand', *The FEBS Journal*, 12(275), pp. 172–183. doi: 10.1111/j.1742-4658.2007.06187.x.

Sariola, H. and Saarma, M. (2003) 'Novel functions and signalling pathways for GDNF', *Journal of Cell Science*, 116(19), pp. 3855–3862. doi: 10.1242/jcs.00786.

Sartori, R. *et al.* (2013) 'BMP signaling controls muscle mass', *Nature Genetics*. Nature Publishing Group, 45(11), pp. 1309–1321. doi: 10.1038/ng.2772.

Savage, C. *et al.* (1996) 'Caenorhabditis elegans genes sma-2, sma-3, and sma-4 define a conserved family of transforming growth factor β pathway components', *Proceedings of the National Academy of Sciences of the United States of America*, 93(2), pp. 790–794. doi: 10.1073/pnas.93.2.790.

Scheufler, C., Sebald, W. and Hülsmeier, M. (1999) 'Crystal structure of human bone morphogenetic protein-2 at 2.7 Å resolution', *Journal of Molecular Biology*, 287(1), pp. 103–115. doi: 10.1006/jmbi.1999.2590.

Schneider, A. *et al.* (2006) 'Polyelectrolyte multilayers with a tunable young's modulus: Influence of film stiffness on cell adhesion', *Langmuir*, 22(3), pp. 1193–1200. doi: 10.1021/la0521802.

Schwab, E. H. *et al.* (2015) 'Nanoscale control of surface immobilized BMP-2: Toward a quantitative assessment of BMP-mediated signaling events', *Nano Letters*, 15(3), pp. 1526–1534. doi: 10.1021/acs.nanolett.5b00315.

Schwartz, A. D. *et al.* (2017) 'A Biomaterial Screening Approach Reveals Microenvironmental Mechanisms of Drug Resistance', *Integr Biol (Camb)*, 9(12), pp. 912–924. doi: 10.1039/c7ib00128b.A.

Seeherman, H. J. *et al.* (2019) 'A BMP/activin A chimera is superior to native BMPs and induces bone repair in nonhuman primates when delivered in a composite matrix', *Science Translational Medicine*, 11(489), pp. 1–21. doi: 10.1126/scitranslmed.aar4953.

Sefkow-Werner, J. *et al.* (2020) 'Heparan sulfate co-immobilized with cRGD ligands and BMP2 on biomimetic platforms promotes BMP2-mediated osteogenic differentiation', *Acta Biomaterialia*. Elsevier Ltd, 114, pp. 90–103. doi: 10.1016/j.actbio.2020.07.015.

Sengle, G. and Sakai, L. Y. (2015) 'The fibrillin microfibril scaffold: A niche for growth factors and mechanosensation?', *Matrix Biology*. Elsevier B.V., 47, pp. 3–12. doi: 10.1016/j.matbio.2015.05.002.

Senn, N. (1889) 'Senn on the Healing of Aseptic Bone Cavities by Implantation of Antiseptic Decalcified Bone', *Annals of Surgery*, 10(5), pp. 352–368.

Shi, Y. *et al.* (1998) 'Crystal structure of a Smad MH1 domain bound to DNA: Insights on DNA binding in TGF- β signaling', *Cell*, 94(5), pp. 585–594. doi: 10.1016/S0092-8674(00)81600-1.

Shore, E. M. *et al.* (2006) 'A recurrent mutation in the BMP type I receptor ACVR1 causes inherited and sporadic fibrodysplasia ossificans progressiva', *Nature Genetics*, 38(5), pp. 525–527. doi: 10.1038/ng1783.

Shu, B. *et al.* (2011) 'BMP2, but not BMP4, is crucial for chondrocyte proliferation and maturation during endochondral bone development', *Journal of Cell Science*, 124(20), pp. 3428–3440. doi: 10.1242/jcs.083659.

- Sims, N. A. and Vrahnas, C. (2014) 'Regulation of cortical and trabecular bone mass by communication between osteoblasts, osteocytes and osteoclasts', *Archives of Biochemistry and Biophysics*. Elsevier Inc., 561, pp. 22–28. doi: 10.1016/j.abb.2014.05.015.
- Smith, W. C. and Harland, R. M. (1992) 'Expression cloning of noggin, a new dorsalizing factor localized to the Spemann organizer in *Xenopus* embryos', *Cell*, 70(5), pp. 829–840. doi: 10.1016/0092-8674(92)90316-5.
- Song, B., Estrada, K. D. and Lyons, K. M. (2009) 'Smad Signaling in Skeletal Development and Regeneration Buer', *Cytokine Growth Factor Rev*, 20(5–6), pp. 379–388. doi: 10.1016/j.cytogfr.2009.10.010.Smad.
- Souchelnytskyi, S. *et al.* (1997) 'Phosphorylation of Ser465 and Ser467 in the C terminus of Smad2 mediates interaction with Smad4 and is required for transforming growth factor- β signaling', *Journal of Biological Chemistry*, 272(44), pp. 28107–28115. doi: 10.1074/jbc.272.44.28107.
- Stefanska, K. *et al.* (2020) 'Mesenchymal stem cells- A historical overview', *Medical Journal of Cell Biology*, 8(2), pp. 83–87. doi: 10.2478/acb-2020-0010.
- Sugiura, K., Su, Y. Q. and Eppig, J. J. (2010) 'Does bone morphogenetic protein 6 (BMP6) affect female fertility in the mouse?', *Biology of Reproduction*, 83(6), pp. 997–1004. doi: 10.1095/biolreprod.110.086777.
- Sultana, A. and Lee, J. E. (2015) 'Measuring protein-protein and protein-nucleic acid interactions by biolayer interferometry', *Current Protocols in Protein Science*, 2015, pp. 19.25.1-19.25.26. doi: 10.1002/0471140864.ps1925s79.
- Sun, J. *et al.* (2015) 'Role of bone morphogenetic protein-2 in osteogenic differentiation of mesenchymal stem cells', *Molecular Medicine Reports*, 12(3), pp. 4230–4237. doi: 10.3892/mmr.2015.3954.
- Suzuki, Y. *et al.* (2010) 'BMP-9 induces proliferation of multiple types of endothelial cells in vitro and in vivo', *Journal of Cell Science*, 123, pp. 1684–1692. doi: 10.1242/jcs.061556.
- Tajer, B. *et al.* (2021) 'BMP heterodimers signal via distinct type I receptor class functions', *Proceedings of the National Academy of Sciences of the United States of America*, 118(15). doi: 10.1073/pnas.2017952118.
- Tazoe, M. *et al.* (2003) 'Involvement of p38MAP kinase in bone morphogenetic protein-4-induced osteoprotegerin in mouse bone-marrow-derived stromal cells', *Archives of Oral Biology*, 48(8), pp. 615–619. doi: 10.1016/S0003-9969(03)00100-6.
- Tillet, E. and Bailly, S. (2014) 'Emerging roles of BMP9 and BMP10 in hereditary hemorrhagic telangiectasia', *Frontiers in Genetics*, 5(DEC), pp. 1–7. doi: 10.3389/fgene.2014.00456.
- Tobias, R. (2013) 'Biomolecular Binding Kinetics Assays on the Octet Platform', *ForteBio Interactions*, p. Pall Life Sciences. Available at: http://www.fortebio.com/doc_download.html?docid=329&source=.
- Tramullas, M. *et al.* (2010) 'BAMBI (bone morphogenetic protein and activin membrane-bound inhibitor) reveals the involvement of the transforming growth factor- β family in pain modulation', *Journal of Neuroscience*, 30(4), pp. 1502–1511. doi: 10.1523/JNEUROSCI.2584-09.2010.
- Trembath, R. C. *et al.* (2001) 'Clinical and Molecular Genetic Features of Pulmonary Hypertension in Patients with Hereditary Hemorrhagic Telangiectasia', *New England Journal of Medicine*, 345(5), pp. 325–334. doi: 10.1056/nejm200108023450503.

- Tsuji, K. *et al.* (2006) ‘BMP2 activity, although dispensable for bone formation, is required for the initiation of fracture healing’, *Nature Genetics*, 38(12), pp. 1424–1429. doi: 10.1038/ng1916.
- Umulis, D., O’Connor, M. B. and Blair, S. S. (2009) ‘The extracellular regulation of bone morphogenetic protein signaling’, *Development*, 136(22), pp. 3715–3728. doi: 10.1242/dev.031534.
- Urist, M. R. and Strates, B. S. (1971) ‘Bone Morphogenetic Protein’, *Journal of Dental Research*. SAGE Publications Inc, 50(6), pp. 1392–1406. doi: 10.1177/00220345710500060601.
- Vactosertib* (2021). Available at: <https://www.selleckchem.com/products/ew-7197.html>.
- Vactosertib (TEW-7197)* (no date). Available at: <https://www.selleckchem.com/products/ew-7197.html>.
- Valcourt, U. *et al.* (2002) ‘Functions of transforming growth factor- β family type I receptors and Smad proteins in the hypertrophic maturation and osteoblastic differentiation of chondrocytes’, *Journal of Biological Chemistry*, 277(37), pp. 33545–33558. doi: 10.1074/jbc.M202086200.
- Valcourt, U. *et al.* (2005) ‘TGF- β and the Smad Signaling Pathway Support Transcriptomic Reprogramming during Epithelial- Mesenchymal Cell Transition’, *Mol Biol Cell*, 16, pp. 1987–2002. doi: 10.1091/mbc.E04.
- Vallejo, L. F. and Rinas, U. (2013) ‘Folding and dimerization kinetics of bone morphogenetic protein-2, a member of the transforming growth factor- β family’, *FEBS Journal*, 280(1), pp. 83–92. doi: 10.1111/febs.12051.
- Voeltzel, T. *et al.* (2018) ‘A new signaling cascade linking BMP4, BMPR1A, Δ Np73 and NANOG impacts on stem-like human cell properties and patient outcome’, *Cell Death and Disease*. Springer US, 9(10). doi: 10.1038/s41419-018-1042-7.
- Walker, R. G. *et al.* (2017) ‘Structural basis for potency differences between GDF8 and GDF11’, *BMC Biology*. BMC Biology, 15(1), pp. 1–22. doi: 10.1186/s12915-017-0350-1.
- Wang, R. N. *et al.* (2014) ‘Bone Morphogenetic Protein (BMP) signaling in development and human diseases’, *Genes and Diseases*. Elsevier Ltd, 1(1), pp. 87–105. doi: 10.1016/j.gendis.2014.07.005.
- Wang, W. *et al.* (2019) ‘The TGF β type I receptor TGF β RI functions as an inhibitor of BMP signaling in cartilage’, *Proceedings of the National Academy of Sciences of the United States of America*, 116(31), pp. 15570–15579. doi: 10.1073/pnas.1902927116.
- Wang, Y. *et al.* (2013) ‘Noggin resistance contributes to the potent osteogenic capability of BMP9 in mesenchymal stem cells’, *Journal of Orthopaedic Research*, 31(11), pp. 1796–1803. doi: 10.1002/jor.22427.
- Wang, Y. *et al.* (2014) ‘Bone morphogenetic protein 2 stimulates noncanonical smad2/3 signaling via the bmp type 1a receptor in gonadotrope-like cells: Implications for FSH synthesis’, *Endocrinology*, 155(5), pp. 1970–1981. doi: 10.1210/en.2013-1741.
- Weber, S. *et al.* (2008) ‘SIX2 and BMP4 Mutations Associate With Anomalous Kidney Development’, *J Am Soc Nephrol*, 19(5), pp. 891–903. doi: 10.1681/ASN.2006111282.
- Weiskirchen, R. *et al.* (2009) ‘BMP-7 as antagonist of organ fibrosis’, *Frontiers in Bioscience*, 14(13), pp. 4992–5012. doi: 10.2741/3583.

- Weiskirchen, R., Weiskirchen, S. and Tacke, F. (2019) 'Organ and tissue fibrosis: Molecular signals, cellular mechanisms and translational implications', *Molecular Aspects of Medicine*. Elsevier, 65(March 2018), pp. 2–15. doi: 10.1016/j.mam.2018.06.003.
- Wente, S. R. and Rout, M. P. (2010) 'The nuclear pore complex and nuclear transport.', *Cold Spring Harbor perspectives in biology*, 2(10). doi: 10.1101/cshperspect.a000562.
- What is Real-Time PCR (qPCR)?* (2021). Available at: <https://www.bio-rad.com/fr-fr/applications-technologies/what-real-time-pcr-qpcr?ID=LUSO4W8UU>.
- Wijayarathna, R. and de Kretser, D. M. (2016) 'Activins in reproductive biology and beyond', *Human Reproduction Update*, 22(3), pp. 342–357. doi: 10.1093/humupd/dmv058.
- Wilkinson, L. *et al.* (2003) 'CRIM1 Regulates the Rate of Processing and Delivery of Bone Morphogenetic Proteins to the Cell Surface', *Journal of Biological Chemistry*. © 2003 ASBMB. Currently published by Elsevier Inc; originally published by American Society for Biochemistry and Molecular Biology., 278(36), pp. 34181–34188. doi: 10.1074/jbc.M301247200.
- Williams, E. and Bullock, A. (2018) 'Structural basis for the potent and selective binding of LDN-212854 to the BMP receptor kinase ALK2', *Bone*. The Authors, 109, pp. 251–258. doi: 10.1016/j.bone.2017.09.004.
- Wills, A., Harland, R. M. and Khokha, M. K. (2006) 'Twisted gastrulation is required for forebrain specification and cooperates with Chordin to inhibit BMP signaling during *X. tropicalis* gastrulation', *Developmental Biology*, 289(1), pp. 166–178. doi: 10.1016/j.ydbio.2005.10.022.
- Winbanks, C. E. *et al.* (2013) 'The bone morphogenetic protein axis is a positive regulator of skeletal muscle mass', *Journal of Cell Biology*, 203(2), pp. 345–357. doi: 10.1083/jcb.201211134.
- Wisotzkey, R. G. and Newfeld, S. J. (2020) 'TGF- β Prodomain Alignments Reveal Unexpected Cysteine Conservation Consistent with Phylogenetic', *GENETICS*, 214(February), pp. 447–465.
- Wozney, J. M. *et al.* (1989) 'Novel regulators of bone formation: Molecular clones and activities', *Obstetrical and Gynecological Survey*, 44(5), pp. 387–388. doi: 10.1097/00006254-198905000-00028.
- Wrana, J. L. *et al.* (1994) 'Mechanism of activation of the TGF- β receptor', *Nature*, 370(6488), pp. 341–347. doi: 10.1038/370341a0.
- Wu, G. *et al.* (2000) 'Structural basis of Smad2 recognition by the smad anchor for receptor activation', *Science*, 287(5450), pp. 92–97. doi: 10.1126/science.287.5450.92.
- Wu, J. *et al.* (2001) 'Crystal Structure of a Phosphorylated Smad2: Recognition of Phosphoserine by the MH2 Domain and Insights on Smad Function in TGF- β Signaling', *Molecular cell*, 8, pp. 1277–1289.
- Wu, M., Chen, G. and Li, Y. P. (2016) 'TGF- β and BMP signaling in osteoblast, skeletal development, and bone formation, homeostasis and disease', *Bone Research*, 4(December 2015). doi: 10.1038/boneres.2016.9.
- Wyatt, A. W. *et al.* (2010) 'Bone Morphogenetic Protein 7 (BMP7) mutations are associated with variable ocular, brain, ear, palate, and skeletal anomalies', *Human Mutation*, 31(7), pp. 781–787. doi: 10.1002/humu.21280.
- Xu, L. *et al.* (2002) 'Smad2 nucleocytoplasmic shuttling by nucleoporins CAN/Nup214 and

- Nup153 feeds TGF β signaling complexes in the cytoplasm and nucleus', *Molecular Cell*, 10(2), pp. 271–282. doi: 10.1016/S1097-2765(02)00586-5.
- Xu, Y. and Pasche, B. (2007) 'TGF- β signaling alterations and susceptibility to colorectal cancer', *Human Molecular Genetics*, 16(R1), pp. 1–13. doi: 10.1093/hmg/ddl486.
- Yaffe, D. and Saxel, O. (1977) 'Serial passaging and differentiation of myogenic cells isolated from dystrophic mouse muscle', *Nature*, 270(5639), pp. 725–727. doi: 10.1038/270725a0.
- Yamaguchi, K. *et al.* (1999) 'XIAP, a cellular member of the inhibitor of apoptosis protein family, links the receptors to TAB1-TAK1 in the BMP signaling pathway', *EMBO Journal*, 18(1), pp. 179–187. doi: 10.1093/emboj/18.1.179.
- Yamamoto, N. *et al.* (1997) 'Smad1 and smad5 act downstream of intracellular signalings of BMP-2 that inhibits myogenic differentiation and induces osteoblast differentiation in C2C12 myoblasts', *Biochemical and Biophysical Research Communications*, 238(2), pp. 574–580. doi: 10.1006/bbrc.1997.7325.
- Ye, L., Kynaston, H. and Jiang, W. G. (2008) 'Bone morphogenetic protein-9 induces apoptosis in prostate cancer cells, the role of prostate apoptosis response-4', *Molecular Cancer Research*, 6(10), pp. 1594–1606. doi: 10.1158/1541-7786.MCR-08-0171.
- Yu, P. B. *et al.* (2005) 'Bone morphogenetic protein (BMP) type II receptor deletion reveals BMP ligand-specific gain of signaling in pulmonary Artery smooth muscle cells', *Journal of Biological Chemistry*, 280(26), pp. 24443–24450. doi: 10.1074/jbc.M502825200.
- Yu, P. B. *et al.* (2008) 'Dorsomorphin inhibits BMP signals required for embryogenesis and iron metabolism', *Nat Chem Biol*, 4(1), pp. 33–41. doi: 10.1016/B978-0-12-384937-3.00023-9.
- Zakin, L. and De Robertis, E. . (2010) 'Extracellular regulation of BMP signaling', *Curr Biol*, 20(3), pp. R89–R92. doi: 10.1016/j.cub.2009.11.021.Extracellular.
- Zhang, Y. E. (2017) 'Non-Smad signaling pathways of the TGF- β family', *Cold Spring Harbor Perspectives in Biology*, 9(2). doi: 10.1101/cshperspect.a022129.
- Zhang, Y., Feng, X.-H. and Derynck, R. (1998) 'Smad3 and Smad4 cooperate with c-Jun/c-Fos to mediate TGF- β -induced transcription', *Nature*, 394, pp. 909–913.
- Zimmerman, L. B., De Jesús-Escobar, J. M. and Harland, R. M. (1996) 'The Spemann organizer signal noggin binds and inactivates bone morphogenetic protein 4', *Cell*, 86(4), pp. 599–606. doi: 10.1016/S0092-8674(00)80133-6.
- Zou, M. L. *et al.* (2021) 'The Smad Dependent TGF- β and BMP Signaling Pathway in Bone Remodeling and Therapies', *Frontiers in Molecular Biosciences*, 8(May), pp. 1–11. doi: 10.3389/fmolb.2021.593310.
- Zuniga, J. E. *et al.* (2011) 'The T β R-I pre-helix extension is structurally ordered in the unbound form and its flanking prolines are essential for binding', *Journal of Molecular Biology*. Elsevier Ltd, 412(4), pp. 601–618. doi: 10.1016/j.jmb.2011.07.046.
- Zuo, W. H. *et al.* (2016) 'Promotive effects of bone morphogenetic protein 2 on angiogenesis in hepatocarcinoma via multiple signal pathways', *Scientific Reports*. Nature Publishing Group, 6(October), pp. 1–9. doi: 10.1038/srep37499.
- Zylbersztejn, F. *et al.* (2018) 'The BMP pathway: A unique tool to decode the origin and progression of leukemia', *Experimental Hematology*. Elsevier Inc., 61, pp. 36–44. doi: 10.1016/j.exphem.2018.02.005.

Abstract

Bone morphogenetic factors (BMPs) are growth factors with several physiological and pathological roles. As their name suggest, they are osteoinductive as they promote stem cells differentiation into osteoblasts, in addition, they are involved in a large panel of physiological and pathological processes, including angiogenesis, adipogenesis, muscle differentiation and embryonic development and cancers. *In vivo*, BMPs bind two types of BMP receptors (BMPR); type –I and type-II. In this thesis, we focused on the early steps of bone tissue formation starting at the molecular scale with the BMP/BMPR interaction. The large number of BMPs associated to a low number of BMPR leads to a phenomenon of promiscuity, where a BMP can bind different BMPRs with various affinities. In the thesis, The binding affinities and kinetic properties of four BMPs: BMP-2, BMP-4, BMP-7 and BMP-9 with five type-I BMPR (ALK1, ALK2, ALK3, ALK5, ALK6) and three type-II BMPRs (BMPR-II, ACTR-IIA, ACTR-IIB) were first studied using biolayer interferometry (BLI) and surface plasmon resonance (SPR). In a second part, biomaterials in the form of polyelectrolytes biomimetic films were used to present BMP to cells in a matrix-bound manner, and to study the combined effect of film stiffness and BMP-2 presentation (for BMP-2, BMP-4, BMP-7 and BMP-9) . C2C12 skeletal myoblasts and human periosteum-derived stem cells (hPDSCs) were used as cellular models of BMP-responsive cells. High content screening (HCS) of cellular responses was done to quantify cell adhesion evaluated by cell number and cell spreading area, and cell differentiation in bone by quantifying Smad and alkaline phosphatase (ALP) activities. Using RNA silencing of BMP receptors and of the adhesion receptors integrins enabled to reveal the specific roles of each receptors. In a third part, a HCS assay to quantify phosphorylated Smad was developed and a proof-of-concept of drug assays on biomaterials was realized, using commercial inhibitors of ALK2, ALK5 inhibitors.

Résumé

Les facteurs morphogénétiques osseux (BMP) sont des facteurs de croissance ayant plusieurs rôles physiologiques et pathologiques. Ils sont ostéoinducteurs favorisant la différenciation des cellules souches en ostéoblastes, de plus ils sont impliqués dans l'angiogenèse, l'adipogenèse, la différenciation musculaire et le développement embryonnaire. In vivo, les BMP se lient à deux types de récepteurs BMP (BMPR) ; type -I et type-II. Dans cette thèse, nous nous sommes concentrés sur les premières étapes de la régénération osseuse en commençant par l'interaction BMP/BMPR. Vu le grand nombre de BMP (environ douze) par rapport à un faible nombre de BMPR (quatre BMPR de type I et trois BMPR de type II), un processus de promiscuité a été décrit où un BMP peut lier différents BMPR avec diverses affinités. Ainsi, dans cette thèse, nous avons d'abord fait une étude comparative pour examiner les affinités de liaison et les constantes cinétiques de quatre BMP : BMP-2, BMP-4, BMP-7 et BMP-9 avec cinq BMPR de type I (ALK1, ALK2, ALK3, ALK5, ALK6) et trois BMPR de type II (BMPR-II, ACTR-IIA, ACTR-IIB) en utilisant l'interférométrie à biocouche (BLI) et la résonance plasmonique de surface (SPR). Deuxièmement, nous avons examiné l'effet de la rigidité sur les activités cellulaires des BMP. Nous avons utilisé des cellules myoblastes squelettiques C2C12 et des cellules souches dérivées du périoste humain (hPDSC) connues dans le domaine de la régénération osseuse pour leurs sensibilités aux BMP. Nous les avons ensuiteensemencés sur des films minces de polyélectrolyte de rigidité contrôlée, préalablement développés par l'équipe, chargés avec l'un des quatre BMP (BMP-2 ou BMP-4 ou BMP-7 ou BMP-9). Nous avons ensuite effectué un criblage à haut contenu des réponses cellulaires, telles que l'adhésion cellulaire évaluée par le nombre de cellules et la zone d'étalement cellulaire, ainsi que la signalisation cellulaire en examinant la signalisation Smad et phosphatase alcaline (ALP). De plus, les rôles de la BMPR et des intégrines dans l'adhésion cellulaire, la signalisation Smad et ALP avec les quatre BMP ont été évalués par des études d'ARN silencing. Enfin, afin d'effectuer des tests de dépistage de drogues sur les films biomimétiques, nous avons optimisé un test d'immunofluorescence pour examiner la translocation du Smad phosphorylé vers le noyau. Nous avons utilisé un inhibiteur connu de la kinase ALK2, LDN-193189, et deux inhibiteurs de la kinase ALK5, le galunisertib et le vactosertib développés dans des essais cliniques, employés avec BMP-2 et TGF- β 1 respectivement.

Annexes

Differential bioactivity of four BMP-family members as function of biomaterial stiffness

Adrià Sales^{1,2} #, Valia Khodr^{1,2*}, Paul Machillot^{1,2*}, Line, Chaar³, Laure Fourel^{1,2,3}, Amaris Guevara-Garcia^{1,2,3}, Elisa Migliorini^{1,2}, Corinne Albigès-Rizo³, Catherine Picart^{1,2,4#}

¹Interdisciplinary Research Institute of Grenoble (IRIG), ERL BRM 5000 (CNRS/UGA/CEA), CEA Grenoble, 17 rue des Martyrs, 38054 Grenoble cedex, France

² CNRS, Grenoble Institute of Technology, LMGP, UMR 5628, 3 Parvis Louis Néel, 38016 Grenoble

³ INSERM U1209, CNRS 5309, Université de Grenoble Alpes, Institut for Advanced Biosciences, Institut Albert Bonniot, Allée des Alpes, Site Santé, 38700 La Tronche, France

4. Institut Universitaire de France (IUF)

* Co-second authors

co-corresponding authors: Adrià Sales, Catherine Picart

E-mail: adria.salesramos@cea.fr ; catherine.picart@cea.fr

Keywords: biomimetic films; stiffness; adhesion; differentiation; BMPs; integrins.

Abstract

Whereas soft biomaterial is not able to induce cell spreading, BMP-2 presented by a soft film has been described to be sufficient to trigger cell spreading, migration and downstream BMP-2 signaling. Based on thin polyelectrolyte films of controlled stiffness, we investigated whether the presentation of four BMP members (2, 4, 7, 9) in a matrix-bound manner may differentially impact cell adhesion and bone differentiation of skeletal progenitors. We performed high content and automated screening of cellular responses, including cell number, cell spreading area, SMAD phosphorylation and alkaline phosphatase activity. The basolateral presentation of the different BMPs allowed us to discriminate the specificity of cellular response and the role of BMP receptors type I, type II, as well as three β integrins, in a BMP type and stiffness-dependent manner.

1. Introduction

Bone morphogenetic proteins (BMPs) belong to the transforming growth factor β superfamily (Massagué, 2000) and are known to participate in a large number of physiological and pathological processes, including cell growth and differentiation (Wagner *et al.*, 2010), tissue development (Salazar, Gamer and Rosen, 2016), as well as cancerous processes (Ehata *et al.*, 2013; Jiramongkolchai, Owens and Hong, 2016). BMP signaling, which is mediated via BMP type I and type II receptors, involves different pathways usually described as SMAD or non-SMAD, and is dependent on the mechanical context of the cell environment (da Silva Madaleno, Jatzlau and Knaus, 2020). BMP signaling pathway is under the control of multiple ligands binding two type I and two type II receptors that interact combinatorically to form distinct receptor-ligand complexes (Antebi *et al.*, 2017). In addition, the repertoire of BMP ligands and of BMP receptors is cell- and tissue-dependent context (Morikawa, Derynck and Miyazono, 2016).

BMPs can either be diffusible molecules or be presented by extracellular matrix (ECM) components (Sedlmeier and Sleeman, 2017). It is known that BMP-mediated signaling depends on the duration of exposure to BMPs and on their spatial localization (Ramel and Hill, 2013; Zhang *et al.*, 2019). A sustained presentation of the BMP ligands can be obtained using biomaterials such as a collagen (Yamachika *et al.*, 2008), a poly(ethyl acrylate) polymer (Llopis-Hernández *et al.*, 2016), or a polyelectrolyte film containing hyaluronic acid and poly(L-lysine) (Crouzier *et al.*, 2009).

Beside their role in cell differentiation, BMPs appear to induce cell spreading and they also appear to control cytoskeleton organization and cell migration (Gamell *et al.*, 2008; Khurana *et al.*, 2013). Increasing evidences highlight a role of BMPs in mechanotransduction (Morrell *et al.*, 2016; da Silva Madaleno, Jatzlau and Knaus, 2020; Migliorini *et al.*, 2020). Mechanotransduction via the ECM is known to involve the adhesion receptors integrins and to be sensitive to matrix stiffness (Hynes, 2009; Tenney and Discher, 2009). Indeed, BMP signaling can be modulated by integrins (Ashe, 2016), matrix stiffness and cytoskeletal tension (Wei *et al.*, 2020).

We have previously shown that a biomimetic material presenting BMP-2 in a matrix-bound manner (bBMP-2) can be used to control stem cell fate *in vitro* (Crouzier, Fourel, *et al.*, 2011; Machillot *et al.*, 2018) and *in vivo* to repair critical-sized bone defects (Bouyer *et al.*, 2016). We have also shown that bBMP-2 presented from a soft film was sufficient to trigger cell spreading and migration (Fourel *et al.*, 2016), overriding the response to film stiffness. The

same effect has been shown on rigid surfaces with a low cRGD surface density (Sefkow-Werner *et al.*, 2020) and on surfaces presenting peptides specific for $\alpha 5\beta 1$ integrins (Posa *et al.*, 2021). This process on soft films involved $\beta 3$ integrins and BMP receptors that worked together to control SMAD signaling and tensional homeostasis (Fourel *et al.*, 2016), thereby coupling cell adhesion and fate commitment. Whether other BMPs are able to induce BMP receptor-integrin crosstalk is poorly known. For instance, BMP-4, which is involved in hematopoiesis, leukemias and cancers (Toofan and Wheadon, 2016), is known to induce the expression of $\alpha 4$ -integrin (Khurana *et al.*, 2013). BMP-7 plays a major role in fibrosis, kidney disease and is involved in the adhesion and migration of human monocytic cells (Sovershaev *et al.*, 2016). BMP-9 is involved in cardiovascular diseases and anemia (Morrell *et al.*, 2016). It also increases cell proliferation on bone grafts (Fujioka-Kobayashi *et al.*, 2017), but its overexpression decreases cell adhesion and migration (Ye, Kynaston and Jiang, 2008). However, whether the signaling induced by BMPs is stiffness-dependent, is still elusive.

Recently, we have developed an automated process to deposit the polyelectrolyte films in various multiwell plate formats, especially 96-well microplates (Machillot *et al.*, 2018). Interestingly, such film-coated microwells enable to study a large number of experimental conditions in parallel. In addition, multiwell plates are compatible with automated methods to quantify cellular processes using plate readers and automated imaging systems.

In this study, four BMPs including BMP-2, -4, -7 and -9 were selected in view of their physiological importance such as skeletal formation, involvement in cardiovascular diseases, cancers, hematopoiesis and leukemias (Wagner *et al.*, 2010; Jiramongkolchai, Owens and Hong, 2016; Morrell *et al.*, 2016; Toofan and Wheadon, 2016). All four BMPs have an osteogenic potential *in vitro* (Rivera *et al.*, 2013). We varied film stiffness to assess the combined effect of bBMP type and substrate mechanics on cell adhesion and differentiation. As BMP-responsive cells, we selected C2C12 skeletal myoblasts (Rivera *et al.*, 2013; Gilde *et al.*, 2016) and human periosteum-derived stem cells (hPDSCs) (Roberts *et al.*, 2011; Duchamp De Lageneste *et al.*, 2018) in view of their physiological relevance for bone regeneration and known sensitivity to a large number of BMPs, including these four BMPs (Rivera *et al.*, 2013; Bolander *et al.*, 2016). We directly compared the effect of the four selected BMPs, on stem cell adhesion and early bone differentiation in response to increasing doses of bBMPs presented by the polyelectrolyte film. Cell adhesion, assessed by the number of adherent cells and the cell spreading area, and early bone differentiation, assessed by quantifying SMAD phosphorylation and alkaline phosphatase (ALP) activation, were quantified in an automated manner. Finally, by means of silencing RNA against the type I and II BMP receptors and against three selected

β integrins, we identify the roles of each BMP receptor and integrins in cell adhesion, SMAD signaling and ALP expression in BMP ligand- and film stiffness-dependent context.

2. Materials and Methods

2.1. Polyelectrolyte film buildup, crosslinking and BMPs loading. Poly(L-lysine) hydrobromide (PLL) and poly(ethylene imine) (PEI) were purchased at Sigma-Alrich (St Quentin Fallavier, France), and hyaluronic acid (HA) at Lifecore medical (USA). PLL and HA were dissolved in a HEPES-NaCl buffer (20 mM HEPES and 0.15 M NaCl at pH 7.4) at 0.5 mg/mL. PEI was dissolved in a NaCl 0.15 M solution at pH ~6.5, at 4 mg/mL. A first layer of PEI was always deposited. All rinsing steps were performed with 0.15 M NaCl at pH ~6.5. LbL films were directly deposited in 96-well cell culture microplates (Greiner bio-one, Germany) using an automated liquid handling robot (TECAN Freedom EVO® 100, Tecan France, Lyon) and a custom-made macro (Machillot *et al.*, 2018). The films were then chemically crosslinked using 1-Ethyl-3-(3-Dimethylamino-propyl)Carbodiimide (EDC) at a final concentration of 30 or 70 mg/mL, and N-Hydrosulfosuccinimide sodium salt (Sulfo-NHS) at a concentration of 11 mg/mL as catalyzer, as previously described (Schneider *et al.*, 2006; Crouzier, Sailhan, *et al.*, 2011). BMP loading in the films was done following an established protocol (Crouzier *et al.*, 2009). BMP-2 was purchased from Bioventus (France), BMP-4 and -9 from Peprotech (France) and BMP-7 from Olympus Biotech (France).

2.2. Cell culture, and quantification of stem cell adhesion, spreading and differentiation.

We used two types of BMP-responsive cells, C2C12 skeletal myoblasts (Crouzier *et al.*, 2009) and periosteum-derived stem cells (hPDSCs) (Bolander *et al.*, 2016) to assess the bioactivity of the biomimetic coatings at high content. C2C12 skeletal myoblasts (<15 passages, obtained from the American Type Culture Collection, ATCC) and hPDSC (<12 passages, obtained from F. Luyten) were cultured as previously described (Crouzier *et al.*, 2009; Bolander *et al.*, 2016) in tissue culture flasks, in a 1:1 Dulbecco's Modified Eagle Medium (DMEM):Ham's F12 medium (Gibco, Life Technologies, France) for C2C12 and in high-glucose Dulbecco's modified Eagle's medium (high DMEM) + pyruvate for hPDSC (Gibco, Life Technologies, France), supplemented with 10% fetal bovine serum (FBS, Gibco, Life TechnologiesFrance) and 1% penicillin/streptomycin (Gibco, Life Technologies, France) in a 37 °C, 5% CO₂ incubator. For analysis of cell adhesion, spreading and pSMAD, 8300 cells/cm² of C2C12 and 7000 cells/cm² of hPDSCs were seeded in each well. For analysis of ALP, 33000 cells/cm² of

C2C12 were seeded in each well. For quantification of cell adhesion and spreading, cells were cultured for 4 or 5 h and then fixed with 4% paraformaldehyde. Nuclei were stained with 4',6-diamidino-2-phenylindole (DAPI) (Invitrogen, Thermofisher Scientific, France) and the actin cytoskeleton with Alexa Fluor 633-phalloidin (Thermofisher Scientific, France). For quantification of cell differentiation, C2C12 cells were stained at 4 or 5 h for pSMAD analysis, and after 3 days of culture for ALP analysis. pSMAD was stained by using a 1:400 dilution of an antibody anti-pSMAD 1,5,9 (Cell Signaling, ref: 13820S) or a 1:800 dilution of an antibody anti-pSMAD 2 (Cell Signaling, ref: 18338S) both diluted in a solution of bovine serum albumin (BSA, Sigma-Aldrich, Merck, Germany) 3% w/v in PBS. A secondary antibody conjugated to Alexa Fluor 555 (Invitrogen, Thermofisher Scientific, France) diluted at 1:500 in BSA 3% w/v in PBS, was used for both SMAD markers since they were always analyzed in different samples. ALP was stained by using fast blue RR salt (Sigma-Aldrich, Merck, Germany) in a 0.01 % (w/v) naphthol AS-MX solution (Sigma Aldrich, Merck, Germany), according to the manufacturer's instructions. ALP was imaged using a scanner and quantified using a TECAN Infinite 1000 microplate reader (TECAN France, Lyon) by measuring the absorbance at 570 nm using the multiple-read/well mode (Machillot *et al.*, 2018). The mean value of 76 measured different positions per microwell was taken.

For the quantification of immunofluorescence stainings, a GE INCA 2500 imaging system (General Electrics Healthcare, France) was used with an inverted 20X objective (Plan Apo N.A.=0.75, Nikon, Japan). 21 images distributed over the well were acquired and, generally, at least 100 cells were analyzed par well and plate. Between 2 and 4 independent experiments (biological replicates) were performed with 2 technical replicates per experiment, making up a total of, generally, at least 400 cells per condition. For comparison of pSMAD 1,5,9 and pSMAD 2 fluorescent signal, the same exposure time was always used for each marker, which was different between both markers.

For image analysis, InCarta software (General Electrics Healthcare, USA) was used to automatically segment nuclei and cells, and to quantify cell number, cell area and pSMAD signal intensity.

For quantitative analysis of the BMP dose-response experiments, the data were fitted with an exponential function:

$$= A_{\max} (1 - \exp(-[BMP]/Cc))$$

Where C_c is the characteristic concentration, and A_{\max} is the plateau value (in number of cells /mm² for the cell number, and in μm^2 for the cell area). In some cases where the curve decayed after reaching a maximum, only the ascending part of the curve was fitted.

In the BMP dose-response experiments, Δ_{\max} was calculated by subtracting the maximum value by the value corresponding to the control condition without BMP.

2.3. Expression of BMP and integrin receptors. Expression of BMP type I, type II and integrin receptors was investigated by mRNA transcript analysis. Total RNA from expanded C2C12 and hPDSCs was extracted by lysing cells in lysis buffer supplemented with β -mercaptoethanol. Further RNA extraction was performed using the RNeasy kit (Qiagen) according to the manufacturer's instructions. Complementary DNA (cDNA) was obtained by reverse transcription of total RNA with Oligo (dT)20 as primer (Superscript III; Invitrogen, Thermofisher Scientific, France). Quantitative PCR was performed in duplicates with a thermocycler (MX4800P; Agilent Technologies, France) as previously described (Fourel *et al.*, 2016) using the SYBER green kit. The primer sequences are given in **Table SI 2**. Primer efficiency was established by a standard curve using sequential dilutions of gene-specific PCR fragments. Data were normalized from the quantitative RT-PCR housekeeping genes EF1, Gusb, and PPIA as an index of cDNA content after reverse transcription.

2.4. SiRNA interference. Cells were transfected with siRNA against β 1, β 3 or β 5 integrins, BMP receptors type I (ALK2, ALK3, ALK5, ALK6), BMP receptors type II (BMPR-II, ACTR-IIA, ACTR-IIB) (ON-TARGET plus SMART pool; respectively, mouse ITGB1, ITGB3, ITGB5, ALK2, ALK3, ALK5, ALK6, BMPR-II, ACTR-IIA, ACTR-IIB) (Dharmacon, France). The gene target siRNA sequences used for transfection are listed in **Table SI 3**. A scrambled siRNA (Dharmacon, France) was taken as control. Cells were seeded at 5,000 cells/cm² in 12-well plates and cultured in 1 ml of GM with 0.5% of antibiotics for 24 h. The transfection mix was prepared as follows: For one well, 2.8 μ l of Lipofectamine RNAiMAX Reagent (Invitrogen, Thermofisher Scientific, France) was added to 60 μ l of Opti-MEM medium (Gibco, Life Technologies, France) and 1.2 μ l of 16.67 μ M siRNA, diluted in RNase free water (5 Prime) was added to another 60 μ l Opti-MEM medium. Lipofectamine-containing mix was added to siRNA-containing mix and incubated for 20 min at RT. Then, 120 μ l of the final mix was added to each well. After 24 h of incubation at 37°C, the cells were transfected for the second time and incubated for another 24 h. The cells were then detached with 0.25% trypsin-EDTA (Gibco, Life Technologies, France), seeded in GM on the films, and allowed to adhere.

2.5. Data representation and statistical analysis: For box plots, the box shows 25, 50 and 75% percentiles, the square shows the mean value and the error bars correspond to the standard deviation. For scatter plots and bar plots, the mean values and the standard error of the mean

(SEM) are represented. Experiments were performed in duplicate, triplicate, or quadruplicate (biological replicates) with 2 wells per condition (technical replicate) in each experiment. Statistical analysis was performed using the non-parametric analysis Kruskal-Wallis analysis of variance (K-W ANOVA) to obtain p values ($p < 0.05$ was considered significant).

In the adhesion and spreading experiments, the mean values of cell number and cell area were obtained by averaging all the values for all the wells (technical and biological replicates). To calculate the mean value of pSMAD signal, first the average of all values per well was calculated, then the average of all wells from all the experiments was calculated. In the ALP experiments, the mean value was obtained by averaging the mean absorbance values of each well from all the experiments. In the knockdown experiments, the relative values were calculated by first averaging all the mean values per well from all the experiments, then normalizing the values by the scrambled condition.

3. Results

3.1. Cell adhesion and spreading of C2C12 and hPDSCs are induced in a BMP-specific and stiffness-dependent manner.

To investigate whether the film stiffness may affect the effect induced by the four BMPs, namely BMP-2, -4, -7 and -9, in early cell adhesion and spreading we bound them non-covalently to a polyelectrolyte film of controlled stiffness made of poly(L-lysine) (PLL) and hyaluronic acid (HA) (Crouzier *et al.*, 2009)(Fourel *et al.*, 2016)(Schneider *et al.*, 2006). The polyelectrolyte films were crosslinked to different levels using a crosslinker EDC, as previously described (Schneider *et al.*, 2006), which leads to low and high crosslinked films (EDC30 and EDC70, respectively), named hereafter for simplicity soft (S) and rigid (R) films. Their stiffness corresponds to ~200 kPa (soft) and ~400 kPa (rigid) (Schneider *et al.*, 2006). The amounts of the four BMPs loaded in the films were quantified (**Table SI 1**). BMP-2, -4, -7, and -9 could all be loaded in the films at 65 to 95% of the loading concentration depending on the BMP type, with only slight stiffness-differences. Surprisingly, BMP-9, which is known to be found circulating in plasma in soluble form (Bidart *et al.*, 2012), was well bound to the matrix, with incorporation percentages of 92 and 88% on soft and rigid films, respectively. Thus, the four BMPs could be presented to cells in a matrix-bound manner (bBMPs).

Cells were fixed and analyzed 4-5 h after cell seeding to enable cell adhesion and spreading on the soft and stiff films. Both cell processes are usually slower on the films than on tissue culture polystyrene or glass, both of which are orders of magnitude stiffer than the films (Crouzier,

Fourel, *et al.*, 2011). Soluble BMPs (sBMPs) in the cell culture medium were used as control, at a constant concentration of 200 ng/ml, which is considered as a high concentration (Crouzier, Fourel, *et al.*, 2011).

Cells were cultured on soft and rigid films with increasing concentrations of bBMPs, obtained by loading the films with BMP solutions from 0 to 20 $\mu\text{g/mL}$. Representative images of cell adhesion are given in **Fig. 1A** and **Fig. SI 1**, together with the quantification of the number of adherent cells (**Fig. 1B**) and cell spreading areas (**Fig. 1C**). At first sight, it appears that the cells adhere and spread on all bBMPs in a concentration-dependent and stiffness-dependent manner, whatever the bBMPs, except on soft films with bBMP-9. After quantitative analysis, we observe that cell number and cell area values are generally higher on rigid films than on soft ones (**Fig. 1B** and **C**). However, on the non-BMP condition, this increase is only observed for cell number but not for cell spreading.

The quantified data were fitted with an exponential function toward a plateau value (see *Methods*) and two quantitative parameters were extracted: Δ_{max} (difference between the highest value and value for the no BMP condition) and $1/C_c$ (**Fig. 1D-G**). C_c (in $\mu\text{g/mL}$) corresponds to the characteristic concentration extracted from the exponential fit of the data. It corresponds approximately to the BMP concentration when half of the plateau value is reached. $1/C_c$ provides a direct quantification of the cell sensitivity to bBMPs: the higher it is, the higher is the sensitivity to a given bBMP. Regarding Δ_{max} , the higher it is, the stronger is the effect for a given BMP.

The increase in cell number (Δ_{max}) was stiffness-dependent for bBMP-4 and -7, being higher on soft than on rigid films (**Fig. 1D**). In cell area, this same parameter was found to be stiffness-dependent for all the bBMPs. However, the increase in cell area was always higher on rigid films than on soft ones (**Fig. 1F**). Regarding the sensitivity parameter ($1/C_c$), it was stiffness-sensitive for bBMP-2 and -4 in cell number (**Fig. 1E**), and for bBMP-2, -4 and -7 in cell area (**Fig. 1G**), being in all cases higher on rigid films than on soft ones. However, a rather large standard deviation was found for bBMP-7 sensitivity parameter on cell area. bBMP-9, in particular, only helped increasing adhesion and spreading on rigid films and no response was observed on soft ones at this time scale (**Fig. 1B** and **D**), indicating a smaller role on adhesion and spreading of this bBMP in comparison to the others.

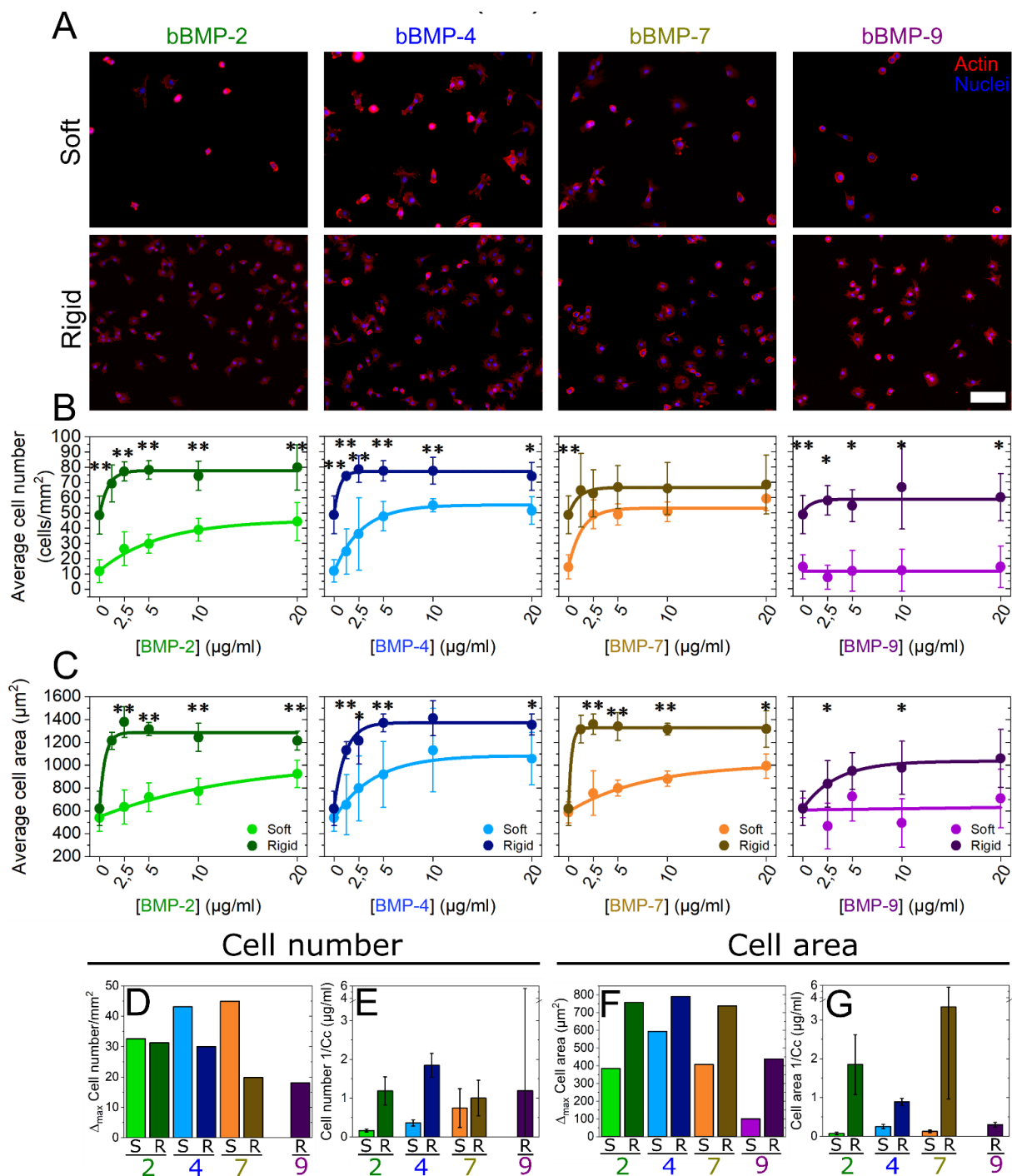


Fig. 1. Quantification of C2C12 cell adhesion and spreading on soft and rigid films with four bBMPs (2, 4, 7, 9) at increasing BMP-loading concentrations. Representative fluorescent images of the actin cytoskeleton for (a) cells cultured for 5 h on soft films (S) and for 4 h on rigid films (R). Images correspond to a BMP loading concentration in solution of 5 µg/mL. Quantification of (b) the average cell number per mm² of substrate area and (c) the cell area as a function of the initial BMP concentration in the loading solution. Results of the data fitting for each BMP-dose response curve (see methods) gave two parameters: Δ_{\max} and Cc (characteristic concentration). (d) Difference (Δ_{\max}) between the maximum cell number and the no bBMP condition, plotted for each of the 4 bBMPs and film stiffness (S, R films). (e) Sensitivity to the BMP concentration (given as 1/Cc that provides a direct information on the sensitivity to the bBMP concentration). (f and g) Same quantitative parameters extracted for the cell spreading area in response to the bBMP-dose. Data represent three independent

biological replicates with two microwells per condition in each independent experiment (technical replicates). Statistical tests were done using non-parametric Kruskal-Wallis ANOVA test to compare S (light color) and R (dark color) films (*p < 0.05; **p < 0.01). Scale bar=100 μm .

Interestingly, plotting the data in relative percentage compared to the no BMP condition, further highlighted the fact that soft films with bBMPs had a stronger role on cell adhesion than rigid films, while rigid films with bBMPs had a stronger role on cell spreading (**Fig. SI 2**). Soluble BMPs (sBMPs) added on cells cultured in the same experimental conditions than with bBMPs, only had an effect increasing cell area on rigid films with sBMP-2 (**Fig. SI 3**), confirming that bBMPs amplify cell adhesive response.

The adhesive response of hPDSCs (**Fig. SI 4 and SI 5**) was qualitatively and quantitatively similar to that of C2C12 myoblasts. However, we noted some differences: regarding the Δ_{max} value, cell adhesion was stiffness-dependent for all four BMPs (**Fig. SI 3**) while the cell area was only stiffness-dependent for bBMP-4 and higher on soft than on rigid films (**Fig. SI 3G**). Regarding the kinetics, faster adhesion kinetics were observed on rigid films with bBMP-7 in comparison to soft ones (**Fig. SI 3F and H**), while no stiffness-dependent differences were observed on C2C12 cells. We also noted that, on rigid films with bBMP-2, bBMP-7, and to a lesser extent with bBMP-4, the cell number and cell area values, decreased after reaching the maximum value, showing a dual response of hPDSCs to high bBMP concentrations. Finally, on bBMP-9, contrary to C2C12 cells, very small adhesion could be measured on soft films (**Fig. SI 3B**). As with C2C12, data in relative percentage further highlighted the fact that soft films with bBMPs had a strong role of both cell adhesion and spreading of hPDSCs (**Fig. SI 5**). Here again, this effect was specific to bBMPs since sBMPs only had an influence increasing cell area on rigid films with sBMP-2 (**Fig. SI 6**).

Altogether, our data showed that the four studied bBMPs positively act either on the cell number, on the spreading area or both. There is BMP-specific response to film stiffness. The increase in cell number thanks to bBMPs was stronger on soft films than on rigid ones, notably for BMP-4 and -7, while cell area was more strongly enhanced by bBMPs on rigid than soft films. In general, cells respond faster, in terms of adhesion and spreading, on rigid films than soft ones. Similar behaviors were observed between C2C12 cells and hPDSCs.

3.2. Early stem cell differentiation in bone is BMP-specific and stiffness-dependent.

SMAD 1,5,9 is a transcription factor known to play a key role in the transduction pathway from BMP receptors to the nucleus (Sieber *et al.*, 2009) and its phosphorylation is often taken as

readout of early cell differentiation (Sieber *et al.*, 2009). While SMAD 2,3 is described as being triggered mainly by TGF- β s and activins (Yadin, Knaus and Mueller, 2016), it was also shown to be triggered by sBMPs (Holtzhausen *et al.*, 2014). We decided to include it in our study and quantify the phosphorylation of the nuclear translocated SMAD 2. One of the markers for the so-called non-canonical pathway is the induction of alkaline phosphatase (ALP) (Sieber *et al.*, 2009), which is often taken as later osteogenic readout (Rivera *et al.*, 2013).

We then studied the phosphorylation and nuclear translocation of SMAD 1,5,9 and SMAD 2 after 4-5 h of culture on the films with increasing BMP concentrations (**Fig. 2**, **Fig. SI 8**). In order to avoid differences in fluorescent signal intensity between experiments, we normalized the fluorescent signals of pSMAD 1,5,9 and pSMAD 2 of each experiment by the non-BMP condition (**Fig. 2A** and **D**). Not-normalized data is shown in **Fig. SI 8**. Representative examples of pSMAD fluorescent signal values distribution, together with representative pictures of C2C12 cells presenting low and high pSMAD signals, are shown in **Fig. SI 7**.

After fitting the curves, as we did with cell adhesion and spreading, and extracting the parameters Δ_{\max} and $1/Cc$, we observed that, for pSMAD 1,5,9 Δ_{\max} value was higher on soft than on rigid films with bBMP-2, -4 and -7 (**Fig. 2B**). The sensitivity value ($1/Cc$) instead, was higher on soft than on rigid films with bBMP-2 and -4, but it was stiffness-independent for bBMP-7, which gave the lowest sensitivity. Nevertheless, attention should be paid due to big error bars (**Fig. 2C**). Curiously, at lower bBMP-7 concentrations on rigid films, the pSMAD 1,5,9 values were below that of the non-BMP condition (**Fig. 2A** and **SI 8A**). Regarding bBMP-9, the cell response could solely be measured for cells cultured on stiff films, since C2C12 cells were barely adhering after 5 h on the soft films. bBMP-9 induced a high pSMAD 1,5,9 response (**Fig. 2A** and **SI 8A**), with a high sensitivity (**Fig. 2C**). To note, pSMAD 1,5,9 response to sBMPs was solely increased for cells on stiff films with sBMP-2 and 9 (**Fig. SI 9**).

pSMAD 2 signal was stiffness-independent in all conditions except for cell sensitivity parameter ($1/Cc$) with bBMP-4, where soft films induced a higher sensitivity than rigid ones. However, the error bar in this condition was big (**Fig. 2F**). bBMP-9 triggered the strongest pSMAD 2 signal, followed by bBMP-2 (**Fig. 2D-F** and **Fig. SI 8B**). bBMP-4 induced a higher pSMAD 2 than pSMAD 1,5,9 signal in terms of Δ_{\max} on both film rigidities (**Fig. 2E**), and sensitivity only on rigid films (**Fig. 2F**). Similarly, to pSMAD 1,5,9, at low concentrations bBMP-7 induced slightly smaller pSMAD 2 signal values than the control, but on soft films instead (**Fig. 2D** and **Fig. SI 8B**).

The ALP response of C2C12 cells was quantified after 3 days of culture (Machillot *et al.*, 2018). The results corresponding to rigid films were extracted and adapted from P. Machillot *et al.* (Machillot *et al.*, 2018). Here, cells on soft films with bBMP-9 could be analyzed, since they could better adhere after 3 days of culture. bBMP-2 and bBMP-9 exhibited a strong stiffness-dependent response, with a significantly higher ALP activation on rigid films than on soft ones (Fig. 2G-I and Fig. SI 10). Conversely, the ALP response to bBMP-4 and -7 was very high for both soft and stiff films with only little stiffness-dependence (Fig. 2G-I). The ALP response to bBMP-4 and -7 on soft films was also higher than that to bBMP-2 and -9. Generally, for the ALP response, the sensitivity of cells to bBMPs was higher on rigid films (Fig. 2I). Altogether, our data for C2C12 cells showed BMP-specific and stiffness-dependent responses. For bBMP-2, ALP response was stiffness-dependent, and to a less extent pSMAD 1,5,9 signal. bBMP-4 induced a strong ALP response whatever the film stiffness, and to a less extent pSMAD 1,5,9 and pSMAD 2 signals. bBMP-7 also strongly activated ALP, to a lesser extent pSMAD 1,5,9 and even less pSMAD 2. Lastly, bBMP-9 induced the highest SMAD response from all the four BMPs, and a high ALP response.

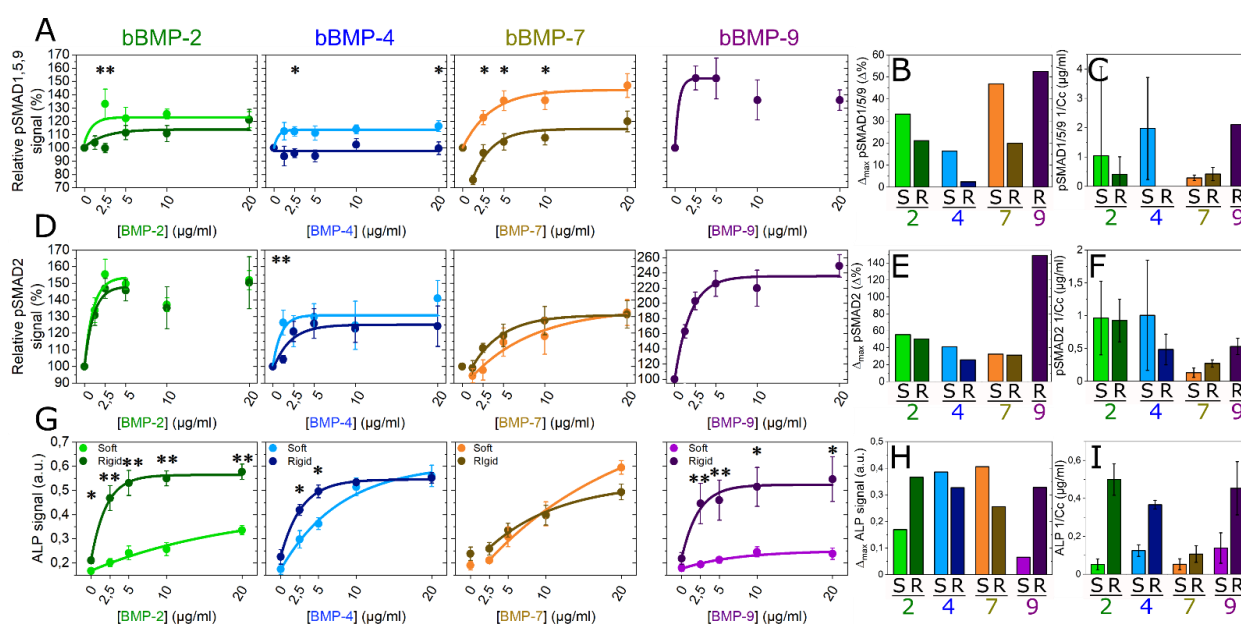


Fig. 2. pSMAD and ALP analyses for the four bBMPs on soft and rigid films. Fluorescent signal quantification of (a) pSMAD 1,5,9, (d) pSMAD 2, and (g) ALP activity as a function of the BMP concentration in soft (S) (light color) and rigid (R) films (dark color). Quantitative parameters Δ_{\max} and $1/Cc$ extracted from the fit of each of the experimental curves for (b, c) pSMAD 1,5,9, (e, f) pSMAD 2 and (h, i) ALP. Data represent the mean \pm SEM of 2 to 4 independent experiments with two samples per condition in each independent experiment (at least 400 cells were analyzed in total). Statistical tests were done using non-parametric Kruskal-Wallis ANOVA test to compare S and R films (* $p < 0.05$; ** $p < 0.01$).

3.3. Involvement of BMP receptors and integrins in the cell adhesive response

Having evidenced that bBMPs can act as adhesive molecules to trigger myoblast and periosteum stem cell adhesion and spreading, we aimed to unravel the specific role of the BMP receptors and of integrins in the cell adhesive response. Firstly, an *in silico* screening was performed using RNA sequencing data from UCSC genome browser (Encode database). Thus, we identified the adhesion receptors expressed in C2C12 cells and expressed their relative abundance by quantifying the percentage (**Fig. SI 11**). We then verified the expression level of the BMP receptors (BMPR) and integrins of C2C12 myoblasts and hPDSCs using quantitative PCR (**Fig. 3A and B**). For C2C12 myoblasts, mRNA transcripts for the type I BMPR, ALK2, ALK3 and ALK5 were detected. ALK1, ALK4 and ALK6 were expressed at a much lower level. For the type II BMP receptors, BMPR-II, ACTR-IIA and to a much lower extent ACTR-IIB were detected. Regarding integrins, in both cell types $\beta 1$ was the most highly expressed followed by $\beta 5$ and $\beta 3$. For hPDSCs, the similar BMP type I, II and integrins were detected, although their expression was quantitatively lower.

Next, we quantified the molecular interactions between the four BMPs and the BMP receptors type I and II using reflectometric interference spectroscopy with the commercially-available biolayer interferometry setup. We obtained the affinity constants (Kd) values for each BMP-BMP receptor couple (**Fig. 3C**), as recently shown in Khodr *et al.* (Valia Khodr, Paul Machillot, Elisa Migliorini, Jean-Baptiste Reiser, 2020). Confirming the literature data (Ehata *et al.*, 2013), BMP-2 and BMP-4 exhibited high affinity for ALK3 and ALK6. BMP-7 exhibited a different behavior since it has the highest affinity for ACTR-IIA and has a moderate, non-specific affinity for all ALK receptors. BMP-9 had the strongest affinity for ALK1 and a similar affinity for the three type II receptors. We did not consider ALK4 for this study since it is an activin receptor and no evidence was found in the literature regarding a possible interaction with BMPs.

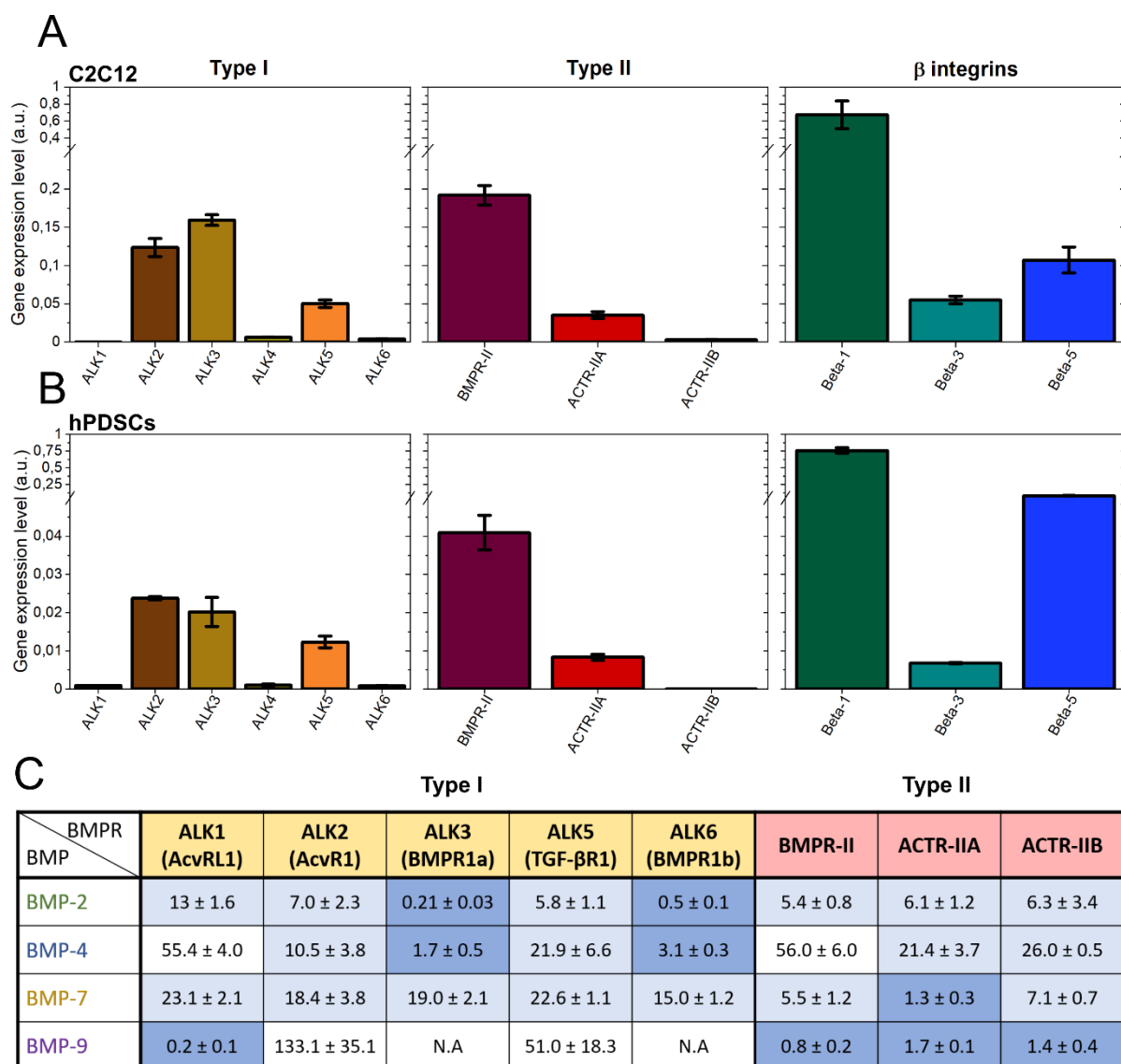


Fig. 3. Relative gene expression analysis of type I, type II BMP receptors and β -integrins. Data corresponding to (a) C2C12 cells and to (b) hPDSCs. The gene expression was analyzed by qPCR and it was normalized to the expression of EF1, PPIA and GUSB genes. Data are represented as mean \pm SEM of three independent experiments. (c) Table of the affinity constants (K_d in nM) of the type I and II BMP receptors with the four selected BMPs. Data was obtained from kinetic experiments performed by bio-layer interferometry (BLI), from the work of Khodr *et al.* (Valia Khodr, Paul Machillot, Elisa Migliorini, Jean-Baptiste Reiser, 2020). The highest affinity couples ($K_d < 5$ nM) are highlighted in dark blue, those with an affinity in the range from 5 to 25 nM are in light blue. N.A means no measurable interaction. Values are given as mean \pm SD of three independent experiments.

In order to assess the specific role of each receptor, type I (ALK2, 3, 5 and 6) and type II BMP receptors (BMPR-II, ACTR-IIA, ACTR-IIB), as well as β integrins (1, 3 and 5) were silenced using siRNA. The efficacy of the silencing was first verified (Fig. SI 12). The cell number and cell spreading area were analyzed on one particular BMP concentration (20 μ g/ml), normalized by the scrambled control condition and averaged, to reveal the contribution of each receptor (Fig. 4 and Fig. SI 13). Non-normalized raw data are plotted in Fig. SI 14.

Among the ALK receptors, on the non-BMP condition, ALK3 enhanced cell adhesion and spreading, while ALK6 promoted adhesion but inhibits spreading (**Fig. SI 13**). The same response was observed on films with bBMPs, with some particularities: ALK3 role on adhesion is stiffness-dependent with bBMP-4, and ALK6 induces adhesion only on rigid films but not on soft ones (**Fig. 4**). Notably, the response of ALK2 to bBMP-2 was mechano-sensitive regarding the cell spreading area. ALK5 was involved in a mechano-sensitive cell adhesion on bBMP-4 and -7, being an inhibitor on soft films and an activator on rigid ones (**Fig. 4A** and **Fig. SI 14A**). It was also mechano-sensitive for cell spreading on bBMP-2, being activator on soft films and no role on rigid films (**Fig. 4B**).

Regarding type II BMP receptors, mainly BMPR-II and ACTR-IIA played a certain role in adhesion and spreading. On the non-BMP condition, both receptors induced adhesion, while BMPR-II inhibited spreading and ACTR-IIA activated it (**Fig. SI 13**). On films with bBMPs, BMPR-II was a slight inhibitor of cell spreading, but a strong activator of cell adhesion on soft films with bBMP-2. ACTR-IIA was mechano-sensitive, being an inhibitor of cell adhesion on soft films with bBMP-4 and -7, and activator on rigid films in response to all BMPs. It had a minor role on cell spreading, except for rigid films with bBMP-9 where it induced cell spreading (**Fig. 4**).

With respect to integrins, $\beta 3$ integrin had an important and consistent role in activating both cell adhesion and spreading, independently of film stiffness and of the BMP presence. The role of $\beta 1$ integrin was generally comparable to that of $\beta 3$. $\beta 1$ integrin was also involved in a mechano-sensitive response to bBMP-7, acting as an inhibitor of cell adhesion on soft films, and an activator on rigid ones. Lastly, $\beta 5$ integrin was involved in a mechano-sensitive cell response to bBMP-2: it was an inhibitor of cell adhesion on soft films and no role on rigid ones. $\beta 5$ integrin was an inhibitor of cell spreading on bBMP-2 and -4, on both film stiffness, and on soft films with bBMP-7 (**Fig. 4** and **Fig. SI 13**).

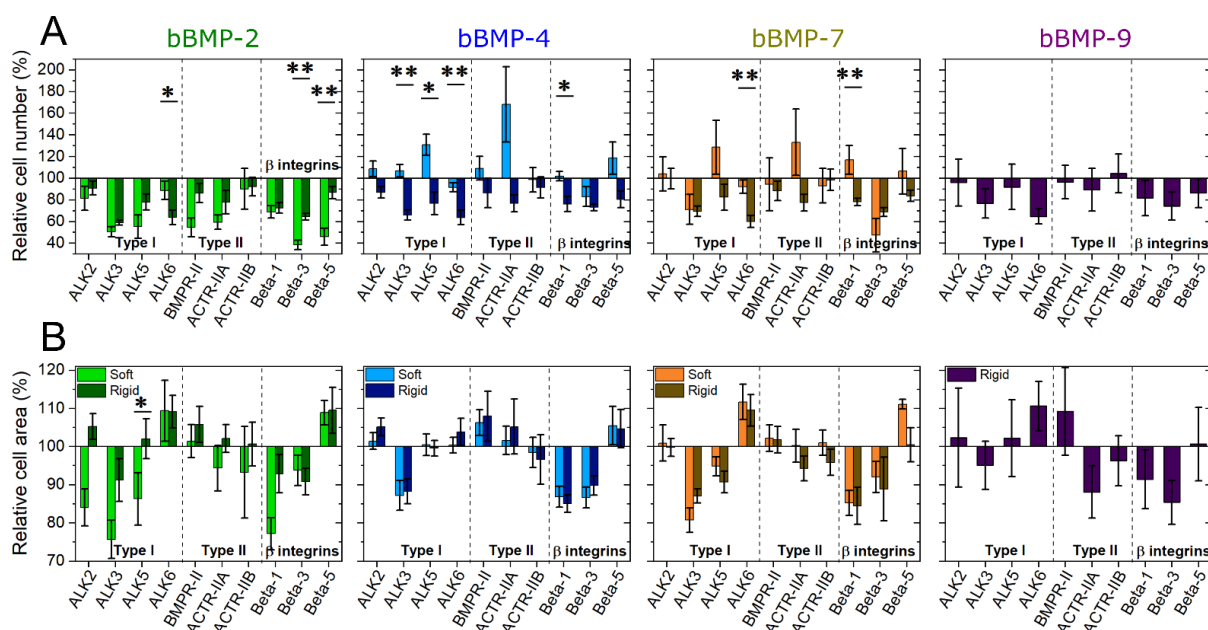


Fig. 4. Effect of BMP receptor and β chain integrin silencing on cell adhesion and spreading. C2C12 cells were transfected with siRNA against BMP receptor type I (ALK2, ALK3, ALK5, ALK6), BMP receptor type II (BMPR-II, ACTR-IIA, ACTR-IIB) and β chain integrins (β 1, β 3, β 5) and plated on soft (light color) and rigid (dark color) films with bBMPs for 5 or 4 h, respectively. The cell number per mm^2 of substrate area and the spreading area were quantified. The relative % is given, in comparison to a control scrambled siRNA. (a) Relative cell number (%), (b) relative cell area (%). Data represent the mean \pm SEM, with 3 biological replicates and 2 technical replicates per experiment. Statistical tests were done using non-parametric Kruskal-Wallis ANOVA test (*, $p \leq 0.05$; **, $p \leq 0.01$). Statistical comparisons were made between soft and rigid films for each condition.

3.4. Involvement of BMP receptors and integrins in early cell differentiation to bone

The effect of receptor silencing on early osteogenic differentiation was also investigated for pSMADs and ALP activity (Fig. 5 and Fig. SI 15). Non-normalized raw data are plotted in Fig. SI 16.

Regarding pSMAD 1,5,9, ALK2 exhibited an important role for all BMPs in a non-specific manner. ALK3 revealed to have a BMP-specific role: it is an activator for bBMP-4 and an inhibitor for bBMP-7 and -9. ALK6 was an activator of pSMAD 1,5,9 on all bBMPs. ALK5 had only a minor inhibiting role for bBMP-2, -4 and -7, which was more visible on soft films than rigid ones (Fig. 5A).

With respect to the BMPR type II receptors, BMPR-II was an important and a non-specific activator for all BMPs on both film stiffness, as well as for the no BMP condition (Fig. 5A and Fig. SI 15A), while ACTR-IIA was an activator of the pSMAD 1,5,9 response to bBMP-7, independently of film stiffness.

Lastly, β integrins were found to have a minor role on SMAD 1,5,9 activation in comparison to ALKs and BMP-type II receptors. β 3 integrin was the most important activator, notably for bBMP-2 and -4, on both film stiffness, and solely on soft films for bBMP-7. β 5 integrin had a minor inhibiting role on soft films with bBMP-4 and -7, and on rigid films with bBMP-9 (**Fig. 5A**).

For pSMAD 2 (**Fig. 5B**), BMPR-II was again an important and non-specific activator for all bBMPs, and the no BMP condition (**Fig. SI 15**), especially on rigid films. Interestingly, here again, ALK3 had a notable role: being a stiffness-dependent activator for the pSMAD 2 response to bBMP-4, a stiffness-dependent inhibitor for the response to bBMP-7, and an inhibitor for bBMP-9, its role being prominent on rigid films in comparison to soft ones.

Regarding the ALP activity (**Fig. 5C** and **Fig. SI 16, 17**), generally, ALK2, ALK3 and ALK6 were activators, whereas ALK5 had only an inhibitor role for bBMP-2 (**Fig. 5C**). BMPR-II and ALK6 played the most important role in activating ALP. However, ALK6 was a stronger ALP activator than BMPR-II on bBMP-2, -4 and -7 for soft films, and on bBMP-9 for rigid ones. ACTR-IIA played a role in ALP activation on bBMP-4 and -7, independently of film stiffness. ACTR-IIB only played a minor role inhibiting ALP on bBMP-2 (**Fig. 5C**). Regarding integrins, β 3 and β 5 integrins were generally activators of ALP for bBMP-2, -4 and -7. β 1 integrin was rather inhibiting ALP notably on soft films and had almost no effect on stiff films, except for BMP-2 (**Fig. 5C**).

Globally, the role of the receptors was related to each readout of the osteogenic differentiation (pSMAD 1,5,9; pSMAD 2 or ALP) with only little differences depending on the film stiffness, and little differences between the bBMPs except for the ALK3 and ACTR-IIA receptors.

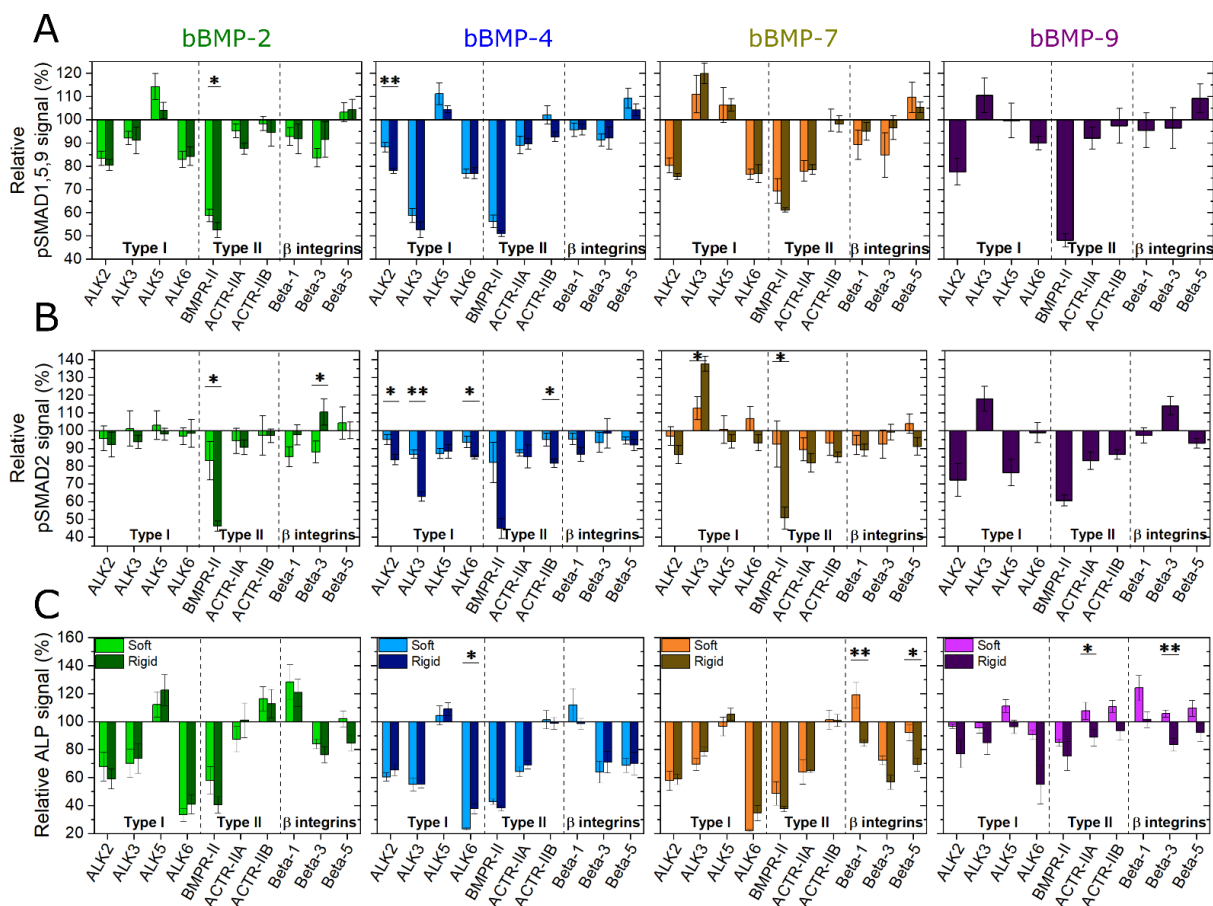


Fig. 5. Effect of BMP receptor and β chain integrin silencing on early cell differentiation to bone. C2C12 cells were transfected with siRNA against BMP receptor type I (ALK2, ALK3, ALK5, ALK6), BMP receptor type II (BMPR-II, ACTR-IIA, ACTR-IIB) and β chain integrins (β 1, β 3, β 5) and plated on soft (light color) and rigid (dark color) films with bBMPs for 5 or 4 h, respectively. (a) pSMAD 1,5,9 signal and (b) ALP activity were quantified, and the relative % is given, in comparison to a control scrambled siRNA. Data represent the mean \pm SEM. Statistical tests were done using non-parametric Kruskal-Wallis ANOVA test (*, $p \leq 0.05$; **, $p \leq 0.01$). Statistical comparisons were made between soft and rigid films for each condition.

4. Discussion

4.1. Stiffness dependence of BMPs and BMP receptors in cell adhesion and spreading

For the first time, the effect of 4 different BMPs, presented in a matrix-bound manner, has been compared on cell adhesion, spreading, SMAD signaling and ALP activity. We show that generally, film stiffness plays a relevant role on the BMP-induced cell responses. Furthermore, we show the role of BMPR type I, type II, and three β -chain integrins, on the aforementioned cell responses for each condition. This study was feasible thanks to a high-content automatized procedure for film preparation (Machillot *et al.*, 2018), image acquisition and analysis

We found that all four studied bBMPs are able to induce both cell adhesion and cell spreading (**Fig. 2**, **Fig. 6A** and **B**, and **Fig. SI 2**, **4** and **5**). This extends our initial findings regarding the role of bBMP-2 on cell adhesion and migration (Crouzier, Fourel, *et al.*, 2011). This effect of BMPs on cell adhesion and spreading was revealed thanks to the matrix-bound presentation of the BMPs together with the variation of film stiffness. Among the four BMPs, bBMP-4 and bBMP-7 induced the most potent adhesion and spreading response, on C2C12 and hPDSCs (**Fig. 1D-G** and **Fig. SI 4D-G**). All four bBMPs have a stronger role inducing cell spreading on rigid films than on soft ones (**Fig. 2F** and **G**). However, on the no BMP condition, only cell number is increased on rigid films with respect to soft ones, but not cell spreading, as it was found in previous works (Crouzier, Fourel, *et al.*, 2011; Fourel *et al.*, 2016). bBMP-9 on soft films did not induce neither cell adhesion nor cell spreading on C2C12 (**Fig. 1B** and **C**), and only a small increase is observed on hPDSCs (**Fig. SI 4B** and **D**). The fact that BMP-9 does not bind to ALK3 and ALK6 could help explaining this observation, since these two receptors are important for cell adhesion (**Fig. 4A**), and ALK3 also for cell spreading (**Fig. 4B**). Our data are consistent with other works showing a positive effect of BMP-2, -4 and -7 on cell adhesion and migration with other cell types (Khurana *et al.*, 2014; Fourel *et al.*, 2016; Sovershaev *et al.*, 2016)

ALK2 appears to be mechano-sensitive in response to bBMP-2 only (**Fig. 4**), by inducing cell spreading on soft films. Our data are consistent with the recently reported mechanosensitivity of ALK2 (Haupt *et al.*, 2019). Interestingly, this mechanosensing appears to be altered during heterotypic ossification associated to fibrodysplasia ossificans progressiva (FOP).

ALK3 appears to be a central receptor in cell adhesion and spreading for all BMPs (**Fig. 4** and **Fig. 6C**). ALK3 has a major role in several cancers (Jiramongkolchai, Owens and Hong, 2016) and plays a role in the adhesion of human epithelial ovarian cancer spheroids to the substratum (Peart *et al.*, 2012).

We found that ALK5 tends to be mechano-sensitive for cell spreading on bBMP-2, and for cell adhesion on bBMP-4 and 7 (**Fig. 4** and **Fig. 6C**). Our data are consistent with the role of ALK5 described in other contexts showing a mechanosensing role of this receptor. In fact, ALK5 is historically known as a TGF- β receptor (Derynck and Budi, 2019) and for its involvement in EMT in breast epithelial (Piek *et al.*, 1999) and endothelial cells (Egorova *et al.*, 2011). It was already shown to be involved in the response to shear stress in the endothelium (Walshe, Dela Paz and D'Amore, 2013), in chondrocyte mechanosensing (Sanz-Ramos, Dotor and Izal-Azcárate, 2014) and in the activation of focal adhesion kinase (FAK) in lung epithelial cells (Ding *et al.*, 2017).

Our data revealed an important mechano-sensitive role of ACTR-IIA in cell adhesion, notably in response to both bBMP-4 and bBMP-7 (**Fig. 4A** and **Fig. 6D**). This finding is in line with a work showing a mechano-sensitive role of ACTR-IIA in tenogenic commitment of adipose stem cells under magnetic stimulation (Matos *et al.*, 2020).

4.2. Identification of integrins in BMP-induced cell adhesion, spreading and BMP signaling

Regarding the role of integrins, $\beta 3$ integrin appears to have a major role in cell adhesion and spreading on all bBMPs. The role of $\beta 3$ integrins is crucial for cell adhesion in soft environment, which corresponds to our finding, whereas both $\beta 1$ and $\beta 3$ integrins cooperate in a stiff environment as already described (Schiller *et al.*, 2013). $\beta 1$ integrin was also important for cell adhesion and spreading on all bBMPs, with a peculiar stiffness-dependent response for cell adhesion to bBMP-7. $\beta 5$ integrin also exhibited a stiffness-dependent response to bBMP-2 and to a lower extent to bBMP-4 (**Fig. 4** and **Fig. 6E**).

Apart from their role in adhesion and spreading, integrins are also important for bone differentiation (Brunner *et al.*, 2011). In our experimental conditions, we found that $\beta 1$ integrin is a slight inhibitor of BMP-2-mediated C2C12 ALP activity for soft and stiff films, while it was stiffness-dependent on bBMP-7 (**Fig. 5C** and **Fig. 6E**). The role of $\beta 1$ integrin in osteoblastic differentiation is recognized, but appears to depend on the cell type and on the context. Previously in our group, Sefkow-Werner *et al.* found an activator role of $\beta 1$ integrin with sBMP-2 and BMP-2 bound to heparan sulphate, by using also C2C12 cells (Sefkow-Werner *et al.*, 2020). Many data have shown that $\beta 1$ integrin plays an important role in osteoblast differentiation and function (Moursi *et al.*, 1997; Wang and Kirsch, 2006; Hamidouche *et al.*, 2009). Mice expressing a dominant-negative $\beta 1$ integrin in mature osteoblasts show reduced bone mass and defective bone formation (Moursi *et al.*, 1997). $\beta 5$ integrin has been shown to be involved in bone differentiation in a non-Smad-dependent manner (Lai *et al.*, 2006).

4.3. Stiffness dependence of BMP and BMP receptors in SMAD and ALP signaling

BMPs are traditionally referred to activate the pSMAD 1,5,9 pathway (Yadin, Knaus and Mueller, 2016) whereas TGF- β activates SMAD 2,3 signaling (Derynck and Budi, 2019). To our knowledge, to date, there was no systematic comparison of the role of BMPs on SMAD and ALP signaling available in the literature. Here, we showed that all four bBMPs are able to activate both pSMAD 1,5,9, pSMAD 2 and ALP pathways in a BMP-specific and, in certain

conditions, in a stiffness-dependent manner (**Fig. 6A and B**). In the stiffness-dependent conditions, pSMAD 1,5,9 and pSMAD 2 Δ_{\max} values were always higher on soft films (**Fig. 2A, B, D, and E**). Notably, bBMP-4 induced a negligible pSMAD 1,5,9 response on stiff films while bBMP-9 induced the highest one.

BMP-2 was recently shown to promote both canonical SMAD 1,5,8 and non-canonical SMAD 2,3 pathways in trophoblast cells (Zhao *et al.*, 2018). Soluble BMP-4 also activates SMAD3 (Upton *et al.*, 2013). Our data is also consistent with SMAD and non-SMAD signaling reported for BMP-7 induced BMP signaling in tenocyte-like cells (Klatte-Schulz *et al.*, 2016).

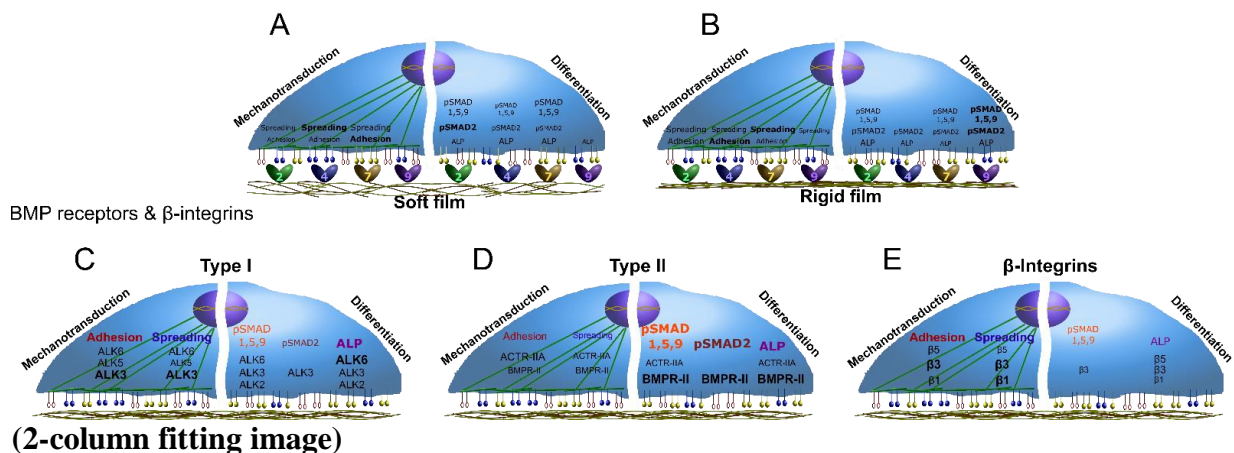
Regarding pSMAD 1,5,9 signaling, ALK2 and ALK6 were found to have a central role independently of the BMP type, while the effect of ALK3 was bBMP-specific: it is a strong activator on bBMP-4 and inhibitor on bBMP-7 and -9 (**Fig. 5A and Fig. 6C**).

BMPR-II had a major activator role for all bBMPs while ACTR-IIA was specifically associated to the response to bBMP-7 (**Fig. 5A and Fig. 6D**). Our data are consistent with the role of ACTR-IIA for BMP7-mediated chemotaxis of monocytes and pSMAD activation (Perron *et al.*, 2019).

The important role of bBMP-9 activating SMAD 1,5,9 and SMAD 2, could be correlated with the strong binding to BMPR-II (**Fig. 3**), which plays a crucial role in SMAD activation (**Fig. 5A and D**), and to ALK1 (**Fig. 3**) which is also important for SMAD 2,3 and SMAD 1,5 activation (Finsson, Almadani and Philip, 2020). Also, the fact that BMP-9 is resistant to the BMP inhibitor Noggin may help to the strong SMAD activation (Rosen, 2006).

ALP is a common marker to assess BMP-induced osteoblastic differentiation (Rivera *et al.*, 2013). We showed that ALP is highly activated in C2C12 cells in response to bBMPs (**Fig. 2G and Fig. SI 10**). Our data are in agreement with the previously demonstrated ALP activities evidenced for soluble BMP-2, -4, -7, and -9 (Rivera *et al.*, 2013). We showed here for the first time a BMP-specific stiffness-dependent ALP response of cells cultured on bBMPs. Indeed, ALP was stiffness-dependent in response to bBMP-2 and -9 and stiffness-independent for bBMP-4 and -7 (**Fig. 2G-I**). The relevant roles of ALK2 and ALK3 in ALP activation that we observed, are consistent with role of ALK2 in ALP activity (Ohte *et al.*, 2011) as well as the role of ALK3 (Aoki *et al.*, 2001), found in the literature. Interestingly, ALK6 was a strong ALP activator despite its low level of expression on C2C12 cells (**Fig. 5C and Fig. 6C**). As with SMAD proteins, BMPR-II played a crucial role activating ALP. Our data also showed that ACTR-IIA is an activator of BMP-4 and 7-mediated ALP activity, while ACTR-IIB was an inhibitor solely for the ALP response to bBMP-2 (**Fig. 5C**). They are consistent with the role of ACTR-IIA and B receptors in the regulation of bone mass (Goh *et al.*, 2017).

BMP type & substrate stiffness



(2-column fitting image)

Fig. 6. Schematic representations summarizing the major results of this study. The influence of the four bBMPs on C2C12 cell adhesion and spreading, as mechanotransduction parameters, and pSMAD 1,5,9, pSMAD 2 and ALP activity, as differentiation parameters, is represented for (a) soft and (b) rigid films. Moreover, the role of the BMP receptors type I, type II and the three β chain integrins analyzed, on the mechanotransduction and differentiation parameters aforementioned, are depicted for each type of receptor: (c) type I BMPR, (d) type II BMPR, and (e) β chain integrins. Since no relevant stiffness-dependent differences were generally observed for the receptors, no specific detailed distinction between soft and rigid films is represented.

5. Conclusion

In this work, we carried out an extensive study where we shed light on the effect of four BMPs non-covalently bound to a biomimetic film, combined with two film rigidities (soft and rigid), on early phases of cell adhesion and spreading, using C2C12 cells and hPDSCs, and osteogenic differentiation, using C2C12 cells. We observed that matrix-bound BMPs (bBMPs) induced cell adhesion, spreading, and differentiation in a bBMP type- and film stiffness-dependent manner. We found that bBMP-2, -4 and -7 play an important role inducing adhesion and spreading, while bBMP-9 does not. On the other hand, bBMP-9 plays a very important role activating SMAD 1,5,9 and SMAD 2 pathways. Moreover, by means of siRNA, we revealed the role of type I and type II BMP receptors, as well as 3 beta-chain integrins, on the aforementioned cell processes. Generally, BMP receptors type I and integrins play an important role in bBMP-mediated cell adhesion and spreading, while BMP receptors type II play the most important role in cell differentiation, followed by type I receptors and integrins.

This study paves the way for the elucidation of the complex interplay between BMPs, substrate physico-chemical properties, BMP receptors and integrins, on cell adhesion, spreading, and on the cell fate towards osteogenic lineage, which are crucial for the development of new, tailored, medical implants.

Acknowledgements

C. Picart is a senior member of the Institut Universitaire de France, whose financial support is acknowledged. The study was supported by Agence Nationale de la Recherche (ANR CODECIDE, ANR-17-CE13-022 to C.A.R. and C.P, ANR GlyCON, ANR-19-CE13-0031-01 E.M.), by the Fondation Recherche Medicale (FRM) (grant DEQ20170336746 to C.P. DEQ20170336702 to C.A.R), by the European Research Council (ERC Biomim, GA 259370, POC BioactiveCoatings, GA692924). We are part of the GDR2088 “BIOMIM” and the GDR “Réparer l’humain” research networks. V.K. was supported by a PhD fellowship from Grenoble Institute of Technology. A. Guevara-Garcia is supported by a CONACYT fellowship from the mexican government (CVU: 532484). We thanks Prof. Franz Luyten for providing the hPDSCs cells and for fruitful discussions. We are grateful to David Pointu for his technical advices.

Author contribution. C.P. supervised the project, designed the experiments, wrote the manuscript, acquired funding and provided the resources. A.S and P.M. designed, and performed experiments, analyzed the data, and wrote the manuscript. V.K. carried out experiments, analyzed the data and edited the manuscript. L.F. and C.A.R provided advice and technical assistance, and edited the manuscript. E.M. and A.G.G reviewed and edited the manuscript.

Competing interests. The authors declare that they have no conflict of interest with the contents of this article.

Materials & Correspondence. Catherine Picart and Adria Sales

Data availability statement

The raw and processed data required to reproduce these findings are available upon request to Catherine Picart and/or Adria Sales.

References

- Antebi, Y. E. *et al.* (2017) 'Combinatorial Signal Perception in the BMP Pathway', *Cell*. Elsevier Inc., 170(6), pp. 1184–1196.e24. doi: 10.1016/j.cell.2017.08.015.
- Aoki, H. *et al.* (2001) 'Synergistic effects of different bone morphogenetic protein type I receptors on alkaline phosphatase induction', *Journal of Cell Science*, 114(8), pp. 1483–1489.
- Ashe, H. L. (2016) 'Modulation of BMP signalling by integrins', *Biochemical Society Transactions*, 44(5), pp. 1465–1473. doi: 10.1042/BST20160111.
- Bidart, M. *et al.* (2012) 'BMP9 is produced by hepatocytes and circulates mainly in an active mature form complexed to its prodomain', *Cellular and Molecular Life Sciences*, 69(2), pp. 313–324. doi: 10.1007/s00018-011-0751-1.
- Bolander, J. *et al.* (2016) 'The combined mechanism of bone morphogenetic protein- and calcium phosphate-induced skeletal tissue formation by human periosteum derived cells', *European Cells and Materials*, 31, pp. 11–25. doi: 10.22203/eCM.v031a02.
- Bouyer, M. *et al.* (2016) 'Surface delivery of tunable doses of BMP-2 from an adaptable polymeric scaffold induces volumetric bone regeneration', *Biomaterials*, 104(0), pp. 168–181. doi: 10.1016/j.biomaterials.2016.06.001.
- Brunner, M. *et al.* (2011) 'Osteoblast mineralization requires β 1 integrin/ICAP-1-dependent fibronectin deposition', *Journal of Cell Biology*, 194(2), pp. 307–322. doi: 10.1083/jcb.201007108.
- Crouzier, T. *et al.* (2009) 'Layer-by-layer films as a biomimetic reservoir for rhBMP-2 delivery: Controlled differentiation of myoblasts to osteoblasts', *Small*, 5(5), pp. 598–608. doi: 10.1002/sml.200800804.
- Crouzier, T., Fourel, L., *et al.* (2011) 'Presentation of BMP-2 from a soft biopolymeric film unveils its activity on cell adhesion and migration', *Advanced Materials*, 23(12), pp. 111–118. doi: 10.1002/adma.201004637.
- Crouzier, T., Sailhan, F., *et al.* (2011) 'The performance of BMP-2 loaded TCP/HAP porous ceramics with a polyelectrolyte multilayer film coating', *Biomaterials*. Elsevier Ltd, 32(30), pp. 7543–7554. doi: 10.1016/j.biomaterials.2011.06.062.
- Derynck, R. and Budi, E. H. (2019) 'Specificity, versatility, and control of TGF- β family signaling', *Science Signaling*, 12(570). doi: 10.1126/scisignal.aav5183.
- Ding, Q. *et al.* (2017) 'Focal adhesion kinase signaling determines the fate of lung epithelial cells in response to TGF- β ', *American Journal of Physiology - Lung Cellular and Molecular Physiology*, 312(6), pp. L926–L935. doi: 10.1152/ajplung.00121.2016.
- Duchamp De Lageneste, O. *et al.* (2018) 'Periosteum contains skeletal stem cells with high bone regenerative potential controlled by Periostin', *Nature Communications*. Springer US, 9(773), pp. 1–15. doi: 10.1038/s41467-018-03124-z.
- Egorova, A. D. *et al.* (2011) 'Lack of primary cilia primes shear-induced endothelial-to-mesenchymal transition', *Circulation Research*, 108(9), pp. 1093–1101. doi: 10.1161/CIRCRESAHA.110.231860.
- Ehata, S. *et al.* (2013) 'Bi-directional roles of bone morphogenetic proteins in cancer: Another molecular Jekyll and Hyde?', *Pathology International*, 63(6), pp. 287–296. doi: 10.1111/pin.12067.
- Finnsen, K. W., Almadani, Y. and Philip, A. (2020) 'Non-canonical (non-SMAD2/3) TGF- β

- signaling in fibrosis: Mechanisms and targets', *Seminars in Cell and Developmental Biology*. Elsevier, 101(November 2019), pp. 115–122. doi: 10.1016/j.semcdb.2019.11.013.
- Fourel, L. *et al.* (2016) ' β 3 integrin-mediated spreading induced by matrix-bound BMP-2 controls Smad signaling in a stiffness-independent manner', *Journal of Cell Biology*, 212(6), pp. 693–706. doi: 10.1083/jcb.201508018.
- Fujioka-Kobayashi, M. *et al.* (2017) 'Osteogenic potential of rhBMP9 combined with a bovine-derived natural bone mineral scaffold compared to rhBMP2', *Clinical Oral Implants Research*, 28(4), pp. 381–387. doi: 10.1111/clr.12804.
- Gamell, C. *et al.* (2008) 'BMP2 induction of actin cytoskeleton reorganization and cell migration requires PI3-kinase and Cdc42 activity', *Journal of Cell Science*, 121(23), pp. 3960–3970. doi: 10.1242/jcs.031286.
- Gilde, F. *et al.* (2016) 'Stiffness-dependent cellular internalization of matrix-bound BMP-2 and its relation to Smad and non-Smad signaling', *Acta Biomaterialia*, 46, pp. 55–67. doi: 10.1016/j.actbio.2016.09.014.
- Goh, B. C. *et al.* (2017) 'Activin receptor type 2A (ACVR2A) functions directly in osteoblasts as a negative regulator of bone mass', *Journal of Biological Chemistry*, 292(33), pp. 13809–13822. doi: 10.1074/jbc.M117.782128.
- Hamidouche, Z. *et al.* (2009) 'Priming integrin α 5 promotes human mesenchymal stromal cell osteoblast differentiation and osteogenesis', *Proceedings of the National Academy of Sciences of the United States of America*, 106(44), pp. 18587–18591. doi: 10.1073/pnas.0812334106.
- Haupt, J. *et al.* (2019) 'ACVR1 R206H FOP mutation alters mechanosensing and tissue stiffness during heterotopic ossification', *Molecular Biology of the Cell*, 30(1), pp. 17–29. doi: 10.1091/mbc.E18-05-0311.
- Holtzhausen, A. *et al.* (2014) 'Novel bone morphogenetic protein signaling through Smad2 and Smad3 to regulate cancer progression and development', *FASEB Journal*, 28(3), pp. 1248–1267. doi: 10.1096/fj.13-239178.
- Hynes, R. O. (2009) 'The extracellular matrix: Not just pretty fibrils', *Science*, 326(5957), pp. 1216–1219. doi: 10.1126/science.1176009.
- Jiramongkolchai, P., Owens, P. and Hong, C. C. (2016) 'Emerging roles of the bone morphogenetic protein pathway in cancer: Potential therapeutic target for kinase inhibition', *Biochemical Society Transactions*, 44(4), pp. 1117–1134. doi: 10.1042/BST20160069.
- Khurana, S. *et al.* (2013) 'A novel role of BMP4 in adult hematopoietic stem and progenitor cell homing via Smad independent regulation of integrin- α 4 expression', *Blood*, 121(5), pp. 781–790. doi: 10.1182/blood-2012-07-446443.
- Khurana, S. *et al.* (2014) 'SMAD signaling regulates CXCL12 expression in the bone marrow niche, affecting homing and mobilization of hematopoietic progenitors', *Stem Cells*, 32(11), pp. 3012–3022. doi: 10.1002/stem.1794.
- Klatte-Schulz, F. *et al.* (2016) 'An investigation of BMP-7 mediated alterations to BMP signalling components in human tenocyte-like cells', *Scientific Reports*. Nature Publishing Group, 6(January), pp. 1–11. doi: 10.1038/srep29703.
- Lai, C. F. *et al.* (2006) 'Four and Half Lim Protein 2 (FHL2) stimulates osteoblast differentiation', *Journal of Bone and Mineral Research*, 21(1), pp. 17–28. doi: 10.1359/JBMR.050915.
- Llopis-Hernández, V. *et al.* (2016) 'Material-driven fibronectin assembly for high-efficiency

- presentation of growth factors', *Science Advances*, 2(8), p. e1600188. doi: 10.1126/sciadv.1600188.
- Machillot, P. *et al.* (2018) 'Automated Buildup of Biomimetic Films in Cell Culture Microplates for High-Throughput Screening of Cellular Behaviors', *Advanced Materials*, 30(27), pp. 1–8. doi: 10.1002/adma.201801097.
- Massagué, J. (2000) 'How cells read TGF- β signals', *Nature Reviews Molecular Cell Biology*, 1(3), pp. 169–178. doi: 10.1038/35043051.
- Matos, A. M. *et al.* (2020) 'Remote triggering of TGF- β /Smad2/3 signaling in human adipose stem cells laden on magnetic scaffolds synergistically promotes tenogenic commitment', *Acta Biomaterialia*. Elsevier Ltd, 113, pp. 488–500. doi: 10.1016/j.actbio.2020.07.009.
- Migliorini, E. *et al.* (2020) 'Learning from BMPs and their biophysical extracellular matrix microenvironment for biomaterial design', *Bone*, 141, p. 115540. doi: <https://doi.org/10.1016/j.bone.2020.115540>.
- Morikawa, M., Derynck, R. and Miyazono, K. (2016) 'TGF- β and the TGF- β family: Context-dependent roles in cell and tissue physiology', *Cold Spring Harbor Perspectives in Biology*, 8(5). doi: 10.1101/cshperspect.a021873.
- Morrell, N. W. *et al.* (2016) 'Targeting BMP signalling in cardiovascular disease and anaemia', *Physiology Nat Rev Cardiol Behavior*, 13(2), pp. 106–120. doi: 10.1016/j.physbeh.2017.03.040.
- Moursi, A. *et al.* (1997) 'Interactions between integrin receptors and fibronectin are required for.pdf', *Jcs.Biologists.Org*, 2196, pp. 2187–2196.
- Ohte, S. *et al.* (2011) 'A novel mutation of ALK2, L196P, found in the most benign case of fibrodysplasia ossificans progressiva activates BMP-specific intracellular signaling equivalent to a typical mutation, R206H', *Biochemical and Biophysical Research Communications*. Elsevier Inc., 407(1), pp. 213–218. doi: 10.1016/j.bbrc.2011.03.001.
- Peart, T. M. *et al.* (2012) 'BMP signalling controls the malignant potential of ascites-derived human epithelial ovarian cancer spheroids via AKT kinase activation', *Clinical and Experimental Metastasis*, 29(4), pp. 293–313. doi: 10.1007/s10585-011-9451-3.
- Perron, J. C. *et al.* (2019) 'Chemotropic signaling by BMP7 requires selective interaction at a key residue in ActRIIA', *Biology Open*, 8(7). doi: 10.1242/bio.042283.
- Piek, E. *et al.* (1999) 'TGF- β type I receptor/ALK-5 and Smad proteins mediate epithelial to mesenchymal transdifferentiation in NMuMG breast epithelial cells', *Journal of Cell Science*, 112(24), pp. 4557–4568.
- Posa, F. *et al.* (2021) 'Surface Co-presentation of BMP-2 and integrin selective ligands at the nanoscale favors $\alpha 5\beta 1$ integrin-mediated adhesion', *Biomaterials*. Elsevier Ltd, 267(October 2020), p. 120484. doi: 10.1016/j.biomaterials.2020.120484.
- Ramel, M. C. and Hill, C. S. (2013) 'The ventral to dorsal BMP activity gradient in the early zebrafish embryo is determined by graded expression of BMP ligands', *Developmental Biology*. Elsevier, 378(2), pp. 170–182. doi: 10.1016/j.ydbio.2013.03.003.
- Rivera, J. C. *et al.* (2013) 'Beyond osteogenesis: An in vitro comparison of the potentials of six bone morphogenetic proteins', *Frontiers in Pharmacology*, 4(125), pp. 1–7. doi: 10.3389/fphar.2013.00125.
- Roberts, S. J. *et al.* (2011) 'Enhancement of osteogenic gene expression for the differentiation of human periosteal derived cells', *Stem Cell Research*. Elsevier B.V., 7(2), pp. 137–144. doi:

10.1016/j.scr.2011.04.003.

Rosen, V. (2006) 'BMP and BMP inhibitors in bone', *Annals of the New York Academy of Sciences*, 1068(1), pp. 19–25. doi: 10.1196/annals.1346.005.

Salazar, V. S., Gamer, L. W. and Rosen, V. (2016) 'BMP signalling in skeletal development, disease and repair', *Nature Reviews Endocrinology*, 12(4), pp. 203–221. doi: 10.1038/nrendo.2016.12.

Sanz-Ramos, P., Dotor, J. and Izal-Azcárate, I. (2014) 'The role of Alk-1 and Alk-5 in the mechanosensing of chondrocytes', *Cellular and Molecular Biology Letters*, 19(4), pp. 659–674. doi: 10.2478/s11658-014-0220-6.

Schiller, H. B. *et al.* (2013) ' β 1 - And α v -class integrins cooperate to regulate myosin II during rigidity sensing of fibronectin-based microenvironments', *Nature Cell Biology*. Nature Publishing Group, 15(6), pp. 625–636. doi: 10.1038/ncb2747.

Schneider, A. *et al.* (2006) 'Polyelectrolyte multilayers with a tunable young's modulus: Influence of film stiffness on cell adhesion', *Langmuir*, 22(3), pp. 1193–1200. doi: 10.1021/la0521802.

Sedlmeier, G. and Sleeman, J. P. (2017) 'Extracellular regulation of BMP signaling: welcome to the matrix', *Biochemical Society Transactions*, 45(1), pp. 173–181. doi: 10.1042/BST20160263.

Sefkow-Werner, J. *et al.* (2020) 'Heparan sulfate co-immobilized with cRGD ligands and BMP2 on biomimetic platforms promotes BMP2-mediated osteogenic differentiation', *Acta Biomaterialia*. Elsevier Ltd, 114, pp. 90–103. doi: 10.1016/j.actbio.2020.07.015.

Sieber, C. *et al.* (2009) 'Recent advances in BMP receptor signaling', *Cytokine and Growth Factor Reviews*, 20(5–6), pp. 343–355. doi: 10.1016/j.cytogfr.2009.10.007.

da Silva Madaleno, C., Jatzlau, J. and Knaus, P. (2020) 'BMP signalling in a mechanical context – Implications for bone biology', *Bone*. Elsevier, 137(April), p. 115416. doi: 10.1016/j.bone.2020.115416.

Sovershaev, T. A. *et al.* (2016) 'A novel role of bone morphogenetic protein-7 in the regulation of adhesion and migration of human monocytic cells', *Thrombosis Research*. Elsevier Ltd, 147, pp. 24–31. doi: 10.1016/j.thromres.2016.09.018.

Tenney, R. M. and Discher, D. E. (2009) 'Stem cells, microenvironment mechanics, and growth factor activation', *Current Opinion in Cell Biology*, 21(5), pp. 630–635. doi: 10.1016/j.ceb.2009.06.003.

Toofan, P. and Wheadon, H. (2016) 'Role of the bone morphogenic protein pathway in developmental haemopoiesis and leukaemogenesis', *Biochemical Society Transactions*, 44(5), pp. 1455–1463. doi: 10.1042/BST20160104.

Upton, P. D. *et al.* (2013) 'Transforming growth factor- β 1 represses bone morphogenetic protein-mediated Smad signaling in pulmonary artery smooth muscle cells via Smad3', *American Journal of Respiratory Cell and Molecular Biology*, 49(6), pp. 1135–1145. doi: 10.1165/rcmb.2012-0470OC.

Valia Khodr, Paul Machillot, Elisa Migliorini, Jean-Baptiste Reiser, C. P. (2020) 'High throughput measurements of BMP/BMP receptors interactions using bio-layer interferometry', *BioRxiv*. doi: <https://doi.org/10.1101/2020.10.20.348060>.

Wagner, D. O. *et al.* (2010) 'BMPs: From bone to body morphogenetic proteins', *Science Signaling*, 3(107). doi: 10.1126/scisignal.3107mr1.

- Walshe, T. E., Dela Paz, N. G. and D'Amore, P. A. (2013) 'The role of shear-induced transforming growth factor- β signaling in the endothelium', *Arteriosclerosis, Thrombosis, and Vascular Biology*, 33(11), pp. 2608–2617. doi: 10.1161/ATVBAHA.113.302161.
- Wang, W. and Kirsch, T. (2006) 'Annexin V/ β 5 integrin interactions regulate apoptosis of growth plate chondrocytes', *Journal of Biological Chemistry*, 281(41), pp. 30848–30856. doi: 10.1074/jbc.M605937200.
- Wei, Q. *et al.* (2020) 'BMP-2 Signaling and Mechanotransduction Synergize to Drive Osteogenic Differentiation via YAP/TAZ', *Advanced Science*, 7(15), pp. 1–15. doi: 10.1002/advs.201902931.
- Yadin, D., Knaus, P. and Mueller, T. D. (2016) 'Structural insights into BMP receptors: Specificity, activation and inhibition', *Cytokine and Growth Factor Reviews*. Elsevier Ltd, 27, pp. 13–34. doi: 10.1016/j.cytogfr.2015.11.005.
- Yamachika, E. *et al.* (2008) 'Immobilized recombinant human bone morphogenetic protein-2 enhances the phosphorylation of receptor-activated Smads', *Journal of Biomedical Materials Research - Part A*, 88(3), pp. 599–607. doi: 10.1002/jbm.a.31833.
- Ye, L., Kynaston, H. and Jiang, W. G. (2008) 'Bone morphogenetic protein-9 induces apoptosis in prostate cancer cells, the role of prostate apoptosis response-4', *Molecular Cancer Research*, 6(10), pp. 1594–1606. doi: 10.1158/1541-7786.MCR-08-0171.
- Zhang, Z. *et al.* (2019) 'Mouse embryo geometry drives formation of robust signaling gradients through receptor localization', *Nature Communications*. Springer US, 10(1). doi: 10.1038/s41467-019-12533-7.
- Zhao, H. J. *et al.* (2018) 'Bone morphogenetic protein 2 promotes human trophoblast cell invasion by upregulating N-cadherin via non-canonical SMAD2/3 signaling', *Cell Death and Disease*. Springer US, 9(2), pp. 4–15. doi: 10.1038/s41419-017-0230-1.

Supporting information, Sales et al,
Differential bioactivity of four BMP-family members as function of biomaterial stiffness

TABLE SI 1. Percentage of BMP proteins (BMP-2, -4, -7 and -9) incorporated in the (PLL/HA)₁₂ films and the corresponding estimated density on the film. The samples analyzed correspond to an initial BMP loading concentration in solution of 20 µg/mL. The amount of BMP was quantified using a micro bicinchoninic acid assay (microBCA) assay. Experiments were performed at least in triplicate (data are mean ± SD of 2 to 3 independent experiments).

BMP type	% of BMPs incorporated		BMPs surface densities (µg/cm ²)	
	Soft film	Rigid film	Soft film	Rigid film
BMP-2	60 ± 3 %	65 ± 5 %	1.81 ± 0.09	1.97 ± 0.15
BMP-4	82 ± 4 %	67 ± 9 %	2.48 ± 0.12	2.03 ± 0.27
BMP-7	94 ± 3 %	85 ± 8 %	2.85 ± 0.09	2.58 ± 0.24
BMP-9	92 ± 1 %	88 ± 1 %	2.79 ± 0.03	2.67 ± 0.03

TABLE SI 2. Primer sequences.

<i>Mouse Gene</i>	<i>Forward sequence (5'-3')</i>	<i>Reverse sequence (5'-3')</i>
ALK1	GACACCCACCATCCCTAACC	TTGGGGTACCAGCACTCTCT
ALK2	AGTGGAAGTCTGGAAAAGGAACA	TTCTCCCAGCAGGCTCCCTAT
ALK3	GGAAGCATAGGTCAAAGCTGTTC	TGAGGGAGGCTTCCTTACAGA
ALK4	ACGAGACAATCAACATGAAGCA	CGGAGGGCACTAAGTCGTAA
ALK5	TTTCAGAGGGCACCACCTTA	AATGGTCTGGCAATTGTTCT
ALK6	CAACCCGGCCATAAGTGAAG	CTCCTTCTGGTGCCACATT
BMPR-II	CCCTCCCTTGACCTGGATAAC	TACAGCAACTGGACGCTCAT
ACTR-IIA	GCGTTCGCCGTCTTTCTTAT	AGCAAGGTTCAACACCAGTCT
ACTR-IIB	AGGGAAGCCTCCTGGGGATA	CCATGGCGTACATGTCGATAC
β 1	CGGACGCTGCGAAAAGATGA	CACATCGTGCAGAAGTAGGC
β 3	CCACACGAGGGCGTGAAGTC	CTTCAGGTTACATCGGGGTGA
β 5	CCCGTTATGAAATGGCCTCA	GCCTAGCTAGCGTGAGCAA
EF1	CCGTCAGAACGCAGGTGTTG	GTTCGCTTGTCGATTCCACC
PPIA	GTCTCCTTCGAGCTGTTTGC	GCGTGTAAGTCACCACCCT
GUSB	CGGGACTTTATTGGCTGGGT	CCATTCACCCACACAAGTGC

<i>Human Gene</i>	<i>Forward sequence (5'-3')</i>	<i>Reverse sequence (5'-3')</i>
ALK1	TGGTGCTGTGGGAGATTGC	TCCTCAAAGCTGGGGTCATT
ALK2	ATGTGACCAAGAGCCTGCAT	CGCAGGAGAGACCTTCACAC
ALK3	GGTAGTGGGTCTGGACTACCT	ACGCCATTTGCCCATCCATA
ALK4	CTCCTCCTTCTTCCCCCTTGTT	CCATCTGTCTCACACGTGTAGTTG
ALK5	TTGCTGCAATCAGGACCATTG	AGATGCAGACGAAGCACACT
ALK6	ATGACTCTGGGTTGCCTGTG	TCAATGGAGGCAGTGTAGGG
BMPR-II	TGAGCCCAACAGTCAATCCA	TGGCACACGCCTATTATGTGA
ACTR-IIA	GGCGTTTGCCGTCTTTCTTA	AACACGGTTCAACACCAGTTT
ACTR-IIB	GGGCCACAAGCCGTCTATT	GGAGGTTTCCCTGGCTCAAA

β1	CCGCGCGGAAAAGATGAAT	CACAATTTGGCCCTGCTTGTA
β3	TGCGAGTGTGACGACTTCTC	GTCAGTACGCGTGGTACAGT
β5	TGCTTCGAGAGCGAGTTTGG	GTCCCGATGTAACCTGCAT
EF1	ATCCACCTTTGGGTCGCTTT	CTGAGCTTTCTGGGCAGACT
PPIA	TCAACCCACCGTGTCTTC	TGCTGTCTTTGGGACCTTGT
GUSB	GTGCGTAGGGACAAGAACCA	GGGAGGGGTCCAAGGATTTG

TABLE SI 3. Gene target siRNA sequences used for transfection.

<i>Gene Target</i>	<i>Reference DHARMACON</i>	<i>siRNA target sequence (5' to 3')</i>
β 1 integrin	L-040783-01-0005, ON-TARGETplus Mouse Itgb1 (16412) - SMARTpool	UGCCAAAUCUUGCGGAGAA UUACAAGAGUGCCGUGACA GUGAAGACAUGGACGCUUA CAAUGAAGCUAUCGUGCAU
β 3 integrin	L-040746-01-0005, ON-TARGETplus Mouse Itgb3 (16416) – SMARTpool	AAACAGAGCGUGUCCCGUA AAACACGUGCUGACGCUAA GAGCAGUCUUUCACUAUCA GUGAAAGAGCUGACGGUAU
β 5 integrin	L-042453-01-0005, ON-TARGETplus Mouse Itgb5 (16419) - SMARTpool	CCGCUUAGGUUUCGGGUCU GCUAGGCACGCACGGAUAA AGAAGAUCGGAUGGCGAAA ACUGCUAAGGACUGCGUUA
ALK2	L-042047-00-0005, ON-TARGETplus Mouse Acvr1 (11477) - SMARTpool	CUAGAUCACUCGUGUACAU GAAAUGGGAUCGUUGUAUG UAUAAGAGGGUCGAUAAUU GAAGGGCUGCUUUCAGGUU
ALK3	L-040598-00-0005, ON-TARGETplus Mouse Bmpria (12166) - SMARTpool	GAGGAAUCGUGGAGGAAUA GCUAGCUGGUUUAGAGAAA GAAAUGGCUCGUCGUUGUA GGCCAUUGCUUUGCCAUAU
ALK5	L-040617-00-0005, ON-TARGETplus Mouse Tgfbr1 (21812) - SMARTpool	GGGCAGUUACUACAACAU CUAGAUCGCCUUUCAUUU GCGAAGGCAUUACAGUGUU UGACAGCUUUGCGAAUUA
ALK6	L-051071-00-0005, ON-TARGETplus Mouse Bmpr1b (12167) - SMARTpool	GACAAUAGCUAAGCAAUUU GGAAUGAGUGUAAUAAAGA

		GCACAGAUGGGUACUGCUU GACGAGAGCUUGAAUAGAA
BMPR-II	L-040599-00-0005, ON-TARGETplus Mouse Bmpr2 (12168) - SMARTpool	GCACAUAGGUCCCAAGAAA GAACGCAACCUGUCACUAU GCAUGAACCUUUACUGAGA CUAAVAAGCUAGAUCCTAAA
ACTR-IIA	L-040676-00-0005, ON-TARGETplus Mouse Acvr2a (11480) - SMARTpool	GAACCUUGCUAUGGUGAUA GGACGCAUUUCUGAGGAUA CAGACUUUCUUAAGGCUAA GCAAUGCUCUGUGAAACGA
ACTR-IIB	L-040629-00-0005, ON-TARGETplus Mouse Acvr2b (11481) - SMARTpool	GCCCAGAAGUCACGUACGA CGGCCUGGCUGUUCGGUUU GAAGAGCGGGUAUCCUGA GGAACGAACUGUGCCACGU
Scrambled	D-001810-01-05) ON-TARGETplus Non-targeting	UGGUUUACAUGUCGACUAA

FIGURE SI 1. Representative fluorescent pictures of C2C12 cell adhesion and spreading on the films with matrix-bound BMPs. C2C12 cells were fixed after 5 h of culture on soft films, and after 4 h of culture on rigid films. Cells were stained for actin (in far-red) and nuclei (in blue) for increasing loading concentrations. Scale bar=100 μm .

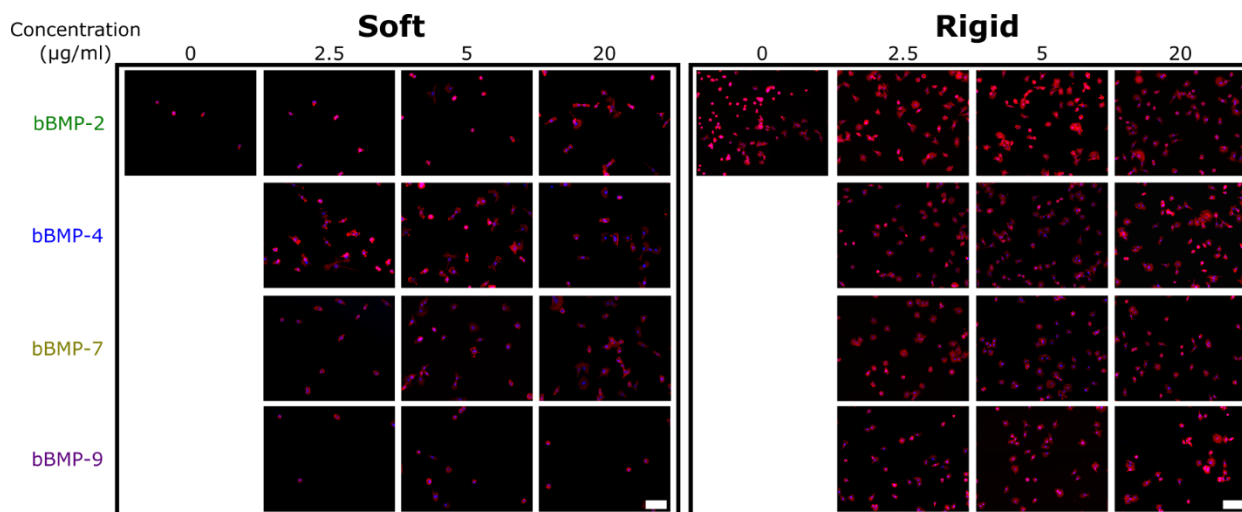


Figure SI 2. Normalized cell number and cell area values to the non-BMP condition on C2C12 seeded on soft and rigid films with different BMP concentrations. (a) Calculation of cell number per mm^2 of substrate area, and (b) cell area both of them normalized by the non-BMP condition. Thus, the effect of each bBMP for each film stiffness is exalted. Data represent three independent biological replicates with two wells per condition in each independent experiment (technical replicates). Statistical tests were done using non-parametric Kruskal-Wallis ANOVA test to compare soft (light color) and rigid (dark color) films (* $p < 0.05$; ** $p < 0.01$).

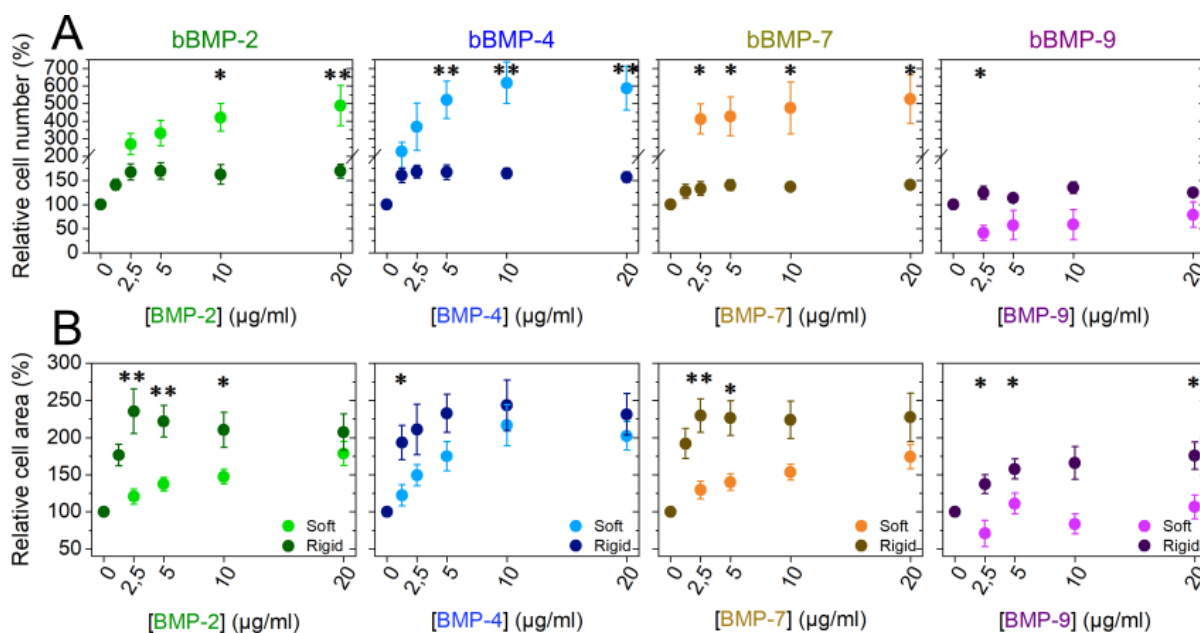


Figure SI 3. Effects of soluble BMPs (sBMP-2, -4, -7, -9) on cell adhesion and spreading of C2C12 cells. Cells were fixed after 5 h, on soft films, and after 4 h on rigid ones.. (a) The cell number (cells/mm² of substrate area) and (b) the cell spreading area (μm²) are given. Data represent the mean ± SEM, with 3 independent biological replicates and 2 technical replicates in each experiment. Statistical tests were done using non-parametric Kruskal-Wallis ANOVA test to compare each BMP condition with the no BMP condition. * p ≤ 0.05.

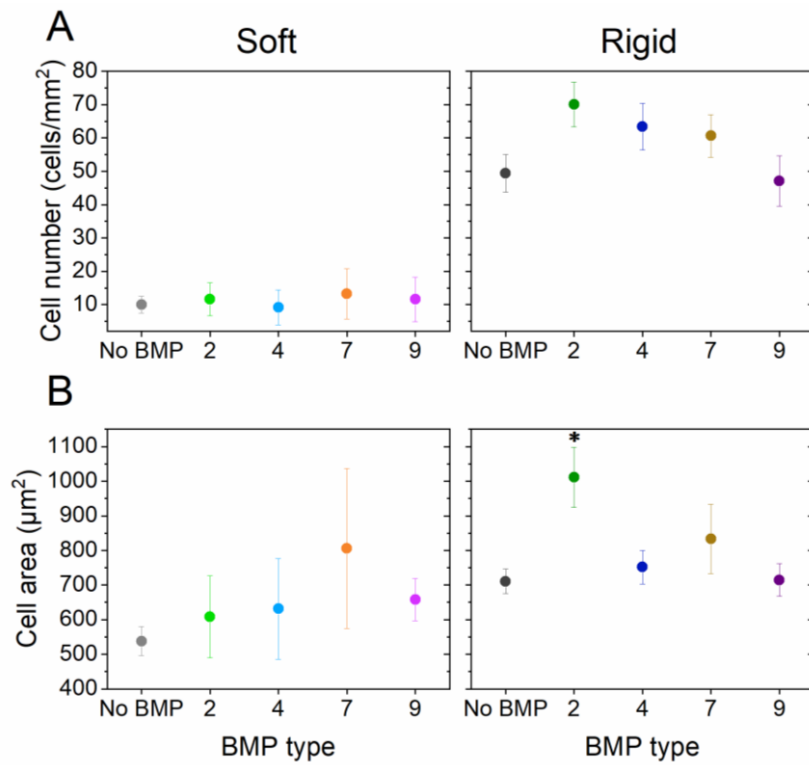


Figure SI 4. Quantification of hPDSCs adhesion on soft and rigid films with four bBMPs (2, 4, 7, 9) at increasing BMP-loaded concentrations. (a) Representative images of the cell actin cytoskeleton (red) on soft films 5 h after cell seeding, and on rigid films 4 h after cell seeding. (b) Cell number per mm² of substrate area and (c) cell area as a function of the BMP concentration in solution are shown. Quantitative parameters extracted from the fit of the experimental curves: (d and e) cell number and (f and g) cell area. Data represent the mean \pm SEM of 3 independent experiments with 2 samples per condition in each experiments (at least a total of 400 cells analyzed per condition). Statistical tests were done between soft (light color) and rigid (dark color) films using non-parametric Kruskal-Wallis ANOVA test (* $p < 0.05$; ** $p < 0.01$). Scale bar=200 μ m.

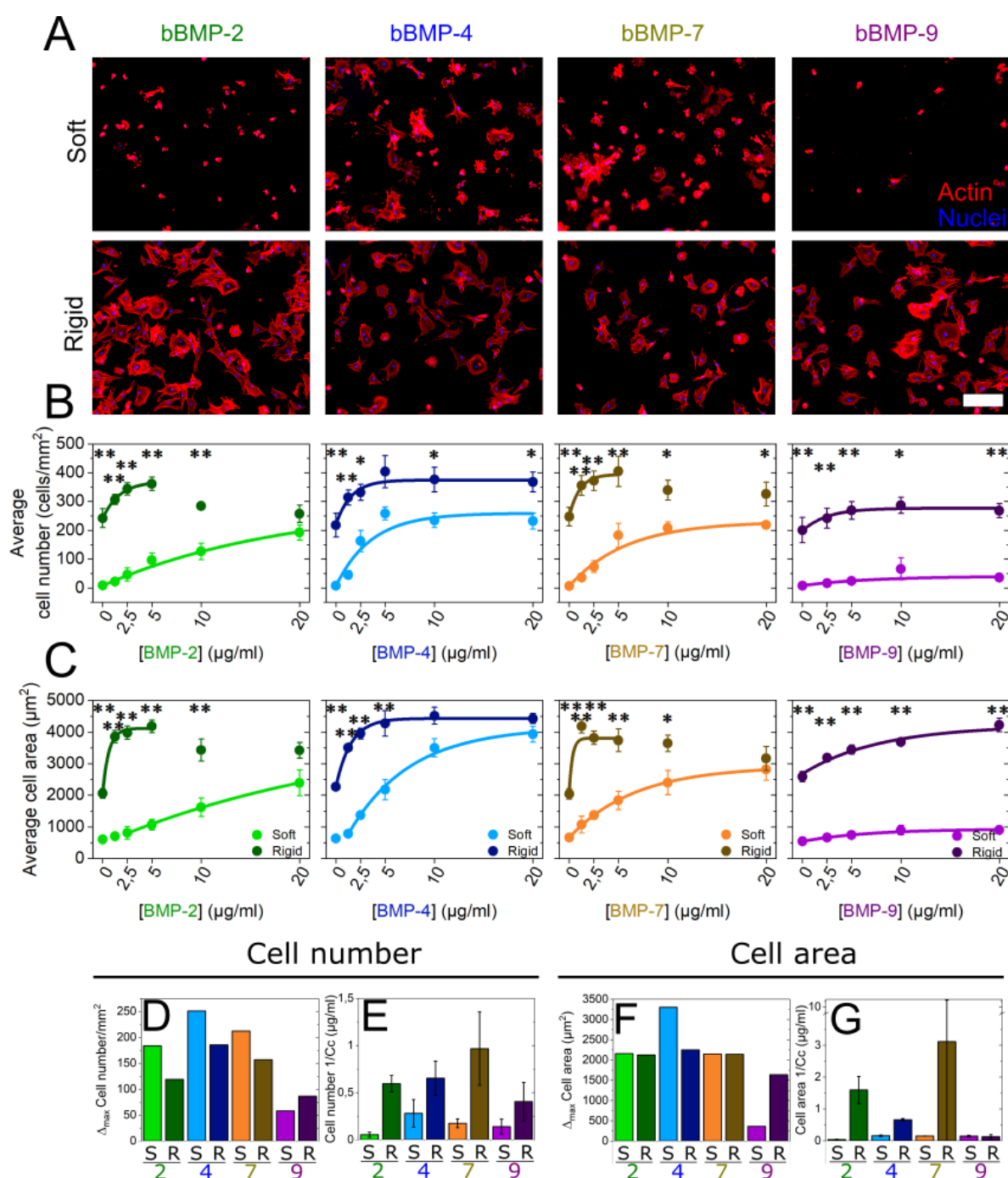


Figure SI 5. Normalized cell number and cell area values to the non-BMP condition on hPDSCs seeded on soft and rigid films with different BMP concentrations. (a) Calculation of cell number per mm² of substrate area and (b) cell area both of them normalized by the non-BMP condition. Thus, the effect of each bBMP for each film stiffness is exalted. Data represent three independent biological replicates with two wells per condition in each independent experiment (technical replicates). Statistical tests were done using non-parametric Kruskal-Wallis ANOVA test to compare soft (light color) and rigid (dark color) films (*p < 0.05; **p < 0.01).

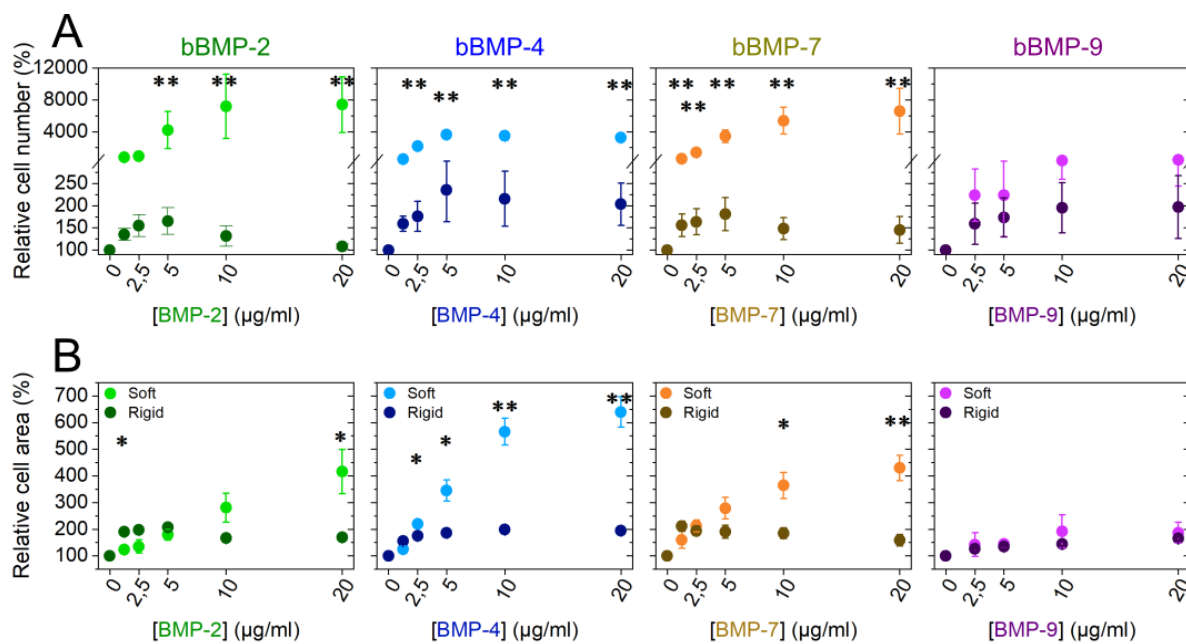


Figure SI 6. Effects of soluble BMPs (sBMP-2, -4, -7, -9) on cell adhesion and spreading of hPDSCs cells. Cells were fixed after 5 h, on soft films, and after 4 h on rigid ones. (a) The cell number (cells/mm² of substrate area) and (b) the cell spreading area (μm²) are given. Data represent the mean ± SEM, with 3 independent biological replicates and 2 technical replicates in each experiment. Statistical tests were done using non-parametric Kruskal-Wallis ANOVA test to compare each BMP condition with the non-BMP condition. * p ≤ 0.05.

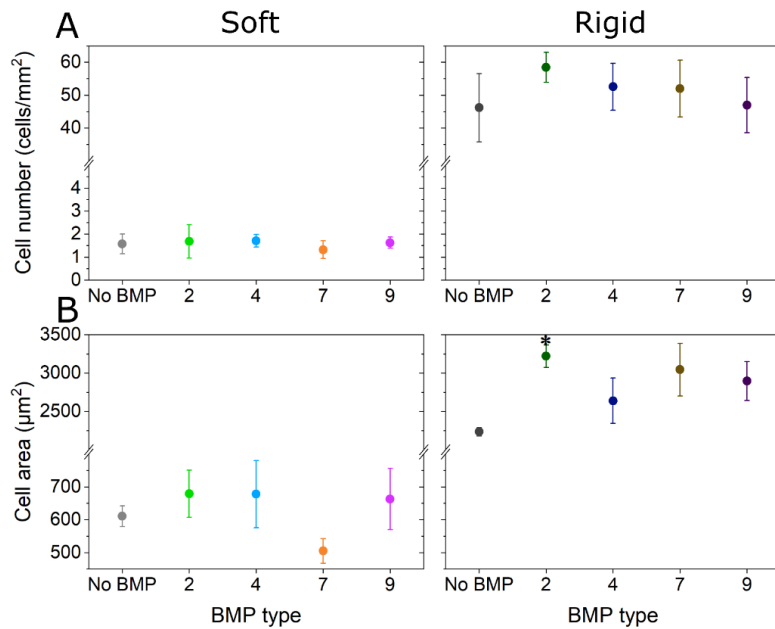


Figure SI 7. Representative example of high and low pSMAD fluorescent signal. Boxplot showing an example of pSMAD 1,5,9 signal distribution of individual cells, represented by the small points. No BMP condition vs bBMP-9 at 20 $\mu\text{g/ml}$ on rigid films are represented. Representative fluorescent images of each condition, representing a cell with low pSMAD 1,5,9 signal, seeded on no-BMP condition, and a cell with a high pSMAD 1,5,9 signal, seeded on bBMP-9 at 20 $\mu\text{g/ml}$. Both conditions correspond to a rigid film. Immunofluorescent staining was performed 4 h after cell seeding. Box plots represent the 25 and 75% percentiles. The horizontal line in the box represent the median (50% percentile). The filled square represent the mean value, and the error bars represent the standard deviation. Scale bar=25 μm .

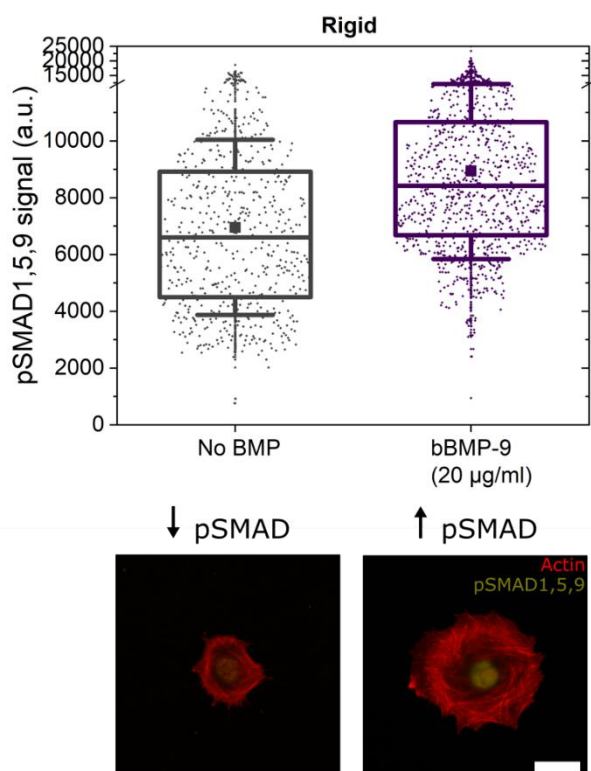


Figure SI 8. pSMAD analyses for the four bBMPs (2, 4, 7 and 9) on soft and rigid films. Fluorescent signal quantification of (a) pSMAD 1,5,9 and (b) pSMAD 2 as a function of the BMP concentration in soft (light color) and rigid films (dark color). Data represent the mean \pm SEM of 2 to 4 independent experiments with two samples per condition in each independent experiment (at least 400 cells were analyzed in total). Statistical tests were done using non-parametric Kruskal-Wallis ANOVA test to compare soft and rigid films. However, no statistical differences were found.

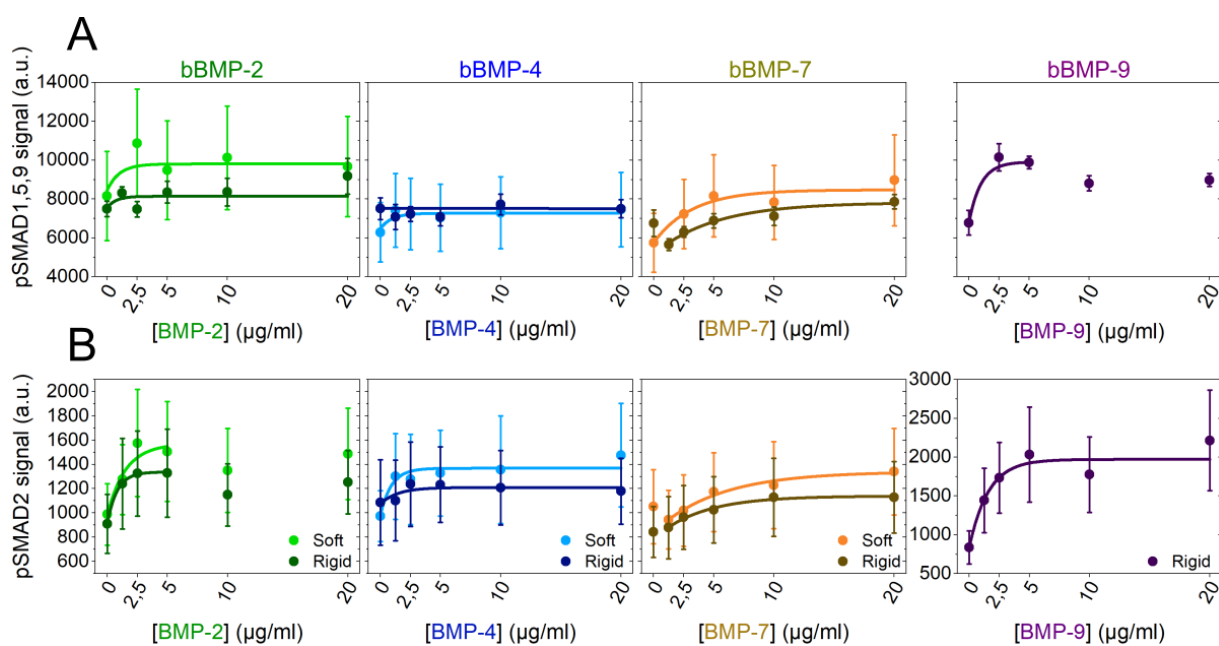


Figure SI 9. Effects of soluble BMPs (sBMP-2, -4, -7, -9) on pSMAD 1,5,9 signal on C2C12 cells. Cells were fixed after 5h, on soft films, and after 4 h on rigid ones. Data represent the mean \pm SEM, with 3 independent biological replicates and 2 technical replicates in each experiment. Statistical tests were done using non-parametric Kruskal-Wallis ANOVA test to compare each BMP condition with the no-BMP condition. * $p \leq 0.05$.

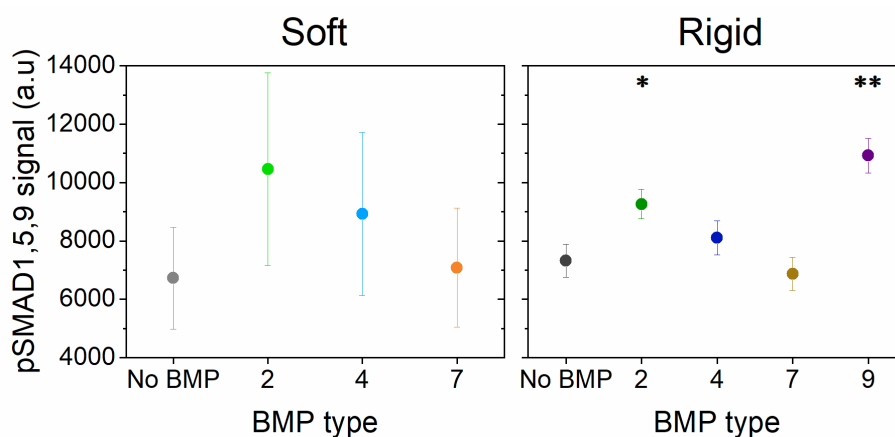


Figure SI 10. Representative images of an ALP staining for C2C12 cells on soft and rigid films with all 4 bBMPs (2, 4, 7, 9). C2C12 cells were fixed and stained 3 days after cell seeding to measure ALP activity. The loading BMP concentration of 20 $\mu\text{g/ml}$ for all BMPs, and the non-BMP condition are shown as representative examples.

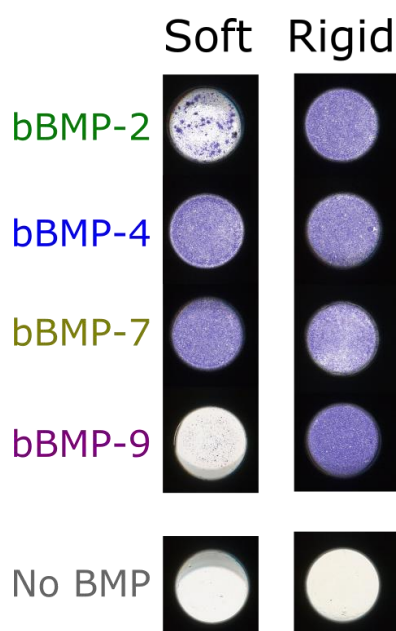


FIGURE SI 11. Identification of C2C12 cells-specific BMP receptors and integrins, using the ENCODE database. Pie chart of the percentage of expression of BMP receptor type I, BMP receptor type II and β integrins (1, 3 and 5), illustrating the predominance of certain adhesion receptors in C2C12 cells. Data were obtained by analyzing RNA sequencing data made for the ENCODE public research project.

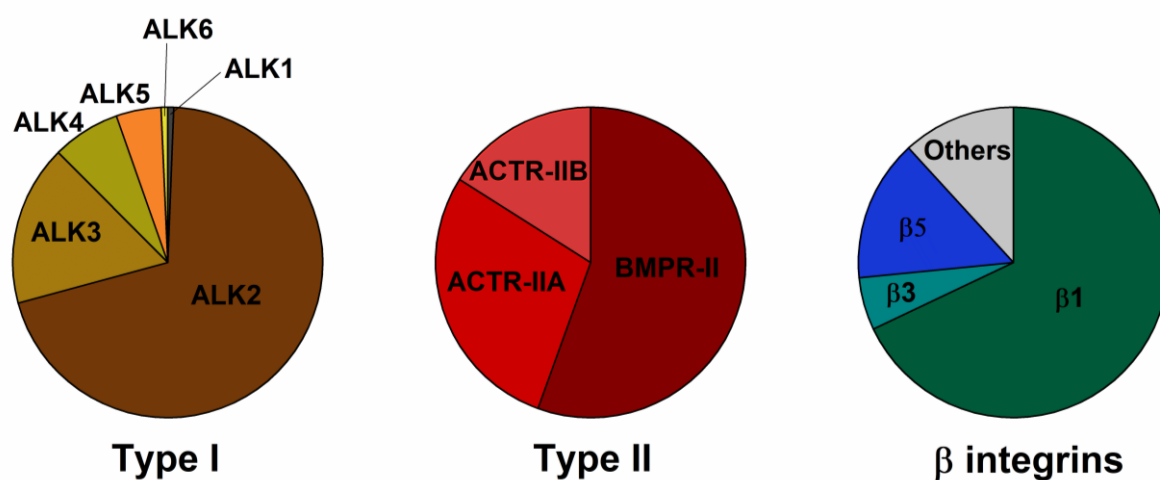


Figure SI 12. C2C12 transfection control. The gene expression level of each knocked down gene, as well as the corresponding scrambled condition, are shown for the BMP receptors type I, type II and the three β integrins studied. All the receptors were correctly silenced, with expression levels below 10% with respect to the scrambled condition. Bars represent the mean and error bars represent the \pm SEM, with 3 biological replicates and 2 technical replicates per experiment.

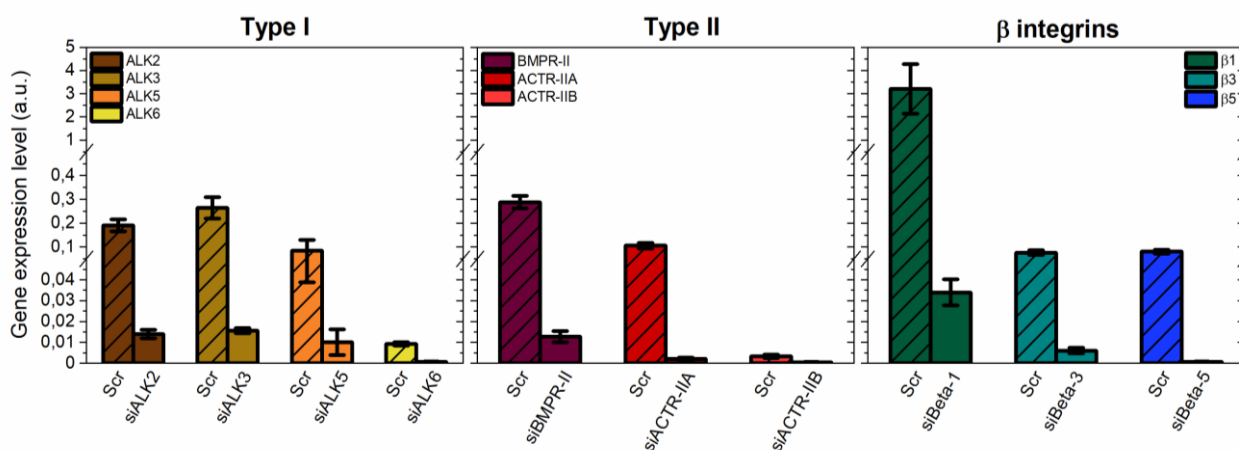


Figure SI 13. Effect of BMP receptor and beta chain integrin silencing on cell adhesion and spreading on rigid films with no BMPs. C2C12 cells were transfected with siRNA against BMP receptor type I (ALK2, ALK3, ALK5, ALK6), BMP receptor type II (BMPR-II, ACTR-IIA, ACTR-IIB) and beta chain integrins (β 1, β 3, β 5) and were plated on rigid films without bBMPs for 4 h. The cell number per mm² of substrate area and the spreading area were quantified, and the relative % is given, in comparison to a control scrambled siRNA. (a) Relative cell number (%), (b) relative cell area (%). Data represent the mean \pm SEM, with 2 to 4 biological replicates and 2 technical replicates per experiment.

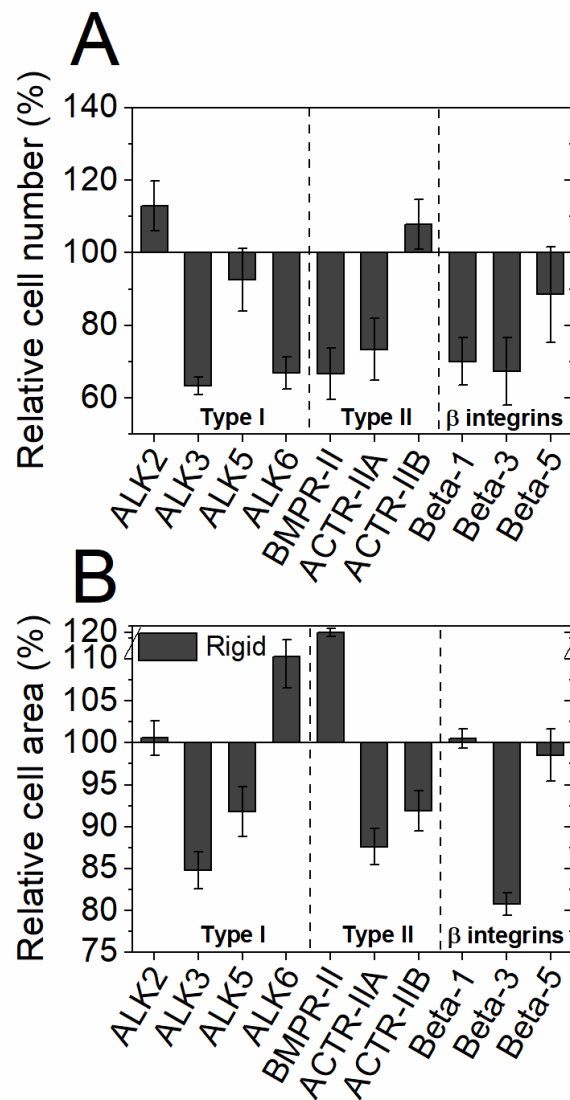


Figure SI 14. Non-normalized data showing the effect of BMP receptor and beta chain integrin silencing on cell adhesion and spreading. C2C12 cells were transfected with siRNA against BMP receptor type I (ALK2, ALK3, ALK5, ALK6), BMP receptor type II (BMPR-II, ACTR-IIA, ACTR-IIB) and beta chain integrins ($\beta 1$, $\beta 3$, $\beta 5$) and were plated on soft and rigid films with or without bBMPs for 5 or 4 h, respectively. **(a)** The cell number per mm^2 of substrate area and **(b)** the spreading area were quantified. Data represent the mean \pm SEM, with 2 to 4 biological replicates and 2 technical replicates per experiment. Statistical tests were done using the non-parametric Kruskal-Wallis ANOVA test (*, $p \leq 0.05$; **, $p \leq 0.01$). Statistical comparisons were made between the different knock down conditions and the scrambled.

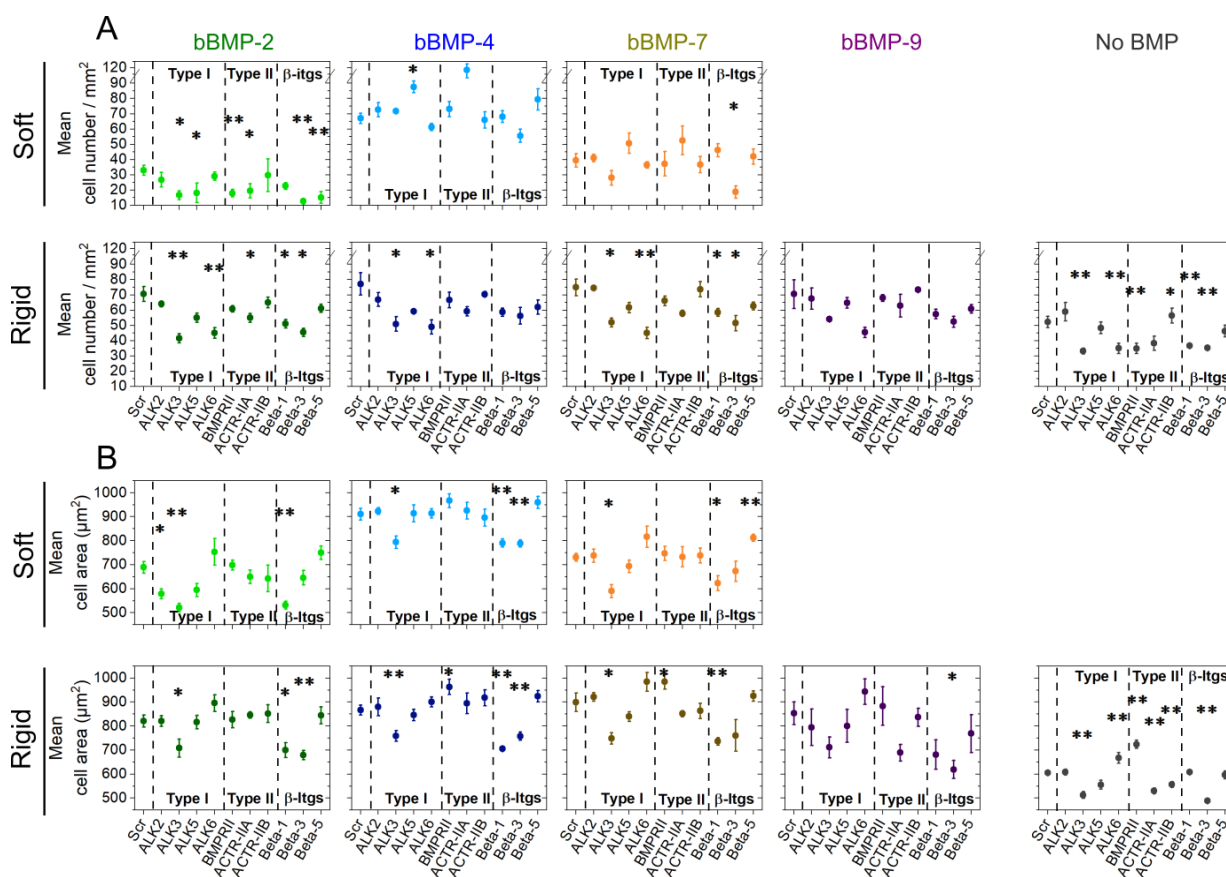


Figure SI 15. Effect of BMP receptor and beta chain integrin silencing on cell differentiation to bone, on rigid films with no BMPs. C2C12 cells were transfected with siRNA against BMP receptor type I (ALK2, ALK3, ALK5, ALK6), BMP receptor type II (BMPR-II, ACTR-IIA, ACTR-IIB) and beta chain integrins (β 1, β 3, β 5) and were plated on rigid films without bBMPs for 4 h. (a) pSMAD 1,5,9 and (b) pSMAD 2 signal, as well as (c) ALP activity were quantified. The relative % is given, in comparison to a control scrambled siRNA. Data represent the mean \pm SEM, with 2 to 4 biological replicates and 2 technical replicates per experiment.

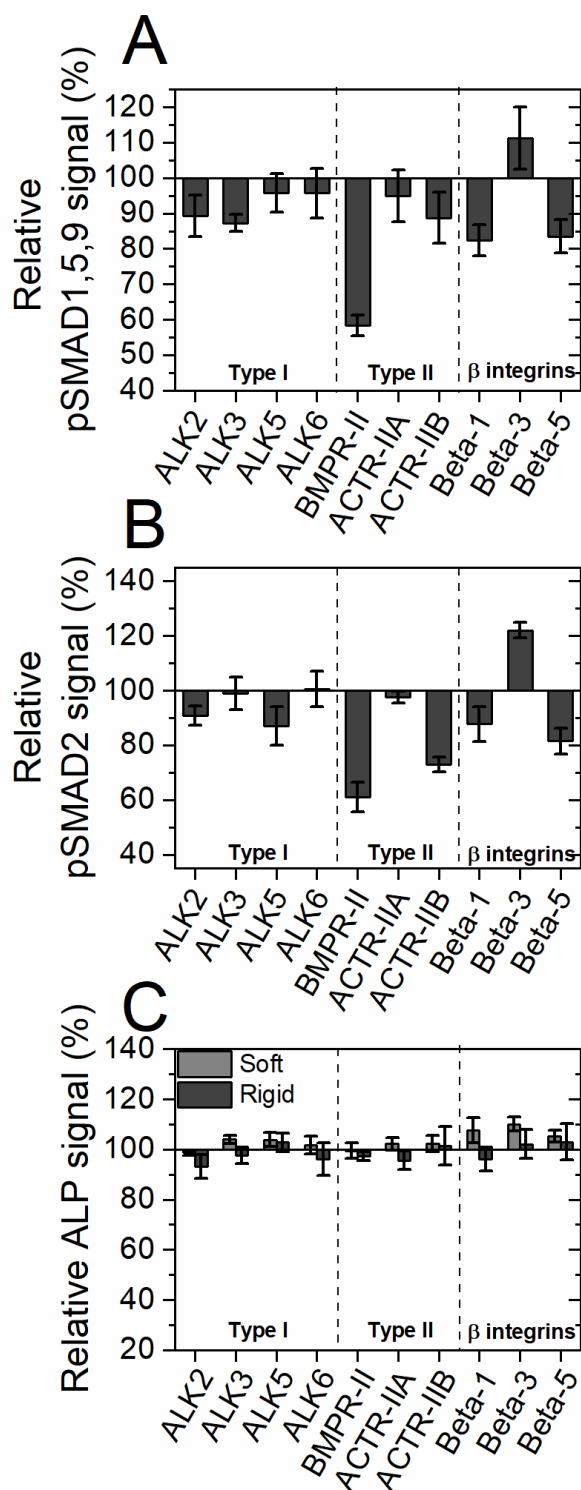


Figure SI 16. Non-normalized data showing the effect of BMP receptor and beta chain integrin silencing on pSMAD 1,5,9, pSMAD 2 and ALP activation. C2C12 cells were transfected with siRNA against BMP receptor type I (ALK2, ALK3, ALK5, ALK6), BMP receptor type II (BMPR-II, ACTR-IIA, ACTR-IIB) and beta chain integrins (β 1, β 3, β 5) and were plated on soft and rigid films with or without bBMPs for 5 or 4 h, respectively. (a) The pSMAD 1,5,9 and (b) pSMAD 2 fluorescent signals, together with (c) the ALP activation level were quantified. Data represent the mean \pm SEM, with 2 to 4 biological replicates and 2 technical replicates per experiment. Statistical tests were done using non-parametric Kruskal-Wallis ANOVA test (*, $p \leq 0.05$; **, $p \leq 0.01$). Statistical comparisons were made between the different knock down conditions and the scrambled condition.

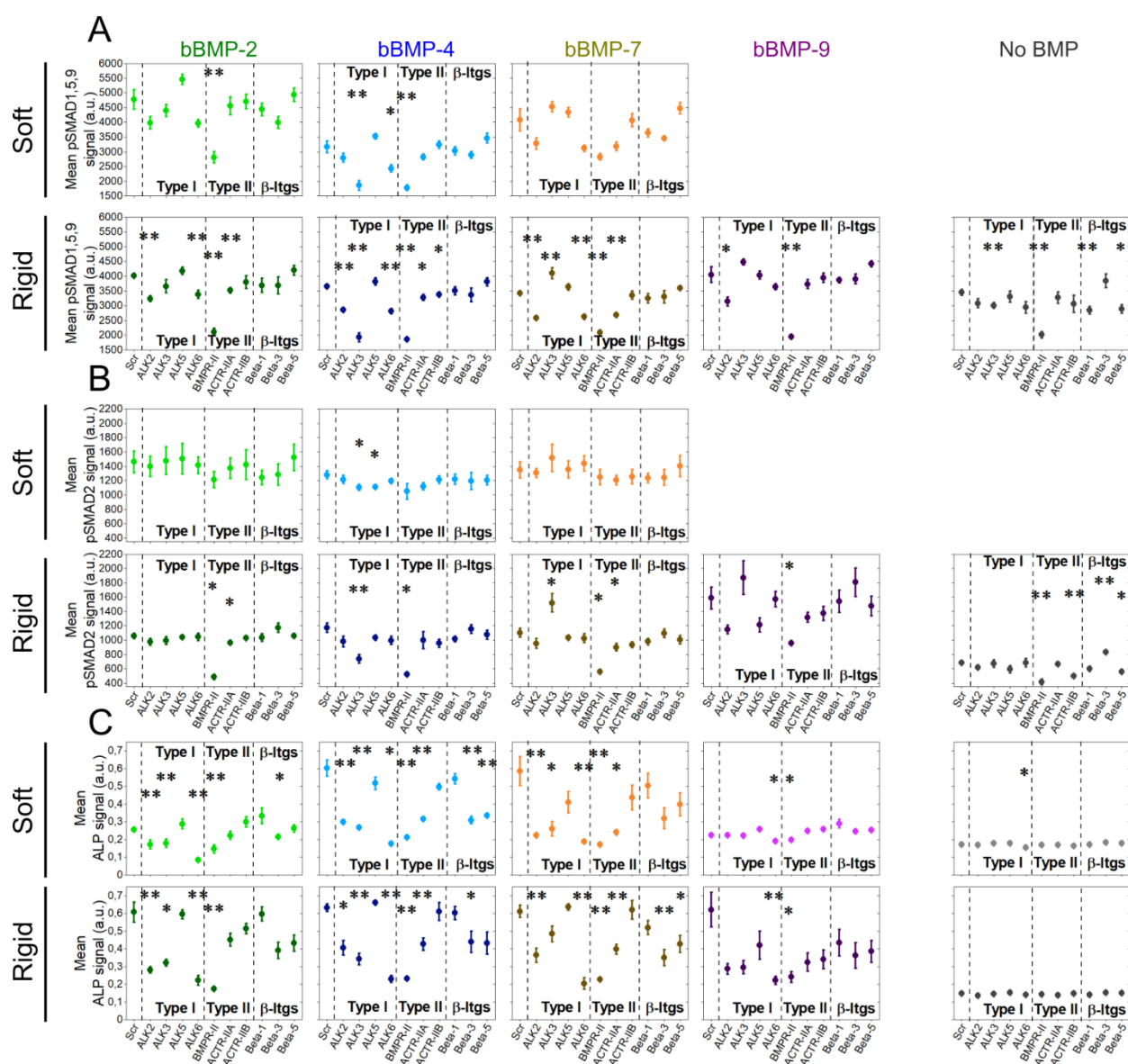
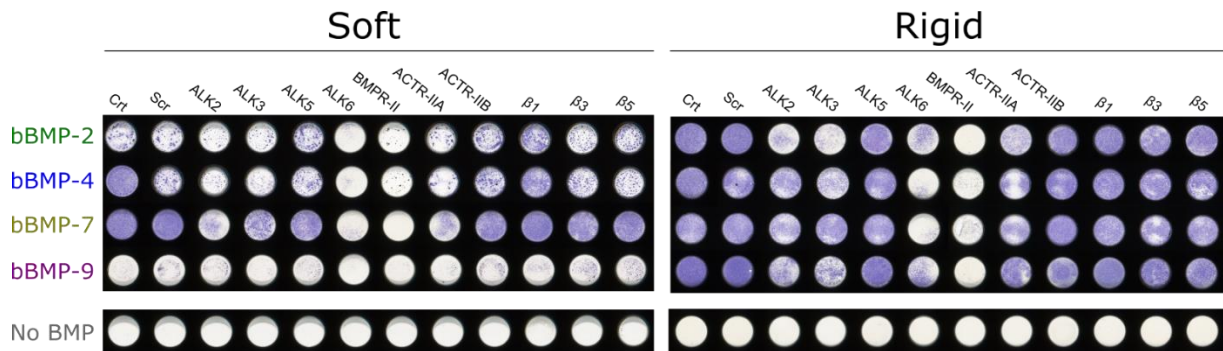


Figure SI 17. Representative pictures of an ALP staining on C2C12 cells for each bBMP (2, 4, 7 and 9) and each knock down condition, on soft and rigid films. C2C12 cells were fixed 3 days after seeding, and were stained for ALP, on soft and rigid films with a BMP loading concentration of 20 $\mu\text{g}/\text{ml}$, as well as on the non-BMP control condition.



CV Valia KHODR

Grenoble, France

khodrvalia@gmail.com - [LinkedIn](#) : valia-khodr



Education

PhD in Biotechnology (ED216: EDISCE) University of Grenoble-Alpes (Some courses: Biomaterials, project management) Title: "Initial molecular steps of bone regeneration: modulation at the cellular scale"	10/2018 – 12/2021 Grenoble, France
Master of Science in Biochemistry and Molecular Biology University of Bordeaux (Some courses: Genetic engineering, cellular imaging, Drug discovery)	09/2016 – 06/2018 Bordeaux, France
Bachelor of Science in Biology specialized in Biochemistry University of Bordeaux	09/2013 – 06/2016 Bordeaux, France

Professional Experience

Researcher - PhD candidate INSERM U1292 Biosanté (Biology and Biotechnology for Health, INSERM-UGA-CEA), CEA-IRIG Institute and CNRS EMR 5000 (Biomimeticism and Regenerative Medicine, CNRS-CEA-UGA) Investigated BMPs' canonical pathway in the context of bone regeneration and developed a high-content immunofluorescence assay to study drugs on biomaterials <ul style="list-style-type: none">• Measured the interaction of BMP with BMPR using surface plasmon resonance (SPR) and biolayer interferometry (BLI)• Developed and optimized an automated cellular immunofluo. assay to study pSMAD signaling in bone regeneration• Performed and compared kinetics analysis of BMP-2 and TGFβ-1 on biomaterials and glass• Conducted and compared drug testing experiments on a biomaterial and glass models using microplates• Examined BMPR, cadherin and integrin gene expression using qPCR in BMP-responsive cells (C2C12 mice cells, human mesenchymal stem cells (hMSCs))• Wrote the BLI protocol and improved the qPCR protocol for the team• Analyzed my results and drafted three scientific journal articles, as well as participated in reviewing a third one• Taught 20 hours of qPCR practical work to engineering and master students at Phelma Grenoble INP	10/2018 – 12/2021 Grenoble, France
Research Assistant - M2 Intern Institut Européen de Chimie et Biologie (IECB) Conducted research to structurally characterize Ab oligomers, involved in Alzheimer's disease <ul style="list-style-type: none">• Produced Aβ peptides by recombinant expression• Purified and analyzed samples by fast protein liquid chromatography (FPLC) and size exclusion chromatography (SEC)• Performed SDS-Page to verify the purity of the oligomers• Conducted solution NMR experiments in order to structurally characterize Aβ oligomers• Performed mass spectrometry experiments to determine the stoichiometry of Aβ oligomers	01/2018 – 06/2018 Bordeaux, France
Research Assistant- M1 Intern Chimie & Biologie des Membranes et des Nano-Objets (CBMN) Analyzed and compared protein A columns from different manufacturers using mAb <ul style="list-style-type: none">• Packed chromatographic columns of protein A• Analyzed the dynamic capacities (by FPLC), precipitation of protein A and host cells proteins (by Elisa and SDS-PAGE), and precipitation of residual host DNA (by qPCR) using antibodies on chromatographic columns of several manufacturers	04/2017 – 06/2017 Bordeaux, France
L3 intern Inserm U1053 <ul style="list-style-type: none">• Evaluated the level of infection by <i>Helicobacter bacteria</i> in a murin model by qPCR	05/2016 Bordeaux, France

Tutor

University of Bordeaux

- Ensured educational support for first and second year students in enzymology, structural and metabolic Biochemistry

12/2015 – 05/2016

Bordeaux, France

Publications

- “High throughput measurements of BMP/BMP receptors interactions using bio-layer interferometry” by [Valia Khodr](#), Paul Machillot, Elisa Migliorini, Jean-Baptiste Reiser, Catherine Picart, *Biointerphases*, 2021, doi: [10.1116/6.0000926](https://doi.org/10.1116/6.0000926)
- “Differential bioactivity of four BMP-family members as function of biomaterial stiffness” by Adrià Sales, [Valia Khodr](#), Paul Machillot, Laure Fourel, Amaris Guevara-Garcia, Elisa Migliorini, Corinne Albigès-Rizo, Catherine Picart, *Biomaterials*, 2022, doi: [10.1016/j.biomaterials.2022.121363](https://doi.org/10.1016/j.biomaterials.2022.121363)
- “Development of an automated high-content screening immunofluorescence assay of pSmad quantification: proof-of-concept with drugs inhibiting the BMP and TGFβ pathways” by [Valia Khodr*](#), Laura Clauzier* Paul Machillot, Adrià Sales, Elisa Migliorini, Catherine Picart (in preparation)
- “Promiscuity of TGF-β superfamily receptor activation and its implication in human diseases” by [Valia Khodr*](#), Tala Al Tabosh, Sabine Bailly, Catherine Picart (in preparation)

Scientific communication

Oral presentation

- Conférence “Société française de Biochimie et Biologie Moléculaire” – Paris (oral presentation) 1-2/07/2021
- The BCI laboratory of biosanté unit bimonthly meeting - CEA Grenoble (oral presentation) 9/11/2020
- “Hydra European Summer School on Stem Biology and Regenerative Medicine” - Hydra Greece (poster + oral presentation) 15 to 22/09/2019
- “Laboratoire des matériaux et du Génie Physique yearly scientific day” - Grenoble (oral presentation) 11/4/2019

Poster presentation:

- Biointerphases Conference Zurich – Online (Poster + flash presentation) 18-19/08/2021
- “AURASem conference 2019” - Lyon France (poster) 8/07/2019
- “Young Scientist Symposium 2018” - Bordeaux France during M2 (poster) 24-25/05/2018
- “Young Scientist Symposium 2017” - Bordeaux France during M1 (poster) 18-19/05/2017

Summary Skills

Technical skills: Biophysics techniques (SPR, BLI), microscopy, immunofluorescence, cell culture (mouse and primary cells), qPCR, μBCA, SDS-PAGE, Purification techniques (FPLC, HPLC...), biomimetic film polymer preparation, recombinant expression, western Blot, solution NMR, mass spectrometry,

Computer skills: Origin, inkscape, imageJ, R Programming, spss, Kaleidagraph, MS Word, Excel, PowerPoint

Languages: Fluent in English, French and Arabic

Soft skills: Writing, Organizational, Time management, Teamwork, Public Speaking, Communication, Leadership

Associative Activities

Association ASSEM (Association de Soutien Scolaire aux Enfants Malades)

01/2016 – 04/2016

Position Held: *Animator*

Bordeaux, France

- Animated several scientific workshops for hospitalized teenagers

Interests and Hobbies

Piano, travelling, yoga and reading

References

Available upon request

